The Mechanisms of Amniote Photoperiodism: from Deep-Brain Photoreceptors to Rhythmic Epigenetics.

Elisabetta Tolla

MSc Biomedical Sciences

BSc Biology

Submitted in fulfilment of the requirements for the Degree of

Doctor of Philosophy

University of Glasgow

2020

Abstract

Seasonal reproduction is a strategy conserved across nature. The duration of light (photoperiod) regulates the reproductive molecular control within the Hypothalamic-Pituitary-Gonadal Axis of seasonal species, and supplementary cues fine-tune the exact timing of breeding. In recent years, epigenetic mechanisms have been shown to be involved in an array of circannual rhythms, including reproduction. The aim of this thesis was to explore the molecular reproductive neuroendocrine processes that underlie the onset of reproduction in two summer-breeding animal models, the Japanese quail (*Coturnix japonica*) and the Siberian hamster (*Phodopus sungorus*). In birds, light penetrates the skull and is detected by deep-brain photoreceptors (DBPs) within the hypothalamus, stimulating the photoperiodic reproductive response. However, the identity of these DBPs is unclear to this day. In the present thesis, the expression of two photoreceptors, Vertebrate-Ancient Opsin (VA Opsin) and Neuropsin (OPN5), was repressed through adeno-associated viral injection, and the breeding response was monitored in control and treated birds maintained under short-days (SD), or long-days (LD) for 2, 7 or 28 days. The data revealed that both opsins may be involved in seasonal reproduction in the Japanese quail, and that OPN5's role includes modulating gonadal sensitivity to gonadotropins during breeding. It was also found that hypothalamic *OPN5, GNRH* and *DNA methyltransferase* (*Dnmt*) expression increases at embryonic day 14 in this species. In addition, higher global methylation levels were found in the pituitary gland of adult LD quail, compared to SD.

In the Siberian hamster, two studies were conducted to investigate the effect of triiodothyronine (T_3) on the photoperiod-dependent regulation of reproductive physiology and hypothalamic DNA methyltransferase enzyme expression in both males and females. Two weeks of daily T_3 injections induced gonadal growth in SD males, but not in females. Female SD hamsters, but not males, were found to express lower levels of *de novo* Dnmts compared to LD individuals. However, exogenous T_3 did not affect hypothalamic *Dnmt* expression in neither males or females. The data indicated sex differences in the gonadal response to T_3, as well as in the regulation of hypothalamic DNA methyltransferase expression. It is likely that female Siberian hamsters require additional cues to initiate reproductive processes. The studies presented allowed for an exploration of reproductive mechanisms in both an avian and a mammalian model, including the role of epigenetic processes in seasonal breeding. Future studies are required to elucidate the precise mechanisms of DBPs, as well as identify downstream targets of maintenance and *de novo* Dnmts.

Table of Contents

List of Tables

List of Figures

Acknowledgements

I would like to thank my supervisor, Dr Tyler Stevenson, for being such a great mentor and friend. The skills and knowledge your training has taught me during these 5 years have shaped me as a researcher and I will take them with me for the rest of my academic career.

Second, I would like to especially thank Professor Neil Evans, for his precious advice and support. Thank you to Dr Jonathan Pérez, working with you has been extremely enjoyable and your *in vivo* experience has been invaluable. I would also like to thank Professor Simone Meddle and Professor Ian Dunn for their guidance throughout the photoreceptor knockdown project. A big thank you to Professor Ian Dunn, Professor Karen Spencer and Jessica-Lily Harvey-Carroll for kindly supplying the quail tissues analysed in chapter 3. Thank you also to Dr Ana Monteiro and Lynne Fleming for always being so helpful around the lab and for bringing a little laughter to work. A special thank you goes to past lab members Dr Chris Coyle and Mahnoor Khalid for their assistance.

I would like to immensely thank Alessandro for his continuous support, especially during the writing of this thesis. I would also like to thank Francesca, Klara, Manuel, Aoife, Suzie, Rodanthi, Carmen, Jess and Pietro for their encouragement and friendship. My PhD experience would not have been the same without all of you.

Finally, I am extremely grateful for the unconditional love and support of my wonderful family, my parents Eleonora and Tito and my brother Federico, throughout my studies. I will forever cherish the opportunities you gave me that have moulded me into the person I am today.

Author's Declaration

I declare that, except where explicit reference is made to the contribution of others, this dissertation is the result of my own work and has not been submitted for any other degree at the University of Glasgow or any other institution.

Printed Name: Elisabetta Tolla

Signature:

Chapter 1 – Introduction

This chapter is drawn from three publications: “Tolla, E., Pérez, J. H., Dunn, I. C., Meddle, S. L., & Stevenson, T. J. (2019). Neuroendocrine Regulation of Seasonal Reproduction. In *Oxford Research Encyclopedia of Neuroscience*.”, “Pérez, J. H., Tolla, E., Dunn, I. C., Meddle, S. L., & Stevenson, T. J. (2019). A comparative perspective on extra-retinal photoreception. *Trends in Endocrinology & Metabolism*, 30(1), 39-53.”, and “Tolla, E., & Stevenson, T. J. (2020). Sex differences and the neuroendocrine regulation of seasonal reproduction by supplementary environmental cues. *Integrative and Comparative Biology*.”, as they provide in-depth descriptions of principles and knowledge that form the basis of the present thesis.

1.1 Seasonal reproduction and the importance of photoperiod

Seasonal rhythms are pervasive across the kingdoms of life, and seasonal species use environmental and internal cues to determine the correct timing for an array of functions, such as sleep, hibernation, reproduction, and migration. Some examples of external cues that can elicit one or all these responses are temperature, food availability and daylength (photoperiod). In time, studies have established a role for light information as the primary external factor involved in the seasonal response (Rowan, 1926; Paul et al., 2008; Stevenson and Ball, 2011). William Rowan in 1926 first showed experimentally the crucial effect photoperiod has on reproduction. Working with the small finch *Junco hyemalis*, he brought the birds into breeding condition using artificial light in the depths of winter. Although seasonal rhythms in reproduction are more common in higher latitudes due to the salient changes in environmental conditions (Hut et al., 2013), it is not uncommon to observe annual variation in reproduction in species that are endemic to equatorial regions (Hau, 2001). Across avian and mammalian species, the hypothalamus is

the key brain region that integrates environmental cues with the endogenous internal timing mechanism, leading to the optimal timing of reproduction necessary for the propagation of the species (Stevenson, Prendergast, & Nelson, 2017; Pérez et al., 2019). One common feature of seasonal reproduction is the robust and predictable molecular oscillations in key neuroendocrine brain regions. These rhythmic-molecular switches are essential to ensure that the birth of the offspring occurs during periods optimal for survival.

In the present chapter, I will introduce the biological concepts that underlie the work presented in this thesis, including mechanisms of light detection, and external and endogenous modulators of the hypothalamic-pituitary-gonadal axis that lead to timing of breeding. I will then outline the hypotheses tested in chapters 2-6.

1.2 Environmental and internal regulation of seasonal reproduction

1.2.1 Environmental control of seasonal reproduction

Environmental cues are divided in proximate and ultimate factors (Baker, 1938). Proximate factors include events essential for the initiation and progression of reproductive processes during the whole breeding period. Ultimate factors are stimuli affecting individual fitness and survival by determining the optimal time for reproduction and birth of the offspring (Baker, 1938). This distinction aids in the categorisation of studies and facilitates research on seasonal rhythms. Seasonal species have developed neuroendocrine processes that respond to both ultimate and proximate factors (Wilson and Donham, 1987; Dawson et al., 2001). Successful timing of seasonal reproduction requires the integration of multiple environmental cues with complex internal, endogenous timing mechanisms (Figure 1.1A). In general, the annual change in day length, known as photoperiod, is the predictive cue that many animals use to anticipate annual changes in the environment (Figure 1.1B) (e.g., Dawson, 2015; Paul et al., 2008; Stevenson & Ball, 2011; MacDougall-Shackleton et al., 2009).

The timing of the termination of breeding is as critical as its stimulation. Photorefractoriness, or loss of a physiological ability to respond to the photoperiodic signal, tightly constrains reproduction to a breeding season. For example, in sheep, short-day refractoriness causes the gonads to regress spontaneously after many months on short days (e.g., Lincoln, Andersson, & Hazlerigg, 2003). Absolute refractoriness in birds is remarkable and rapid. For instance, in white-crowned sparrows (*Zonotrichia leucophrys*) and European starlings (*Sturnus vulgaris*), long days stimulate gonadal growth but after two to three months there is a spontaneous shutdown of the HPG axis resulting in gonadal regression (e.g., Nicholls, Goldsmith, & Dawson, 1988; Meddle et al., 2006; Stevenson et al., 2009). For hamsters and other hibernating species, three to four months of short days result in refractoriness to the inhibitory effects and the gonads recrudesce (e.g., Ebling, 2015; Hut et al., 2014). The complex neuroendocrine machinery underlying photorefractoriness and its disappearance by the next breeding season still requires deciphering. One suggestion is that two separate photoperiodic mechanisms (photo-induction and photo-inhibition) are players in the asymmetrical breeding cycle (Dawson, 2015; Ebling, 2015) and thyroid hormones are key for timing these seasonal transitions; for instance, in sheep, thyroid hormones are crucial for the transition from the reproductive state to anoestrus (e.g., Goldsmith & Nicholls, 1984, Nicholls et al., 1988, Parkinson et al., 1995; Moenter et al., 1991; Webster et al., 1991; Dahl et al., 1994). It is important to highlight that many animals use long summer days to time breeding (e.g., hamsters, quail) and other animals use short winter day lengths to initiate reproduction (e.g., sheep, emu). Following the photoinduction of a breeding state, other supplementary cues, such as temperature, food availability, and social information serve to fine tune the timing of reproduction to maximize offspring survival (Wingfield & Kenagy, 1991).

A)

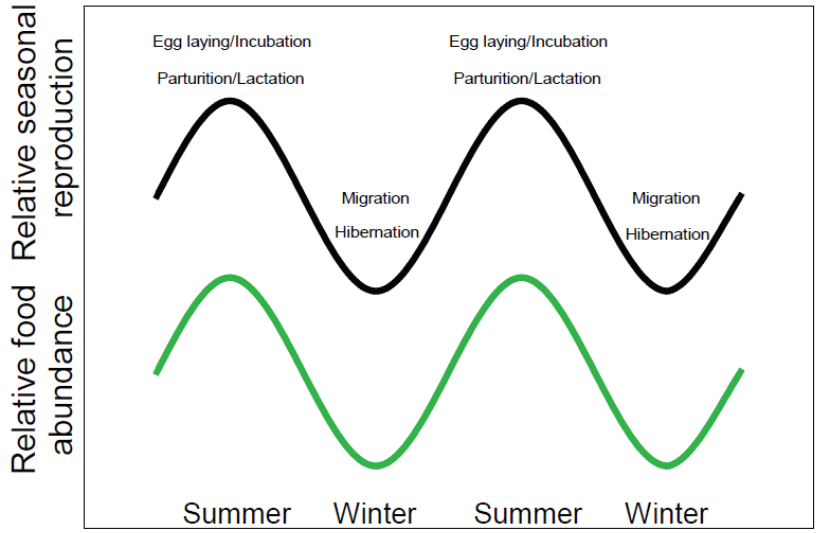
Relative seasonal reproduction
Relative food abundance
Egg laying/Incubation
Parturition/Lactation
Egg laying/Incubation
Parturition/Lactation
Migration
Hibernation
Migration
Hibernation
Summer
Winter
Summer
Winter

B)

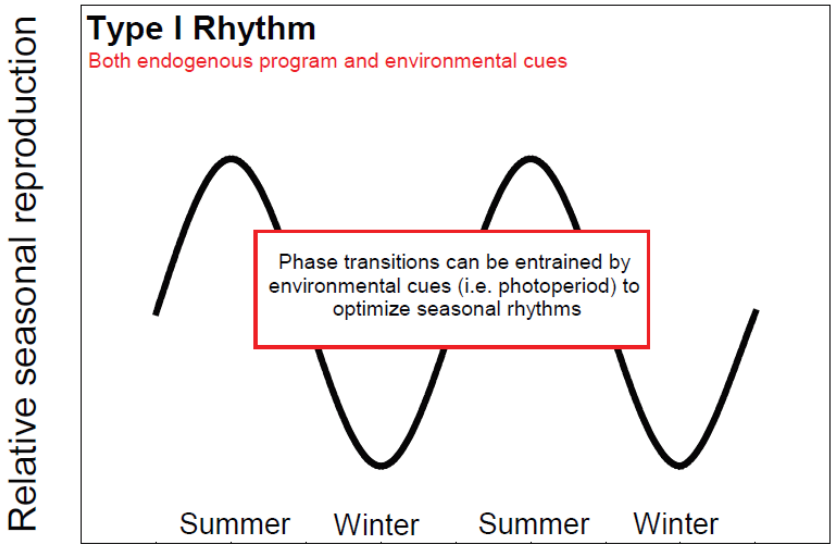
Relative seasonal reproduction
Type I Rhythm
Both endogenous program and environmental cues
Phase transitions can be entrained by environmental cues (i.e. photoperiod) to optimize seasonal rhythms
Summer
Winter
Summer
Winter

C)

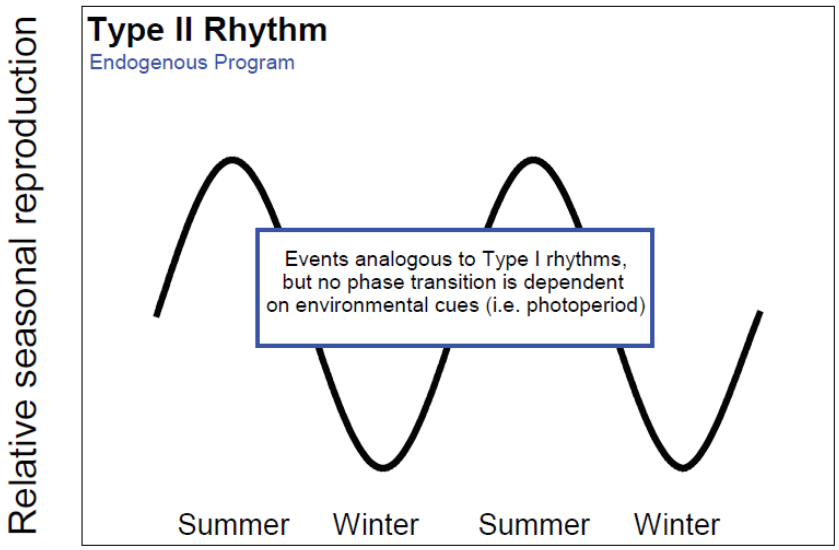
Relative seasonal reproduction
Type II Rhythm
Endogenous Program
Events analogous to Type I rhythms, but no phase transition is dependent on environmental cues (i.e. photoperiod)
Summer
Winter
Summer
Winter

Figure 1.1. Schematic representation of seasonal reproductive rhythms. (A) Many northern hemisphere vertebrates time reproduction to occur during the long-day summer periods due to the significant increase in biomass. Annual cycles of long-day breeding animals are depicted by the black line and relative food abundance is represented by the green line. The two cycles are intrinsically linked, as species have evolved to lay eggs/give birth during times of high food abundance to maximize both parent and offspring survival. During winter when food availability is at its lowest, many temperate zone animals escape the harsh environments by annual endogenous programs in migration or hibernation. The principal forms of seasonal rhythms that have been characterized are Type I and Type II. (B) Type I (mixed) seasonal rhythms are dictated by both endogenous (interval timer) programming and environmental cues, for example, photoperiod. Long day breeders increase reproductive function in response to vernal increase in photoperiods and either terminate reproduction after prolonged exposure to long days (i.e., birds) or exhibit gonadal involution after exposure to decreasing day lengths (i.e., mammals). (C) Type II (circannual) seasonal rhythms are entirely generated by endogenous programs and typically have a period less than 12 months. Adapted from Stevenson et al. (2017). Figure from Tolla et al., 2019.

1.2.2 Supplementary cues and timing seasonal reproduction in birds

As mentioned above, the duration of light is considered the initial predictive cue for sexual maturation in seasonally breeding species of birds and mammals (Wingfield and Kenagy, 1991; Wingfield et al., 1992; Stevenson et al., 2012). However, it has been shown that supplementary cues impact the neuroendocrine regulation of reproduction in a sex-dependent manner in both avian and mammalian systems (Ball and Ketterson, 2008). In seasonally reproducing birds, sexual differences in response to external supplementary cues have been documented for over a century (Riley and Witshi, 1938; Ball and Ketterson, 2008). For example, the vernal increase in light duration is sufficient to induce testes growth in male house sparrows (*Passer domesticus*), although the same treatment is not able to stimulate full ovarian development (Riley and Witschi, 1938). The lack of photostimulation to fully induce reproductive competence in female birds has been widely demonstrated (Farner and Lewis, 1971). These studies suggested that other cues drive female reproductive physiology, and since then, food cues, temperature, and auditory and

visual stimuli have been identified as important supplementary cues for reproductive development.

In ring doves (*Streptopelia risoria*), females exposed to male presence respond with a significant increase in mating and maternal behaviour (Lehrman, 1965). Females that were able to see the male and hear males engaging in directed courting reached full reproductive growth (Friedman, 1977). Subsequently, using female canaries (*Serinus canaria*), Robert Hinde and Elizabeth Steel identified that simply hearing male vocalizations was sufficient to induce sexual development and behaviour (Hinde and Steel, 1976). It is now well characterized that immediate early gene expression in the auditory brain region, the caudal mesopallium (CMM) and the dorsal nidocaudal mesopallium (NCMd), is associated with song attractiveness and female mate preferences in canaries (Haakenson et al., 2019), white-crowned sparrows (*Zonotrichia leucophrys*; Maney et al., 2003), house finches (*Carpodacus mexicanus*; Hernandez and MacDougall-Shackleton, 2004), European starlings (*Sturnus vulgaris*; Genter and Hulse, 2000) and zebra finches (*Taeniopygia guttata*; van Ruijssevelt et al., 2018).

The presence of male vocalizations alone can stimulate the neuroendocrine axis leading to egg-laying in female birds. Female house sparrows (*Passer domesticus*) paired with males increased ovarian follicle size and body compared to birds that were housed alone or paired with a non-breeding male (Stevenson et al., 2008). When female budgerigars (*Melopsittacus undulates*) were kept in the dark and were exposed to male vocalizations, there was a significant increase in the number of eggs laid, indicating that auditory cues are capable of inducing full reproductive competence (Vaugien, 1951). To determine the specificity of male vocalizations that are required for egg laying, Bentley and colleagues (2000) exposed female songbirds to both heterospecific and conspecific songs. Both songs were identified to induce follicle development. In addition, a surge in plasma LH and egg laying was observed in females that heard male songs, compared with females exposed to no songs (Bentley et al., 2000). How auditory cues perceived in the

CMM and NCMd project to and regulate the neuroendocrine axis remains uncharacterized in birds.

It is important to note that variation between populations in the response to supplementary cues has been previously reported and should be a factor when analysing data. For instance, one study found different effects of temperature on the onset of breeding in two distinct populations of great tits (Husby et al., 2010). Although both populations experienced a similar increase in temperature during the spring, only one showed a significant variation in timing of egg-laying (Husby et al., 2010). It is essential then to take into consideration not only species-specific effects, but also inter-population differences that could be given by genetic variances.

1.2.3 Supplementary cues and timing seasonal reproduction in mammals

Although the literature describing the role of supplementary cues in avian reproduction is abundant, most of the studies on mammalian seasonal reproduction predominantly focus on the effect of photoperiod. Some studies have focused on the effects of food availability, food quality and social cues (i.e. olfaction) for reproductive development, however these are rarely considered in a seasonal context. Here I will cover some of the evidence shown to underlie potential sex differences in the timing of seasonal reproduction in mammals. Due to the paucity of information of supplementary cues to time seasonal rhythms, supplementary cues in male mammals will primarily be considered.

The availability of food resources can have an impact on reproductive development and seasonal breeding in some rodent species (Stephan, 2001; Bronson, 1989). California voles (*Microtus californicus*) are a seasonally-breeding rodent species and reduce testicular mass and seminal vesicles in response to short days. The simple addition of spinach leaves was observed to counteract the inhibitory effects of short-day lengths (Nelson et al., 1983). Moreover, water restriction was found to lower testicular mass suggesting that both food availability and water can augment seasonal rhythms in the reproductive competence of

male California voles. In tropical species such as the cloud forest mouse (*Peromyscus nudipes*), food availability significantly increased the probability of producing viable offspring. Female cloud forest mice exhibit oestrus cycles and readily engage in copulatory behaviours during both dry and wet seasons. Only during the wet season, when food and water are readily available, will cloud forest mice produce offspring (Heideman and Bronson, 1992). These findings indicate that food availability can impact the neuroendocrine control of gonadal growth in both male and female mammals. Yet, the investment in the production of offspring by the female is entirely dependent on sufficient food resources.

In addition to food availability, the composition of food resources can impact the seasonal rhythm in reproductive physiology. In ewes (*Ovis aries*), feeding on dry lot resulted in a higher percentage of females reaching ovulation even in the non-breeding period, compared with individuals feeding on pasture (Hulet et al., 1986). In female voles, but not in males, the addition of the plant compound 6-Methoxybenzoxazolinone (6-MBOA) to food during the non-breeding season caused a 4-week advance in sexual maturation and breeding (Korn and Taitt, 1987). In addition, voles maintained at a constant photoperiod of 12L:12D that were fed 6-MBOA showed an increase in serum FSH and uterus and ovary weights (Schadler et al., 1988). In the southern hemisphere, Australian cashmere goats reproduce in the late summer and early autumn (Walkden-Brown et al., 1997). To assess the impact of diet composition on reproductive traits, goats were fed with either a high-protein (17.6 % protein) or low-protein (6.9 % protein) diet for sixteen months. In individuals that were fed the high-protein diet, there was a luteinizing hormone (LH) surge earlier in the season and LH levels were significantly higher than low-protein diet feeders (Walkden-Brown, 1994). These changes indicated that macronutrient levels in food can have an effect in advancing reproduction and increase the production of reproductive hormones. However, this study did not consider male-female differences,

suggesting more research is required to understand the role of nutrition on sex-dependent reproductive neuroendocrine signalling.

In mammals, social cues, primarily via olfaction, are well established to regulate female reproductive cycles (i.e. oestrous) and copulatory behaviour in females and males. However, less is known regarding the impact of other social cues on the neuroendocrine timing of seasonal reproduction. Adult female Angora goats were kept in different social settings, from having no male contact to only visual, olfactory or tactile cues, or all visual, olfactory and tactile cues (Shelton, 1960). More females reached ovulation after either visual, olfactory or tactile stimulation compared to females that did not receive tactile cues from a potential male mate. This study suggests that in female mammals, social cues facilitated the onset of reproduction, manifested as an additive effect of vision, sound and presence of a prospective male partner.

1.2.4 Organizational effects during development establish sex differences

The differences in how males and females respond to supplementary environmental cues is likely the effect of organizational effects on brain morphology (Raisman and Field, 1973; Gorski et al., 1978; Arnold and Gorski, 1984; Juraska, 1991). In 1959, Phoenix and colleagues proposed that steroid hormones, specifically testosterone, act on the mammalian brain during a critical window during development to organize its structure so that sex-specific genes can be activated later, during puberty (Phoenix et al., 1959). The 'Organizational-Activational Hypothesis' for the establishment and development of sex differences continues to explain how mammalian and avian species detect, integrate and respond to environmental and social stimuli (Beatty, 1984; Arnold, 2009). The preoptic area (POA) in the anterior hypothalamus is a critical node for the regulation of reproductive physiology and behaviour. Lesions to the POA in male rats result in a reduction in mating behaviour, however in females this decrease did not occur indicating a

marked sex difference in the role of the POA to regulate reproductive physiology (Hitt et al., 1970).

In mammals, a female-like brain has generally been considered the default during development, as the differentiation into a female brain results from the lack of steroid hormone action. The organizational-activational hypothesis has also been applied to the avian brain. In Japanese quail (*Coturnix japonica*), males and females have distinct sex differences in reproductive behaviour, where mounting and cloacal contact attempts are male-only traits. This has been attributed to sexual differences in the medial preoptic nucleus (POM) structure and the action of testosterone in males (Panzica et al., 1996; for a review see Balthazart et al., 1996). Although the POA is considered the site of the majority of sexual differences in reproductive behaviour, other brain regions have been found to differ between the sexes, such as the mammalian cortex (Juraska, 1991) as well as the telencephalon in songbirds (Nottebohm and Arnold, 1976).

1.3 Endogenous seasonal timing mechanisms

In addition to environmental cues, seasonal species possess internal timing mechanisms that act as an endogenous annual clock (Figure 1.1C) (Helm & Stevenson, 2015). The first suggestion that animals, and birds in particular, possess an endogenous circannual clock was demonstrated by Gwinner (1996). Using constant environmental conditions, Gwinner demonstrated that several tropical bird species, such as the East African stonechat (*Saxicola torquatus*) and the Garden warbler (*Sylvia borin*), maintain circannual rhythms in migratory behavior that showed period lengths ranging from 9 to 13 months (Gwinner, 1996). The presence of circannual timing mechanisms has since been identified in a range of species from single-celled organisms (*Alexandrium tamarense*; Anderson & Keafer, 1987) to mammals (*Spermophilus lateralis*; Dark et al., 1985). The exact molecular and cellular processes that underpin circannual rhythms are unknown. Two prevailing hypotheses have been proposed: the annual birth of new neurons (i.e.,

neurogenesis: Hazlerigg & Lincoln, 2011) and epigenetic modifications (Stevenson & Lincoln, 2017). A third conjecture is the involvement of *circannual clock genes* providing seasonal timing information in a manner similar to that of circadian clock genes. Several prospective hypothalamic regions have been proposed to act as the neural node for the central control of seasonal reproduction and include: the suprachiasmatic nucleus (SCN) (Ruby et al., 1998), the pars tuberalis (PT) (Lincoln et al., 2003), and the tanycyte cells that line the ependymal layer of the third ventricle (3V) (Meddle & Follett, 1997; Lewis & Ebling, 2017). The SCN is critical for the circadian regulation of daily rhythms of physiological, immunological, behavioural, and cognitive processes (Hastings et al., 2018). However, given that golden-mantled ground squirrels maintain circannual rhythms in body weight despite lesioned SCN, it is likely that an alternative brain region provides the neural representation of seasonal time. Moreover, the argument for the PT is not supported from a comparative reproductive perspective as fish do not possess a PT, suggesting the anatomical structure is not evolutionarily conserved. Given that female rainbow trout show robust and consistent circannual rhythmicity in gonadal function, an alternative cell substrate must provide long-term annual timing (Duston & Bromage, 1991). Overall, the present data support the proposition that the tanycytes in the ependymal layer of the 3V are an evolutionarily conserved cell population that are likely the anatomical substrate for the endogenous neuroendocrine timing of seasonal reproduction beyond mammals and birds.

1.4 Neuroendocrine circuits involved in seasonal reproduction in birds and mammals

1.4.1 Light detection in the avian brain

For seasonal reproduction to be possible, organisms need to be able to detect sunlight and its duration. Until the start of the 20th century, the eyes were the only organ thought to be involved in this. For mammals, this is still true. Mammals possess photoreceptors in the retina that are linked to downstream neuroendocrine pathways and

that allow them to initiate different aspects of the reproductive response, such as gonadal recrudescence during long days (LD) in summer-breeding species (Foster et al., 1989; Yamazaki et al., 1999). However, non-mammalian species, e.g. reptiles and birds, have been shown to retain a seasonal rhythm despite lacking the eyes, implying the existence of extra-retinal photoreceptors (ERPs) (fish: Von Frisch, 1911; birds: Benoit, 1935; Menaker and Keatts, 1968; lizards: Underwood and Menaker, 1976; reviewed in Pérez, Tolla et al., 2019).

The first evidence for ERPs emerged in 1911, when Von Frisch showed that light stimulation caused skin colour changes in enucleated and pinealectomized minnows (Von Frisch, 1911). In 1935, Benoit provided the first piece of evidence correlating seasonality with the brain. In his study, the hypothalami of blind ducks were illuminated artificially with both winter and summer durations (Benoit, 1935). It was found that the avian skull is permeable to light and, despite lacking the eyes, summer-like day lengths stimulated gonadal growth, while short, winter-like day lengths did not. In 1976, Menaker and colleagues continued Benoit's research and further established a role for ERPs as part of the seasonal framework that integrates light stimuli and translates them into a reproductive response (Menaker et al., 1976). In his studies, Menaker and colleagues injected india ink superficially inside the skull of house sparrows (*Passer domesticus*), blocking the passage of light, and observed reproductive inhibition even after light stimulation, highlighting the fact that birds possess light detection mechanisms within the brain that translate into signals able to target peripheral systems and stimulate sexual maturation (Menaker and Keatts, 1968). In 1979, Oliver et al illuminated different regions of the brain to determine the exact location of the avian DBPs, and found that only after illuminating the medio-basal hypothalamus (MBH) they were able to induce testes growth, as opposed to brain regions such as the POA (Oliver et al., 1979). After the MBH was implicated in this process as the most important site for photoreception in the brain, research efforts lead to

the identification of DBPs in virtually all non-mammalian vertebrates (Young, 1935; Archer, 1999). The evolutionary reason for ERP loss in mammals is still unknown.

ERPs consist of an opsin protein and a retinal chromophore, a type of vitamin A. The opsin protein is sensitive to light and it interacts with the chromophore component, either 11-cis-retinal or all-trans-retinal, through G protein-coupled receptors. The chromophore absorbs photons of light and alters its structure from 11-cis to all-trans, which begins a downstream signalling cascade. Opsins have been classified into five different groups, depending on various factors, such as species where they can be found, absorption spectra and location. The five groups are OPN1, OPN3, OPN4, OPN5 and retinal G protein-coupled receptor (RGR) opsin (Reviewed in Perez, Tolla et al., 2019). Each opsin has a different absorption spectrum by which it is activated, with maximal absorption occurring at the wavelength that triggers the highest production of energy. This difference in absorption spectra is likely due to the evolutionary pressure to respond to the appropriate wavelength of light, depending where a species may live. For instance, ERPs of fish living in deep water will have evolved sensitivity to green and blue wavelengths, as they are able to penetrate deeper in the water, while fish living in surface waters will have evolved different opsin absorption spectra.

In 1983, Vigh-Teichmann and colleagues isolated the first opsin from the pineal gland of the thornback ray (*Raja clavata*). In 1994, Okano and colleagues were able to isolate a form of pinopsin from the pineal gland of chicken. Since then, a combination of immunochemistry methods and molecular and sequencing techniques have been used to characterise novel ERPs and attribute downstream physiological functions to them. The presence of opsins has been linked to an array of different functions, such as movement, migration and reproduction, in virtually all non-mammalian vertebrates, including amphibians, reptiles and birds. A large number of opsins has been found in the brain, including discrete nuclei of the hypothalamus and the pineal gland. The opsins found in the brain are also called deep-brain photoreceptors (DBPs). Figure 1.2 summarises the

opsins that have been reported in the brain of non-mammalian vertebrates, separating them by species and class of opsin. However, despite a century of research and the emergence of novel molecular techniques, the identity of the specific avian DBPs responsible for triggering reproduction in seasonal species has not yet been established, and a functional link between candidate photoreceptors and reproduction has not yet been investigated.

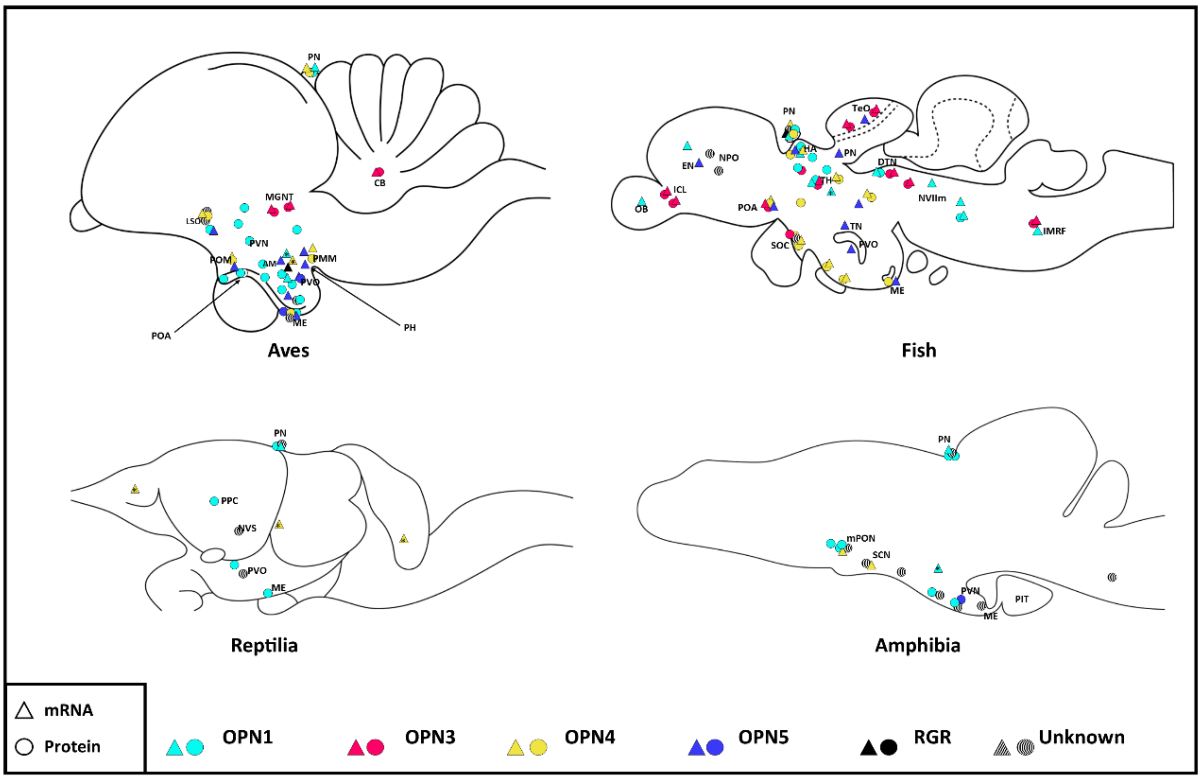

Figure 1.2. The neural distribution of opsins in non-mammalian vertebrates (amphibians, reptiles, birds and fish) displayed on generalized sagittal sections. Protein (circle) and mRNA (triangle) localizations are indicated independently. An * indicates that the tagged marker represents expression of that opsin was characterized in a broad brain region (e.g. hypothalamus, telencephalon, mesencephalon etc.) not at the specific location of the marker. Abbreviations: lateral septal organ (LSO); premammilary nucleus (PMM); (POM); preoptic area (POA); periventricular nucleus (PVN); median eminence (ME); (PVO); AM; suprachiasmatic nucleus (SCN); and pituitary (PIT). From Pérez, Tolla et al., 2019.

1.4.2 Vertebrate-Ancient Opsin and Neuropsin

During the search for the opsins responsible for seasonal reproduction in birds, various scientific communities started to identify a number of photoreceptors located in the MBH, specifically in the lateral septal region (LSO), premammillary nucleus (PMM), paraventricular organ (PVO) and paraventricular nucleus (PVN). In 1985, Foster and Follett determined that the maximal light absorption (λmax) for the greatest LH release in the Japanese quail, a common seasonal model, is 492 nm (Foster and Follett, 1985). Because of the significance of LH in the reproductive axis of the Japanese quail, this finding initiated the hunt in the scientific community for an opsin molecule of a sensitive at 492 nm. Foster and Follett's study also provided an additional method of determining whether opsins found in the brain could be classified as potential DBPs. In 1998, Soni and Foster successfully isolated a novel retinal opsin in the Atlantic salmon (*Salmo salar*.; Soni and Foster, 1998), and named it Vertebrate-Ancient Opsin (VA Opsin). It was found that VA Opsin has two functional isoforms, a longer one (cVAL) and a shorter one (cVAS). Later, VAS was identified in the hypothalamus of the chicken, and cVAS-expressing neurons found to be projecting to the median eminence (ME) (Halford et al., 2009). VA Opsin was proposed as a potential avian photoreceptor mediating the reproductive response. In addition, the maximal spectrum for VA Opsin in the hypothalamus of birds was determined to be 490 nm both *in vivo* and *in vitro*, matching the absorption spectrum for the initiation of reproduction in birds (Davies et al, 2011). Immunoreactive VA Opsin cells are localized to the preoptic area, and paraventricular nucleus and fibers were identified in the anterior hypothalamus and basal hypothalamus. Of particular interest was the observation that fibers terminated adjacent to the PT (Halford et al., 2009).

Based on the information gathered from prior studies, the candidate DBP must be expressed in the hypothalamus (Halford et al., 2009), activated by wavelength of ~ 492 nm (Foster and Follett, 1985), linked to circadian genes, and be associated with the activation of downstream reproductive pathways (as reviewed in García-Fernández et al., 2015).

However, it is still unclear whether VA Opsin in involved in the stimulation of the reproductive axis.

In the meantime, a different opsin molecule started to gather attention from the scientific community: neuropsin (OPN5). OPN5 was initially isolated from neural tissue of mouse in 2003 and assigned to a new family of opsins, as it shares only about 30% of amino acids with other known photoreceptor molecules (Tarttelin et al., 2003). It was later found to be localised to the cerebrospinal fluid-contacting neurons of the PVO in the MBH of the Japanese quail (Nakane and Yoshimura, 2010), fulfilling the location criteria for candidate DBPs. Immunoreactive fibers were shown to project from the PVO directly adjacent to the PT (Nakane et al., 2010). However, the maximal absorption for OPN5's two isoforms were found to be 360 nm and 474 nm (Yamashita et al., 2010), two lower values compared to the λmax required for the stimulation of reproduction determined by Foster (Foster and Follett, 1985). Recently, OPN5 has also been detected in the mouse POA and suggested to be involved in body temperature regulation (Zhang et al., 2020). Since OPN5's characterisation, numerous studies have investigated the possible role of neuropsin in the avian reproductive system. However, despite a century of research and the emergence of novel molecular techniques, the identity of DBPs has not yet been established, mainly because a functional link between VA Opsin, OPN5 and reproduction has not yet been investigated. In addition, how opsins in the brain are able to initiate downstream reproductive pathways in seasonal vertebrate species is still unknown. Figure 1.3 provides a schematic summary of the possible mechanisms adopted by DBPs to trigger the avian reproductive axis. In the present thesis, the two candidate photoreceptors that have been examined are VA Opsin and OPN5.

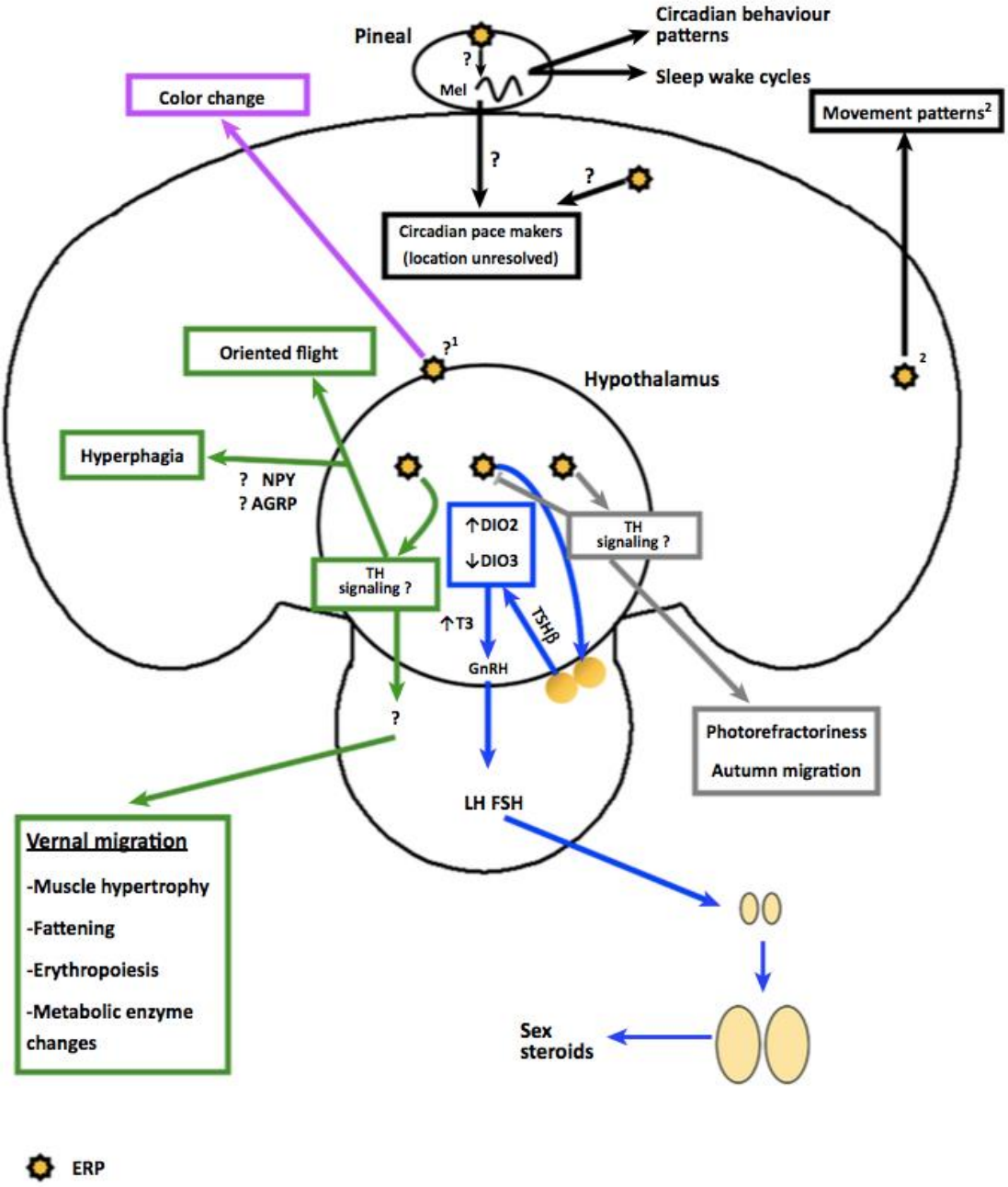

Figure 1.3. Schematic summary of both already established and hypothesised (symbolised by '?') pathways of extra-retinal photoreception. Although numerous physiological and behavioural processes are linked to perception of light cues and/or circadian rhythms, most of the neural control mechanisms remain poorly elucidated. 1, localization of minnow colour change receptors resolved to diencephalon. 2, location of ERPs associated appears to vary by species and taxa. AGRP, Agouti-related protein; DIO2, deiodinase 2; DIO3, deiodinase 3; FSH, follicle-stimulating hormone; GnRH, gonadotropin-releasing hormone; LH, luteinizing hormone; Mel, melatonin; NPY, neuropeptide Y; T3, triiodothyronine; TH, thyroid hormone; TSH-b, thyroid-stimulating hormone-b. From Pérez, Tolla et al., 2019.

In birds, one of the earliest confirmed molecular change in response to long-day exposure is an increase in thyrotrophin-stimulating hormone-β (*TSHβ*) in the PT (Nakao et al., 2008). Therefore, the photoreceptor that links photoperiodism with the seasonal reproductive response must also link with *TSHβ* expression. In 2012, Stevenson and Ball (2012) used siRNA that targeted OPN5 in the Border canary (*Serinus canaria*) and observed a significant increase in hypothalamic *TSHβ* expression. A similar negative correlation between OPN5 and *TSHβ* expression has been reported in the migratory redheaded bunting (Emberiza bruniceps) (Majumdar et al., 2014). This inhibitory output could potentially be discontinued during the breeding period, allowing for an increase in gonadal size and initiation of reproduction. Conversely, in Japanese quail (Coturnix japonica), the inhibition of OPN5 was observed to inhibit *TSHβ* expression (Nakane et al., 2014). Overall, the neuroendocrine circuit that underlies the seasonal regulation of reproduction in birds requires light detection by hypothalamic ERPs that are connected to the PT thyrotrophs. The mechanism(s) by which ERPs are linked to the PT are currently unknown. The long-day increase in *TSHβ* secretion signals the tanycytes to induce T_3-dependent morphological changes that permit the release of GnRH from the median eminence (Figure 1.4). Supplementary environmental cues are then integrated across a diverse range of hypothalamic and extra-hypothalamic nuclei that converge on reproductive neuropeptides, GnRH and GnIH (Meddle et al., 2006; Stevenson et al., 2012A; Kriegsfeld et al., 2015).

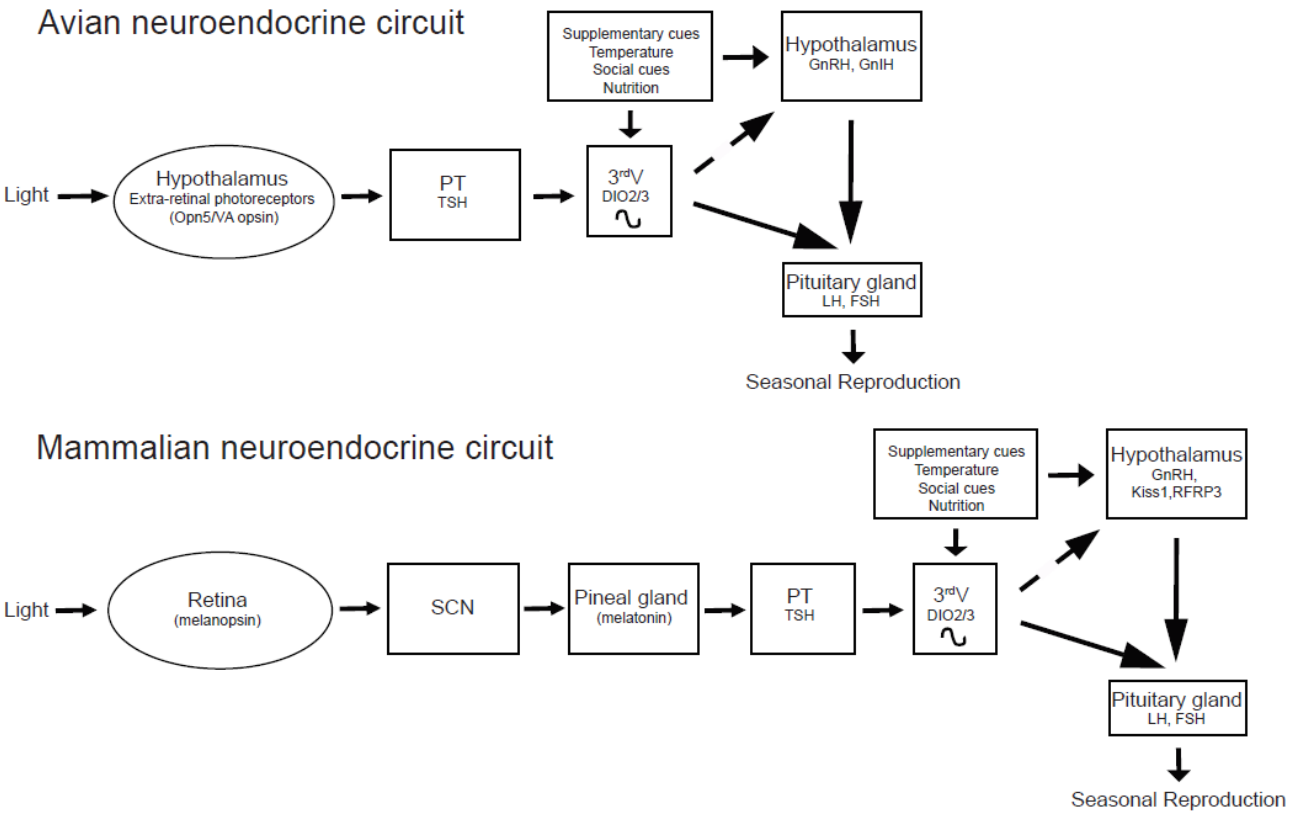

Figure 1.4. Neuroendocrine pathways for the photoperiodic regulation of seasonal reproduction in mammals and birds. In avian species, light is detected by extra-retinal photoreceptors (ERPs) located in the hypothalamus. The identity of the photopigments responsible for deep brain photoreception is currently unknown, however two major candidate genes are neuropsin (*OPN5*) and vertebrate-ancient opsin (*VA Opsin*). ERPs are connected to the pars tuberalis (PT) which stimulates thyrotropin-stimulated hormone-β (TSH) expression in response to long days. Photoperiodic regulation of TSH triggers tanycytes along the ependymal layer of the third ventricle (3^{rd}V) to increase the expression of deiodinase Type-2 (*DIO2*) and decrease Type-3 (*DIO3*). The localized synthesis of thyroid hormone, triiodothyronine (T_3) then induces a morphological change in the tanycytes that permits the pituitary gland to release gonadotrophs: luteinizing hormone (LH) and follicle-stimulating hormone (FSH). Annual changes in day length also regulate neuropeptide expression, gonadotropin-releasing hormone (*GNRH*) and gonadotropin-inhibitory hormone (*GNIH*). In mammals, annual changes in photoperiod are initially detected by the retina photoreceptors (*e.g.* melanopsin) and light information is then transmitted to the circadian pacemaker nucleus, the suprachiasmatic nucleus of the hypothalamus (SCN). The SCN provides an internal code for daily secretion of melatonin by the pineal gland. The annual variation in nocturnal melatonin secretion regulates the levels of TSH produced by the PT. Similar to birds, long-day mammalian breeders have high TSH levels that trigger the tanycytes to stimulate *Dio2* expression leading to the release of LH and FSH from the pituitary gland. Other supplementary environmental cues also converge on tanycytes and neuropeptides in the hypothalamus to fine-tune the timing of seasonal reproduction. The sinewave symbol represents the putative location for the endogenous circannual pacemaker. Solid arrows indicate well described direct connections, the dash arrow between the tanycytes and hypothalamic neuropeptides represents current undescribed connection. From Tolla et al., 2019.

1.4.3 The role of melatonin in mammals

Although extra-retinal photoreceptors such as encephalopsin have been identified in the mammalian diencephalon and pineal gland (Blackshaw et al., 1999), it is likely that extra-retinal photoreceptors in the mammalian brain are not involved in photoperiodism as the evidence to support the capability of light to pass the skull and regulate these opsins is lacking. Instead, photoreceptors in the retina are linked to downstream neuroendocrine pathways via the daily nocturnal pineal secretion of melatonin (Stevenson et al., 2017). Melanopsin expression in the photosensitive retinal ganglion cells is critical for the daily entrainment of circadian rhythms and is likely required for annual photoperiodism (Hankins, Peirson, & Foster, 2008). In mammals, light integration by the SCN is critical for circadian regulation and the photoperiodic control of melatonin secretion by the pineal gland. Nocturnal melatonin provides an internal physiological code for the annual change in night length (Goldman & Nelson, 1993). Long days result in a small nocturnal duration of melatonin, whereas short winterlike days result in a greater nocturnal duration of melatonin (Reiter, 1991; Bartness et al., 1993; Wehr, 1991). The duration of melatonin is sufficient for mammals to initiate different aspects of the reproductive response, such as gonadal recrudescence during long days in summer-breeding species such as hamsters (Foster et al., 1989; Yamazaki et al., 1999) and a long duration melatonin signal is stimulatory for short-day breeding species such as sheep (*Ovis aries*; e.g., Lincoln et al., 2003; Weems et al., 2015; Karsch et al., 1984; Bittman & Karsch, 1984). A simple injection of melatonin in long days in the early afternoon is sufficient to extend the duration of exposure and subsequently induce reproductive involution in hamsters (Bartness et al., 1993). Thus, melatonin provides the internal representation of annual day length and acts in multiple brain regions, including the PT, to drive seasonal variation in reproduction. It is well established that melatonin binds to the melatonin receptor 1b (MT2) to inhibit hamster reproductive physiology (Prendergast, 2010).

Although the precise mechanisms are not well established, annual changes in melatonin have powerful effects on the expression of multiple neuropeptides (described in section 4.1), neurotransmitters and receptor function in discrete neuroendocrine cell populations. In mammals, melatonin receptors have been shown to be expressed in the PT (Williams & Morgan, 1988), where thyrotrophs are predominantly located. Melatonin binding in the thyrotrophs reduces TSHβ levels (Hanon et al., 2008). TSHβ triggers an upregulation of the enzyme deiodinase 2 (DIO2), which is responsible for converting thyroxine (T_4) into triiodothyronine (T_3) during the reproductive period (Klosen et al., 2013). Work by Hanon et al. (2008) indicated the TSHβ-signalling system to be evolutionary conserved in seasonally breeding vertebrates (Hanon et al., 2008). In addition, TSHβ injections were sufficient to drive the long-day reproductive response in male Siberian and Syrian hamsters, through an increase in kisspeptin and RFRP expression (Klosen et al., 2013), implicating these neuropeptides in the seasonal control of reproduction. The mechanism for DIO3 action, responsible for inactivating T_3 during the non-reproductive period, is currently unknown. However, its expression is likely to be affected by melatonin. In birds, nocturnal melatonin does not appear to be involved in the hypothalamic timing of seasonal reproduction (Juss et al.,1993) and instead, functions to synchronize peripheral tissues, particularly the gonads (McGuire et al., 2011).

1.5 Neuroendocrine substrates that regulate reproduction in birds and mammals

1.5.1 The role of neuropeptides: GnRH, Kisspeptin and GnIH/RFRP3

The master neuroendocrine peptide in the regulation of reproduction is gonadotropin-releasing hormone (GnRH) (Herbison, 2016). GnRH is released from the median eminence in response to photostimulation and targets the gonadotrophs in the anterior pituitary, which, in turn, release the gonadotropins—luteinising hormone (LH) and follicle-stimulating hormone (FSH)—linking the brain to peripheral endocrine systems. LH

and FSH both play key roles in the development of characteristics essential for reproductive success. GnRH-secreting cells are expressed in the anterior hypothalamus, POA in all sexually reproducing species (Stevenson et al., 2012a). In birds, the number of cells that express GnRH exhibit robust variation; in some species such as the European starling (*Sturnus vulgaris*), there is a 10-fold change in the number of detectable cells (Stevenson et al., 2009; Dawson and Goldsmith, 1997) between seasons. However, in other species, such as Galliformes (e.g., chickens) the level of annual mRNA changes in GnRH is significantly less (Dunn & Sharp, 1999).

The primary driver of annual plasticity in GnRH expression in birds is the change in photoperiod, as increased day length in the summer triggers a rapid increase in expression leading to a reproductive state (Dawson et al., 2001). However, long days also initiate a cascade of events that terminate the reproductive period (Stevenson et al., 2012b; Dawson and Goldsmith, 1997). How light directly regulates GnRH expression is not entirely clear and may be driven by the localization of photoreceptors in GnRH cells such as VA Opsin (Halford et al., 2009) in avian species, or by the coordinated activity of other neuropeptides such as Gonadotropin-inhibitory hormone (GnIH) also referred to as RFamide-related peptide-3 (RFRP3) in mammals.

GnIH neurons are predominantly localized to the paraventricular nucleus (PVN) and have widely distributed projections into diencephalic and mesencephalic regions in birds (Kriegsfeld et al., 2015; Ubuka, Bentley, & Tsutsui, 2013a). GnIH receptors are expressed in the median eminence in quail and gonadotropes in the pituitary gland in quail and chickens (Tsutsui et al., 2000; Ubuka et al., 2013b). Unlike GnRH, the photoperiodic regulation of GnIH expression is minimal. For example, house sparrows (*Passer domesticus*) show only a small increase in immunoreactive GnIH cells during the non-breeding season (Bentley et al., 2003). The mammalian ortholog, RFRP3, is expressed in the dorsomedial nucleus of the hypothalamus (DMH), projects to the median eminence and inhibits gonadotropin release in hamsters (Kriegsfeld et al., 2006). However, the direct link

between RFRP3 signaling and gonadotropin function has not been clearly delineated. Exposure to short days was found to significantly reduce RFRP3 expression in hamsters (Prendergast et al., 2013; Mason et al., 2010), and appears to be downregulated by melatonin (Revel et al., 2008). In sheep, RFRP3 does not directly regulate LH secretion and may instead have indirect effects on reproduction via food intake or stress (Decourt et al., 2016).

In mammals, kisspeptin is generally located in two distinct hypothalamic brain regions, the arcuate nucleus (Arc), and the anteroventral periventricular nucleus (AvPv) in rodents (Yeo & Colledge, 2018). In Siberian hamsters, exposure to reproductively inhibitory short days resulted in a significant increase in Arc kisspeptin cell numbers and a reduction in AvPv cell numbers (Greives et al., 2007). Castration significantly reduced AvPv kisspeptin cells indicating a role for gonadal-dependent regulation of expression (Greives et al., 2008). Conversely, in Syrian hamsters, SD was observed to significantly reduce Arc kisspeptin cell numbers. Syrian hamsters that were pinealectomized and moved to short days showed elevated kisspeptin expression (Revel et al., 2006), suggesting a primary regulatory role for melatonin. This is consistent with the knowledge that short days stimulate weight gain in this species, while causing weight loss in Siberian hamsters (Bartness & Wade, 1984), although they are long-day breeders as well. To date, kisspeptin has not been identified in an avian genome, nor the cognate receptor, G-protein coupled receptor 54 (KISS1R) (Kim et al., 2012; Tena-Sempere et al., 2012). The complete absence of these two genes provides strong evidence that kisspeptin-KISS1R signalling is not an evolutionarily conserved mechanism for the control of reproduction. The evidence provided suggests that the neuroendocrine network responsible for seasonal species is complex and differs not only between birds and mammals but also within mammalian species.

1.5.2 The role of thyroid hormones in the hypothalamus

Thyroid hormones, specifically the bioactive form, triiodothyronine (T_3), are thought to play a central role in the seasonal photoperiodic reproductive response (Wu & Koenig, 2000). Thyroid hormones have been tied to the induction of the hypothalamic-pituitary-gonadal (HPG) axis hormonal cascade responsible for development of the physiological characteristics associated with breeding in multiple species (Follett & Nicholls, 1985; Follett & Nicholls, 1988; Nicholls et al., 1988; Wilson & Reinert, 1995; Reinert & Wilson, 1996; Wilson & Reinert, 1999; Dawson et al., 2001, Pérez et al., 2018). Thyroid hormone delivered directly to the hypothalamus rescues gonadal growth in thyroidectomized animals (Wilson & Reinert, 2000) and induce HPG activation in Japanese quail held under short day lengths (Watanabe et al., 2007). Localized thyroid signaling within the brain is mediated by the diodinase enzyme system. T_3 is generated from the corresponding prohormone thyroxine (T_4) by the enzyme deiodinase 2 (DIO2) in most tissues (Yoshimura et al., 2003). Deiodinase 1 (DIO1) can also catalyze this reaction; however, it is mainly found in peripheral tissues (Bianco et al., 2002). Conversely, DIO3 is the enzyme responsible for inactivating T_3 (Bianco & Kim, 2006; Schweizer et al., 2014). Increasing day-length results in the release of TSHβ from thyrotroph cells of the PT, which act in a paracrine manner to trigger a shift in deiodinase expression within tanycytes lining the 3rdV of the hypothalamus (Yoshimura et al., 2003; Yasuo et al., 2005). The resulting increase in DIO2 and decrease in DIO3 expression results in increased net conversion of T_4 to T_3 (Watanabe et al., 2007; Nakao et al., 2008; Nakane & Yoshimura, 2010; Mishra et al., 2017). This local increase in T_3 has a downstream effect on tanycytes to permit the release of GnRH from the median eminence in long-day breeding species (Figure 1.4) (Whitlock, 2005; Yamamura et al., 2004; Lehman et al., 1997), and the inhibition of reproduction in short-day breeders such as sheep (Webster et al., 1991).

1.5.3 Sex differences in the neuroendocrine regulation of reproduction function

The early action of steroid hormones on the developing brain primes the organism for puberty, and the neuroendocrine control of reproduction by the GnRH pathway is essential across all sexually reproducing species (Stevenson et a., 2012). In female murine models, there is a significantly higher (10X) number of kisspeptin cells in AvPv compared to males (Clarkson and Herbison, 2006). Interestingly, kisspeptin action can overcome the negative effects of food restriction on reproductive aspects in rats (Castellano et al., 2005) suggesting a short-term responsiveness to food cues. In mammals, the population of GnRH cells appears relatively constant in seasonal breeders, but kisspeptin cells in both the AvPv and Arc exhibit large scale plasticity (Simonneaux, 2020; Clarke and Caraty, 2013). Food restriction in male Siberian hamsters can significantly suppress kisspeptin expression in the arcuate nucleus (Paul et al., 2009) suggesting that nutritional cues can fine tune the timing of reproduction upstream of GnRH. Thus, kisspeptin-secreting cell populations can be considered optimal targets for the regulation of the mammalian reproductive neuroendocrine axis by supplementary cues in a sex-specific manner.

Neither kisspeptin, nor the receptor GPR54 have been identified in an avian genome. The available evidence suggests that GnRH cells in the POA are directly responsible for the integration of supplementary seasonal cues. The presence of a potential mate was found to significantly increase GnRH expression and/or release in European starlings (Stevenson and Ball, 2009) and house sparrows (Stevenson et al., 2008). Other supplementary cues have been shown to modulate GnRH content such as temperature and food cues. GnRH mRNA levels in redheaded buntings (*Emberiza bruniceps*) were significantly increased in response to elevated temperature (Trivedi et al., 2019). Food restriction in male house finches significantly increased the number of GnRH cells compared to *ad libitum* fed birds (Valle et al., 2015), reflecting a reduced GnRH secretion and increased GnRH storage indicated by high levels of cGnRH-ir perikarya (Foster et al., 1988; Valle et al., 2015). However, food resources do not appear to impact the amount of GnRH in Albert's

Towhees POA (Davies et al., 2015). Furthermore, the opportunistically seasonally breeding songbird, White-winged crossbills (*Loxia leucoptera*) maintain constant levels of GnRH content despite variation in food resources (MacDougall-Shackleton et al., 2001). Highly plastic GnRH responses may be an evolutionarily conserved trait, as supplementary cues also significantly impact expression levels in amphibians (Burmeister and Wilcsynki, 2005) and fish (White et al., 2002).

Seasonal variation in body mass is another well characterized physiological response (Ebling, 2015). In female mammals, growth hormone (GH) has a continuous-release pattern, while in males it is released in a pulsatile manner (Waxman et al., 1995; Udy et al., 1997; Waxman, 2000). These different forms of GH release have important downstream effects, some of which are critical for the expression of sex differences in physiological traits. For instance, GH stimulates tyrosine phosphorylation of Signal Transducer and Activator of Transcription 5 (STAT5b) in the male liver, but not in females (Waxman et al., 1995). STAT5b gene repression through knockdown studies in mice has confirmed the hypothesis that this gene is responsible for the regulation of certain sex-specific traits: STAT5b K/D in males causes a slower growth rate compared to intact males, and an altered liver transcription profile, both effects comparable to characteristics of the female phenotype (Waxman et al., 1995; Udy et al., 1997; Waxman, 2000). This suggests that STAT5b is differentially regulated in males compared to females, and that it plays a key role in the development of sex differences in liver function. STAT5 is also one factor shown to be able to control ER alpha in the hypothalamus (Champagne et al 2006). The sex-dependent effects of GH and STAT5 may account for some variation in the organized brain and liver signalling pathways and therefore contribute to how supplementary cues fine tune the timing of reproduction.

1.6 Tanycytes function as an evolutionary conserved neuroendocrine regulator

Tanycytes along the 3rdV in the hypothalamus have been proposed to be the predominant neuroendocrine cell population for the regulation of long-term physiological processes, such as seasonal breeding (Figure 1.5) (e.g., Meddle & Follett, 1997; Lewis & Ebling, 2017). Since tanycytes are derived from an evolutionarily ancient neuroepithelium in vertebrates, these cells are well positioned to be the conserved brain region for endogenous seasonal rhythmicity (Szele & Szuchet, 2003). Furthermore, these cells have been shown to exhibit a photoperiodic change in epigenetic modifications (Stevenson & Prendergast, 2013) as well as contain a stem cell niche (Lee et al., 2012) that could serve as a source of cyclical histogenesis (Hazelrigg and Lincoln, 2011). In addition, tanycytes integrate a range of environmental cues such as photoperiodic information from the PT (Wood & Loudon, 2018), peripheral endocrine changes in energetic state (Bolborea & Dale, 2013) and respond to gonadal steroids (i.e., estrogen) (de Seranno et al., 2010). Tanycytes also send long projections into adjacent nuclei, such as the Arc, POA, and DMH and have direct contacts with multiple neuroendocrine systems, such as reproductive, orexogenic, and anorexigenic neuropeptides (Figure 1.5) (Lechan & Fekete, 2007). The evolutionarily conserved nature of the tanycyte cells, the endogenous regulation of timing mechanisms, and the interaction with well-characterized reproductive neuroendocrine systems, all support the conjecture that tanycytes are critical for the regulation of seasonal reproduction.

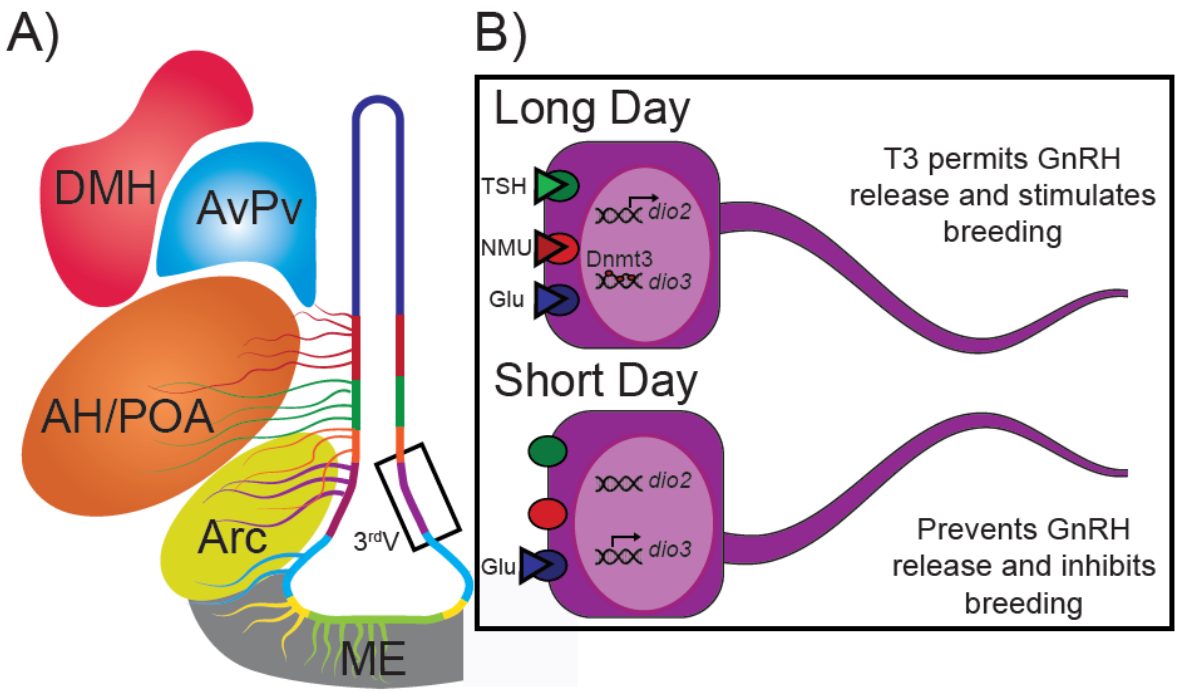

Figure 1.5. Tanycytes are an evolutionarily conserved cell population for neuroendocrine function. All vertebrates have tanycyte cells that line the third ventricle (3rdV) and project into the adjacent parenchyma (e.g., Arcuate nucleus [Arc] and median eminence [ME]). (A) representative schematic of a coronal section through the hypothalamus to highlight the distribution of tanycytes along the 3rdV. The black box is represented at a higher resolution in (B). Tanycytes indicated in purple integrate photoperiodic information derived from the PT via thyrotropin-stimulating hormone (TSH) binding to the cognate receptor in long-day photoperiods. TSH triggers the synthesis of triiodothyronine (T3), which induces a morphological change in tanycytes that permits neuropeptide release from the median eminence (e.g., GnRH). Tanycytes also respond to peripheral signals of energy balance such as neuromedin U (NMU) and Glucose (Glu). NMU is photoperiodically regulated in rodents and provides an internal cue of energy state by binding receptors located on tanycytes. Acute, short-term signalling of energy balance is also provided by Glu binding to the GLUT2 receptor on tanycytes. TSH and NMU are downregulated in short-day conditions. These findings indicate that tanycytes integrate environmental and endogenous cues and are therefore a key cell population for the neuroendocrine timing of seasonal reproduction. From Tolla et al., 2019.

1.7 Epigenetics

One mechanism by which environmental conditions can modulate patterns of gene expression (Bird & Wolffe, 1999) is through epigenetics. Epigenetics studies the ways in which the environment is able to cause changes to an organism that do not involve alterations to the underlying genetic sequence. Instead, environmental conditions are able to shape the patterns by which genes are expressed (Bird and Wolffe, 1999). This can be seen as an adaptive response to ensure optimal fitness and survival of an individual, especially for species living in extreme environmental settings.

Well-documented epigenetic mechanisms include DNA methylation and histone methylation and acetylation (Bird and Wolffe, 1999; Zhang, 2001; Snowden et al., 2002; Fuks et al., 2005; Ding et al., 2007). DNA methylation is by far the most studied epigenetic modification, as it has been characterised in a range of species, from unicellular organisms (Harony and Ankri, 2008) to plants (Zhang et al., 2006), to complex mammals. The main enzymes that carry out this process, the DNA methyltransferases (DNMTs), add a methyl group to mostly cytosine nucleotides in promoter regions (Boyes and Bird, 1991; Bird and Wolffe, 1999; Santoro and Grummt, 2005), although methylation at other nucleotides may occur. Since methylated DNA is more tightly packaged compared to non-methylated DNA, therefore less exposed to transcription components, DNA methylation is most commonly associated with gene inactivation (Bird and Wolffe, 1999). In contrast, the removal of methyl groups allows for accessible DNA and implicates gene expression. Different types of DNMTs have been associated with maintaining DNA methylation patterns through cell division (Dnmt1) (Bestor et al., 1988), as well as establishing new ones (Dnmt3a and Dnmt3b) (Okano et al., 1998; Okano et al., 1999; Jones, 2012).

Histone modifications are also considered part of the epigenetic landscape of an organism. DNA is packaged in histones, proteins that organise the genetic code into units called nucleosomes. Five histone variants have been characterised so far: H1, H2A, H2B, H3 and H4 (Lachner and Jenuwein, 2002). Histone methylation involves the addition of a

methyl group to lysine and arginine residues of histones, or ‘tails’, and is associated with both activation and repression of transcription, depending on the site of methylation and the form of histone (Hoffmann et al., 2012). On the other hand, histone acetylation is the addition of an acetyl group to histone tails, and is associated with gene activation (Struhl, 1998).

DNA methylation and histone acetylation patterns are two of the main mechanisms forming the “epigenome” of an organism. Their expression in human tissues is summarised in Figure 1.6. These conserved epigenetic processes provide a framework for studies in fields that analyse the ways the environment influences an organism. One of the first studies conducted to determine their existence in humans was carried out by Holliday and Pugh (1975). At that time, it was known that bacteria possess methylation mechanisms for the modification of DNA at adenine loci, and that methyl groups are an important part of human genes. It was then hypothesised that methylation of genetic information in humans plays a similar role to DNA methylation in bacteria (Holliday and Pugh, 1975). It was also suggested that DNA methylation patterns are not random but associated with the activation or deactivation of a particular gene. This switch was observed to be a possible “molecular clock” for development, or a chemical mechanism that regulates the growth and reproductive cycle of the organism. It was also compared to stem cell differentiation in order to explain how the turning “on” and “off” of genes determines cell type, and therefore function of a cell. Shortly after this experiment, Riggs (1975) also explored the idea that DNA methylation has a deep effect on the interaction between certain enzymes and DNA, as a regulatory process. He emphasised the fact that there needs to be a mechanism that is able to maintain methylation patters (Riggs, 1975) throughout cell growth and division. This growing interest in epigenetics lead to another study in 1999 that produced compelling evidence for the idea that the role of DNA methylation in mammals is to deactivate the expression of genes (Jones and Laird, 1999). The experiment followed this mechanism in certain genes that inhibit the rise of tumours, also known as tumour-

suppressor genes, *e.g.* p53. When in a methylated state, their expression was “turned off”. This caused a rapid increase in cancerous cells, facilitating cancer growth.

In 1988, DNA methyltransferase 1 (DNMT1), was shown to be an important maintenance methylation enzyme in mammals (Bestor et al., 1988; Sharif et al., 2007). DNMT3a and DNMT3b are essential in cell function as they set up *de novo* methylation patterns: designing structural cell function and regulation when an individual is first born (Okano et al., 1998; Okano et al., 1999). DNA methylation has been shown to be essential for survival in certain mammals, such as mice (Li, Bestor and Jaenisch, 1992; Okano et al., 1999). The absence of DNMTs in DNMT Knockout (KO) mice results in embryonic lethality (Li, Bestor and Jaenisch, 1992). These major findings opened the scientific community to novel possibilities regarding epigenome analysis and the mechanisms that allow the environment to cause morphological, behavioural and physiological changes to individuals. All of these studies provided the basic knowledge needed to investigate epigenetic changes and relate them to variations in the surrounding environmental conditions. Recent research has been focusing on analysing DNA methyltransferase activity in an array of different genes and tissues in order to assess its function in depth and understand just how much daily cell function depends on it.

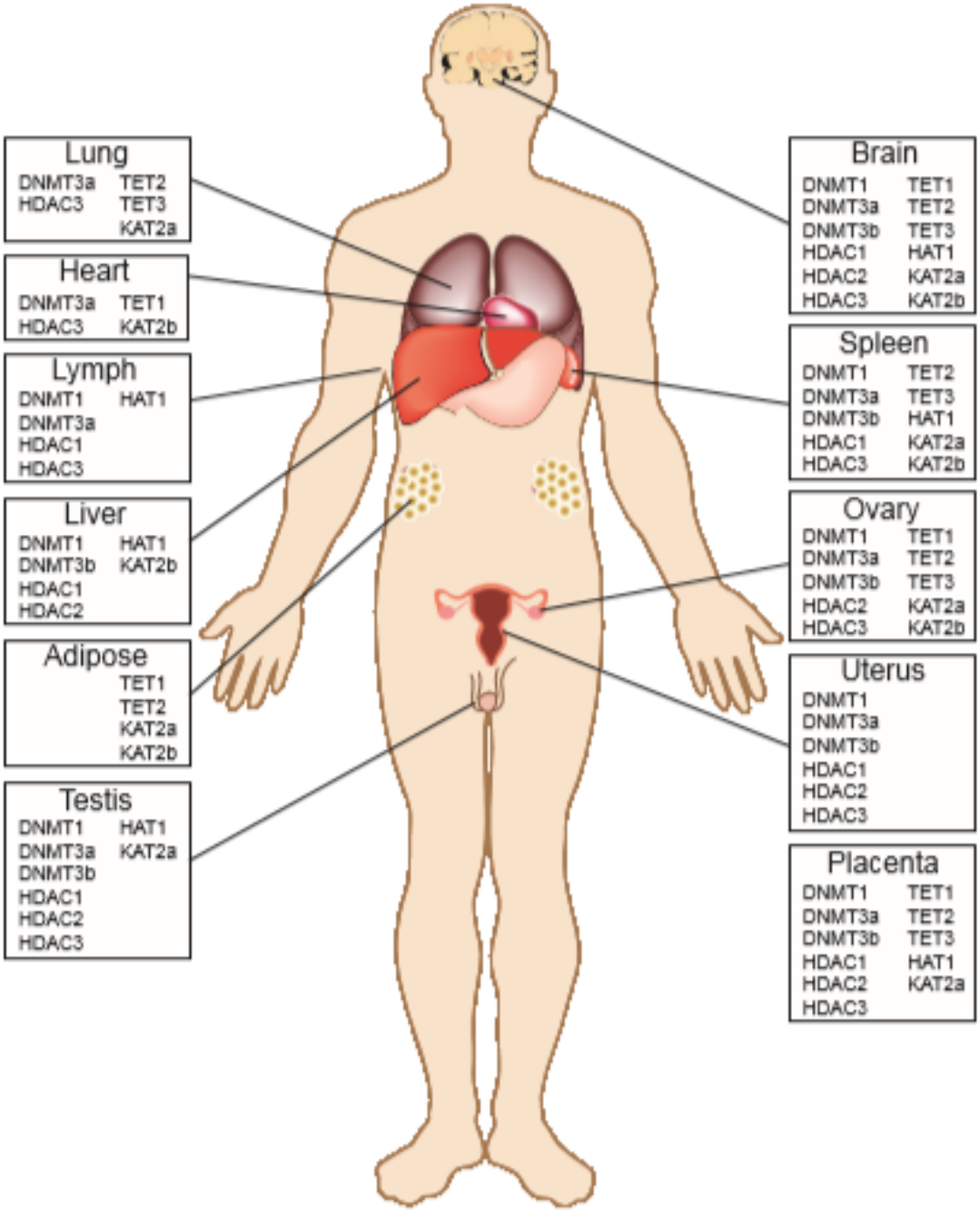

Figure 1.6. Distribution and relative abundance of epigenetic enzymes. A representative diagram to highlight the tissue specific and expression levels of epigenetic enzymes in multiple tissues. Epigenetic enzymes presented in tissue boxes were selected based on higher than average RPKM expression levels across all tissues. Most enzymes involved in DNA methylation and histone modifications are expressed in neuroendocrine substrates (i.e. brain) as well as reproductive tissues (i.e. testes, ovary and uterus). RPKM data were obtained from PUBMED and are based on Fagerberg et al., (2014). From Coyle, Tolla and Stevenson, 2018 (see Appendix B).

1.7.1 Rhythmic epigenetics involved in the seasonal regulation of reproduction

In recent years, epigenetics has grown into a field with applications in countless research areas, one of them being seasonal biology. Recently, DNA methylation has been associated with both daily and annual changes in light in seasonally breeding species. In the wasp (*Nasonia vitripennis*), *y*early changes in DNA methylation have been linked to the stimulation of seasonal diapause (Pegoraro et al., 2015). A seasonal increase in DNA methylation has also been observed in the testes and uteri of Siberian hamsters (*Phodopus sungorus*. Lynch et al., 2016) and in squirrel (*Ictidomys tridecemlineatus*) livers (Alvarado et al., 2015) during non-reproductive winter periods. In addition, exposure to short days in Siberian hamsters resulted in a significant decrease in DNA methylation in the proximal promoter regions for DIO3; suggesting a direct link between epigenetic regulation and enzymes involved in the local thyroid hormone catabolism (Stevenson & Prendergast, 2013). Recently, high-throughput analyses have revealed widespread tissue- and nuclei-specific genomic variation in DNA methyltransferase and histone deacetylase enzymes expression (Yoshimura et al., 2003; Mukai et al., 2009; Stevenson et al., 2012c; Cubuk et al., 2017; Lomet et al., 2018).

The precise downstream genomic targets and functional outcome of rhythmic oscillations in epigenetic modifications remain uncharacterized. Taken together, these studies indicate that epigenetic enzymes show predictable rhythmic patterns that regulate genomic regions critical for the neuroendocrine timing of seasonal reproduction. Thus, it is possible that these rhythmic epigenetic modifications are an adaptive response, especially for species living in extreme environmental settings (Stevenson, 2018), to ensure that reproductive physiological changes occur at the most appropriate time of the year, when factors such as temperature and food availability are able to favour optimal fitness and survival of an individual. It is likely that epigenetic modifications beyond DNA methylation show cell-tissue- and nuclei-specific patterns that are ultimately critical for species variation in the neuroendocrine regulation of seasonal reproduction.

1.7.2 Epigenetic modifications as causes of sex differences in response to supplementary cues

In mammals, during the early stages of embryonic development, DNA methylation and histone modifications silence the expression of genes located on one of the X chromosomes (Avner and Heard, 2001), as a dosage compensation mechanism between the X and Y chromosomes. However, the genes that remain activated are determinants in certain somatic and neuronal sex differences (Chen et al., 2008) that could explain sex-specific disease vulnerability (Chen et al., 2008). X chromosome silencing can be considered as one of the first actions of epigenetic processes on an organism (McCarthy et al., 2009). As described above, brain masculinization is an active process that requires the action of estrogen during a critical window of time during embryonic development (Naftolin and Ryan, 1975). Recent evidence suggests that brain feminization may also involve active processes (Nugent et al., 2015) and that epigenetic modifications including DNA methylation organize neuroendocrine masculinization.

A male-like brain develops due to the result of aromatization of testosterone to estrogens (Naftolin and Ryan, 1975). In murine models, 17β-estradiol (E2) has a key role in brain sexual differentiation (MacLusky and Naftolin, 1981; McCarthy, 2008). Alpha-fetoprotein in females binds to E2 and prevents E2 from crossing the blood-brain barrier and inducing brain masculinization (Bakker et al., 2006). The POA is a primary target and underlying substrate of sexual differences in the control of male sexual behavior and regulation of GnRH release. Nugent and colleagues examined levels of DNA methyltransferase enzymes activity in order to establish a link between DNA methylation in the brain and its masculinization. It was found that gonadal steroids repress the activity of DNMTs, decreasing DNA methylation at the promoters of masculinizing genes, leading to their transcription, and therefore the development of a male-like brain (Nugent et al., 2015). Both chemical inhibition and molecular knockdown of DNMTs, particularly

DNMT3A, in female rats causes a shift towards male-like markers and behaviour (Nugent et al., 2015).

In the avian system, males are homogametic (ZZ) and females are heterogametic (ZW). It is unclear whether birds possess a dosage compensation mechanism that is similar to X chromosome inactivation in mammals. RNA-seq and microarray data show higher Z-linked gene expression in male chicken embryos than in female embryos in both the gonads and soma, suggesting the lack of a dosage compensation process (Julien et al., 2012; Ellegren et al., 2007). However, it is possible that a balance is reached through other means. For instance, male hypermethylated region (MHM) is hypermethylated on both male Z chromosomes, but in a hypomethylated state in the female Z chromosome (Teranishi et al., 2001), indicating that perhaps avian dosage compensation exists via sex differences in transcription of specific regions. In addition, Smith and colleagues reported that this difference in dosage is precisely the cause of sex determination, as opposed to a result of it (Smith et al., 2009). They found that silencing Z-linked gene doublesex and mab-3-related transcription factor 1 (DMRT1) in male chicken embryos lead to gonad feminization, suggesting that avian sex determination is dependent upon the dosage of Z-linked genes present (Smith et al., 2009). Further research is required in order to fully understand sexual differentiation and dosage compensation in birds.

The extent to which seasonal variation in epigenetic modifications is regulated by supplementary cues is poorly understood. Given the consistent observation of food availability, social signals, and temperature cues to impact the timing of seasonal rhythms, it is likely that supplementary cues will drive sex-dependent effects on tissue-specific epigenomes.

1.8 The Japanese quail and the Siberian hamster as seasonal models

In time, an array of species has been used for research on the effects of seasonality on reproductive endocrinology and physiology. Some of these species include sheep, hamsters, mice, and quails. The method by which a particular species is selected for a specific project is by taking into consideration the timings of the study, availability of funds, and the type of behavioural or molecular analyses necessary.

The Japanese quail (*Coturnix japonica*) and the Siberian hamster (*Phodopus sungorus*) are both well-characterised animal models, especially studied in the context of seasonal reproduction. They are both summer breeders and long daylengths initiate physiological, morphological and behavioural changes that lead to breeding (Shimakura, 1940; Kato and Konishi, 1968; Bartness and Wade, 1985; Finley et al., 1995), thus allowing scientists to manipulate the external environment and accurately study its effects on physiology and reproduction (Robinson and Follett, 1982; Finley et al., 1995; Ball and Balthazart, 2010). The Siberian hamster exhibits marked changes in fur colour (white in the winter and dark in the winter), gonadal size, energy balance (Bao et al., 2019) and immune function (Banks et al., 2016) (Figure 1.7). Japanese quail also present significant differences between the seasons, where a LD condition stimulates an increase in gonadal size, cloacal gland area, and abdominal fat (Robinson and Follett, 1982) (Figure 1.8). In addition, this species is optimal for research on reproductive physiology and behaviour, as it reaches sexual maturity seven to eight weeks post-hatching (Huss et al., 2008), allowing for the possibility of more studies in a relatively short period of time. The Japanese quail and the Siberian hamster provide then two excellent animals models for the study of seasonal reproduction in a laboratory setting.

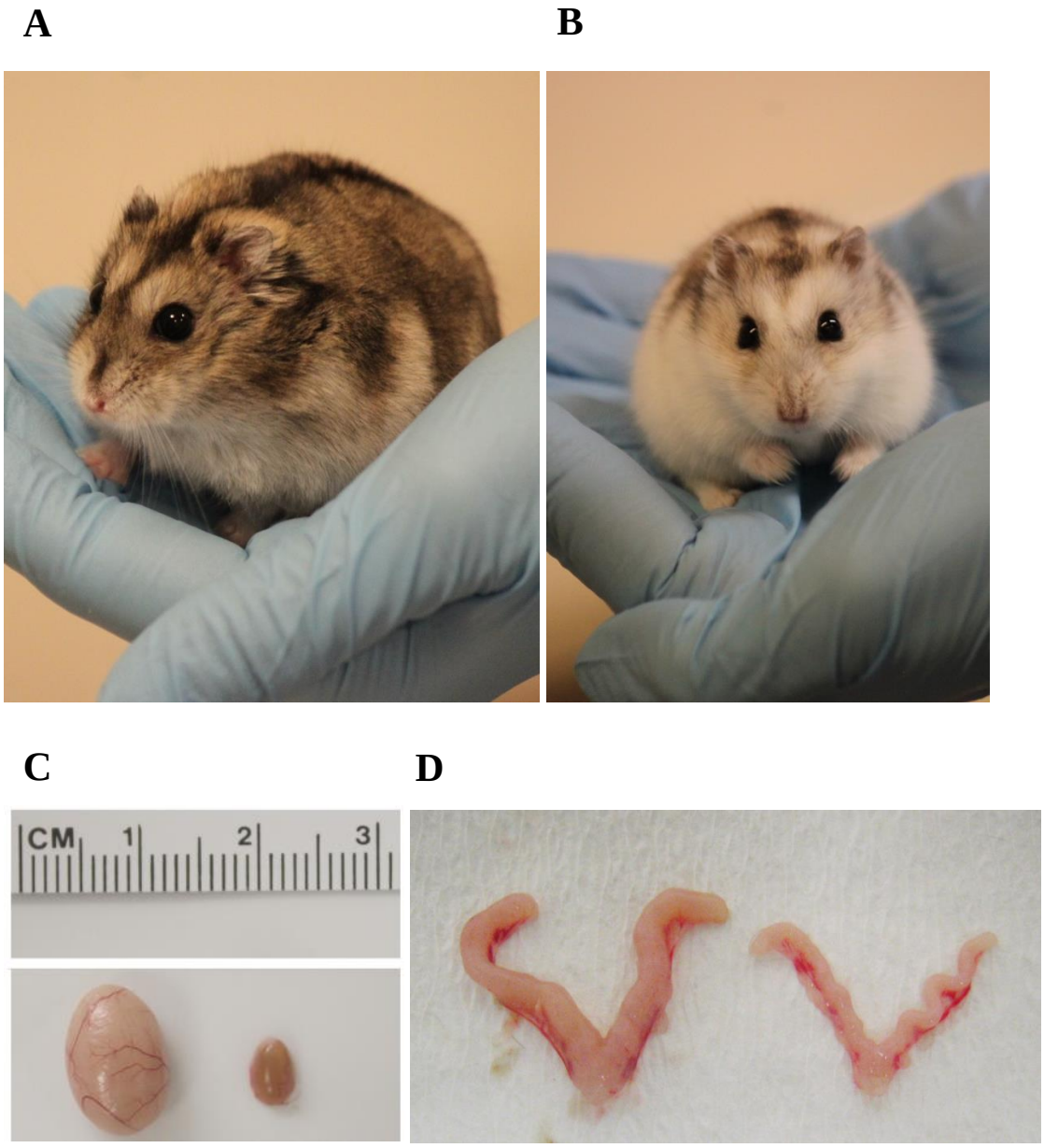

Figure 1.7. Seasonal phenotypic differences in the Siberian hamster. (A) Siberian hamster maintained under long-day (LD) conditions exhibiting dark brown fur. (B) Hamster maintained under short-day (SD), non-breeding conditions exhibiting white fur. (C) Seasonal difference between LD (left) and SD testes (right). Photo credit Tyler Stevenson. (D) Size variation between LD (left) and SD uteri (right). Photo credit Christopher Coyle.

Figure 1.8. Testes size and seasonal abdominal fat change in male Japanese quail. (A) Male quail maintained under long-day (LD) conditions (B) SD testes. Similar to the Siberian hamster, testes volume and mass significantly increase in LD individuals (not pictured). (C) Seasonal difference between SD (left) and LD abdominal fat (right).

1.9 Thesis aims

The present thesis uses a comparative approach to explore the neuropeptides and neural circuits regulating seasonal reproductive mechanisms in the seasonal species of Japanese quail and Siberian hamster. One recurring theme throughout the chapters is DNA methylation, as it is becoming apparent that epigenetic alterations play an essential role in the regulation of seasonal reproduction. Chapter 2 addresses the lack of a functional link between VA Opsin/ OPN5 and downstream reproductive mechanisms using RNA interference methods, testing the hypothesis that either VA Opsin and OPN5, or both, play a role in stimulating the neuroendocrine pathways that lead to sexual maturation in the Japanese quail. Chapter 3 explores VA Opsin and OPN5 expression during embryonic development of the quail and whether stress plays a role in photoreceptor mRNA levels or DNA methyltransferase expression during critical developmental stages. Chapters 4 and 5 describe sex-specific effects of thyroid hormone on the hypothalamic-pituitary-gonadal axis of Siberian hamsters, and epigenetic enzyme control of seasonal breeding. Finally, chapter 6 illustrates two studies in Japanese quail aimed at understanding the reversibility of epigenetic mechanisms and the daily patterns of DNA methyltransferase enzymes in the quail.

Chapter 2 – The Role of Vertebrate Ancient Opsin and Neuropsin in Mediating Seasonal Reproduction in the Japanese Quail

2.1 Introduction

2.1.1 Seasonal Reproduction in Avian Species

As with mammals, seasonal reproduction is a conserved mechanism for many avian species. Breeding needs to occur at the most favourable time of year in order to ensure rich food availability for offspring survival and fitness (Dawson et al., 2001). Birds, especially temperate avian species, have evolved a photoperiod-dependent system for the initiation of reproductive traits, where the duration of light dictates the organism's morphology, physiology, and behaviour. Until the 1920's, reproduction in birds was believed to be triggered by the temperature increase observed in spring. In 1926, Rowan's pioneering work in dark-eyed juncos (*Junco hyemalis*) demonstrated that light, specifically an increase in daylength, is the primary cue birds living in the northern hemisphere require to initiate gonadal growth and reproduction (Rowan, 1926). Conversely, the gradual decrease in duration of light during autumn and winter causes reproductive organs to decrease in size and the dampening of reproductive behaviour.

Supplementary cues, such as food quality and availability, temperature and social cues play an important role in precisely defining the timing of breeding, however this is both species- and sex-specific (for review: Tolla and Stevenson, 2020a). Integrating photoperiod and supplementary environmental cues allows for the activation of gonadotropin-releasing hormone (GNRH) neurons in the hypothalamus to release GNRH, which, in turn, stimulates gonadotroph cells in the anterior pituitary gland to secrete luteinising hormone (LH) and follicle-stimulating hormone (FSH). LH and FSH are essential in stimulating gonadal function in males and females. In males, LH stimulates testosterone production from the Leydig cells, and FSH and testosterone lead to testes

growth (Follett, 1976; Ubuka et al., 2008). In females, LH is responsible for signalling mature follicles to release androgen and oestrogen, and follicle-stimulating hormone targets granulosa cells in the ovaries to secrete progesterone. FSH in females also stimulates ovarian maturation and selection of follicles. Sex steroids, *i.e.* androgen and oestrogen, are responsible for complete sexual maturation, behaviour, and regulate negative feedback to the brain.

Gonadotropin-inhibitory hormone (GNIH) also plays role in avian seasonal breeding in repressing LH and FSH, although minimal. Studies have shown that GNIH action is species-specific, depending on whether a species is strictly seasonal (Perfito et al., 2011; Kriegsfeld et al., 2015). In addition, male Japanese quail show an increase in GNIH release in response to female presence (Tobari et al., 2014). The role of GNIH in avian breeding and in the inhibition of the hypothalamic-pituitary-axis is still largely unclear.

2.1.2 Light detection and Deep Brain Photoreceptors

For the neuroendocrine processes described above to be possible, organisms need to be able to detect sunlight and its duration. As described in chapter 1, light is able to penetrate the avian skull and is detected by deep-brain photoreceptors (DBPs). DBPs initiate the reproductive response, leading to breeding state. The precise identity of the DBPs responsible for seasonal reproduction is still unclear, as no functional link has been investigated yet. Based on the information gathered from prior studies, the candidate DBP must exhibit the following properties (as reviewed in García-Fernández et al., 2015): (1) The candidate opsins must be expressed in the hypothalamus (Halford et al., 2009); (2) They must be activated by wavelength of ~ 492 nm (Foster and Follett, 1985); (3) They must be linked to circadian genes; (4) They need to be associated with the activation of downstream reproductive pathways. Based on these criteria, the two candidate photoreceptors examined in the present study were VA Opsin and OPN5.

2.1.3 Epigenetics, seasonality, and photoreceptors

As discussed in chapter 1, epigenetic processes are conserved across taxa and throughout tissues. DNA methylation and histone modifications are studied in a range of diverse fields, from cancer research to chronobiology, to maternal behaviour. DNA methylation is by far the most studied form of epigenetic modification, and it has been associated with both daily and annual changes in light in seasonally breeding species. The enzymes that carry out DNA methylation are the DNA methyltransferase enzymes (DNMTs), and the most well-characterised are *DNMT1, DNMT3A* and *DNMT3B* (see chapter 1).

Epigenetic mechanisms have also been shown to play a role in opsin function. In a study by Nasonkin et al. (2010) in mice, animals that lacked *Dnmt1* in the retina exhibited deficiencies in the structural development of retinal photoreceptors (Nasonkin et al., 2010). Retinal *Dnmt1* knockdown also results in impaired photoreceptor differentiation and decreased photoreceptor survival in mice (Rhee et al., 2012). In addition, increased *Dnmt3a* expression has been shown in retinitis pigmentosa (RP), a disease that causes loss of photoreceptors in the eyes, in an RP mouse model (Farinelli et al., 2014). Finally, Rao et al. (2010) found that methylation of lysine residues 4 and 27 of histone 3 plays an essential role in the correct development of photoreceptors in embryonic mice (Rao et al., 2010). Taken together, the studies described above suggest that epigenetics plays a key role in retinal photoreception. However, the role of epigenetics in deep brain photoreception has not yet been explored, leaving the opportunity for this study to finally link not only DBPs to seasonality, but also to epigenetic changes.

2.1.4 Hypotheses and aims

The goal of this study was to identify the gene(s) responsible for deep brain photoreception in the Japanese quail. The two candidate opsins are VA Opsin and OPN5.

Therefore, to determine whether these two opsins account for the avian seasonal reproductive response, the first aim was to create an adeno-associated virus able to target the VA Opsin and OPN5 sequences and inhibit their expression in the hypothalamus, specifically the third ventricle (3V) (García-Fernández et al., 2015), of male adult Japanese quail. The second aim was to monitor reproductive characteristics after maintaining the animals in SD or Long day (LD) condition for either 2, 7 or 28 days, testing the hypothesis that VA Opsin and OPN5 knock-down in male Japanese quail exhibit a significant decrease in reproductive characteristics, such as LH and FSH release, testosterone levels, testes mass, cloacal volume and reproductive neuroendocrine hormone expression. Finally, epigenetic enzyme expression in the hypothalamus and pituitary complex was analysed, comparing control and treated individuals. It was hypothesised that DNA methyltransferase enzyme expression would decrease in knock-down birds compared to control individuals, to reflect a SD-induced phenotype.

2.2 Materials and Methods

2.2.1 Validation of AAV2 vector transfection

An adeno-associated virus containing OPN5 and VA Opsin target sequences was developed (Figure 2.1) and sent to Virovek© for production. The two target sequences were placed between the capsid serotype 2, a CMV promoter to target both glia and neurons, and GFP for detection. The ability of a commercially available AAV2 vector (Virovek inc.) was first assessed via transfection of primary cell culture of avian neural cells by Dr Jonathan Pérez at the Roslin Institute, University of Edinburgh. Fresh brain explant sections were taken from quail chicks at embryonic day 10 and rinsed in ice cold PBS. Explant sections were cultured in sterile 24 well culture plates with 500 µl of media. Media contained DMEM base with 1% PenStrep and 10% Fetal Bovine serum. Explants were incubated overnight at 37°C with 5% CO_2 to stabilise cultures. 400 µL of media was

removed and replaced with 600 µL either a CMV or heF1a promoter. All tests were replicated in duplicate. Due to rapid depletion of media an additional 500 µL of fresh media was added the following day. Explants were cultured for 5 days prior to imaging to visualize presence of transfected cells via GFP. GFP was visualized via fluorescence microscopy and found to be present using both promoters, but stronger expression was seen under the CMV promoter.

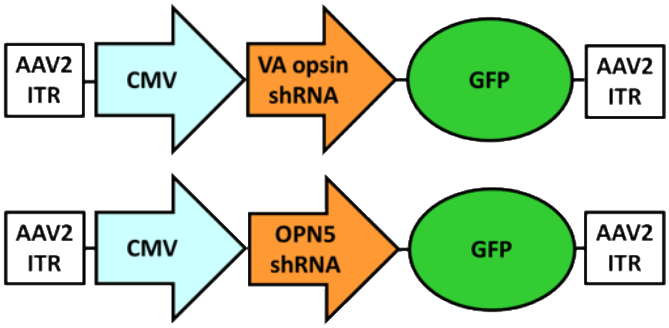

Figure 2.1. Schematic representation of generated AAV2 constructs. The target sequences, VA Opsin (above) and opn5 (below) are sandwiched between the virus capsid serotype (AAV2), a CMV promoter, and GFP.

2.2.2 Stereotaxic ICV injection coordinate verification

Based on previously published studies, a series of stereotaxic coordinates were tested using quail cadavers and India ink. Brains were removed and dissected to establish site of ink within the brain and the following test coordinates were adjusted. This process was repeated until the coordinates were found to reliably target 3V of the medial basal hypothalamus. The conclusive coordinates based of bursa as a starting point are x=0 mm, y= 3.8 mm, z = -6.3 mm, then up to -6.0 mm for injection. 1 µL of AAV2 (2.34E+13 vg/mL) was injected per bird. Isofluorane (4-5%) with O2 at 1-1.5 L/minute was used to anesthetize the animals. Once induced, birds received analgesia via subcutaneous injection of meloxicam (0.5 mg/kg) and butorphanol (1.5 mg/kg). Quails were then positioned into a

stereotaxic frame (Kopf Instruments) and their head feathers were plucked, and the head disinfected. A ~1cm small incision was made on the head and sterile gauze was used to keep the skull exposed during surgery. Then, the injection needle was aligned to the bursa and digital readouts on the stereotaxic frame were zeroed. The needle was then moved to the coordinates of the injection and a small mark was made before clearing the needle. A small dental drill was used to drill through the skull of the animals. Then, the needle was realigned to the stereotaxic coordinates, then loaded with AAV2 solution before injecting the quails. Either veterinary adhesive (VetBond 3M) or suture were used to close the wound. Animals were kept in isolation, allowing them to recover until they were able to stand, then they were transferred to a communal recovery pen and provided with a heat lamp and food and water access. All surgical procedures were carried out in accordance with protocols approved by local AWERB under Home Office Project Licence held by Dr Ian Dunn at the Roslin Institute, University of Edinburgh.

Animals were maintained under short photoperiod (6L:18D) before surgery to ensure short-day, non-breeding phenotypes. Once surgeries began, photoperiod was altered to 7L:17D to allow additional time for recovery during light hours post-surgery. Surgeries were carried out between 0845 and 1330 (lights on at 0800) each day.

2.2.3 Experimental design

2.2.3.1 Study 1: Baseline/ control study

Once sexually mature, a group of male quails (N=5) was pseudo-randomly selected, kept in SD and received a blank virus (CV) injection. Other three groups of male quails were randomly selected to receive either a CV (N=5), VA Opsin (both short and long; N=8) or OPN5 (N=5) injection, maintained in a 7L:17D condition for 2 weeks, and then individuals were photostimulated by transferring to a 16L:8D condition for 2 days, to mimic a summer breeding condition.

2.2.3.2 Studies 2 and 3: Acute study and chronic study

Two studies were conducted to examine the impact of RNAi after 7 days (acute study; N=33) or 28 days (chronic study; N=33) of photostimulation on male Japanese quail. Quail were pseudo-randomly selected and assigned to a treatment: aside from a control virus group (CV; acute study:N=9; chronic study: N=8), treatment groups were injected with RNAi viruses that targeted VA Opsin (acute study: N=9; chronic study: N=9) or OPN5 (acute study: N=7; chronic study: N=9). A group of birds that received both OPN5 and VA Opsin RNAi was also included ('Both' group; acute study: N=8; chronic study: N=7). Following a 2-week incubation and transfection period (7L:17D), quails were photostimulated by transferring them to a 16L:8D condition for either 7 or 28 days. Cloacal gland size was measured throughout the 28 days of the chronic study. Body and testes weights were also taken from the start to the end of each study. The animals were culled, and the following tissues were extracted: brain, pituitary gland, gonads, liver, retina/eyes, adipose tissue, thymus, spleen, heart, muscle, adrenal, kidney. Tissues were collected and frozen at -80°C until analysis.

2.2.3.3 Exclusion criteria

Animals were selected for inclusion in subsequent analyses based on the following criteria. Quails that exhibited enlarged gonads within the short-day or 2-day groups were excluded, as it implied having broken the short-day, non-breeding state, prior to long-day transfer. One animal was excluded from OPN5 western blot analyses because of a technical error in gel loading. 28-day individuals were included based on the presence of GFP signalling within and around the third ventricle (3V) in 30 μm coronal sections of fresh frozen brain mounted to Polysine slides and immediately wet mounted using VECTASHIELD Antifade Mounting Media (Vector Labs) containing DAPI.

2.2.4 Antibody descriptions

Antibodies against VA Opsin and Opn5 were made polyclonal in rabbit hosts and custom made by Cambridge Biochemicals. Opn5 antibody antigen: CISSHRDSAALSETQLEV (Nakane et al., 2010). VA Opsin antibody antigen: PARWDPFHHPLDSI (Halford et al., 2009).

2.2.5 Western blot protein analyses

Opsin expression in birds in the short-day, 2-day and 7-day timepoints was analysed by western blot. Whole hypothalami were dissected because of the extreme challenge in dissecting the 3V alone because of its small size, as well as to investigate whole-hypothalamus interactions, as the downstream mechanisms of VA Opsin and OPN5 are currently unknown. The hypothalamus was dissected from frozen brains and homogenized in 700 μL of 100 mM Tris-HCL buffer with 4% w/v SDS and protease inhibitors (Halt™ Protease Inhibitor Cocktail, EDTA-free, Thermo Fisher Scientific). The anatomical boundaries for hypothalamus dissection were the tractus septopalliomesencephalicus (TrSM) at the anterior border, the cerebellum posterior at the posterior border, then 1-1.5mm on either side of the mid-line were trimmed, and, from the remaining chunk, the dorsal 2 mm were removed. Samples were then centrifuged at 20,000 *x g* for 20 minutes at 4°C. Supernatant was collected and stored at -80°C. Total protein concentration was determined using 1 μL of supernatant using a BCA Protein Assay (Pierce™ BCA Protein Assay Kit). Supernatant volume for use in western blots was then standardized to 10 μg of protein to each well by diluting with water. 20 μL of diluted sample was mixed with 10 μL of LDS buffer (NuPAGE™ LDS Sample Buffer, Thermo Fisher Scientific), before incubating at 98°C for 2 minutes prior to loading. 10 μL of each sample were loaded onto 4-12% Bis-Tris pre-cast gels (NuPAGE™, Thermo Fisher Scientific). Samples were loaded onto two separate gels that were run in parallel in the

same gel tank. Gels were run at 90V for 5 minutes to ensure even entry of samples into the gel, then at 175V for 1 hour. One duplicate gel was then immediately incubated in 40 ml of OptiBlue protein stain for 1 hour to quantify total protein loading on an orbital shaker. The second gel was then processed for western blot transfer. Protein was transferred to a PDVF membrane (iBlot™ Transfer Stacks, PVDF, regular size, Thermo Fisher Scientific) using the iBlot 2 system on preset setting 3. Then, membranes were washed in 1X PBS 5 times for 5 minutes before being blocked for 30 minutes in Odyssey blocking buffer in 50 ml falcon tubes. Blocking buffer was removed and 5 ml of primary antibody solution (5 ml Odyssey buffer, 1 AB, 0.1% Tween 20) were added. After primary antibody incubation, samples were washed with PBS for 5 minutes, 6 times. Incubation with secondary antibody was performed using IRdye 680RD Goat Anti-Rabbit antibody (LI-COR) at 1:10,000 in 5 ml Odyssey Blocking Buffer with 0.1% Tween-20 Detergent. Secondary Antibody incubation was done for 90 minutes at room temperature. Membranes were then rinsed with PBS 5minutes for 6 times, before imaging. Membranes were visualised on a LI-COR Odyssey imager using Image Studio software (Image Studio™ LI-COR). Western blots were imaged at 3.5 Intensity, Medium image quality at 169 μm resolution. Total protein gels were rinsed in distilled water and then imaged on the 700 nm channel at lowest image quality, Intensity 3, 169 μm resolution. Protein work was carried out by Dr Jonathan Pérez at the Roslin Institute, University of Edinburgh.

2.2.6 RNA isolation and cDNA synthesis

RNA was extracted from pituitary gland and gonadal tissues using TRIzol (Thermo Fisher Scientific). For the pituitary gland, the entire gland was used for extraction. For the testes, a 100 mg piece of tissue was used. 1 mL of TRIzol was added to the tissue and homogenized using Kinematica™ Polytron™ PT1200E handheld homogenizer (Thermo Fisher Scientific). Then, after a 5 min incubation at room temperature, 200 μL of

chloroform were added to the homogenized sample and the tubes were incubated for 3 min at room temperature. The samples were centrifuged for 15 min at 12,000 g at 4°C. After centrifugation, the samples separate into an upper aqueous phase, interphase and a lower red phase. The upper aqueous phase was pipetted out of the tube and transferred to a fresh tube. 500 µL of isopropanol were added to the new tubes and incubated for 10 min. The tubes were then centrifuged for 10 min at 12,000 g at 4°C. The supernatant was discarded, and the white RNA pellet was resuspended in 1 mL of 75% ethanol, vortexed and centrifuged for 5 min at 7,500 g at 4°C. The supernatant was discarded, and the tubes were air-dried for 5-10 min. Finally, the pellet was resuspended in 30 µL of RNase-free water. Nucleic acid quality (260/280 ratio) and concentration were determined by using a spectrophotometer (Nanodrop; Thermo Fisher Scientific). cDNA was synthesised using Precision nanoScript2 Reverse Transcription Kit (Primerdesign Ltd) (2 µg RNA) and stored at -20 °C until quantitative PCR (qPCR) assays.

2.2.7 Primer design and optimisation

Primers for target genes were designed using the NCBI Primer Design Tool (https://www.ncbi.nlm.nih.gov/tools/primer-blast/). Primers were designed to include a 40-60% GC content and have an annealing temperature of 55-65°C, then ordered from Invitrogen (Thermo Fisher Scientific). Primers were then suspended in RNAse- and DNAse-free water to 10 µM concentration and optimised using PCR and gel electrophoresis. Each PCR tube consisted of 45 µL of PCR SuperMix (Thermo Fisher Scientific), 1 µL of 10 µM forward primer, 1 µL of 10 µM reverse primer, 100 ng of quail cDNA, and water until 50 µL. The tubes were then placed in a thermal cycler (Thermo Hybaid Px2, Thermo Fisher Scientific) to follow a gradient program: (I) initial denaturation, 94°C for 2 minutes, 1 cycle; (II) denaturation, 94°C for 15 seconds, followed by a gradient annealing temperature (55°C – 62°C) for 30 seconds, followed by extension,

72°C for 1 minute/kb, 35 cycles; (III) hold step at 4°C. A 1% agarose gel was made by mixing 1.2 g agarose, 120 ml 1X TBE buffer (Thermo Fisher Scientific) and 4 µL SYBR Safe DNA Gel Stain (Thermo Fisher Scientific), heating it in a glass beaker for ~2 minutes, then pouring it in a gel cast and letting it set for 40 minutes. 10 µL of each PCR product were then loaded onto the gel. Running was carried out for 50 minutes, at 100 V and 100 mA. The gels were visualised using a UV light transilluminator (GeneFlash, Syngene) and the ideal annealing temperature was identified for each primer pair by selecting the one that yielded the clearer quality and most amount of product. See Table 2.1 for detailed primer information.

Gene	Forward primer	Reverse primer	Annealing Temp
GAPDH	ACGGTGGATGGCCCCTCTGG	GGCCCATCAGCAGCAGCCTT	60˚C
B-ACTIN	AATCAAGATCATTGCCCCAC	TAAGACTGCTGCTGACACC	60˚C
TSH	CTCTTTGGCCTGACTTTTGG	TGTGCACACGTTTTGAGACA	60˚C
GNRH	CGCTGAAAATCTGGTGGAAT	TTGTTGGCGTTGTGGATTTA	60˚C
GNIH	ATGGTGCGTGCCTAGATGAAC	AGCAACTGAATTTGGCACTTTG	60˚C
DNMT1	GTGACAGCCCTATGGGAGGAC	TCCACCATGAACAGCTCCAAC	61˚C
DNMT3A	AGCGTGCAAGAGAGCGATG	GCTCTGTCCTAAGGTGACCC	60˚C
DNMT3B	AATCTCAGAGAACGGGGCTC	TTTGTTCTCGGGTCTGGTCC	59˚C
OPN5	ATGGCATCAGACTGCAACTCC	AAGGAACAGTAGCCCAGAACG	60˚C
VA Opsin	CCTTGCGTACCCCTCTTAGC	GGTGCCACCAGTCAAAGAGA	60˚C
LH	TTTACCGCAGCCCTTTGGGT	AGAGCCACGGGTAGGATGACTTT	55˚C
FSH	CTGCGGTGACCATCCTGAATCTTT	GCTTCCATTGTGACTGAAGGAGCA	62˚C
GNRH-R	CTTCTCCTGTTCAGCCTCAT	CTCACAGAGTGCCATCCTCA	60˚C
FSH-R	ATGGAACCTGCCTGGATGAG	CTTGTATGTAGACCTCGCTCTTAG	56˚C
LH-R	CAGACGTCCTGGACATTTCTTC	GCTGGGGTAGGTCAGAACAG	58˚C
AR	AAGTACCTGTGTGCTAGCCG	CTTTGCGGGCTCCAAGAGTC	60˚C

Table 2.1. List of Japanese quail target genes, primer sequences, and relative annealing temperatures used.

2.2.8 Real-time PCR (qPCR)

qPCRs were performed on a Stratagene Mx3000 Real Time PCR machine in 20 µl reactions. For each well, the qPCR mix consisted of 5 µl cDNA template, 10 µl SYBR green (Primerdesign Ltd), 0.5 µl (300 nM) forward primer, 0.5µl (300nM) reverse primer and 4µl RNase-free H2O. Samples were run in duplicate in a 96-well plate format under

the following conditions: i) denaturing at 95°C for 5 min, then 39 cycles of ii) 95°C for 10 secs, iii) 30 secs at annealing temperature dependent on primer (Table 2.1), and finally iv) an extension step of 72°C for 30 secs. Melt curves were analysed to ensure the specificity of each reaction through only a single peak. PCR Miner (Zhao and Fernald, 2005) was used to determine reaction efficiencies and quantification cycle (Ct). Fold expression of each gene of interest was measured in relation to the average Ct for two reference genes (*GAPDH* and *B-ACTIN*) and calculated using 2-(ΔΔCt).

2.2.9 Testosterone assay

To measure plasma testosterone levels, the Parameter™ Testosterone Assay (R&D Systems, Bio-Techne) was used according to manufacturer's instructions. DNA was extracted from the blood of Japanese quail using Qiagen DNeasy Blood and Tissue Kit (Qiagen, UK). Samples for the testosterone assay were prepared by mixing 50 µl DNA (1 µg/ µl) of each sample with 450 µl of Calibrator Diluent RDS-48. 50 µl of Primary Antibody Solution were added to each well, apart from the non-specific binding (NSB) wells. Then, the plate was incubated on an horizontal shaker for 1 hour at room temperature at 500 rpm. After incubation, the wells were emptied by blotting on a dry paper towel and washed four times with wash buffer. 100 µl of Calibrator Diluent were added to the NSB wells and the zero standard wells. 100 µl of prepared standard, control or sample were added to the residual wells. Then, 50 µl of Testosterone Conjugate were added to each well and the plate was covered with an adhesive film and incubated at room temperature for 3 hours on an horizontal shaker at 500 rpm. After incubation, the wells were washes four times with wash buffer. Next, 200 µl of Substrate Solution were added to each well and the plate was incubated for 30 minutes at room temperature, away from light. Finally, 50 µl of Stop Solution were added to each well. The plate was then carried to a microplate reader (LT-4500, Labtech) and the absorbance of each well was measured at 450 nm and at 570 nm as a control.

2.2.10 Statistical Analysis

All statistical analyses were performed using SigmaPlot 13.0. Data were log-transformed in the event of a violation of normality or equal variance. Significance was determined at $p < 0.05$. For detailed statistical analysis information, refer to Tables A.1 and A.2 (Appendix A).

2.3. Results

2.3.1 Adeno-associated virus silencing of target deep-brain photoreceptors

Confirmatory qPCRs and Western blots were performed on study 1 and 2 hypothalami to ensure the silencing of VA Opsin and OPN5. For mRNA and protein results (Figure 2.2A and B), average expression of control virus-injected individuals was taken. Then, mRNA and protein expression of VA Opsin, OPN5 or 'Both' groups was measured, and the average control value was subtracted from each treatment group, and the knockdown percentage was calculated. *VA Opsin* and *OPN5* mRNA expression showed around 95% knockdown (K/D) in all treatment groups for both genes (Figure 2.2A). The viral constructs were effective in knocking down around >40% of protein expression in all treatment groups except the 2-day VA Opsin K/D group, which showed an increase in VA Opsin protein expression (Figure 2.2B).

Immunohistochemistry showed effective transport of AAV into the hypothalamus by GFP signalling, and stronger expression was seen under the CMV promoter compared to the heF1a promoter (Figure 2.2C and D). By using OPN5 and VA Opsin antibodies, it was possible to identify immunoreactivity in cells lining the 3V (Figure 2.2 E and F), confirming photoreceptor localisation. OPN5-expressing cells were found in the PVO (Figure 2.2E) and VA-immunoreactive cells were identified within the POA (Figure 2.2F). Protein work/ immunohistochemistry was carried out by Dr Jonathan Pérez at the Roslin Institute, University of Edinburgh.

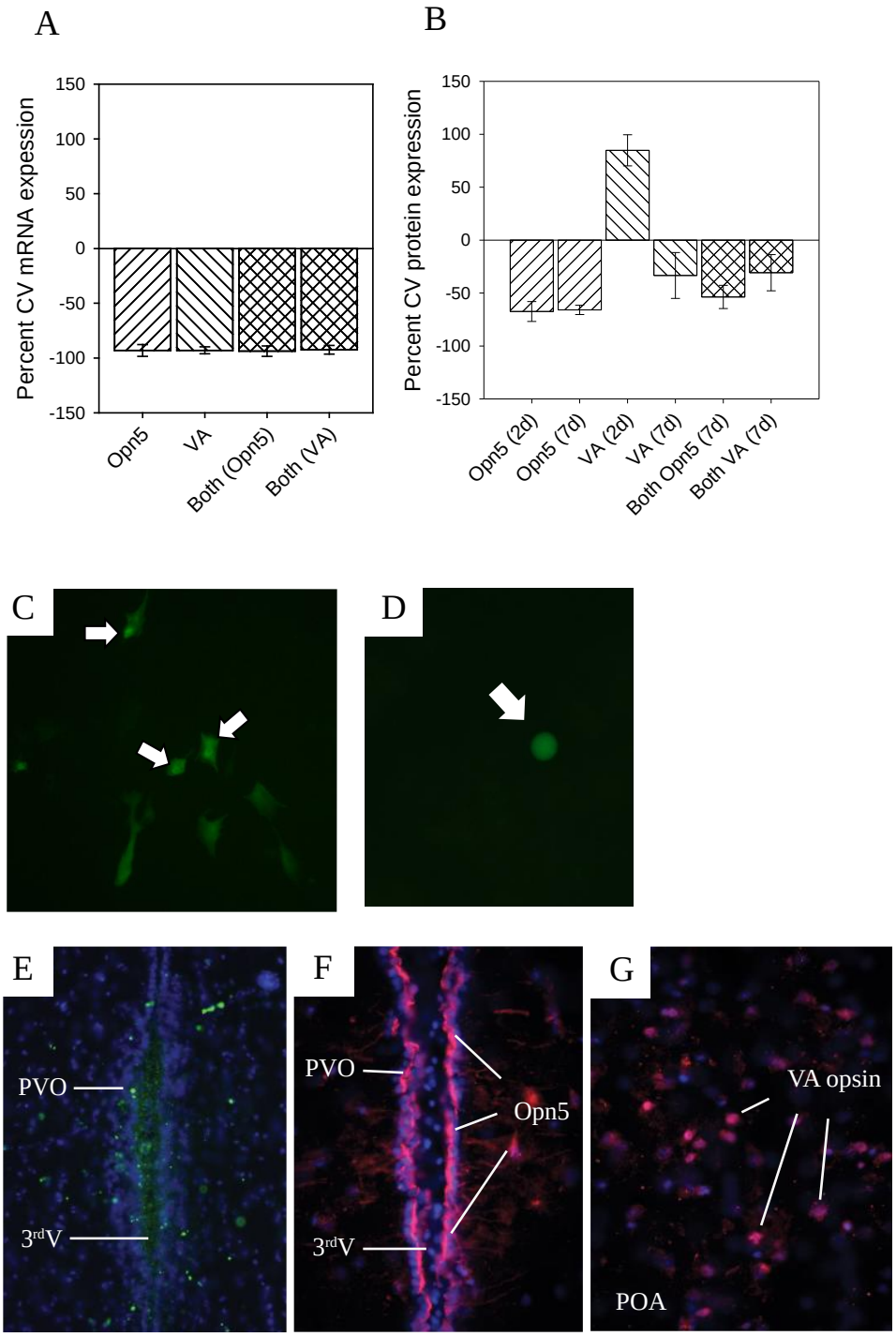

Figure 2.2. Confirmation of knockdown analyses. (A) Percent knockdown of VA Opsin and OPN5 mRNA in the hypothalamus of 2-day and 7-day study treatment groups at around 95% per group. (B) Percent knockdown of VA Opsin and OPN5 protein expression in the hypothalamus of 2-day and 7-day study treatment groups. All groups present 40-60% knockdown levels, except for the 2d VA group. (C)(D) Representative blots showing effective transport of AAV into the hypothalamus of embryonic day 10 quails by GFP signalling using either a CMV promoter (C) or a heF1a promoter (D). Stronger GFP expression was seen with the CMV promoter. (E) Representative blots showing GFP localisation within the third ventricle (3^{rd}V) of the hypothalamus. (F)(G) Representative blots showing VA and OPN5 immunoreactivity in cells lining the 3^{rd}V within the paraventricular organ (PVO) and preoptic area (POA) of the hypothalamus. Protein work/ immunohistochemistry was carried out by Dr Jonathan Pérez at the Roslin Institute, University of Edinburgh.

2.3.2 Peripheral measurements

Testes and body weights were taken at each collection time point (2d, 7d and 28d) (Figure 2.3). After 2 days of photostimulation, there was no difference in testes mass between treatment groups ($F=0.205$, $p=0.892$). However, after RNAi treatment and a 7-day photostimulation, there was a significant increase in testes mass in all treatment groups compared to SD individuals ($F=11.334$; $p<0.001$). Although not significant, there was also a pattern for an additive increase in testes mass in OPN5, VA and Both groups. After 28 days of photostimulation, no significant difference between treatment groups was found ($F= 0.205$; $p= 0.892$). When analysing body mass data, no significant effect of RNAi was detected at 2 days ($F=0.805$; $p=0.462$), 7 days ($F=0.717$; $p=0.549$), or 28 days ($F=0.664$; $p=0.580$) (Figure 2.4).

Cloacal gland area was measured in 28-day individuals. The change in cloacal gland growth rate (*k* value) between weeks 1-4 was then calculated (Figure 2.4). CV individuals showed higher overall *k* throughout the weeks, compared to RNAi-treated birds (Figure 2.5). 2-way ANOVA indicated a significant effect of both injection ($F=3.512$; $p=0.009$) and week ($F=33.363$; $p<0.001$) on cloacal *k.* Fisher's post-hoc LSD method revealed a significant difference between CV and VA *k*, and CV and 'Both' *k* for all weeks (Figure 2.5; see tables A.1 and A.2 in Appendix A for statistical analysis details).

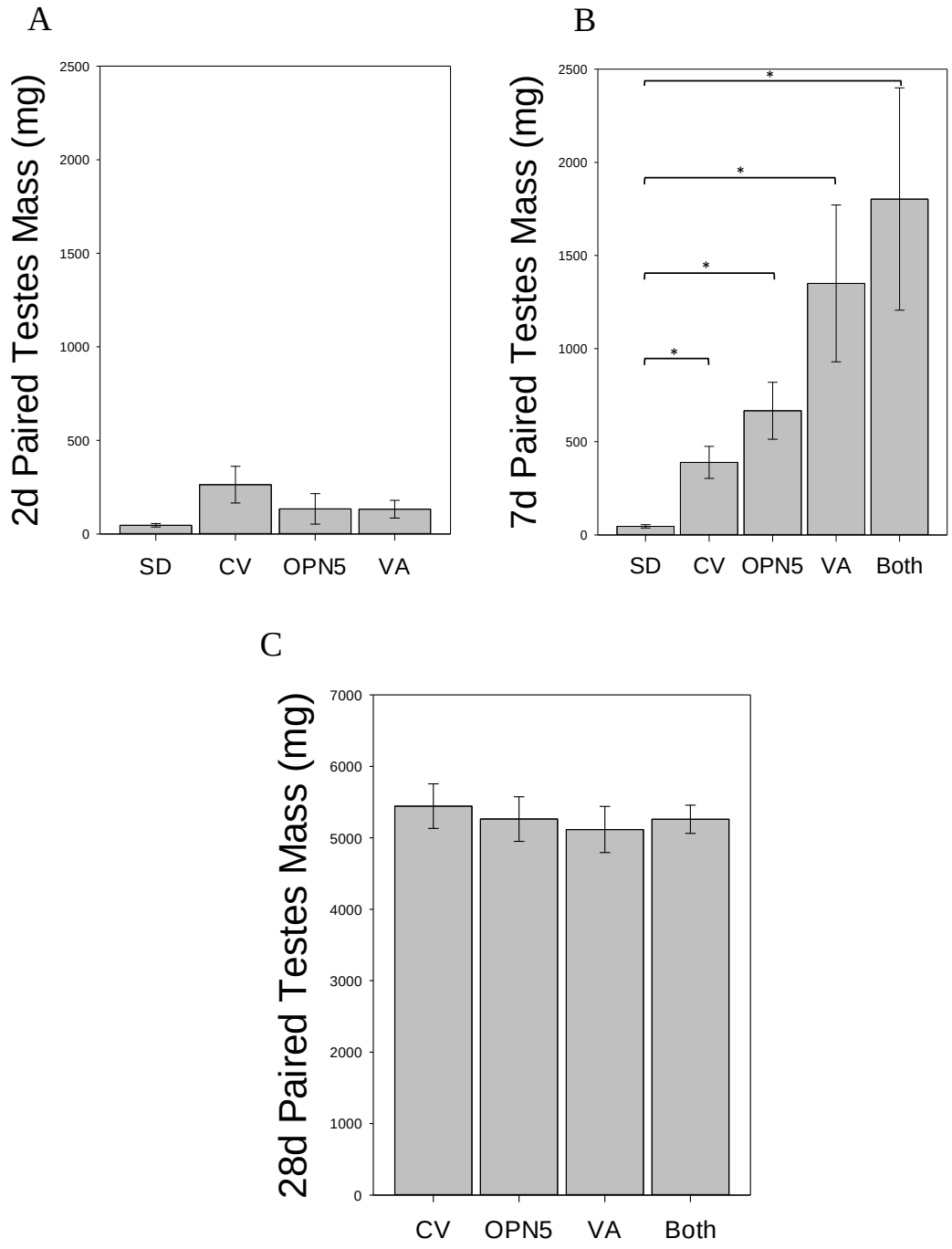

Figure 2.3. Testes mass in adult male quail treated with a control virus, or with an AAV construct to silence the expression of OPN5, VA Opsin or both (OPN5+VA), and photostimulated for either 2 days (A), 7 days (B) or 28 days (C). Asterisks (*) represent significance between groups. Results are mean ± SEM. SD= short-day, control virus (N=5); CV= long-day, control virus (2d: N=5; 7d: N=9; 28d: N=8); OPN5= OPN5 knockdown group (2d: N=5; 7d: N=7; 28d: N=9); VA= VA Opsin knockdown group (2d: N=8; 7d: N=9; 28d: N=9); Both= OPN5 and VA Opsin knockdown group (7d: N=8; 28d: N=7).

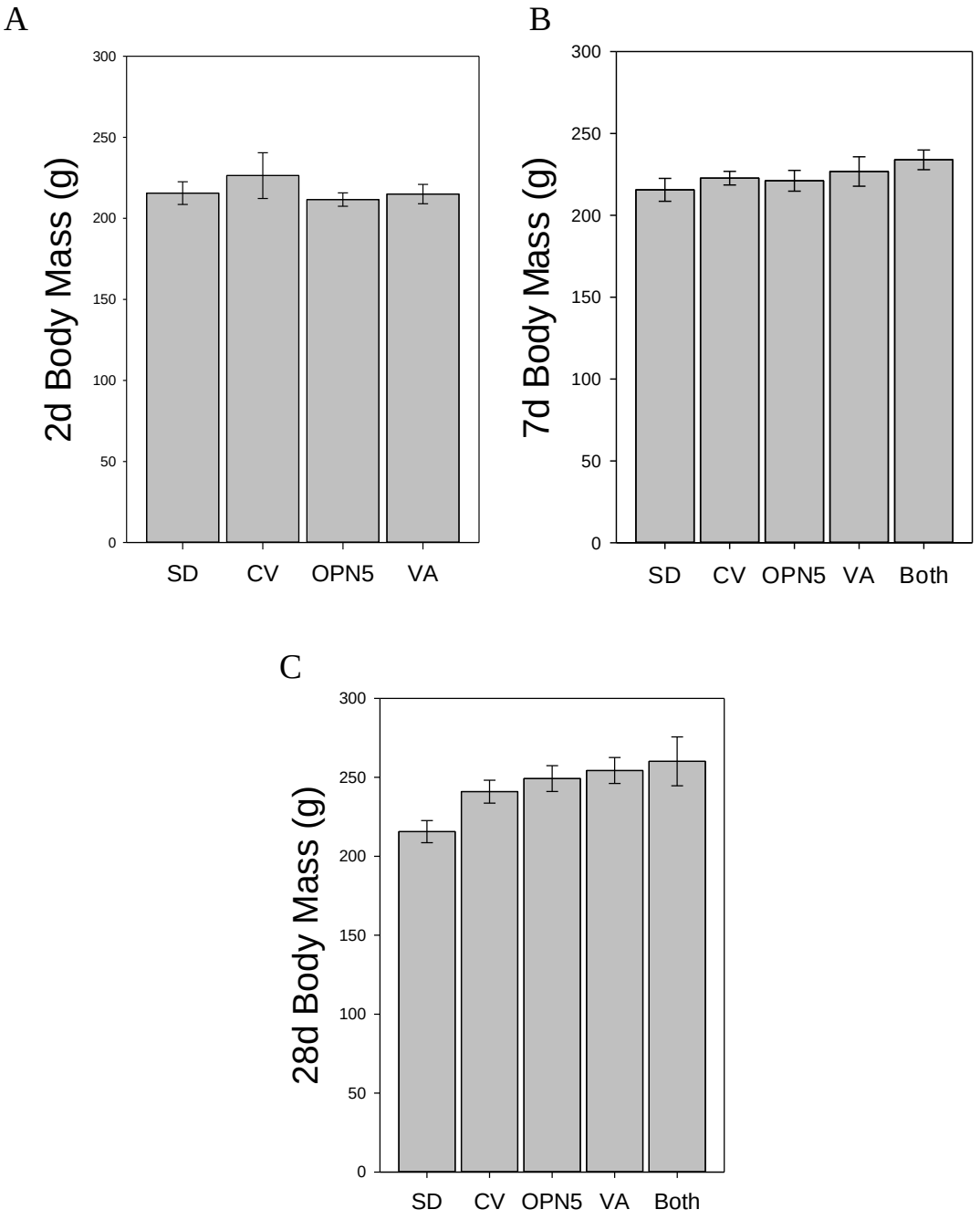

Figure 2.4. Body mass in adult male quail treated with a control virus, or with an AAV construct to silence the expression of OPN5, VA Opsin or both (OPN5+VA), and photostimulated for either 2 days (A), 7 days (B) or 28 days (C). Results are mean ± SEM. SD= short-day, control virus (N=5); CV= long-day, control virus (2d: N=5; 7d: N=9; 28d: N=8); OPN5= OPN5 knockdown group (2d: N=5; 7d: N=7; 28d: N=9); VA= VA Opsin knockdown group (2d: N=8; 7d: N=9; 28d: N=9); Both= OPN5 and VA Opsin knockdown group (7d: N=8; 28d: N=7).

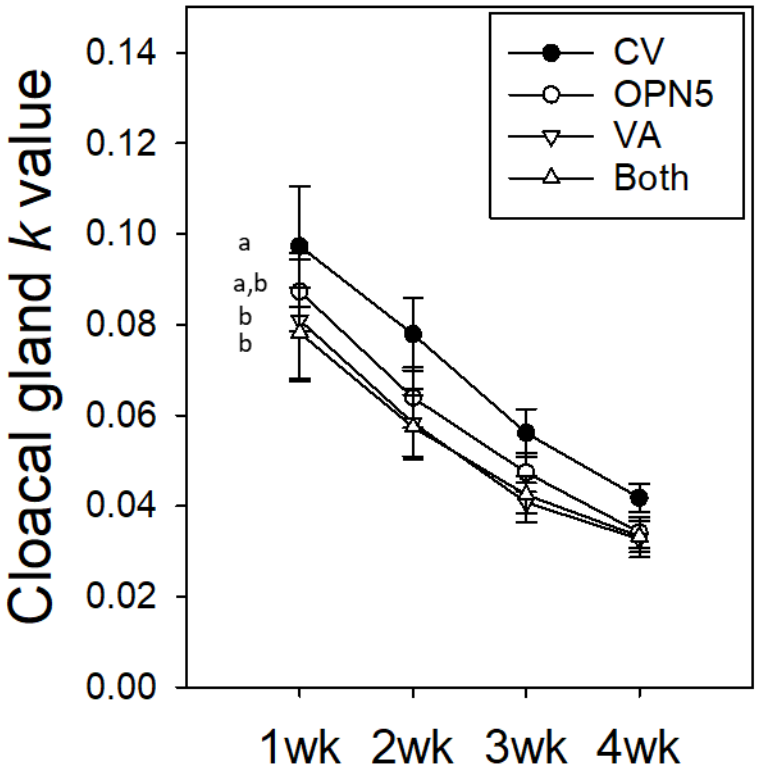

Figure 2.5. Change in cloacal gland growth rate (*k* value) in birds injected with a control virus, or with an AAV construct to silence the expression of OPN5, VA Opsin or both (OPN5+VA), and photostimulated for 28 days. Different letters represent a significant difference. Here, a significant difference was found between CV and VA *k*, and between CV and 'Both' *k* for all weeks. CV= long-day, control virus (N=8); OPN5= OPN5 knockdown group (N=9); VA= VA Opsin knockdown group (N=9); Both= OPN5 and VA Opsin knockdown group (28d: N=7).

2.3.3 Gene expression

2.3.3.1 Hypothalamus

Gene expression in the hypothalamus was measured at 2 days and 7 days after photostimulation. Hypothalamic *GNRH* expression did not change between control virus SD individuals and treated quails (F=0.237, p=0.869) in the 2d study (Figure 2.6A). However, after 7 days of photostimulation, a one-way ANOVA revealed a significant effect of treatment (F=3.858, p=0.012). Tukey's *post-hoc* test indicated an increase in *GNRH* expression in VA individuals compared to SD individuals (p=0.018; Figure 2.6B).

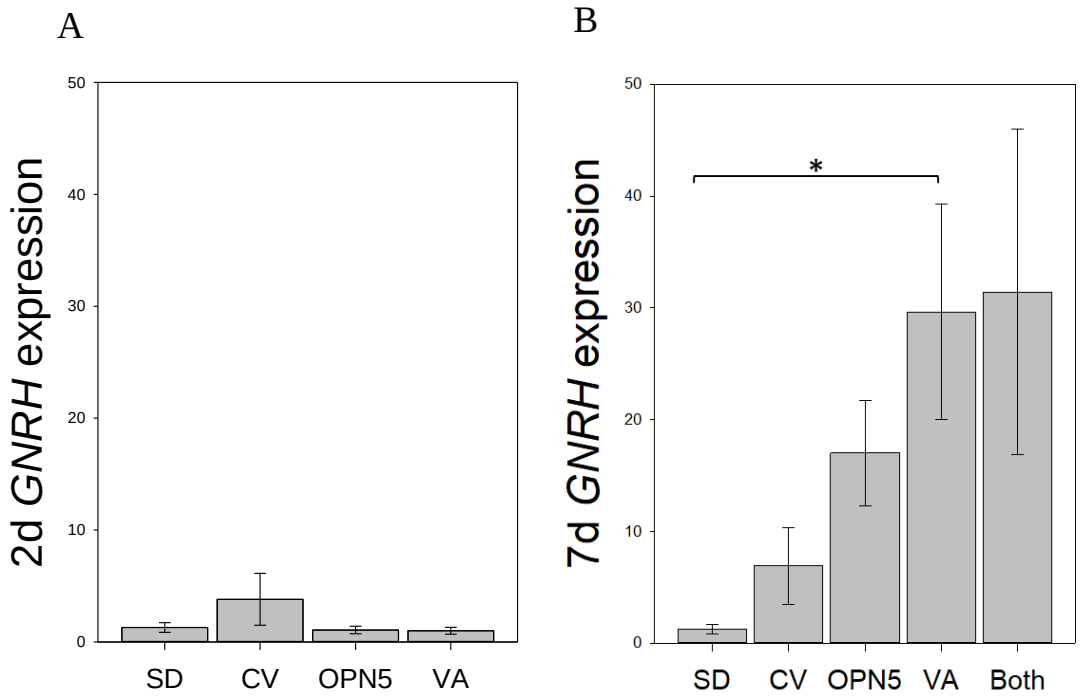

Figure 2.6. Average gene expression for *GNRH* for the 2-day study (A) and 7-day study (B). Asterisks (*) represent significance between groups. Results are mean ± SEM. SD= short-day, control virus (N=5); CV= long-day, control virus (2d: N=5; 7d: N=9); OPN5= OPN5 knockdown group (2d: N=5; 7d: N=7); VA= VA Opsin knockdown group (2d: N=8; 7d: N=9); Both= OPN5 and VA Opsin knockdown group (N=8).

When investigating *GNIH* expression in the hypothalamus, no significant change was detected after 2 days of photostimulation (F=0.104, p=0.957), or after 7 days (H=3.237; p=0.519) (Figure 2.7).

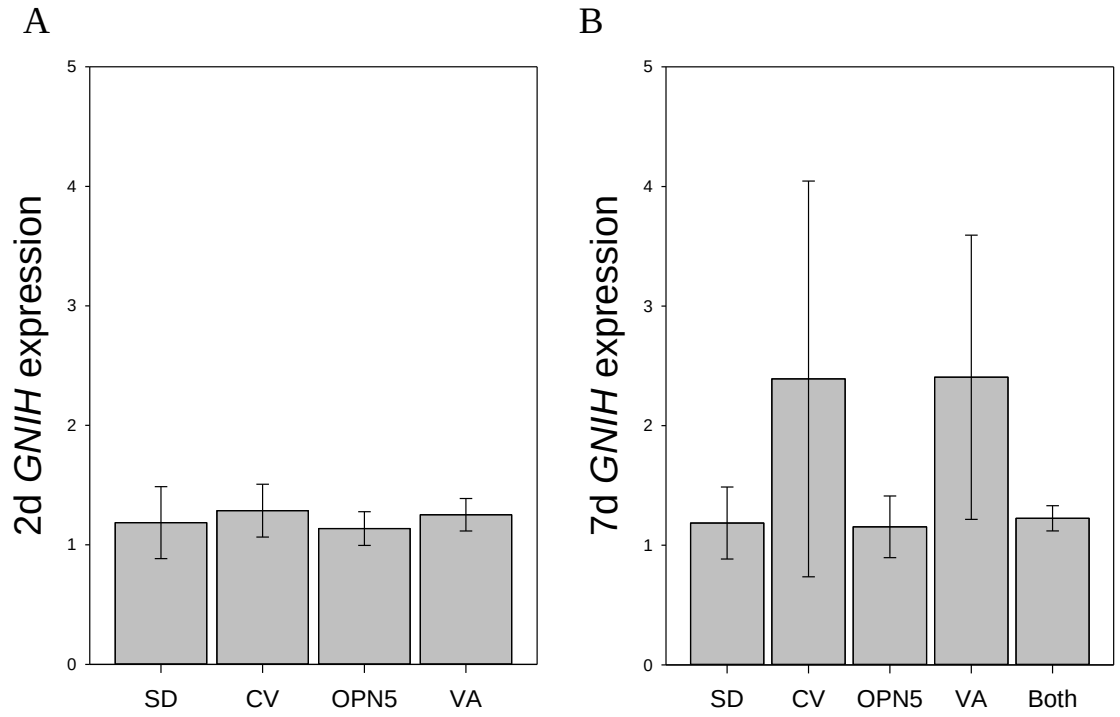

Figure 2.7. Average gene expression of *GNIH*, for the 2-day study (A) and 7-day study (B). Results are mean ± SEM. SD= short-day, control virus (N=5); CV= long-day, control virus (2d: N=5; 7d: N=9); OPN5= OPN5 knockdown group (2d: N=5; 7d: N=7); VA= VA Opsin knockdown group (2d: N=8; 7d: N=9); Both= OPN5 and VA Opsin knockdown group (N=8).

Next, expression of DNA methyltransferase enzymes *1*, *3A* and *3B* was analysed. At 2 days post-photostimulation, there was no significant effect of treatment on expression of *DNMT1* (F=0.214; p=0.885), *DNMT3A* (F=0.120; p=0.947), or *DNMT3B* (F=0.134; p=0.939) (Figure 2.8). OPN5-treated individuals appear to present slightly higher levels of hypothalamic *DNMT1, 3A* and *3B* expression compared to the rest of the treatment groups, although not statistically significant. Kruskal-Wallis One Way Analysis of Variance on Ranks revealed that after 7 days of photostimulation, there was no significant effect of treatment on *DNMT1* (H=4.833; p=0.305), *DNMT3A* (H=8.601; p=0.072), or *DNMT3B* (H=4.222; p=0.377) (Figure 2.9). *DNMT3A* and *DNMT3B* levels appear to decrease in OPN5 and 'Both' birds, although not statistically significant (Figure 2.9). A t-test between OPN5 birds showed a decrease in *DNMT3B* expression in the 7-day group, compared to 2-day hypothalami.

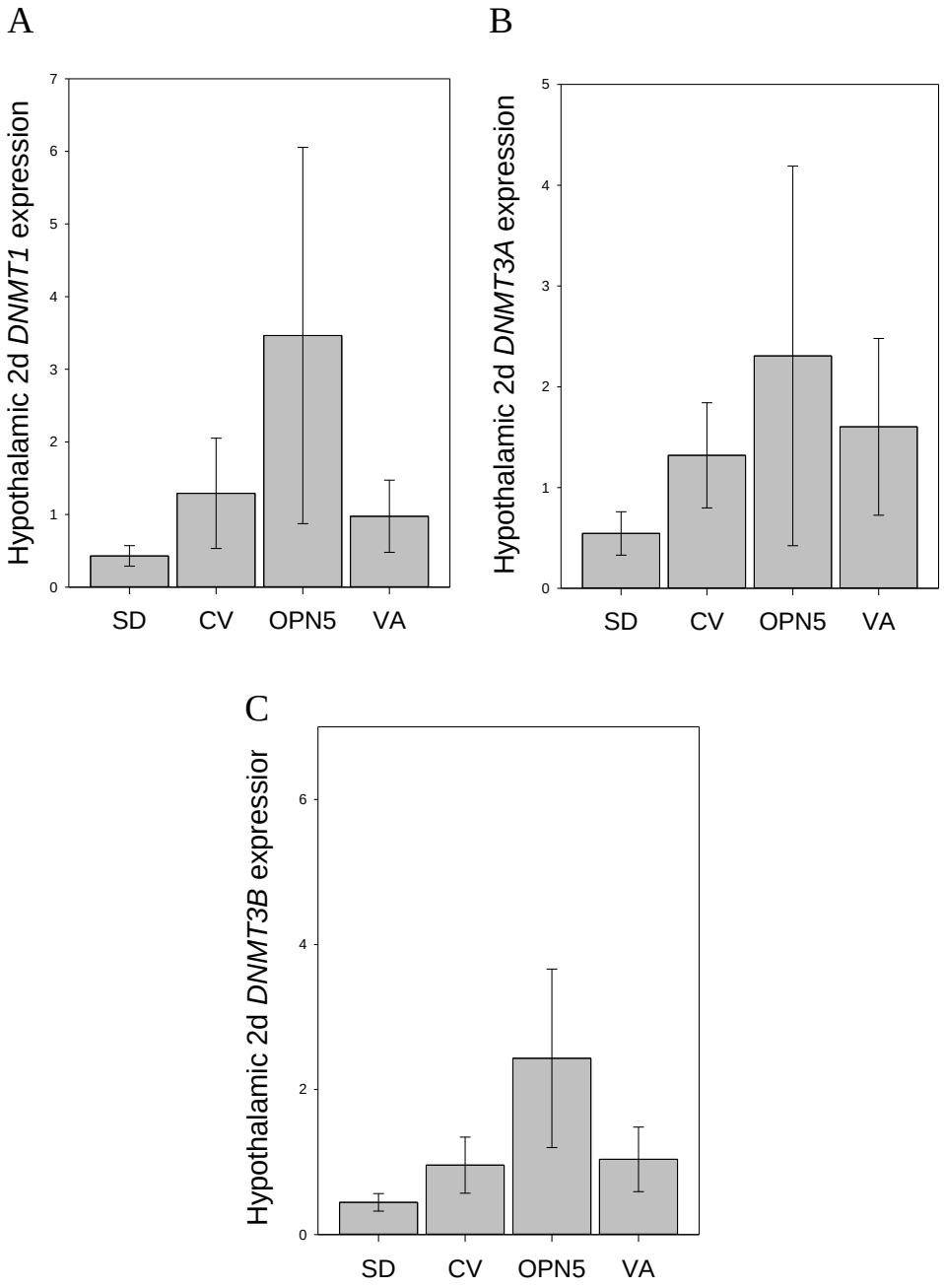

Figure 2.8. DNA methyltransferase *1* (A), *3A* (B), *3B* (C) expression in the hypothalamus of control virus short-day individuals (SD), and birds that were injected with either a control virus (CV), OPN5-silencing virus (OPN5), or VA Opsin-silencing virus (VA) and photostimulated for 2 days. SD= short-day, control virus (N=5); CV= long-day, control virus (N=5); OPN5= OPN5 knockdown group (N=5); VA= VA Opsin knockdown group (N=8).

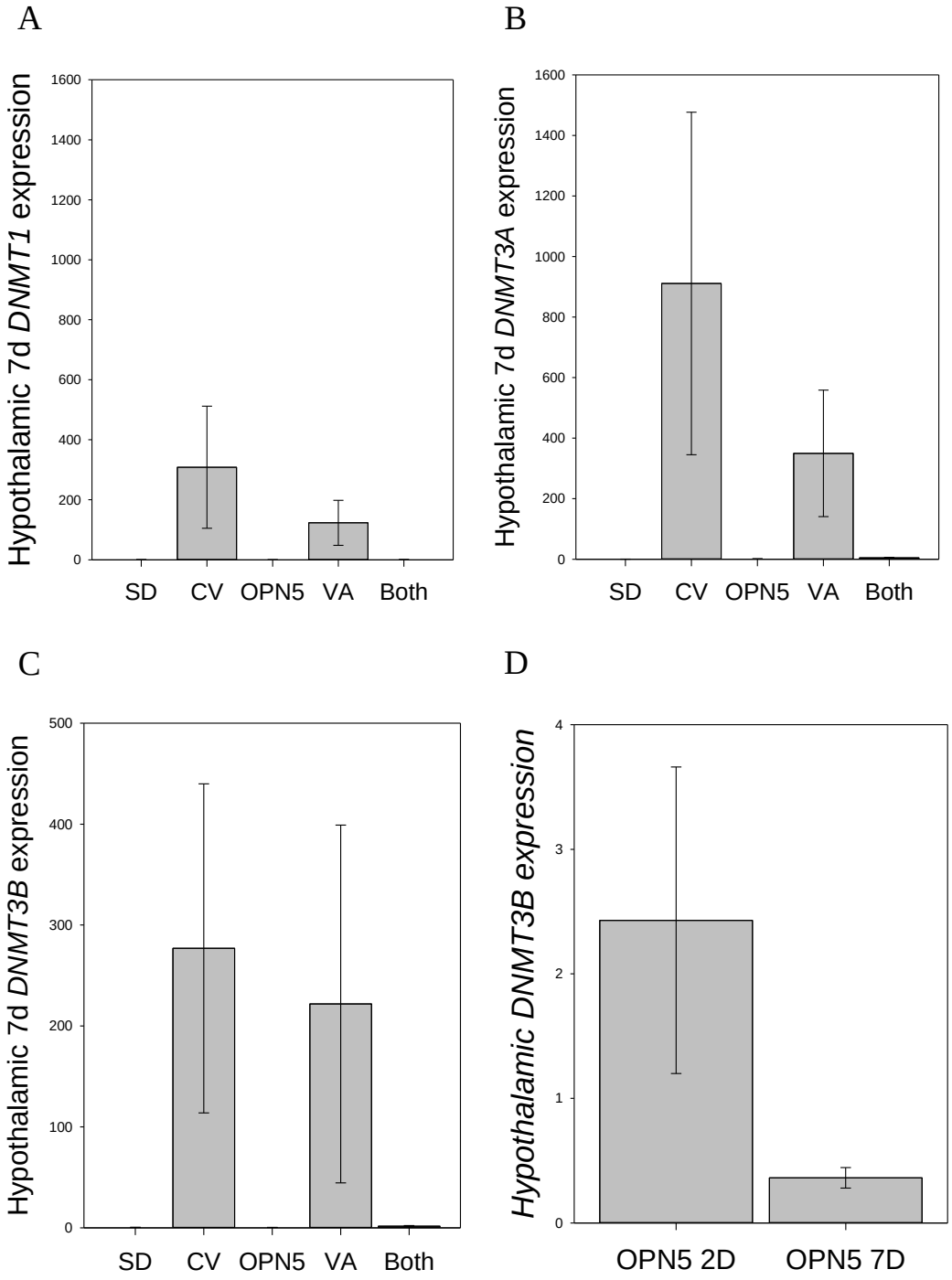

Figure 2.9. DNA methyltransferase *1* (A), *3A* (B), *3B* (C) expression in the hypothalamus of control virus short-day individuals (SD), and birds that were injected with either a control virus (CV), OPN5-silencing virus (OPN5), or VA Opsin-silencing virus (VA) and photostimulated for 2 days. (D) Comparison of *DNMT3B* levels between 2-day and 7-day OPN5 individuals (p=0.0536). SD= short-day, control virus (N=5); CV= long-day, control virus (N=9); OPN5= OPN5 knockdown group (2d: N=5; 7d: N=7); VA= VA Opsin knockdown group (N=9); Both= OPN5 and VA Opsin knockdown group (N=8).

2.3.3.2 TSHB, LHB, and FSH expression in the pituitary gland

Key reproductive genes were analysed in the anterior pituitary gland of quail at 2, 7, and 28 days. Target genes include thyroid-stimulating hormone (*TSHB*), luteinising hormone (*LHB*), follicle-stimulating hormone (*FSH*), and gonadotropin-releasing hormone receptor (*GNRH-R*). In addition, the expression of DNA methyltransferases *1* and *3A* was investigated.

TSHB expression was found not to vary between treatment groups at 2 days ($F=1.632$; $p=0.219$) (Figure 2.10A), 7 days ($H=2.129$; $p=0.712$) (Figure 2.11A), or 28 days ($H=5.681$; $p=0.128$) (Figure 2.12A). No significant effect of treatment was found on *LHB* expression at 2 days ($F=0.663$; $p=0.586$) (Figure 2.10B), 7 days ($H=1.865$; $p=0.761$) (Figure 2.11B), or 28 days ($H=4.372$; $p=0.224$) (Figure 2.12C). There was a significant effect of treatment on *FSH (*$F=9.346$; $p<0.001$) levels at 2 days, with levels increasing in CV, OPN5, and VA groups, compared to SD (Figure 2.10C). At 7 days, *FSH* expression was significantly affected by treatment ($F=3.139$; $p=0.028$), with a significant increase in 'Both' treated individuals, compared to SD (Figure 2.11C). 28-day *FSH* expression did not change with treatment ($H=5.943$; $p=0.114$) (2.12D). *FSH* levels at after 2 days were also greatly higher than levels at 7 or 28 days. *GNRH-R* levels were also monitored in 28-day individuals. There was no effect of treatment on its expression ($F=2.899$; $p=0.051$) (Figure 2.12B).

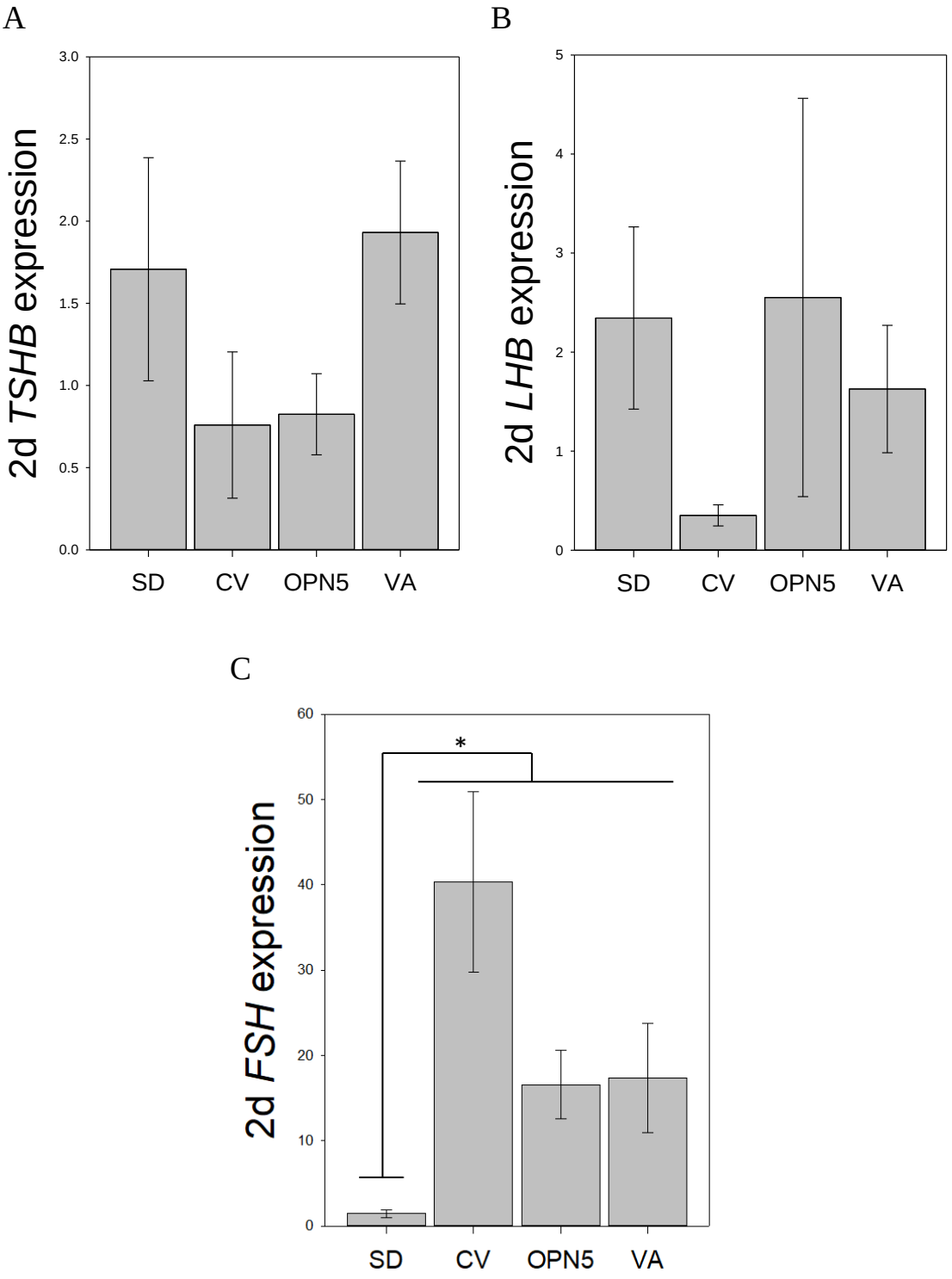

Figure 2.10. Changes in key molecular targets in the pituitary gland between treatments at 2 days. qPCR analyses of pituitary expression of thyrotropin-stimulating hormone (*TSHB*) (A), luteinizing hormone beta subunit (*LHB*) (B), and follicle-stimulating hormone (*FSH*) (C) from adult male quail. Note – quail were collected between zt2 and zt7 to capture the increase in gonadotropin levels (Meddle and Follett, 1997). Asterisks (*) represent significance between groups. Results are mean ± SEM. SD= short-day, control virus (N=5); CV= long-day, control virus (N=5); OPN5= OPN5 knockdown group (N=5); VA= VA Opsin knockdown group (N=8).

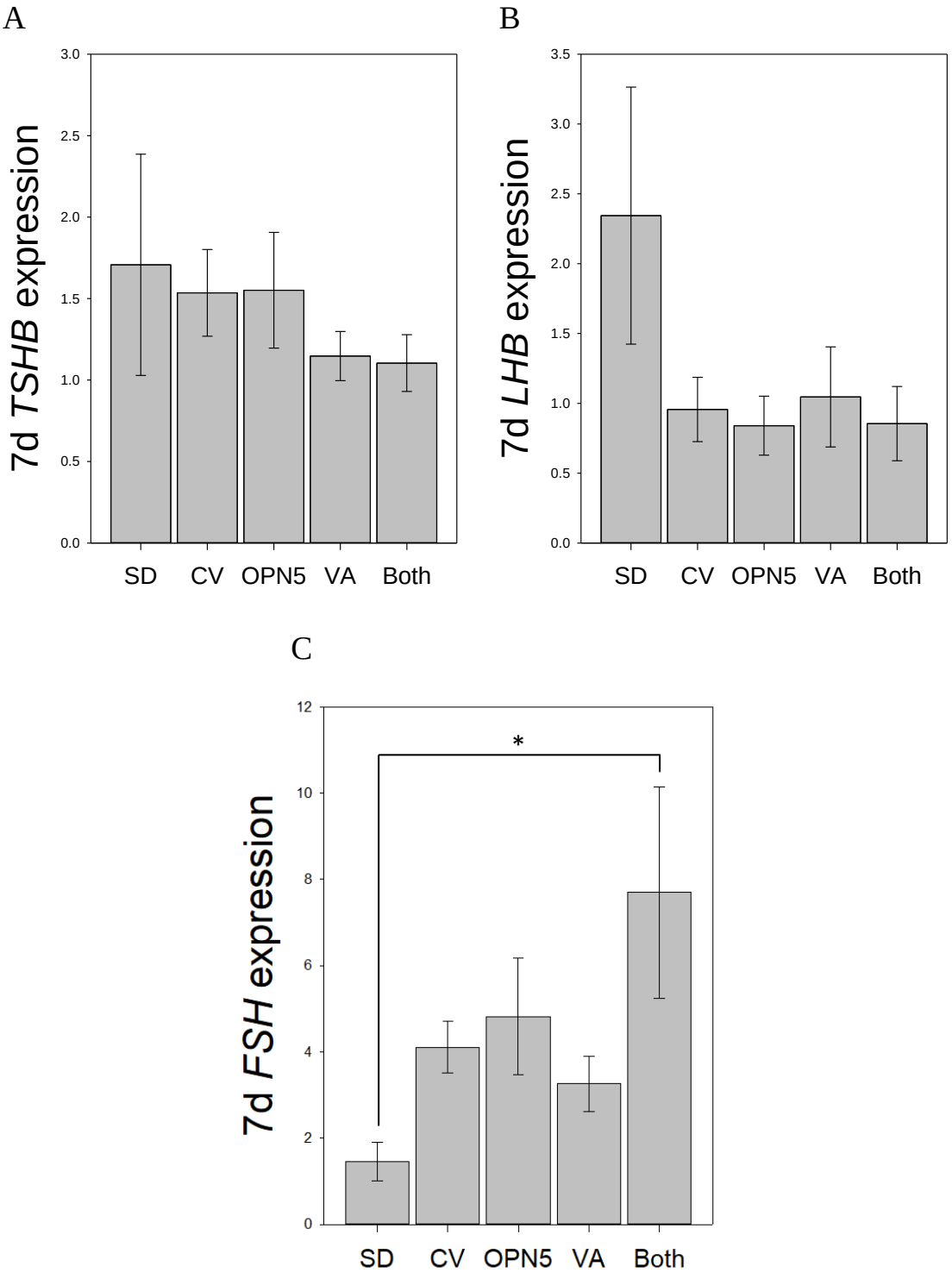

Figure 2.11. Changes in key molecular targets in the pituitary gland between treatments at 7 days. qPCR analyses of pituitary expression of thyrotropin-stimulating hormone (*TSHB*) (A), luteinizing hormone beta subunit (*LHB*) (B), and follicle-stimulating hormone (*FSH*) (C). Note – quail were collected between zt2 and zt7 to capture the increase in gonadotropin levels (Meddle and Follett, 1997). Asterisks (*) represent significance between groups. Results are mean ± SEM. SD= short-day, control virus (N=5); CV= long-day, control virus (N=9); OPN5= OPN5 knockdown group (N=7); VA= VA Opsin knockdown group (N=9); Both= OPN5 and VA Opsin knockdown group (N=8).

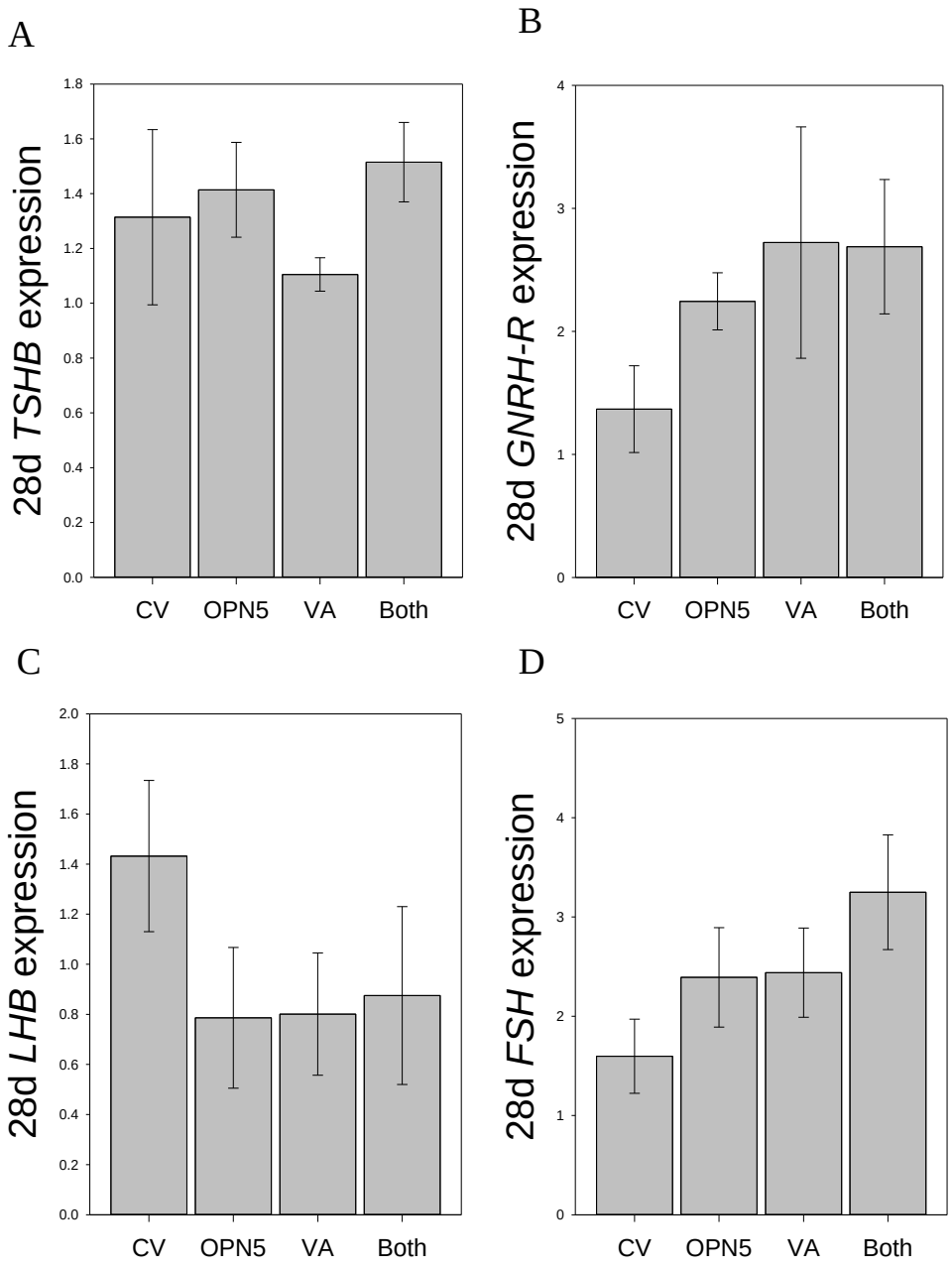

Figure 2.12. Changes in key molecular targets in the pituitary gland between treatments at 28 days. qPCR analyses of pituitary expression of thyrotropin-stimulating hormone (*TSHB*) (A), Gonadotropin-releasing hormone receptor II (*GNRH-R*) (B), luteinizing hormone beta subunit (*LHB*) (C), and follicle-stimulating hormone (*FSH*) (D). Note – quail were collected between zt2 and zt7 to capture the increase in gonadotropin levels (Meddle and Follett, 1997). Results are mean ± SEM. CV= long-day, control virus (N=8); OPN5= OPN5 knockdown group (N=9); VA= VA Opsin knockdown group (N=9); Both= OPN5 and VA Opsin knockdown group (28d: N=7).

2.3.3.3 DNMT1 is reduced in the pituitary gland of 28d VA birds

DNA methyltransferase 1 and 3A expression was measured in the pituitary gland of 28-day individuals. VA-treated animals exhibited a decrease in *DNMT1* expression, compared to CV individuals (H=9.523; p=0.023). No change was found in *DNMT3A* expression between treatment groups (F=0.988; 0.412) (Figure 2.13).

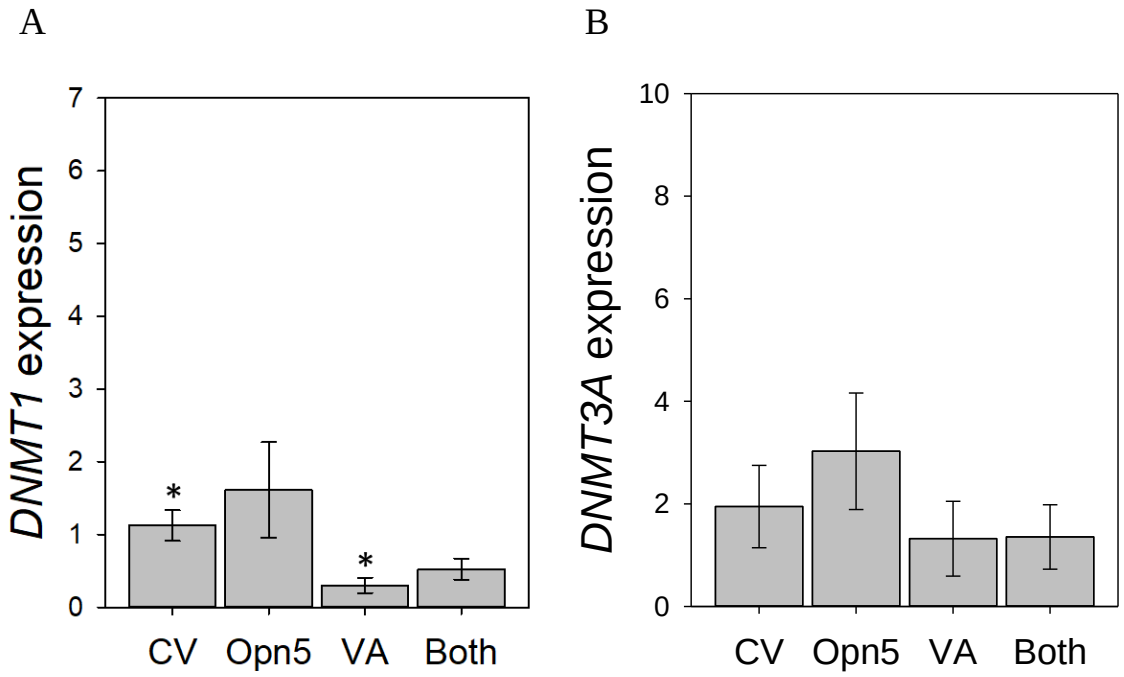

Figure 2.13. Pituitary gland expression of *DNMT1* (A) and *DNMT3A* (B) for each treatment group in the pituitary gland after 28 days of photostimulation (Study 3). *DNMT1* is significantly reduced (p = 0.023) in VA Opsin K/D individuals compared to controls (CV). Asterisks (*) represent significance between groups. Results are mean ± SEM. CV= long-day, control virus (N=8); OPN5= OPN5 knockdown group (N=9); VA= VA Opsin knockdown group (N=9); Both= OPN5 and VA Opsin knockdown group (28d: N=7).

2.3.3.4 Testes

The expression of FSH receptor (*FSH-R*), LH receptor (*LH-R*), and Androgen receptor (*AR*) was analysed in the testes of 2-day, 7-day and 28-day individuals. Treatment did not significantly alter *FSH-R* expression at 2 days (F=0.907; p=0.458) (Figure 2.14A), or 7 days (F=7.395; p=0.116) (Figure 2.15A). However, at 28 days, there was a significant reduction of *FSH-R* in OPN5-treated individuals compared to the CV group (F=3.028; p=0.044) (Figure 2.16A). When considering *LH-R*, there was no effect of treatment on *LH-R* levels at 2 days (H=5.309; p=0.151) (Figure 2.14B), 7 days (H=0.554; p=0.968) (Figure 2.15B), or 28 days (H=1.164; p=0.762) (Figure 2.16B). Finally, *AR* did not exhibit a change in expression between treatment groups at 2 days (F=0.718; p=0.555) (Figure 2.14C), 7 days (H=3.527; p=0.474) (Figure 2.15C), or 28 days (F=1.478; p=0.240) (Figure 2.16C).

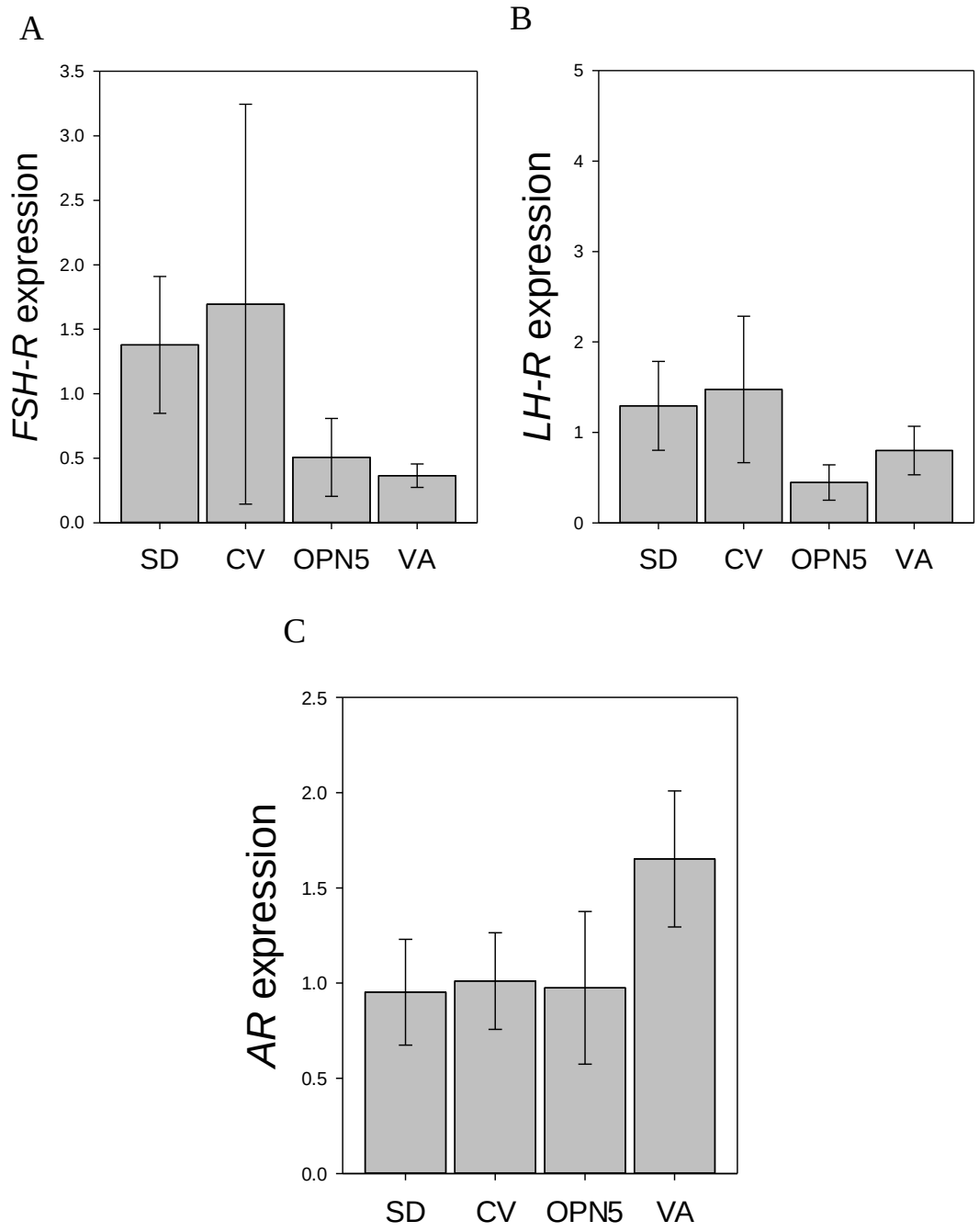

Figure 2.14. Photoperiodic regulation of receptor expression in the testes for the 2-day study. mRNA levels of follicle stimulating hormone receptor (*FSH-R*) (A), luteinizing hormone receptor (*LH-R*) (B) and androgen receptor (*AR*) (C) in quail testes. In short days (SD), male quail received ICV injections that consisted of control virus (CV). A subset of SD-CV quail was collected and used as a reference group (CV). All birds were then moved to long days and collected after 2 days. Results are mean ± SEM. SD= short-day, control virus; CV= long-day, control virus; OPN5= OPN5 knockdown group; VA= VA Opsin knockdown group. SD= short-day, control virus (N=5); CV= long-day, control virus (N=5); OPN5= OPN5 knockdown group (N=5); VA= VA Opsin knockdown group (N=8).

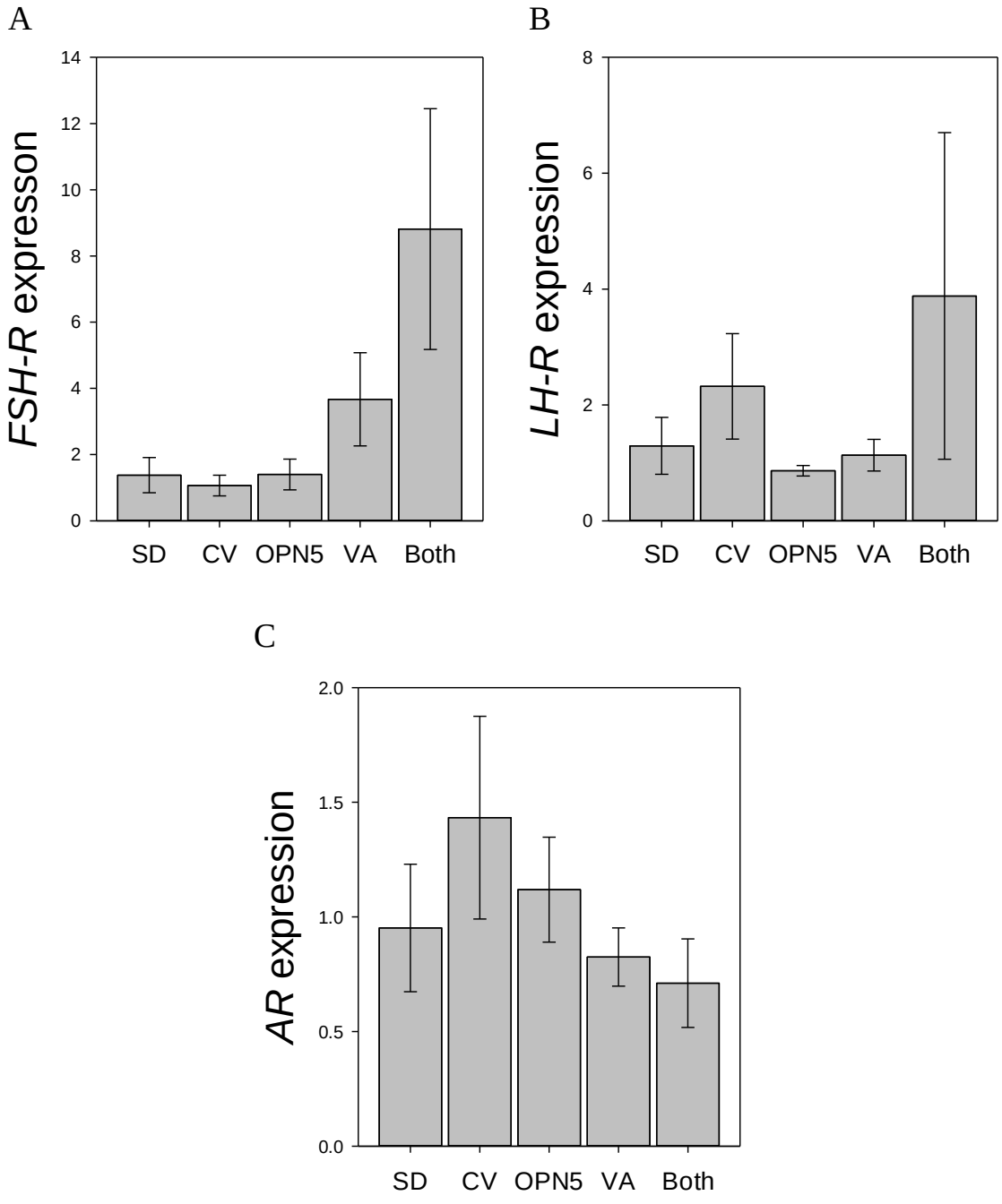

Figure 2.15. Photoperiodic regulation of receptor expression in the testes for the 7-day study. mRNA levels of follicle stimulating hormone receptor (*FSH-R*) (A), luteinizing hormone receptor (*LH-R*) (B) and androgen receptor (*AR*) (C) in quail testes. In short days (SD), male quail received ICV injections that consisted of control virus (CV). A subset of SD-CV quail was collected and used as a reference group (CV). All birds were then moved to long days and collected after 7 days. Results are mean ± SEM. SD= short-day, control virus (N=5); CV= long-day, control virus (N=9); OPN5= OPN5 knockdown group (N=7); VA= VA Opsin knockdown group (N=9); Both= OPN5 and VA Opsin knockdown group (N=8).

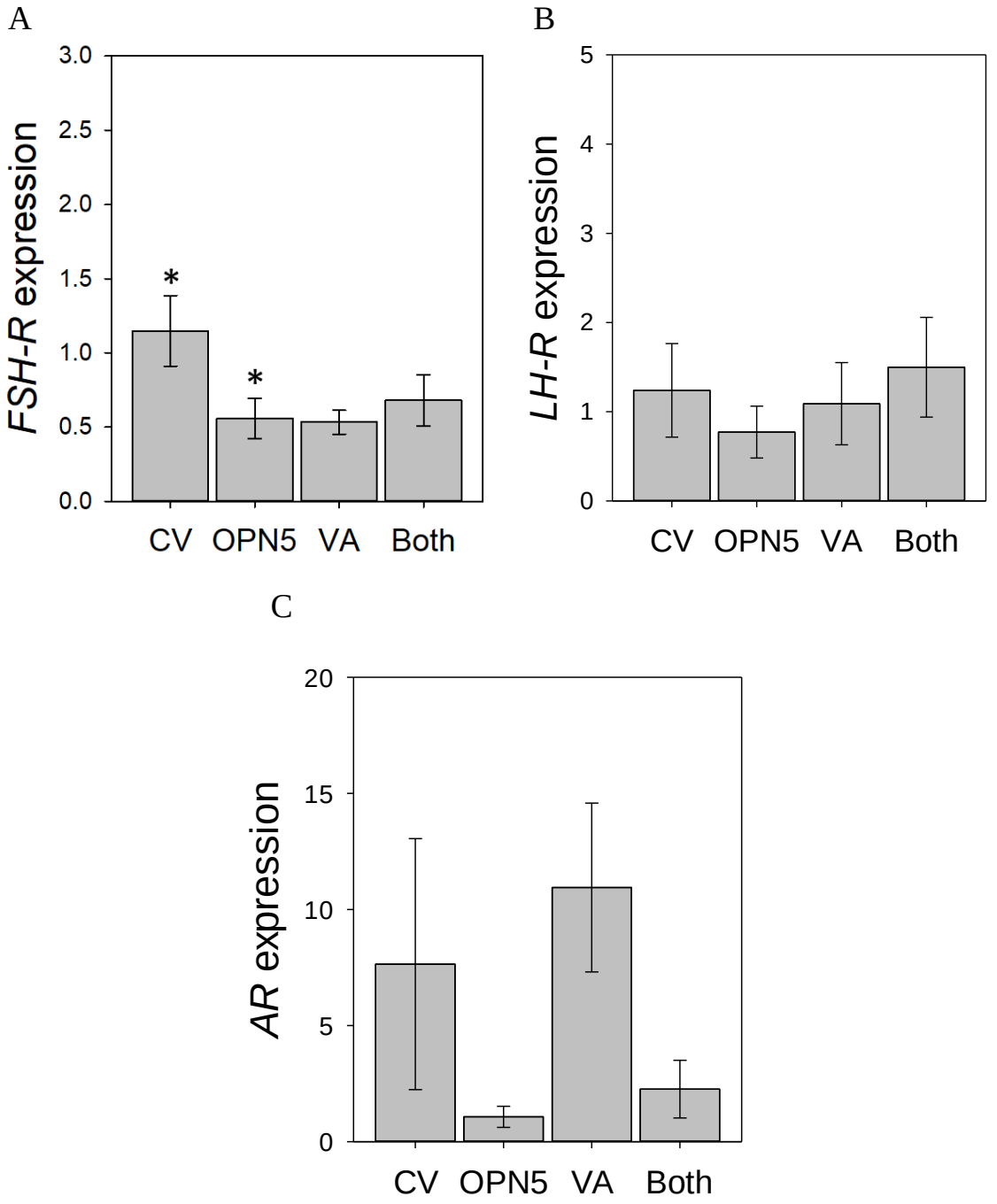

Figure 2.16. Photoperiodic regulation of receptor expression in the testes for the 28-day chronic study. mRNA levels of follicle stimulating hormone receptor (*FSH-R*) (A), luteinizing hormone receptor (*LH-R*) (B) and androgen receptor (*AR*) (C) in quail testes. A subset of SD-CV quail was collected and used as a reference group (CV). All birds were then moved to long days and collected after 28 days. Asterisks (*) represent significance between groups. Results are mean ± SEM. CV= long-day, control virus (N=8); OPN5= OPN5 knockdown group (N=9); VA= VA Opsin knockdown group (N=9); Both= OPN5 and VA Opsin knockdown group (28d: N=7).

2.3.4 Plasma testosterone

Finally, plasma testosterone levels were measured in 2-day, 7-day and 28-day quail. At 2 days, there was no effect of treatment on plasma testosterone ($F=0.922$; $p=0.451$) (Figure 2.17A). After 7 days of photostimulation however, there was a significant effect of treatment ($F=31.693$; $p<0.001$), specifically an increase in testosterone in CV, OPN5, VA and Both groups, compared to SD (Figure 2.17B). At 28 days no change was seen between treatment groups, but there was a significant increase in CV, OPN5 and VA testosterone levels, compared to the SD group ($F=8.105$; $p<0.001$) (Figure 2.17C).

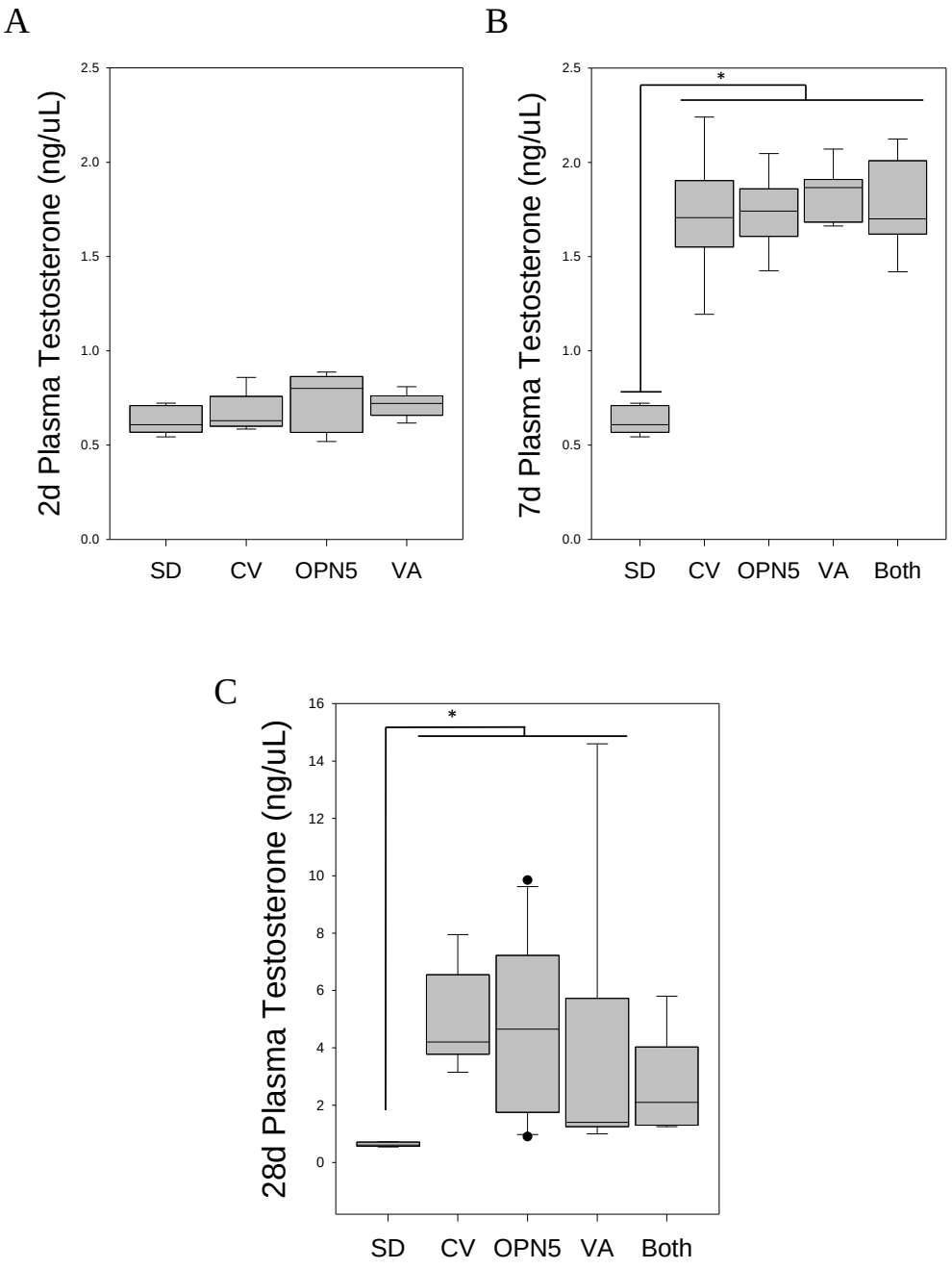

Figure 2.17. Plasma testosterone across the photoperiodic response. In short days (SD), male quail received ICV injections that consisted of control virus (CV). A subset of SD-CV quail was collected and used as a reference group. All birds were then moved to long days and collected after 2 days, 7 days, or 28 days. Plasma testosterone levels are similar to previous reports (Follett and Maung, 1978). Asterisks (*) represent significance between groups. Results are mean ± SEM. SD= short-day, control virus (N=5); CV= long-day, control virus (2d: N=5; 7d: N=9; 28d: N=8); OPN5= OPN5 knockdown group (2d: N=5; 7d: N=7; 28d: N=9); VA= VA Opsin knockdown group (2d: N=8; 7d: N=9; 28d: N=9); Both= OPN5 and VA Opsin knockdown group (7d: N=8; 28d: N=7).

2.4 Discussion

2.4.1 Confirmation of knockdown

This study aimed to explore the function of two candidate deep-brain photoreceptors, VA Opsin and OPN5, and their role in regulating seasonal reproduction in the Japanese quail, *Coturnix japonica*. To achieve this, two adeno-associated viral constructs were designed that targeted VA Opsin and OPN5 sequences, silencing their expression, and were injected in the third ventricle (3V) of the hypothalamus. After receiving the injections, quails were either maintained at SD or photostimulated for 2, 7 or 28 days.

To confirm photoreceptor knockdown, both mRNA and protein levels of OPN5 and VA Opsin were measured in 2-day and 7-day hypothalami. It was found that around 95% of gene expression was silenced in all treatment groups. Regarding protein levels, around 40-50% of protein was knocked down, except for the 2-day VA group.

GFP expression was then examined in 28-day quail hypothalami (Figure 2.2C and D). Fluorescence was detected in cells lining the 3V and the paraventricular organ (PVO) of the hypothalamus, confirming successful AAV injection in target brain regions. VA and OPN5 antibodies were also used on hypothalamic sections of 28-day quail. OPN5-expressing cells were found in the PVO and 3V, which parallels previous findings (Nakane and Yoshimura, 2010). VA-immunoreactivity was identified in the preoptic area (POA), consistent with earlier studies on VA Opsin (Halford et al., 2009). Taken together, these data show successful AAV injection and viral transfection in Japanese quail target brain areas.

2.4.2 Peripheral measurements

In order to evaluate reproductive effects, different indicators of reproductive maturation were used, including gonadal mass, cloacal area, whole-tissue gene expression, and plasma testosterone levels. Testis mass exhibited no change between SD control virus animals and treated individuals after 2 days (2d) of LD. Both the 2d SD CV group and the 2d treated groups had small testes, consistent with the phenotypic differences between Japanese quail in a LD summer condition and a SD non-breeding condition. However, when observing testes after 7 days (7d) of photostimulation, there was a significant increase in gonadal mass in LD treated birds, irrespective of injection, compared to SD control animals, consistent with the known effect of long photoperiods on gonadal mass increase. There was a pattern, though not statistically significant, for an increase in testes weight in LD treated birds compared to LD CV animals, the largest effect seen in animals that received both VA Opsin and OPN5 viral constructs, suggesting that the suppression of opsin expression may be able to facilitate testicular growth. This non-significant increase in testes mass in 'Both' birds can be attributed to an additive effect of the knockdown of both opsins, suggesting a possible inhibitory role for one or both photoreceptors. By silencing the opsins, the inhibitory input is removed, causing a surge in gonadal mass. The lack of significance in this pattern may be due to low samples size and incomplete protein knockdown (Figure 2.2B). After 28 days (28d) of exposure to LD, there was no significant change in testes mass between long-day control and treated birds. This was expected, as 28 days of photostimulation induces marked gonadal growth in Japanese quail (Follett and Maung, 1978). Since complete gonadal recrudescence is achieved at around 28-30 days after exposure to a 16L:8D photoperiod (Follett and Maung, 1978), removing the photoreceptor(s)' inhibitory output did not elicit an even bigger increase in testes mass. Taken together, this data suggests that both photoreceptors may be tied to the control of seasonal reproduction in Japanese quail. Regarding body mass, no change was seen

between treatment. This constant body mass between long and short photoperiods is consistent with previous reports in the Japanese quail (Follett, Nicholls and Mayes, 1988).

In addition to measuring gonadal size as a proxy for seasonal reproduction, cloacal size was also monitored throughout the study. In normal long-day conditions, Japanese quail show an increase in cloacal size, and in non-breeding conditions cloacal size is decreased. In males, the cloaca functions as a sperm-storage organ. In this study, cloacal gland growth rate (*k*) was reduced in all three treatment groups (VA Opsin, OPN5 and Both) compared to control animals in the course of the 28 days. Taken together, the data suggests that there may be two distinct pathways involved in maturation of sexual characteristics, one leading to testes growth and one affecting cloacal size growth rate. Interestingly, previous studies have shown an increase in cloacal size in SD quail after testosterone treatment, suggesting long days are not required for cloacal gland enlargement during the breeding period (Schumacher and Balthazart, 1983). However, it appears that photoreceptors are, at least in part, involved in cloacal growth.

2.4.3 GNRH and GNIH

One of the most important components of seasonal reproduction in both mammals and birds is gonadotropin-releasing hormone (GNRH) (Herbison, 2016). GNRH is released from the median eminence in response to photostimulation and targets the gonadotrophs in the anterior pituitary, which, in turn, release LH and FSH, linking the brain to peripheral endocrine systems. No significant change was found in *GNRH* expression in the hypothalamus at 2 days post-photostimulation, as 2 days may not be sufficient time for *GNRH* expression to increase. This is also consistent with the small testes phenotype seen in 2-day birds (see section 4.1). However, at 7 days post-photostimulation, there was a significant increase in *GNRH* expression in VA-treated birds compared to SD individuals. In addition, similar to gonadal mass, there appears to be a pattern for a gradual increase in *GNRH* expression when inhibiting VA Opsin and OPN5, reaching its peak in individuals

that received both VA Opsin- and OPN5-targeting viral sequences. However, this gradual increase was found not to be statistically significant. As stated previously, this may be due to low samples size and/or incomplete protein knockdown (Figure 2.2B). This data may again suggest an inhibitory role of one or both candidate photoreceptors, consistent with the testes data presented above.

Unlike GNRH, the role of GNIH in avian seasonal reproduction is unclear. Gonadotropin-inhibitory hormone (GNIH) receptors are expressed in the median eminence in quail and gonadotropes in the pituitary gland in quail and chickens (Tsutsui et al., 2009; Ubuka et al., 2013). In this study, *GNIH* expression in the hypothalamus did not exhibit a change at 2 days or 7 days post-photostimulation. This result suggests that inhibiting VA Opsin and OPN5 in male Japanese quail does not change *GNIH* levels in the hypothalamus.

2.4.4 DNA methyltransferase expression in the hypothalamus

As discussed in the introductory section, rhythmic and predictable oscillations of epigenetic enzymes have been shown to be involved in the onset of seasonal reproduction. In this study, DNA methyltransferase *1, 3A* and *3B* expression was explored in the hypothalamus. When comparing 2-day control virus (CV) and short-day control virus (SD) individuals, there was no change in hypothalamic expression of *DNMT1, 3A* and *3B* enzyme in SD animals, although there was a pattern in lower *DNMT1, 3A* and *3B* expression in SD, although not significant. This reduction in DNA methyltransferase expression is consistent with previous studies (Stevenson and Prendergast, 2013; Lynch et al., 2016; Tolla and Stevenson, 2020b). After 2 days of photostimulation, no change in expression of *DNMT1, 3A* or *3B* was shown. However, after 7 days of LD, there is an overall reduction in gene expression of all three Dnmt enzymes in OPN5 and 'Both' treated birds. Since levels are maintained at higher levels in the VA group, this implies that the decrease in 7-day hypothalami in 'Both' animals may be caused by the OPN5-silenced

group. Interestingly, when comparing OPN5 individuals at 2 days and OPN5 individuals at 7 days, there is a trend for a reduction in *DNMT3B* expression in 7-day animals (p=0.0536). Contrary to what the testes data suggests, this *DNMT3B* decrease after 7 days of photostimulation in OPN5-silenced birds points to a possible stimulatory role for OPN5, but only if *DNMT3B* levels are reduced in normal short-day quail hypothalamic, similar to other seasonal species (Stevenson and Prendergast, 2013; Tolla et al., 2020b). Further experiments, such as examination of *DNMT* expression and global methylation in the hypothalamus of LD and SD Japanese quail, and the investigation of promoter region of VA Opsin and OPN5, are required in order to delineate the association between DNA methyltransferase enzymes and deep-brain photoreceptors.

2.4.5 Pituitary gene expression

Expression of *TSHB, LHB,* and *FSH* was analysed in the pituitary gland of 2-day, 7-day and 28-day animals. In 28-day quails, gonadotropin-releasing hormone receptor (*GNRH-R*) levels were also measured, as *GNRH-R* has been shown to be strongly regulated between SD and LD photoperiods in chickens, increasing during the breeding period (Bédécarrats et al., 2006). Two important components of the reproductive axis in eliciting reproductive characteristics are LH and FSH. In this study, *LHB* expression did not change in response to AAV treatment. However, at 28 days there was a pattern for decreased *LHB* expression in response to RNAi treatment in a similar manner to the decrease in cloacal area, although not statistically significant. On the other hand, *FSH* expression increased at 2 days in VA Opsin, OPN5 and Both groups, compared to the SD group. At 7 days, there was significant rise in *FSH* levels in ‘Both’ individuals compared to SD, but again not between LD treatments. This *FSH* increase in ‘Both’-injected quail at 7 days reflects testes mass and *GNRH* expression pattern in the hypothalamus (section 4.3), further suggesting that at least one of the two candidate photoreceptors is involved in seasonal breeding mechanisms in the Japanese quail. After 28 days of photostimulation, there was no

difference in *FSH* expression between treatment groups. In addition, overall *FSH* levels were much higher after 2 days of photostimulation, compared to 7 or 28-day pituitaries. This may be because of negative feedback: after 4 weeks of long-day, increased sex steroid production, caused by FSH and LH action, inhibits GNRH release from the hypothalamus, preventing gonadotropin release. In future studies, it will be useful to determine FSH levels via radioimmunoassay to correlate gene expression to circulating FSH and the effect of injection on reproductive characteristics, as well as analysing *GNRH* gene levels in the hypothalamus of 28-day quail. The differential expression of *LHB* and *FSH* may be the driving factor leading to the opposite patterns of testes mass and cloacal growth rate. Taken together, this data again suggests that there may be two pathways acting separately, one that involves *LHB* and cloacal growth and one that involves *FSH* expression and testes mass, although this is yet to be investigated.

2.4.6 DNA methyltransferase enzyme expression in the pituitary gland

DNMT1 and *DNMT3A* expression was measured in 28-day quail pituitary glands. A significant decrease in *DNMT1* was found in VA K/D birds compared to control individuals, but no change was detected in *DNMT3A* levels between treatment groups. This *DNMT1* reduction in VA quails suggests that this enzyme may control the transcription of reproductive genes in the pituitary gland, and disrupting photoreceptor expression, specifically *VA Opsin*, down-regulates *DNMT1* expression. This may indicate that genes expressed in the pituitary, such as *LHB* and *FSH* may be differentially regulated in VA animals, affecting downstream pathways, such as steroid release from the gonads. Further experiments are needed to clarify the role of *DNMT1* in the pituitary gland of the Japanese quail.

2.4.7 Receptor expression in the testes

In birds, gonadotropins target Leydig and Sertoli cells in the testes to stimulate the production of androgens, such as testosterone. The expression of FSH receptors (*FSH-R*), LH receptors (*LH-R),* and androgen receptors (*AR*) has been shown to rise during the breeding period in the Japanese quail, allowing for increased gonadotropin and androgen sensitivity (Brown and Follett, 1977; Tsutsui and Ishii, 1978; Ottinger et al, 2002). This increase leads to the maturation of reproductive characteristics, such as enlarged gonads and marked reproductive behaviour. In this study, mRNA expression of *FSH-R, LH-R,* and *AR* was measured in the testes of 2d, 7d and 28d quail, in order to relate it to testes mass and plasma testosterone patterns.

In 2d gonads, no difference in receptor expression was found between treatments. This was expected, as testes mass and *GNRH* expression did not exhibit any change after 2 days of photostimulation. However, given that 2d *FSH* expression did increase in LD treated animals, but its receptors did not, this may suggest that 2 days of LD are sufficient to increase *FSH* expression, but not sufficient to reflect receptor levels in the gonads. Similar to 2d, at 7d no significant effects were found in receptor expression. Finally, 28 days of LD did not elicit a change in *LH-R* and *AR* expression. Chronically silencing the two candidate photoreceptors caused a significant reduction in *FSH-R* in OPN5 animals, compared to control quails. This suggests that OPN5 may play a role in increasing sensitivity to gonadotropins during the breeding months, at least after 28 days of LD, even if not directly affecting *FSH* release.

2.4.8 Plasma testosterone

In order to understand the testes and cloacal effects in this study, testosterone levels were measured in both control and treated quails. No changes were found in plasma testosterone between SD birds and treated individuals after 2 days, reflecting *GNRH*

expression. After 7 days of photostimulation, there was an expected increase in testosterone concentration in all LD groups, compared to SD. Similarly, at 28 days, a significant increase in testosterone was observed in CV, OPN5 and VA individuals, compared to birds maintained in SD. This suggests that even though overall *FSH* and *LH* levels are lowered after 28 days, compared to 2 and 7 days, testosterone is kept at high levels even after 28 days of LD. No change was detected between LD treatment groups at any time point.

2.5 Conclusions

The main aim of this study was to determine whether VA Opsin, OPN5, or both photoreceptors are involved in seasonal reproduction in the Japanese quail. It was hypothesised that silencing these two opsins through AAV injection in the 3V of the hypothalamus would cause a marked reduction in reproductive characteristics, such as testes mass, gonadotropin release and plasma testosterone levels. At 2d and 7d, values were compared to a short-day control group injected with a blank virus. At 7d, an additional 'Both' treatment group was added, that received a mix of both AAV, targeting both OPN5 and VA Opsin. After 2 days of photostimulation, *FSH* expression in the pituitary gland significantly increased in the LD treated groups compared to SD animals, regardless of treatment. However, other reproductive indicators, such as testes mass, *GNRH* and *LHB* expression and plasma testosterone did not change. This suggests that 2 days of photostimulation are sufficient for *FSH* expression to increase, but not sufficient to stimulate opsin function. At 7d, there was a pattern for an overall gradual increase in gonadal mass, *GNRH* expression and pituitary *FSH* expression with opsin knockdown, peaking when both photoreceptors were silenced. Although not statistically significant, this gradual increase may indicate that at least one of the two opsins is involved in regulating the hypothalamic-pituitary-gonadal axis through an inhibitory role. By disrupting the photoreceptors, therefore the inhibitory output, there is an increase in reproductive

indicators. The reason for the lack of significance between LD treatments at 7d may be due to the incomplete opsin protein knockdown in 7d animals (Figure 2.2B) and the low sample size of each treatment group. In future experiments, it will be essential to successfully knockdown more than 40% of VA Opsin and OPN5 protein expression in the hypothalamus. Interestingly, at 28d, a significant decrease in *FSH-R* levels was found in the testes in OPN5 animals compared to the CV group, although no change was seen in testes mass, *FSH* or *LHB* expression between treatments. This may point to a chronic role for OPN5 in controlling sensitivity to gonadotropins during breeding through a stimulatory output. By removing this stimulatory output, *FSH-R* levels are reduced, decreasing the reproductive response in quail.

Given the emerging role of DNA methylation and DNA methyltransferase enzyme in seasonal reproduction in mammals, *DNMT1, 3A* and *3B* expression was also investigated, both in the hypothalamus and pituitary gland of Japanese quail. In the hypothalamus, a non-significant decrease in *DNMT3B* expression was found in 7d hypothalami of OPN5 quail compared to 2d OPN5 animals ($p=0.0536$). This trend in reduction may further suggest a stimulatory role for OPN5: by silencing OPN5, there is a decrease in *DNMT3B* levels, perhaps reflecting a SD expression pattern. This hypothesis was further explored in chapter 3. This trend may not be statistically significant due again to the lack of complete protein knockdown at 7d. When analysing gene expression in the pituitary gland, a significant decrease was also shown in *DNMT1* in 28d VA individuals, compared to CV. This difference in *DNMT1* may suggest that silencing VA Opsin leads to a reduction in DNA methylation, perhaps in promoter regions of pituitary genes involved in reproduction, such as LH and FSH. Taken together, these data point to potential differential effects of VA Opsin and OPN5, as well as LH and FSH, in regulating reproductive physiology in the Japanese quail. The pilot data presented in this chapter can be used to power future, larger-scale experiments.

It is possible that either VA Opsin or OPN5 are not acting alone, and instead that the activation of reproduction in birds is the result of the interaction between a variety of photoreceptors in the hypothalamus. Moreover, each opsin could be responsible for different aspects of avian reproduction. The interaction of different opsins could potentially be advantageous, as they would be able to respond to a range of wavelengths, activate diverse reproductive pathways or brain regions, and as a result, provide increased efficiency and reproductive success during breeding seasons. Additional studies are needed to map the molecular pathways that deep-brain photoreceptors utilise to trigger seasonal reproduction in the Japanese quail.

Chapter 3 – Expression of Deep-Brain Photoreceptors During Development of the Japanese Quail and the Role of Corticosterone

3.1 Introduction

3.1.1 Seasonal rhythms and stress

As discussed in the previous chapters, seasonally-breeding species exhibit a range of physiological, behavioural and morphological changes between the breeding and non-breeding periods. These changes are modulated by pathways such as the Hypothalamic-Pituitary-Gonadal (HPG) axis, responsible for reproduction, and the Hypothalamic-Pituitary-Adrenal (HPA) axis, or the stress axis. The HPA axis mediates the stress response through glucocorticoid (GC) release, such as corticosterone (CORT). Stress can be defined as any condition which causes allostatic load to an organism, an increase in the cost of maintaining physiological homeostasis (Henriksen et al., 2011). High GC levels have been associated with inhibition of the reproductive response in order to redirect energy expenditure to survival of the individual (Free and Tillson, 1973; Sapolsky, 1987). However, numerous studies have shown that in non-mammalian vertebrates, GC levels are often increased during the breeding period, in both stressed and non-stressed animals, *e.g.* white-crowned sparrows (*Zonotrichia leucophrys*) (Romero and Wingfield, 1999; Casagrande et al., 2018). In addition, testosterone exposure elevated GC levels in free-living birds (Ketterson et al., 1991), suggesting an intricate interaction between the adrenal and gonadal pathways (Romero, 2002). In 2018, Casagrande and colleagues proposed that levels of GC during the year, especially during the breeding months, vary between species depending on the degree of reproductive investment in each species (Casagrande et al., 2018). If energy expenditure is higher, GC levels will likely be elevated as well (Casagrande et al., 2018). Further studies are required to precisely determine the causes of yearly changes in GC release.

3.1.2 Avian response to pre-natal stress

During both development and adulthood, organisms are affected by a multitude of environmental stressors, such as limited food availability. During development, maternal hormonal signals, including corticosterone release, reach the embryo through crossing the placental barrier in viviparous species, and through targeting the egg yolk in oviparous organisms (Hayward et al., 2005). The hormonal transfer between mother and embryo provides the embryo with an indication of external surrounding environmental conditions (Gluckman and Hanson, 2004), aiding in adaptation and survival in the postnatal environment. Stress during development and the physiological responses to stress have been shown to persist into adulthood to maximise offspring survival, although chronic exposure to negative conditions, such as limited food availability, has been shown to be linked to a higher risk of adverse health conditions (Cottrell and Seckl, 2009). However, there is some evidence suggesting that environmental stressors at low levels can have a beneficial effect on the health and survival of the organism (Costantini et al., 2010), especially if embryonic conditions match environmental conditions postnatally (Gluckman and Hanson, 2004; Zimmer, Boogert and Spencer, 2009; Henriksen et al., 2011). Most research on stress and embryonic development has been done in mammals, and it appears that sex-specific effects exist, where females are more susceptible to stress exposure during the prenatal period (Benoit et al., 2015). Birds, however, are excellent models to explore the effects of glucocorticoid exposure in early-life stages, as avian embryonic development occurs outside the mother and inside an egg. In chicken, offspring of stressed mothers have a significantly lower body mass compared to those of healthy mothers, both at hatching (Love et al., 2005) and later in adult life (Hayward and Wingfield, 2004; de la Cruz et al., 1987). If the postnatal environment of these smaller offspring matches the stressful conditions of the mother prenatally, for instance limited food supply, having a smaller body mass may be beneficial, as the organism would need less food to survive (Henriksen et al., 2011). However, if the environmental conditions do not match pre-hatching

hormonal cues, lower body mass may be a disadvantage to the animal and decrease its survival. The ways by which glucocorticoids contribute to animal fitness are then either advantageous or detrimental depending on the differences between pre- and post-natal environments (Henriksen et al., 2011). Studies that explored the effects of elevated CORT levels in stressed female chickens also found gonadal size reduction, reduced sexual maturity and a decrease in immune response in offspring (Satterlee et al., 2007; Love et al., 2005), indicating that stressful conditions in mothers can negatively impact offspring development. In addition, a maternal plasma CORT-dependent shift in offspring sex ratio has been reported in Japanese quail (Pike and Petrie, 2006) and the house finch (*Carpodacus mexicanus*; Badyaev et al., 2002), generally favouring females. These data suggest that maternal elevated glucocorticoid levels can cause profound physiological changes to offspring during critical embryonic stages.

3.1.3 Epigenetics and the stress response

Epigenetics and the stress response are closely linked, as they are both mechanisms of response to the surrounding external environment. Stress is able to alter an individual's epigenome, and epigenetic processes can modulate an organism's response to stressful conditions. In mammals, prenatal exposure to glucocorticoids has been associated with altered gene expression caused by a change in DNA methylation patterns (Crudo et al., 2012; Oberlander et al., 2008; Alikhani-Koopaei et al., 2004). The epigenetic response to glucocorticoid exposure has been investigated in both mammals and birds. In 2004, Weaver and colleagues explored changes in DNA methylation patterns in offspring of stressed rat mothers (Weaver et al., 2004). They found that stressed mothers showed reduced licking and grooming behaviour towards their pups, causing an increase in glucocorticoid receptor (GR) promoter methylation in the hippocampus of offspring. This switch in DNA methylation patterns at the GR level was shown to be reversible through cross-fostering and was supported by later studies (Weaver et al., 2004; Kosten et al.,

2013). The study by Weaver *et al* suggests a stress-dependent maternal epigenetic programming of the HPA axis in offspring. In later studies, maternal prenatal stress during critical developmental stages in mice was shown to increase methylation of the GC promoter in the hippocampus and decrease methylation of corticotropin-releasing hormone (CRH) (Mueller and Bale, 2008), as well as an increase in DNA methyltransferase 1 (DNMT1) protein in the same region of the brain (Benoit et al., 2015). Recent experiments have also shown changes to the foetal epigenome in peripheral tissues, such as adrenal gland and liver (Thomassin et al., 2001; Crudo et al., 2012) following glucocorticoid treatment. Taken together, these studies suggest that glucocorticoid exposure during early stages in mammalian development alters the epigenome of an individual in a range of tissues, including the brain.

Avian embryonic exposure to glucocorticoids and tissue-specific epigenetic effects are not as well-characterised as they are in mammals. In neonatal male chicken kept in a LD condition, food restriction for 12 continuous hours caused an increase in *DNMT1* and *DNMT3B* expression compared to individuals fed normally (Kang et al., 2017). Exposure to predatorial stress, experimentally simulated by predatorial alarm calls, has also been shown to significantly increase global methylation levels in yellow-legged gull (*Larus michahellis*) embryos (Noguera and Velando, 2019). This increase in DNA methyltransferase enzymes and global DNA methylation following nutritional and predatorial stress respectively, suggests that stress is able to modulate the epigenetic profile in the avian brain as well as the mammalian one. Taken together, these data indicate a role for epigenetic mechanisms, especially DNA methylation, in mediating stressful conditions in both the embryo and later in life in mammals and birds. However, most of the reports concerning the effects of stress in developmental stages have been carried out in mammals, and avian studies in the field generally investigate hippocampal epigenetic plasticity. The hippocampus is often studied in the context of stress and epigenetic modifications because

it is a region of the brain which is highly plastic and sensitive to environmental changes and learned behaviour (Cunha et al., 2010; Sweatt, 2009).

3.1.4 Deep-brain photoreceptor development

As outlined in chapters 1 and 2, the identity of the deep-brain photoreceptor(s) that are responsible for seasonal reproduction in the avian brain is still unclear. In addition, the development of brain opsins and how they can affect the development of an embryo is currently not known, as most of studies focus on retinal development rather than the brain, especially in mammals. In chicken embryos, Vertebrate Ancient opsin (VA Opsin) expression was found in the midbrain, hindbrain and diencephalon from embryonic day 2 (E2) (Tomonari et al., 2007). OPN5-like proteins have been detected in the retina of chick embryos at E7 (Rios et al., 2019), however no detailed report of OPN5 expression in the avian brain has been published yet. To explore whether opsins are essential for embryonic development, Hang and colleagues inserted a VA Opsin mutation in zebrafish embryos through CRIPR/Cas methods (Hang et al., 2016). Crossing a mutant female with a wild-type male resulted in foetal death, but caused late hatching in offspring of mutant males and wild-type females (Hang et al., 2016). It is important to note that extra-retinal photoreceptor function in fish is distinct from the role of deep-brain photoreceptors in birds. However, no similar studies have been done in the avian system to investigate opsin embryonic development and the role of stress in modulating photoreceptor maturation during early stages.

3.1.5 Aims and Hypotheses

In this chapter, two distinct studies allow for an exploration of both opsin expression during embryonic development and the role that glucocorticoid exposure plays in modulating epigenetic mechanisms. In study 1, Japanese quail (*Coturnix japonica*) eggs

were treated with corticosterone at various developmental stages. It was hypothesised that expression of neuropsin (OPN5) and vertebrate ancient opsin (VA Opsin) would increase in late embryonic development, and that DNA methyltransferase enzyme expression would increase with corticosterone injections.

In study 2, adult, sexually mature Japanese quail were maintained in either a long-day (LD; 18L:6D) or short-day (SD; 6L:18D) condition. The purpose of study 2 was to explore hypothalamic DNA methyltransferase expression in adult individuals, as well as investigate VA Opsin and OPN5 levels in birds kept under reproductive photoperiodic conditions or non-breeding light conditions. It was hypothesised that both DNA methyltransferase and opsin expression would decrease in SD.

3.2 Methods

3.2.1 Animals

3.2.1.1 Study 1

All procedures were approved by the local ethics committee at the University of St. Andrews and in accordance with the Animals (Scientific Procedures) Act 1986 ASPA regulations under PIL IE1CF3B75 held by Jessica-Lily Harvey and PPL 70/8159 held by Dr Karen Anne Spencer. All procedures were in accordance with the ARRIVE Guidelines for ethical research on animals.

78 Japanese quail (*Coturnix japonica*) eggs (Moonridge farm, Exeter, UK) were kept under constant darkness on a rotating platform at 37.4^{o}C with 60% humidity. They were incubated all at the same time (Ova-Easy 190A, Brinsea Products Ltd, UK) and injected at embryonic day 5 at the apex with l0µl of 850 ng/ml corticosterone (CORT) diluted in sterile peanut oil (Sigma Aldrich, Poole, UK), similar to a previous study (Zimmer et al., 2013). This dose has been shown to increase CORT concentration in the yolk within 1.8 standard deviation of natural egg CORT ranges (Zimmer et al., 2013; Zimmer et al., 2017), and is similar to the CORT concentration that is deposited in the yolk following natural stressors (Love et al., 2008; Pitk et al., 2012). Control eggs were injected only with 10µL sterile peanut oil. All eggs were returned to the incubator within 30 minutes of the procedure. Tissue was collected from the eggs at embryonic day 11 (CORT n=8, control n=8), day 14 (CORT n=8, control n=7), and day 17 (CORT n=7, control n=5). A post-natal group was kept under 12L:12D conditions with *ad libitum* food (minced Turkey crumb, BOCM, UK) and food, and chicks were culled at postnatal day 10 (CORT n=14, control n=20). The brain and hypothalami were collected immediately and frozen at -80^{o} until further analyses.

3.2.1.2 Study 2

Adult male and female Japanese quail were maintained at the Roslin Institute, University of Edinburgh. All procedures were carried out under the Animals (Scientific Procedures) Act 1986, project license 70/7909 held by Dr Ian Dunn and individual experiments were approved by the institutional ethics committee. 3-week female and male quail were either photostimulated (18L:6D; n=9) or maintained in SD (6L:18D; n=8) for 12 days. Dissections were performed by A Yingua, IC Dunn and PJ Sharp 4 hours after lights off (Dunn et al., 2017).

3.2.2 RNA extraction

3.2.2.1 Study 1

RNA was extracted via Absolutely RNA miniprep kit (Agilent, UK) as per manufacturer's instruction. RNA concentrations were measured on a QuBit 2.0 flourometer using RNA HS Assay Kit (Thermofisher, UK).

3.2.2.2 Study 2

RNA was extracted by A Yingua, IC Dunn and PJ Sharp at the Roslin Institute, University of Edinburgh, using Ultraspec II reagent (AMS Biotechnology, Abingdon, UK) and Lysing Matrix D tubes in a FastPrep Instrument (MP Biomedicals, Cambridge, UK), as described in Dunn et al., 2017.

3.2.3 cDNA synthesis

For study 1, cDNA synthesis was carried out using Nanoscript2 Reverse Transcription Kits (Primer Design, UK). RNA concentration was normalized across all samples to 1.2 μg/μl made up to 10 μl in RNase free H2O, then 1 μl of primer (50 μM oligo dT) and 1 μl of annealing buffer were added. RNase-free H_2O was added to take the volume up to 100 μl before being stored at −20 °C until quantitative PCR (qPCR) assays.

For study 2, RNA was transferred on dry ice to the University of Glasgow, and cDNA synthesis was carried out using the same method used for study 1.

3.2.4 Real-time PCR (qPCR)

To measure mRNA expression, cDNA was assayed using qPCR for both studies. Primers for target genes were ordered from Invitrogen and optimised using gel electrophoresis as described in chapter 2, section 2.2.7. See Table 2.1 for detailed primer information. qPCRs were run on a BioRad CFX96 Real time PCR machine in a 20 µl reaction. For each well the qPCR mix consisted of 5 µl cDNA template, 10 µl SYBR green (PrecisionPLUS qPCR Master Mix with SYBR green) 0.5 µl (300 nM) forward primer, 0.5 µl (300 nM) reverse primer and 4 µl RNase-free H2O to make up to 20 µl. See Table 1 for primer information. All samples were run in duplicate in a 96-well plate format under the following cycling conditions; i) initial denaturing at 95 °C for 5 min, then 39 cycles of ii) 95 °C for 10 secs, iii) 30 secs at annealing temperature dependent on gene of interest (See Table 1), then iv) an extension step of 72 °C for 30 secs. For each gene analysed, including reference genes, there were no-template H2O controls included in the plate. Melt curve analysis was carried out to ensure only a single peak was produced for each reaction. PCR Miner (Zhao and Fernald, 2005) was used to determine reaction efficiencies (E) and quantification cycle (Ct). According to MIQE guidelines, samples with effciency values below 0.8 and above 1.2 were excluded from analyses (Bustin et al., 2009). Fold expression of each target gene was measured in relation to the average Ct for two reference genes (*Gapdh* and *Hprt*) and calculated using 2- (ΔΔCt).

3.2.5 Statistical Analyses

All statistical analyses were performed using SigmaPlot 13.0. Significance was determined at $p < 0.05$. Data were log-transformed in the event of a violation of normality

or equal variance. Study 1's results were analysed using Two Way ANOVA. For study 2, student's t-tests were used. For detailed statistical analysis information, refer to Tables A.1 and A.2 (Appendix A).

3.3 Results

3.3.1 Study 1

3.3.1.1 GNRH expression changes at different embryonic stages but is not affected by CORT treatment

Two Way Analysis of Variance revealed no interaction between age and treatment (F=0.397, p=0.756). A significant effect of age on *GNRH* expression was found (F=6.242, p=0.001), but there was no effect of CORT treatment (F=0.0310, p=0.861) (Figure 3.1).

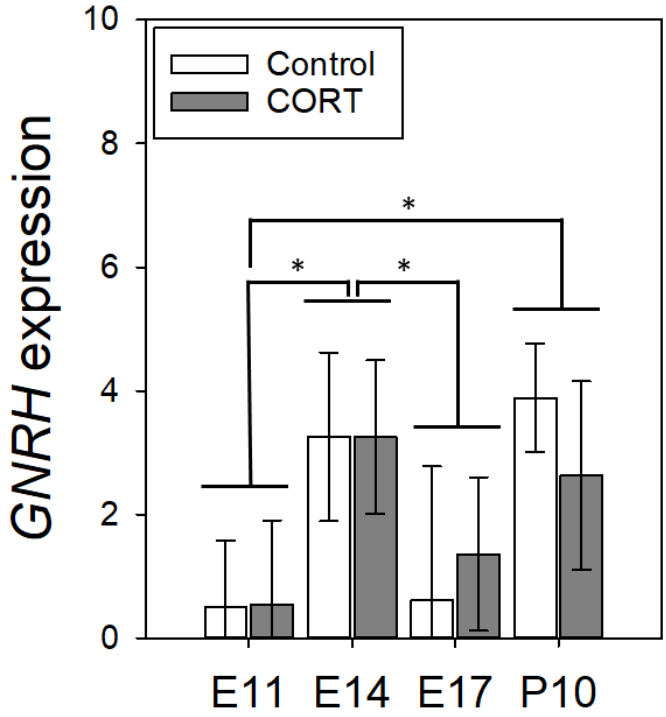

Figure 3.1. *GNRH* expression in control and corticosterone-treated samples (CORT). Asterisks (*) represent significance between groups. Results are mean ± SEM. E11= embryonic day 11 (control: N=8; CORT: N=8); E14= embryonic day 14 (control: N=8; CORT: N=7); E17= embryonic day 17 (control: N=7; CORT: N=5); P10= postanal day 10 (control: N=14; CORT: N=20).

3.3.1.2 DNA Methyltransferase expression varies between ages and CORT treatment has a significant effect on DNMT1 and DNMT3B levels

When analysing *DNMT1* expression, no interaction effect of age and CORT treatment was detected ($F=0.655$; $p=0.584$). However, there was a significant effect of age ($F=18.392$; $p<0.001$) and CORT treatment ($F=8.594$; $p=0.005$) (Figure 3.2A). Fisher's LSD post-hoc test revealed a significant increase in *DNMT1* expression in E14, E17 and P10 animals, compared to E11. There was also a significant *DNMT1* decrease in E17 hypothalami compared to E14.

There was no interaction effect of age and CORT on *DNMT3A* expression ($F=1.345$, $p=0.271$). A significant effect of age on *DNMT3A* expression ($F=3.824$, $p=0.016$) was detected, but no effect of CORT ($F=0.858$, $p=0.359$) was found (Figure 3.2B). Fisher's post-hoc method indicated a significant increase in *DNMT3A* levels in E14 and E17 animals, compared to E11.

Finally, two-way ANOVA analysis revealed a significant interaction of age and treatment ($F=4.683$, $p=0.006$) on *DNMT3B* levels (Figure 3.2C). E17 *DNMT3B* expression was significantly increased in control individuals compared to the E11 control group. Within CORT-treated treatment groups, a significant difference was found in E14, E17 and P10 compared to E11. Similar to *DNMT1* expression patterns, *DNMT3B* was significantly decreased in E17 compared to E14 individuals.

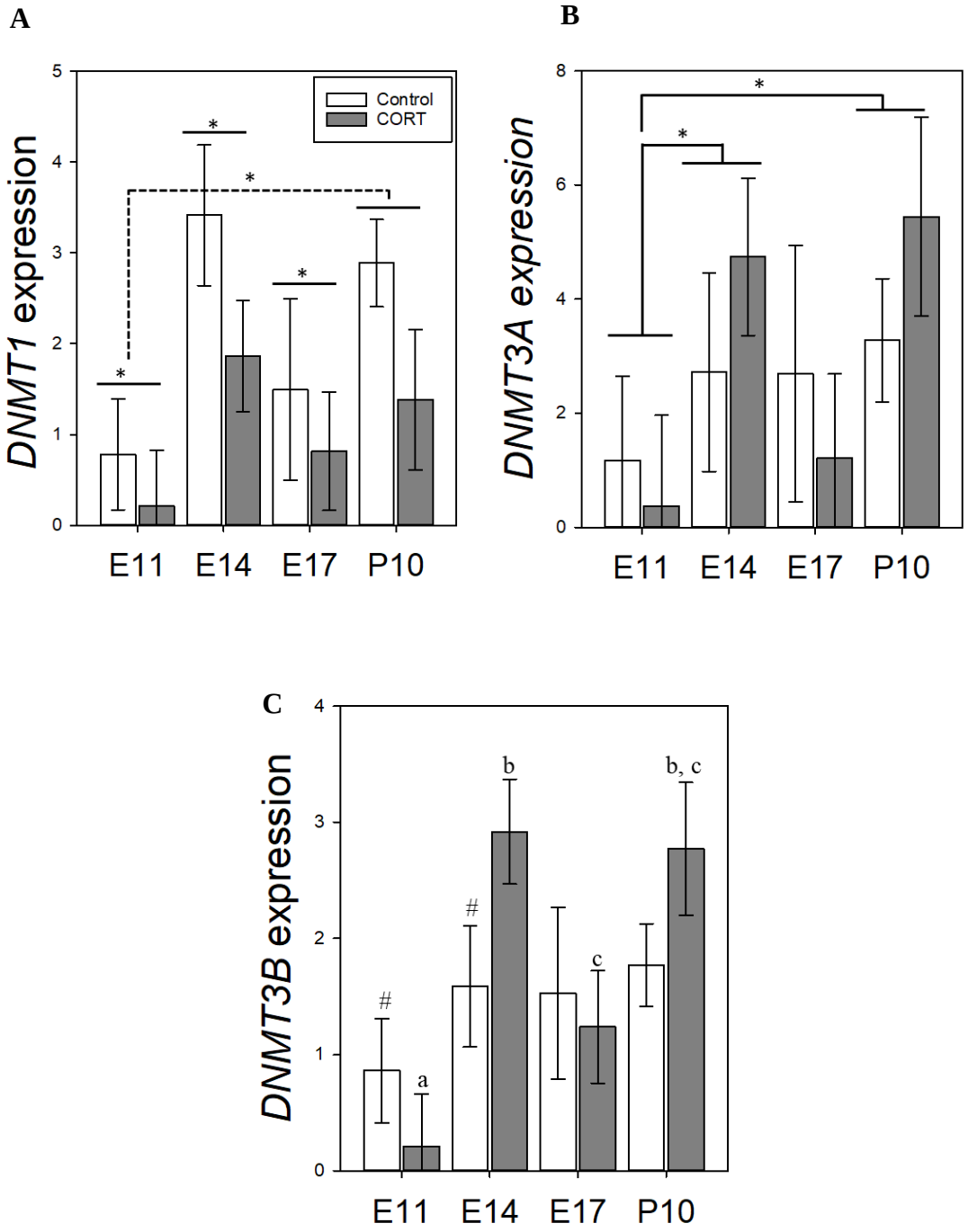

Figure 3.2. Average gene expression of *DNMT1* (A), *DNMT3A* (B) and *DNMT3B* (C) in the hypothalamus of quail at embryonic day 11, 14, 17 and post-natal day 10. Asterisks (*) represent significance between groups. In (C), # represent a significant difference between E11 and E14 controls; different letters represent significance within the CORT-treated group. Results are mean ± SEM. E11= embryonic day 11 (control: N=8; CORT: N=8); E14= embryonic day 14 (control: N=8; CORT: N=7); E17= embryonic day 17 (control: N=7; CORT: N=5); P10= postanal day 10 (control: N=14; CORT: N=20).

3.3.1.3 OPN5 expression increases at E14, decreasing again at P10

The expression of *VA Opsin* and *OPN5* was analysed in the quail hypothalami, both pre-natally at embryonic day 11, 14, 17 and post-natally at day 10. There was no effect of the interaction of age and treatment (F=0.693, p=0.564) on *VA Opsin* expression. *VA Opsin* expression did not change in response to CORT treatment (F=0.0632, p=0.803), or between ages (F=1.692, p=0.191) (Figure 3.3A). When analysing the expression of *OPN5*, there was no significant effect of the interaction between age and CORT (F=3.010, p=0.069). However, a significant effect of age was found (F=7.103, p=0.004), but no effect of CORT (F=3.729, p=0.066). A significant surge in *OPN5* levels was observed at embryonic day 14 (Figure 3.3B), decreasing again at postnatal day 10, similar to the pattern of *GNRH, DNMT1* and *DNMT3B* expression (Figure 3.1).

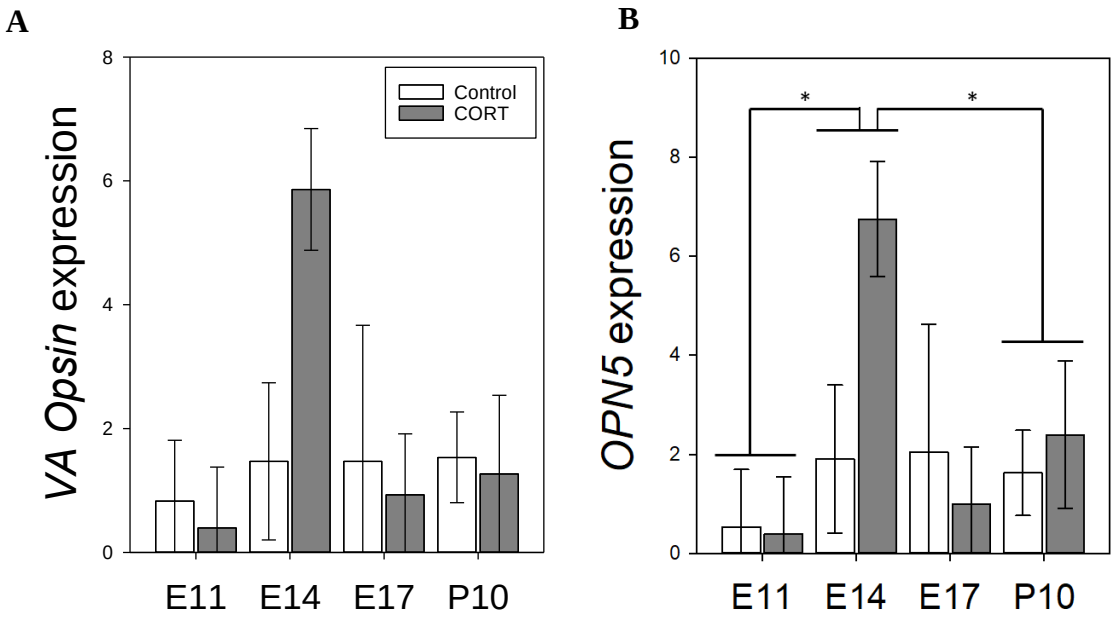

Figure 3.3. Hypothalamic expression of *VA Opsin* in quail at embryonic day 11, 14, 17 and postanal day 10 (A), and *OPN5* in quail at embryonic day 11, 14 and postnatal day 10. Asterisks (*) represent significance between groups. Results are mean ± SEM. E11= embryonic day 11 (control: N=8; CORT: N=8); E14= embryonic day 14 (control: N=8; CORT: N=7); E17= embryonic day 17 (control: N=7; CORT: N=5); P10= postanal day 10 (control: N=14; CORT: N=20).

3.3.2 Study 2

3.3.2.1 TSHB expression decreases in SD

In study 2, adult quail were either photostimulated for 12 days or maintained under short-day conditions. No significant change was detected in *GNRH* (p=0.159) or *GNIH* (p=0.140) expression. *TSHB* levels significantly decreased during SD (p<0.001) (Figure 3.4).

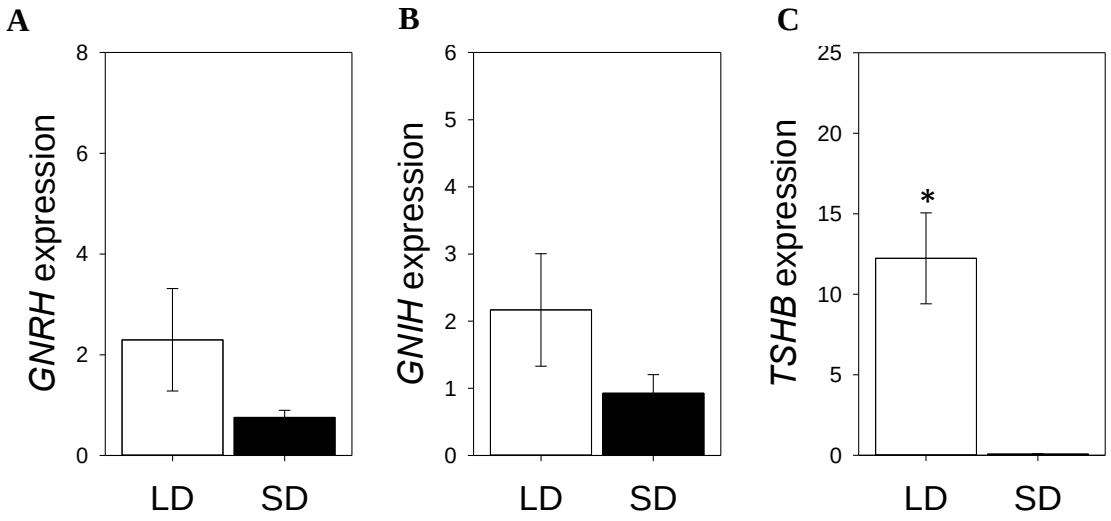

Figure 3.4. Hypothalamic expression of *GNRH* (A), *GNIH* (B) and *TSHB* (C) in adult quail maintained in long day (LD) or short day (SD). Results are mean ± SEM. LD= 18L:6D; N=9; SD= 6L:18D; N=8. Asterisks (*) represent significance between groups.

3.3.2.2 DNMT3A and DNMT3B expression tends to decrease in SD

DNA methyltransferase *1*, *3A* and *3B* levels were examined in the hypothalamus of adult quail. No difference in *DNMT1* (p=0.727), *DNMT3A* (p=0.436), or *DNMT3B* (p=0.334) expression was detected between the two photoperiodic conditions (Figure 3.5). There was a pattern for lower *DNMT3A* and *DNMT3B* expression in SD compared to LD, although it was not statistically significant.

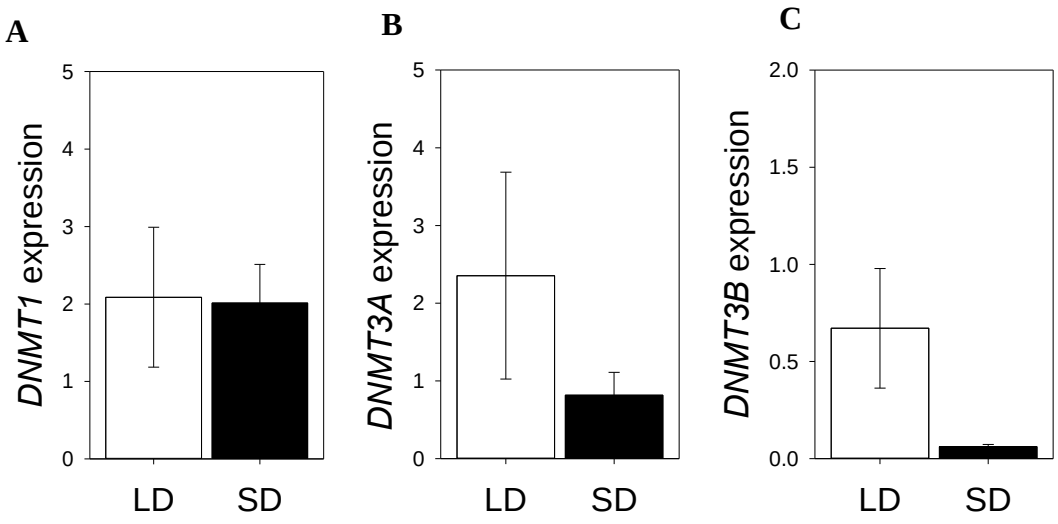

Figure 3.5. Hypothalamic expression of *DNMT1* (A), *DNMT3A* (B) and *DNMT3B* (C) in adult quail maintained in long day (LD) or short day (SD). Results are mean ± SEM. LD= 18L:6D; N=9; SD= 6L:18D; N=8.

3.3.2.3 Deep-brain photoreceptor expression tends to decrease in SD

The expression of two photoreceptors involved in seasonal reproduction was analysed in the adult quail hypothalamus. No significant change was seen in *OPN5* (p=0.194) or *VA Opsin* (p=0.475) gene levels between LD and SD hypothalami. However, there seemed to be a pattern of decreased photoreceptor expression in SD (Figure 3.6).

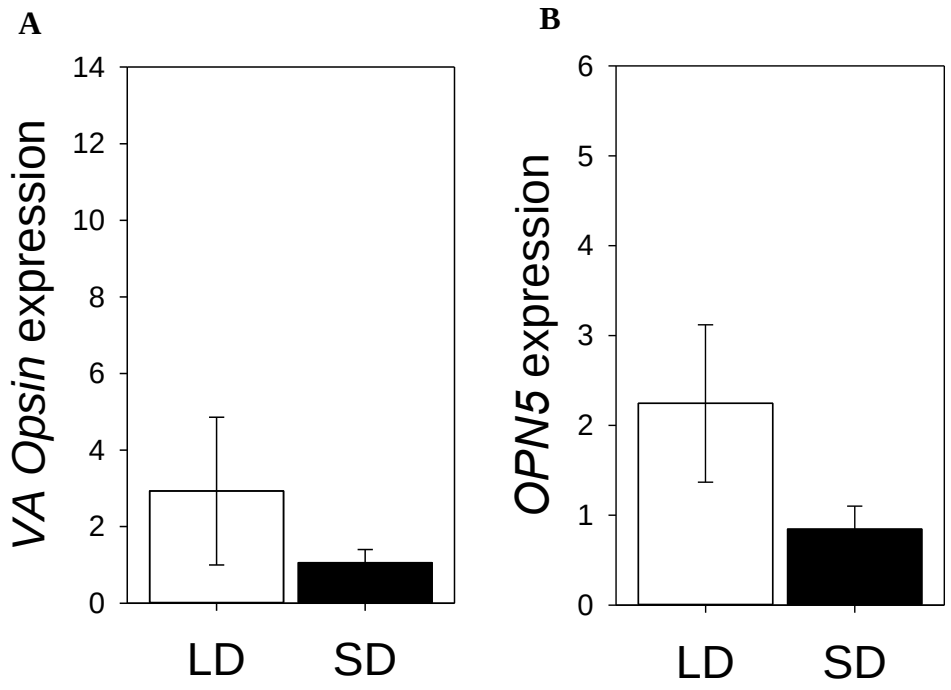

Figure 3.6. Hypothalamic expression of *VA Opsin* (A) and *OPN5* (B) in adult quail maintained in long day (LD) or short day (SD). Results are mean ± SEM. LD= 18L:6D; N=9; SD= 6L:18D; N=8.

3.4 Discussion

In this chapter, I presented data gathered from two different studies, both in *Coturnix japonica.* In study 1, gene expression levels were measured in the hypothalami of Japanese quail at three different embryonic stages (E11, E14 and E17) and at postnatal day 10. Quails were either injected with corticosterone or with peanut oil as a control. Study 2 examined hypothalamic gene expression in adult quails maintained either under long-day photoperiods or short-day photoperiods.

In Study 1, a significant effect of age was found in *GNRH* expression, with levels increasing at E14 compared to E11, decreasing again at E17. *GNRH* levels were also found to be upregulated postnatally, compared to E11. The temporary increase in *GNRH* expression at E14, comparable to P10 expression levels, may indicate a critical developmental day in Japanese quail embryos. The upregulation of *GNRH* at P10 may reflect reproductive maturation development in young birds maintained at 12L:12D. CORT injections did not elicit a change in hypothalamic *GNRH* expression at any age. One study that investigated long-term effects of embryonic CORT injections in chickens, found a significant reduction in hypothalamic *GNRH* mRNA in adults that were previously treated with CORT, compared to controls (Ahmed et al., 2014). However, the experiment did not take into consideration photoperiod, therefore a markedly-seasonal species such as the Japanese quail may exhibit different effects in reproductive markers. Nonetheless, in future studies, it would be useful to measure *GNRH* expression in the hypothalamus of adult, sexually mature quail that were treated with CORT during embryonic development.

Adult quail samples from study 2 show a significant reduction in *TSHB* levels in SD quail, but no significant difference was seen in *GNRH* or *GNIH* expression between photoperiods. *GNRH* expression appears to decrease in SD, however this is not significant. The decrease in *TSHB* expression is consistent with seasonal breeding patterns, as the Japanese quail reproduces in the summer, long-day condition. As discussed in chapter 1, *TSHB* is an important component of the photoperiodic reproductive response, as it acts

upstream of the DIO2 switch and leads to GNRH, LH and FSH release, and therefore reproduction. *TSHB* is also therefore upregulated in the summer and decreased in SD, consistent with the data presented here. GNRH is responsible for stimulating the release of LH and FSH from the pituitary gland to activate the seasonal reproductive cascade. *GNRH* is therefore reduced, although not significantly, in the winter, SD conditions, when the reproductive axis is repressed.

The process of adding methyl groups to the DNA, more commonly cytosine-guanine bonds, is well-characterised in a myriad of plant and animal models and in the context of a range of physiological functions, including seasonal reproduction (see Chapter 1). The addition of a methyl group to DNA is associated with repression of gene expression. DNA methylation patterns are heritable, reversible and can be altered by changing environmental conditions and external stresses. DNA methylation plasticity, thus, provides researchers with a measurable method of linking changes in the surrounding environment to gene expression patterns. Stresses such as limited food availability and predatorial stress elicit a rise in the stress hormone corticosterone, and have been correlated to changes in DNA methylation patterns (Kang et al., 2017; Noguera and Velando, 2019). In this study, it was hypothesised that artificially injecting eggs with corticosterone would cause an increase in the main enzymes involved in catalysing DNA methylation, DNA methyltransferases *1*, *3A* and *3B* (*DNMT1*, *DNMT3A*, *DNMT3B*, respectively). DNMT1 is traditionally thought of as the maintenance methyltransferase, conserving DNA methylation patterns through cell division. Because of its maintenance function, DNMT1 has an essential role during developmental stages in both mammals and birds. DNMT3A and DNMT3B are also called the *de novo* methyltransferases, as they establish new methyl marks on the DNA, important in X silencing in mammals (McCarthy et al., 2009) and perhaps Z-linked gene expression in birds (Teranishi et al., 2001), although the latter requires further research. In study 1, the expression of *DNMT1* increased at embryonic day 14, decreasing again at E17, similarly to *GNRH* expression. A similar age-dependent

increase at E14 was seen in *DNMT3A* and *DNMT3B* levels. *DNMT3B* expression also increased in E14 individuals in response to CORT treatment, decreasing again at E17. *DNMT3B* levels, however, were significantly higher in E17 CORT animals compared to E11 CORT hypothalami. The increase in *DNMT1* may further point to E14 as a critical day during development, or an 'epigenetic resetting', where more cell division occurs, therefore more *DNMT1* is required to maintain DNA methylation patterns. In addition, it is possible that embryonic development at E14 is connected to avian Z-linked differentiation, which has been proposed as the equivalent of dosage compensation mechanisms in mammals (X-silencing) (Teranishi et al., 2001; Smith et al., 2009). Upregulation of *DNMT1,3A* and *3B* could be involved in the epigenetic modulation of Z-linked genes, such as male hypermethylated region (MHM) or gene doublesex and mab-3-related transcription factor 1 (DMRT1), as both have been found to play a role in avian sex determination during early developmental stages (Teranishi et al., 2001; Smith et al., 2009).

On the other hand, in study 2, expression of *DNMT3A* and *DNMT3B* decreased in SD, although not significantly, and *DNMT1* levels did not change. This reduction in *de novo* methyltransferase expression in short photoperiods in consistent with previous mammalian studies (Stevenson and Prendergast, 2013; Tolla et al., 2020b) and perhaps indicates a sort of 'epigenetic switch' between the reproductive and non-reproductive seasons, altering expression patterns of downstream reproductive components. It is also possible that DNA methyltransferase enzymes are themselves part of a circannual endogenous mechanism in seasonally-reproducing avian species. However, further research is required in order to test the hypothesis that Dnmts are regulated by their own seasonal clock. Taken together, the Dnmt data from study 1 and study 2 suggest that there are distinct gene expression profiles between embryonic hypothalamic at different critical developmental stages and adult hypothalami kept under LD and SD conditions. Both maintenance and *de novo* DNA methyltransferase enzymes may act during high cell division foetal stages, and *de novo* methyltransferase enzymes may be part of the

circannual machinery that allows seasonal species to reproduce at the most favourable time of the year. In future avian studies, it will be important to precisely identify the downstream effects of altered epigenetic mechanisms and exposure to stress during early developmental stages.

Deep-brain photoreceptor mRNA expression was also measured in both studies. So far, no studies have investigated avian brain opsin expression across development and/or any effect maternal stress could have on DBP expression. One study by Hang and colleagues in 2016 found altered chorion structure and even foetal death after inserting a mutation in the VA Opsin protein in zebrafish (Hang et al., 2016). However, no study has explored the role of opsin development in bird embryos. In both study 1 and study 2, the expression of *VA Opsin* and *OPN5*, two deep-brain photoreceptors involved in seasonal reproduction (see Chapter 2), was measured. It was found that CORT injections did not alter the levels of *VA Opsin* nor *OPN5*, at any age. However, *OPN5* expression significantly increased at E14, similarly to the pattern of expression of *GNRH* and *DNMT1/3A/3B* expression. *OPN5* expression was also shown to decrease at day 10 post-hatching. This *OPN5* level surge at E14 may further indicate that embryonic day 14 in Japanese quail is a critical day not only in setting up DNA methylation patters, but also in the development of hypothalamic photoreceptors involved in sexual maturation later in life. This critical window of time appears to be restricted, as expression of *GNRH*, and *DNMT1/3A/3B* decreased again at E17, and *OPN5* was reduced at P10. *VA Opsin* also exhibits an increase in its expression at day E14, however it is not significant. In previous studies, rhodopsin expression in the pineal gland was first detected at embryonic day 13 in Japanese quail, and retinal rhodopsin expression was first detected at embryonic day 13 in quail and 14 in chicken (Yamao et al., 1999; Araki et al., 1992; Araki et al., 1990). From the data collected in different studies, Yamao and colleagues suggested that opsin synthesis first occurs on the same developmental day (Yamao et al., 1999), and from the results of the present study, it appears that opsin synthesis in the brain also occurs around the same

time as the pineal gland and the retina, given that incubation time in quail is slightly shorter than chicken. Opsin expression at specific embryonic stages could have different implications. For instance, *OPN5* expression in the developing mouse retina has been shown to stimulate a dopamine-dependent pathway that leads to postnatal vascular regression needed for postnatal vision (Nguyen et al., 2019). It is then possible that OPN5 in the brain is also connected to downstream pathways that elicit essential physiological changes later in life, specifically in preparation to reproductive stimulation. Indeed, other photoreceptors in the brain, such as melanopsin, have been found to be co-expressed in dopamine neurons in the avian hypothalamus, perhaps playing a role in seasonal reproduction (El Halawani et al., 2009). The possible link between photoreceptor expression and dopamine pathways during critical embryonic stages in the Japanese quail has yet to be investigated.

Corticosterone treatment did not alter opsin expression in the hypothalamus, which suggests that offspring of stressed mothers do not have disrupted development of the two candidate deep-brain photoreceptors and may, later in adult life, undergo sexual maturation and reproduce at the appropriate time of the year. Further experiments are required to elucidate brain opsin development in the avian embryonic brain and the effect that different stressors may have on it, by perhaps silencing their expression at critical foetal stages and monitoring seasonal reproduction once adulthood is reached. However, RNAi in specific regions of the brain during development has its limitations, as Japanese quail embryos are significantly smaller than chicken embryos, and specific intracerebral injections may be problematic. Finally, in study 2, *OPN5* and *VA Opsin* expression was reduced in SD, although it was not statistically significant. This decrease in photoreceptor expression may suggest a stimulatory role for both opsins, activating the reproductive cascade in the summer and expressed at lower levels in SD. However, as it was not a statistically significant reduction, further research will need to examine a greater number of adults, as well as discern male-female differences that could be present and could impact

on photoreceptor gene patterns within the hypothalamus.

3.5 Conclusions

The present chapter presented data from two separate studies on Japanese quail. Study 1 focused on the effect of embryonic CORT exposure on hypothalamic expression of *GNRH, DNMT1/3A/3B* and *VA Opsin/OPN5* at different embryonic stages and at postnatal day 10. The second study analysed hypothalamic expression of adult male and female Japanese quail either maintained in LD or SD. Taken together, the data collected suggest an important role of E14 as a critical developmental stage for epigenetic resetting, where DNA methyltransferase *1*,*3A* and *3B* expression is upregulated, independent of CORT. Z-linked genes such as MHM or DMRT1 are both potential targets for the epigenetic modulation required for dosage compensation in birds (Teranishi et al., 2001; Smith et al., 2009). Overall *DNMT3A* and *DNMT3B* expression was reduced in SD adults, indicating their possible involvement in underlying seasonal reproduction in quail, however statistical analysis did not find this reduction significant, and a significant effect may be masked by sex-differences.

OPN5 expression was also found to be upregulated at E14, decreasing in later stages. One hypothesis for its upregulation during a limited window of time could signify a functional role of *OPN5* in the set-up of molecular processes that will modulate later mechanisms postnatally, such as embryonic OPN5-dependent dopamine pathways in the mouse retina that later allow for adult vision (Nguyen et al., 2019). The lack of a CORT-dependent effect in photoreceptor expression may indicate that pre-natal stress in the Japanese quail does not affect the way light is detected in sexually mature adults. In adults, both *VA Opsin* and *OPN5* appear to be decreased in SD, although not significantly, and again this could be an effect of sex-specific differences. It is also possible that the lack of significance in study 2, *i.e. GNRH, DNMT3B, VA, OPN5* expression, is due to low sample size and high variation. In future studies, it will be necessary to account for male-female

differences when analysing photoreceptor expression in the brain of adult Japanese quail, as well as examine the long-term effects of embryonic CORT exposure in this species, especially at E14, and increase sample size. The epigenetic basis of avian dosage compensation and seasonal reproduction is largely unknown, however the emergence of advanced sequencing techniques and novel RNAi methods will aid in the unravelling of the role that epigenetics plays in these fundamental physiological processes.

Chapter 4 – Effects of Exogenous Triiodothyronine on DNA Methyltranferase Enzyme Expression and Neuroendocrine Reproductive Pathways in Male Siberian Hamsters (*Phodopus sugorus*).

4.1 Introduction

4.1.1 The Siberian hamster as a seasonal model

This study focuses on the role of thyroid hormones in seasonal reproduction in male mammals, specifically the Siberian hamster, *Phodopus sungorus.* Siberian hamsters are well-characterised animal models, most commonly used in studies concerning seasonal changes in physiology. They are long-day breeders, initiating the reproductive cascade during the spring/summer (Bartness and Wade, 1985), and nocturnal animals. They are excellent models of seasonal plasticity, as one single long day can stimulate reproduction in this species, allowing for easy environmental manipulation and study design (Finley et al., 1995). Photoperiod drives a range of morphological, physiological and behavioural differences between LD and SD individuals: animals maintained in a LD condition exhibit weight gain and a dark fur, along with enlarged gonads, whereas SD hamsters become more aggressive, undergo gonadal regression, lower their body mass and their fur changes to white (Bartness and Wade, 1985). Siberian hamsters are therefore an excellent animal model for exploring seasonal physiological changes between the reproductive and non-breeding periods.

4.1.2 The importance of thyroid hormones in seasonal reproduction

Thyroid hormones are crucial components in the physiology of most seasonal breeders, including birds, reptiles and mammals (Wu and Koenig, 2000; Ebling, 2015). Some of their essential functions include regulating development and metabolism,

initiating reproduction, and they are also involved in the stress response, avian feather moulting (Vézina et al., 2009), and hibernation (Tomasi, Hellgren and Tucker, 1998). In the mammalian system, thyroid hormones exist as two main isoforms, thyroxine (T4) and triiodothyronine (T_3), and are synthesised by the thyroid gland. T_4 is considered the inactive prohormone of T_3, which is converted into T_3 when required by the organism. Because of their multiple functions, thyroid hormones have been the focus of many studies concerning endogenous mechanisms and seasonal rhythms in mammals.

Similar to the avian brain, mammalian neuropeptides involved in seasonal reproduction include gonadotropin-releasing hormone (*Gnrh*), kisspeptin (*Kiss*), and the mammalian ortholog of gonadotropin-inhibitory hormone (*Gnih*), RFamide-related peptide 3 (*Rfrp3)* (Greives et al., 2007; Stevenson et al., 2012a; Tsutsui et al., 2013). The increase in day length during the spring/summer increases the production of T_3 in summer-breeding species, triggering release of GnRH and downstream reproductive pathways (Yoshimura et al., 2013). *Rfrp3* expression has also been shown to increase in the hypothalamus of Siberian hamsters during LD summer conditions (Ubuka et al., 2012), and in Siberian hamsters that received daily T_3 injections (Henson et al., 2013). In addition, Rfrp3 has been shown to increase LH levels in SD Siberian hamsters, but to inhibit LH release in LD, breeding hamsters (Ubuka et al., 2012). Studies on Syrian hamsters (*Mesocricetus auratus*) indicate that Rfrp3 is able to stimulate the action of GNRH, therefore aiding in gonadotropin release (Ancel et al., 2012). Previous studies in Siberian hamsters have also shown that triiodothyronine injections or implants are able to stimulate gonadal growth in SD individuals (Barrett et al., 2007; Freeman et al., 2007). Taken together, these studies suggest that triiodothyronine is an essential component of the reproductive response by being able to modulate important reproductive neuropeptides in seasonal mammals, such as *Gnrh* and *Rfrp3*.

4.1.3 The effect of photoperiod and T_3 on body mass, testes volume and reproductive neuropeptide expression in male Siberian hamsters

The study I will describe in this chapter includes data gathered from findings published in Banks et al., 2016, for which I was of technical assistance during tissue collections. In this paper, male hamsters were maintained in SD or a LD condition, and received daily T_3 or saline injections for 2 weeks. Hamsters exhibited an increase in body mass in response to LD, and a decrease in response to exogenous T_3 treatment (Banks et al., 2016; Figure 4.1A). Individuals injected with saline for 2 weeks did not show altered body mass. Interestingly, exogenous T_3 significantly increased testes volume in SD hamsters (Figure 4.1B) but did not change testes volume in LD individuals. In addition, the expression of *Gnrh* and *Rfrp3* in the hamsters' hypothalami was measured (Figure 4.1C and 4.1D). No change was found in *Gnrh* expression as a result of different photoperiods, nor T_3 treatment. However, *Rfrp3* levels were found to significantly decrease in SD hamsters compared to LD, and also in response to T_3 injections. In summary, this study not only showed the short day-dependent decrease in body weight and testicular volume, but also reported that T_3 injections were able to stimulate gonadal recrudescence in SD male Siberian hamsters. In addition, *Rfrp3* was shown to decrease in response to short photoperiods and T_3 treatment (Banks et al., 2016). The *Dnmt1/3a/3b* expression results presented in this chapter were gathered in the hypothalami collected by this previous study.

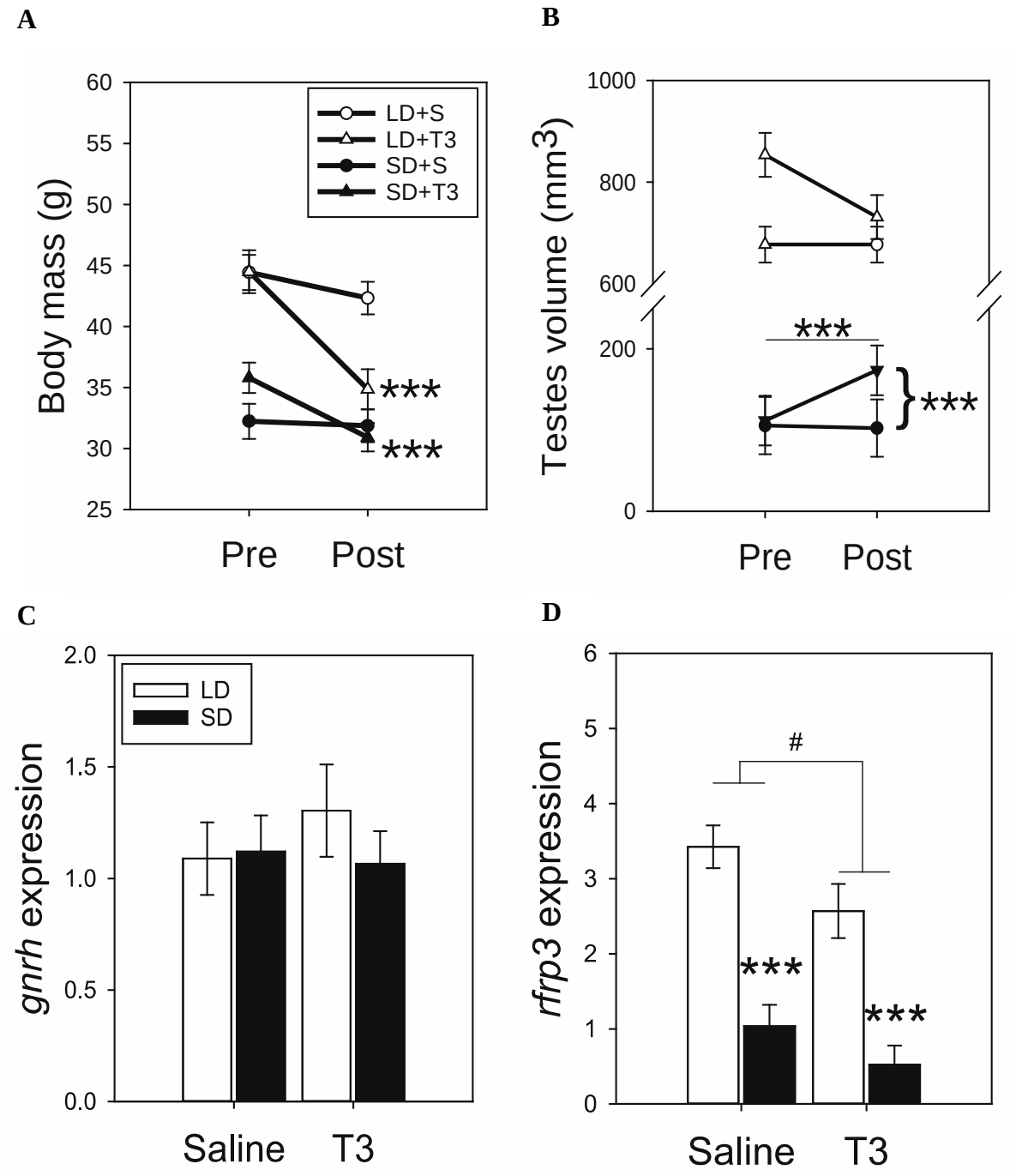

Figure 4.1. Body mass (A) and testes volume (B) of male Siberian hamsters maintained either in a long day (LD) or short day (SD) condition and treated with either saline (+S) or exogenous triiodothyronine (+T_3) for two weeks. (C) *Gnrh* and (D) *Rfrp3* expression in the hypothalami of male Siberian hamsters maintained either in a long day (LD) or short day (SD) condition and treated with either saline or exogenous T_3 for two weeks. LD Saline: N=9; SD Saline: N=8; LD T3: N=6; SD T3: N=8. Adapted with permission from Banks et al., 2016.

4.1.4 DNA methyltransferase expression and seasonality

As discussed in previous chapters, recent studies in the field of seasonality and epigenetics have highlighted the role of DNA methylation in the transition between the breeding and non-breeding periods in seasonally-reproducing species (Stevenson and Prendergast, 2013; Alvarado et al., 2015; Wilschut et al., 2016; Pegoraro et al., 2015; Lynch et al., 2016; Tolla and Stevenson, 2020b). Specifically, DNA methyltranferase enzyme 1 (*Dnmt1*), 3a (*Dnmt3a*) and 3b (*Dnmt3b*) expression in the hypothalamus of these species significantly increased during the summer in long-day breeding animals. One target gene that has been shown to undergo seasonal changes in its promoter methylation is enzyme deiodinase 3 (*Dio3*), which catalyses the deactivation of T_3 during the winter in Siberian hamsters (Stevenson and Prendergast, 2013). DNA methylation is therefore emerging as a regulator of seasonal reproduction. However, the upstream modulators of DNA methyltransferases (Dnmts) are still unknown. As T_3's upstream hormonal signal, thyroid-stimulating hormone (TSH), was shown to have no effect on DNA methyltransferase expression in the hypothalamus (Ashton and McCaffery, 2017, unpublished data), this study seeks to explore whether T_3 is part of the network that modifies Dnmt expression between breeding and non-breeding seasons.

4.1.5 Hypotheses and Aims

This study aimed to analyse the effects of exogenous triiodothyronine and photoperiod on DNA methyltransferase expression in male Siberian hamsters. The indicators of seasonal reproduction used were testes volume and hypothalamic neuroendocrine peptide expression. It was hypothesised that T_3 treatment would lead to a surge in hypothalamic DNA methyltransferase *1*, *3a* and *3b* expression in SD individuals comparable to the known increase in these enzymes during LD photoperiods.

4.2 Methods

4.2.1 Animals

Adult male hamsters (3-8 months; N=31) were obtained from a colony maintained at the University of Aberdeen. Hamsters were housed in polypropylene cages illuminated for 15h/day (15L: 9D). Food and water were provided *ad libitum* and nesting material was provided in the cages. All procedures were approved by the University of Aberdeen Animal Welfare and Ethics Committee and Home Office (PPL 70/7917). All procedures were in accordance with the ARRIVE Guidelines for ethical research on animals.

4.2.2 Study design

Adult male hamsters were maintained on the colony photoperiod (15L:9D). Hamsters were pseudo-randomly assigned to either long day (LD; 15L:9D) (n=15) or short day (SD; 9L:15D) (n=16) conditions for 8 weeks. The transfer to a SD photoperiod reliably induces reproductive involution in Siberian hamsters (Banks et al., 2016; Bao et al., 2019). After 8 weeks of either LD or SD treatment, body mass was measured (Ohaus Scale) to the nearest 0.1g to confirm photoperiod manipulations. Then, hamsters were divided into saline-treated controls LD+SAL (n=9), SD+SAL (n=8) or males that received exogenous triiodothyronine, LD+T_3 (n=6) and SD+T_3 (n=8). Hamsters were injected daily with 5 µg T_3 (T2877, Sigma-Aldrich) dissolved in 1M sterile phosphate buffered saline (PBS) subcutaneously for 2-weeks. LD and SD saline controls received the same solution volume during the 2-week period. Baseline pre-treatment body mass were recorded and collected weekly until the termination of the study. aeADAM scales (Adam Equipment PGL2002; Adam Equipment, Milton Keynes, UK) were used to determine body mass. Testes mass was used to confirm the reproductive involution in response to the SD photoperiodic treatment. There were no non-responders identified. At the end of the experiment, males

were euthanized by cervical dislocation, the brains were rapidly dissected and frozen in dry ice for approximately 5 minutes. Then, brains were moved to -70°C until RNA extraction.

4.2.3 RNA extraction and cDNA synthesis

Hypothalami and infundibulum (i.e. pars tuberalis) were dissected as previously described (Stevenson and Prendergast 2013; Bao et al., 2019). In brief, the anatomical boundaries for hypothalamus dissection were: the optic chiasm at the anterior border, the mammillary bodies at the posterior border, and laterally at the hypothalamic sulci. Extracted tissue was cut dorsally 3-4 mm from the ventral surface. Tissues were homogenized in Trizol (ThermoFisher Scientific) and RNA extracted as per manufacturers guidelines. RNA concentrations (260/280 ratio) were measured by NanoDrop (ThermoFisher Scientific). cDNA synthesis was carried out using First Strand cDNA synthesis kit (Invitrogen). RNA concentration was normalized across all samples to 1.2µg/µl made up to 10µl in RNase free H_2O, then 1µl of primer (50 uM oligo dT) and 1µl of annealing buffer were added. RNase-free H_2O was added to take the volume up to 100µl before being stored at -20°C until quantitative PCR (qPCR) assays.

4.2.4 Primer design and optimisation

Primers for target genes were designed using the NCBI Primer Design Tool (https://www.ncbi.nlm.nih.gov/tools/primer-blast/). Primers were designed to include a 40-60% GC content and have an annealing temperature of 55-65°C, then ordered from Invitrogen (Thermo Fisher Scientific). Primers were then suspended in RNAse- and DNAse-free water to 10 µM concentration and optimised using PCR and gel electrophoresis. Each PCR tube consisted of 45 µL of PCR SuperMix (Thermo Fisher Scientific), 1 µL of 10 µM forward primer, 1 µL of 10 µM reverse primer, 100 ng of hamster cDNA, and water until 50 µL. The tubes were then placed in a thermal cycler

(Thermo Hybaid Px2, Thermo Fisher Scientific) to follow a gradient program: (I) initial denaturation, 94°C for 2 minutes, 1 cycle; (II) denaturation, 94°C for 15 seconds, followed by a gradient annealing temperature (55°C – 62°C) for 30 seconds, followed by extension, 72°C for 1 minute/kb, 35 cycles; (III) hold step at 4°C. A 1% agarose gel was made by mixing 1.2 g agarose, 120 ml 1X TBE buffer (Thermo Fisher Scientific) and 4 µL SYBR Safe DNA Gel Stain (Thermo Fisher Scientific), heating it in a glass beaker for ~2 minutes, then pouring it in a gel cast and letting it set for 40 minutes. 10 µL of each PCR product were then loaded onto the gel. Running was carried out for 50 minutes, at 100 V and 100 mA. The gels were visualised using a UV light transilluminator (GeneFlash, Syngene) and the ideal annealing temperature was identified for each primer pair by selecting the one that yielded the clearer quality and most amount of product. See Table 2.1 for detailed primer information.

4.2.5 Real-Time Polymerase-Chain Reaction (qPCR)

To measure mRNA expression, cDNA was assayed using qPCR. Primers for target genes were ordered from Invitrogen and optimised using gel electrophoresis, as described in chapter 2, section 2.2.7. qPCRs were run on a BioRad CFX96 Real time PCR machine in a 20µl reaction. For each well the qPCR mix consisted of 5µl cDNA template, 10µl SYBR green (PrecisionPLUS qPCR Master Mix with SYBR green) 0.5µl (300nM) forward primer, 0.5µl (300nM) reverse primer and 4µl RNase-free H_2O to make up to 20µl. Primers were all ordered from Invitrogen, sequences for *Gnrh*, *Rfrp3*, *Dnmt1*, *Dnmt3a*, and *Dnmt3b* were optimised and published previously (Stevenson and Prendergast, 2013; Lynch et al., 2016; Bao et al., 2019) as well and the primer sequences for the reference genes glyceraldehyde 3-phosphate dehydrogenase (*Gapdh*) and hypoxanthine phosphoribosyltransferase 1 (*Hprt*) (Lynch et al., 2016). See Table 1 for primer information. All samples were run in triplicate in a 96-well plate format under the following cycling conditions; i) initial denaturing at 95°C for 5 min, then 39 cycles of ii)

95°C for 10 secs, iii) 30 secs at annealing temperature dependent on gene of interest (See Table 4.1), then iv) an extension step of 72°C for 30 secs. For each gene analysed, including reference genes, there were no-template H_2O controls included in the plate. Melt curve analysis was carried out to ensure only a single peak was produced for each reaction. PCR Miner (Zhao and Fernald 2005) was used to determine reaction efficiencies (E) and quantification cycle (Ct). According to MIQE guidelines, samples with efficiency values below 0.8 and above 1.2 were excluded from analyses (Bustin et al., 2009). A two-way ANOVA was conducted to assess the stability of the reference RNA expression levels across experimental groups. Using the average reference Cts, no variation between photoperiod (P=0.34), treatment (P=0.19) or an interaction (P=0.73) was detected. Fold expression of each target gene was measured in relation to the average Ct for two reference genes (*Gapdh* and *Hprt*) and calculated using 2-(ΔΔCt).

Gene	Forward primer	Reverse primer	Annealing Temp
GnRH	TCTGGTCATGTTGTCCGTGT	CTTGCTGGTGTGTGGTATGC	61˚C
Rfrp3	GCCCCTGCCAACAAAGTG	CAGGGTCCTCCCAAATCTCA	60˚C
Tshβ	GCCCTCTCCCAGGATGTTTG	GTGGCTTGGTGCAGTAGTTG	60°C
Dnmt1	CTGAGGCCATGTTGCCGGGG	TCTCAGCTCAGCCAGCCGGA	60˚C
Dnmt3a	CTCTGCAGGAGAGGGCAAAGAACAG	TAGCATTCTTGTCCCCAGCATCCCC	60˚C
Dnmt3b	GCTGCTGCAGATGCTTCTGTGTG	TTGCTGGGTACAACTTGGGTGGC	60˚C
Gapdh	TTCTTGTGCAGTGCCAGCCTCG	CTGTGCCGTTGAACTTGCCGTG	60˚C
Hrpt	AGTCCCAGCGTCGTGATTAGTGATG	CGAGCAAGTCTTTCAGTCCTGTCCA	62˚C

Table 4.1. List of Siberian hamster target genes, primer sequences, and relative annealing temperatures used.

4.2.6 Statistical analyses

Statistical analyses were performed using SigmaPlot 13.0. Two-way ANOVA was conducted on hypothalamic mRNA expression. Data were log-transformed in the event of a violation of normality or equal variance. Significance was determined at $p<0.05$. For detailed statistical analysis information, refer to Tables A.1 and A.2 (Appendix A).

4.3 Results

4.3.1 DNA methyltransferase expression does not vary in response to photoperiod or T_3 treatment in male Siberian hamsters

When analysing *Dnmt1,* there was no interaction effect of daylength and T_3 treatment (F=0.420, p=0.522). No change in its expression was found as a result of daylength (F=0.00006, p= 0.994) or T_3 treatment (F=0.189, p=0.667) (Figure 4.2A). *Two*-way ANOVA analysis showed no change in *Dnmt3a* expression as a result of the interaction between daylength and T_3 treatment (F=0.233, p=0.633). There was also no change in *Dnmt3a* expression in response to daylength (F=0.129, p= 0.722) or T_3 treatment (F=0.203, p=0.656) (Figure 4.2B). Finally, *Dnmt3b* expression was not altered by the interaction between daylength and T_3 treatment (F=0.00006, p=0.993), daylength alone (F=0.094, p= 0.762), or T_3 treatment alone (F=0.350, p=0.559) (Figure 4.2B).

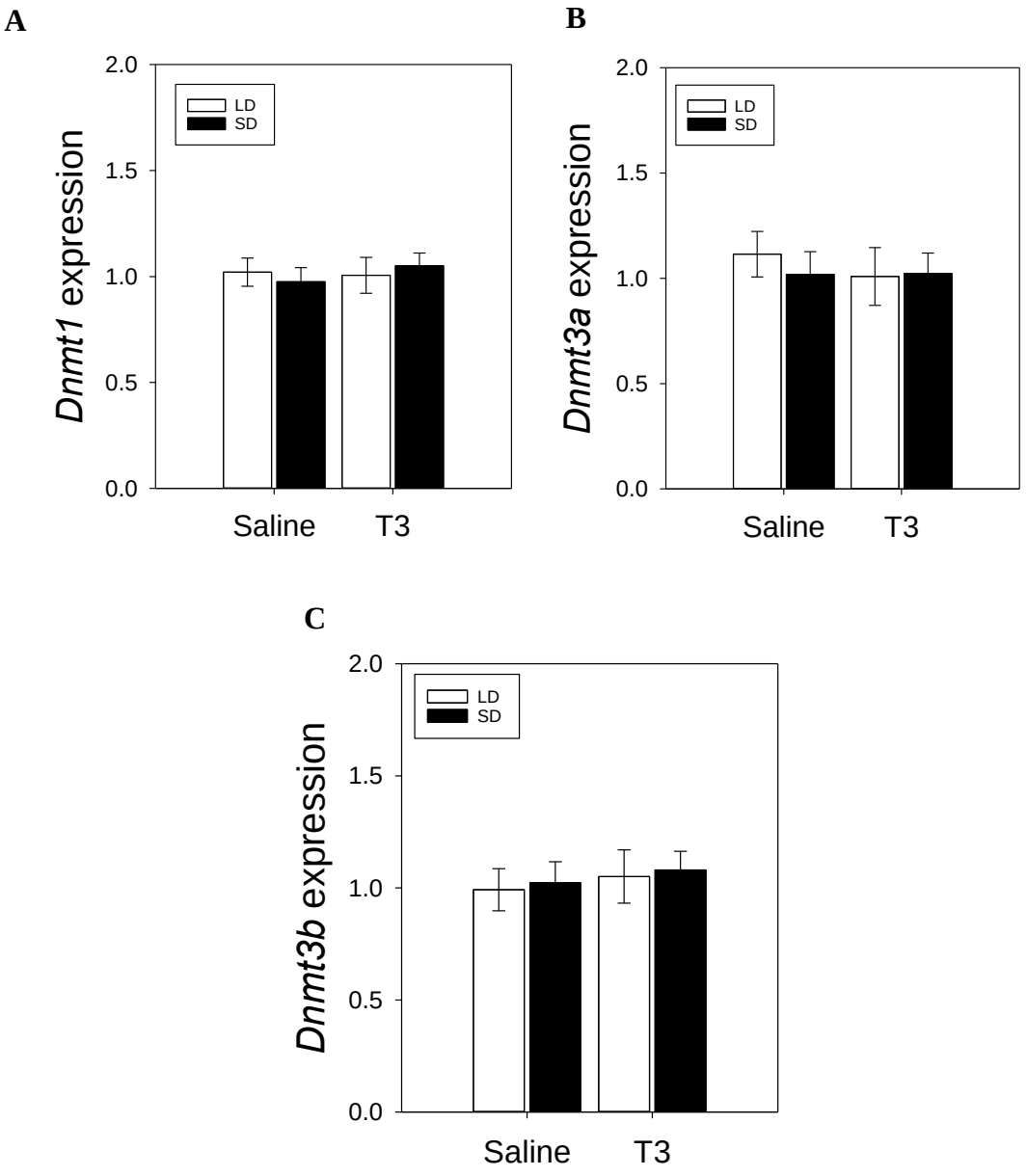

Figure 4.2. Photoperiod- and T_3- dependent expression of *Dnmt1* (A), *Dnmt3a* (B) and *Dnmt3b* (C) in the hypothalami of male Siberian hamsters maintained either in a long day (LD) or short day (SD) condition and treated with either saline or exogenous T_3 for two weeks. LD Saline: N=9; SD Saline: N=8; LD T3: N=6; SD T3: N=8.

4.4 Discussion

In the present study, the effect of photoperiod and T_3 on hypothalamic DNA methyltransferase expression was analysed. Banks and colleagues confirmed the breeding status of the hamsters by measuring body mass and testes volume. In addition, it was shown that daily exogenous T_3 injections are able to stimulate gonadal growth in SD male hamsters (Banks et al., 2016), consistent with previous studies (Freeman et al., 2007; Barrett et al., 2007). When considering DNA methyltransferase expression, the results suggest that neither photoperiod nor T_3 drive DNA methylation in the hypothalamus of the male Siberian hamster brain. There are a few possible interpretations of this data. In previous studies, hypothalamic DNA methyltransferase expression has been shown to increase in response to long day lengths (Stevenson and Prendergast, 2013; Tolla and Stevenson, 2020). However, circadian rhythms have also been shown to dictate Dnmt expression in both the hypothalamus (Azzi et al., 2014; Stevenson, 2017) and the pituitary gland (see chapter 6) of seasonal species. Therefore, it may be possible that not accounting for circadian effects is masking alterations in Dnmt levels between SD and LD. Future studies will have to take into consideration time of day when sampling tissues for seasonal experiments. It may also be possible that male Siberian hamsters require longer than 2 weeks to exhibit a change in Dnmt expression in the hypothalamus.

When considering triiodothyronine treatment, the absence of an effect of T_3 injections on hypothalamic Dnmt levels may be because: 1) a different hormonal signal may be driving Dnmt expression in LD hamsters, or 2) Dnmts may be part of the endogenous circannual machinery within the brain of male Siberian hamsters, therefore not being driven by other hormonal signals at all. In addition, seasonal 'clock' genes in seasonal vertebrate species have not been identified yet, and epigenetic mechanisms have been hypothesised to underlie circannual rhythms (Stevenson and Lincoln, 2017). It may also be possible that other epigenetic enzymes, *e.g.* Hdacs or Tets, are regulated by reproductive components such as T_3, leading to the modulation of the reproductive axis.

However, the association between other epigenetic enzymes and seasonal reproductive processes in the hypothalamus has not yet been investigated. An alternative experimental design could consist of exposing the animals to thyroid hormone injections for longer than a two-week period, along with sampling tissues at different times during the day following a daily T_3 injection regimen.

Finally, *Rfrp3* expression in the hypothalamus appears to be reduced by T_3 treatment in SD hamsters, suggesting a role for triiodothyronine in inhibiting *Rfrp3* levels in male Siberian hamsters. *Rfrp3* expression was also shown to significantly decrease in response to short photoperiods, consistent with previous reports (Klosen et al., 2013; Henson et al., 2013). It could be useful to analyse *Rfrp3* promoter methylation via bisulfite sequencing, to determine whether DNA methylation is linked to the differential expression of this peptide between seasons.

One important aspect of the hypothalamic-pituitary-gonadal axis is differences between male and female integration of stimuli that initiate the reproductive response (Ball and Ketterson, 2008). It may be possible that *Dnmt1, 3a* and *3b* in certain regions of the brain involved in seasonal reproduction, *e.g.* the hypothalamus, exhibit sex differences in expression that later in life account for sex differences in physiology or behaviour, and may account for the absence of variation in Dnmt expression I presented in this chapter. For instance, the preoptic area of the hypothalamus (POA) is a critical node for the control of mammalian reproduction, and GnRH neurons are largely concentrated in this area. Lesions to the POA in rats cause a decrease in breeding behaviour in males, but not in females (Hitt et al., 1970), suggesting that the POA is involved in integrating signals that lead to sex differences in reproduction. Thus, differences in the seasonal or circadian expression of DNA methyltransferase enzymes may be found in anatomically localised hypothalamic regions, such as the POA.

4.5 Conclusions

In the present chapter, I presented data collected from the hypothalami of male Siberian hamsters exposed to either SD or LD, and to either daily saline or T_3 injections for 2 weeks. This study hoped to shed some light on neuroendocrine pathways underlying seasonal reproduction in this mammalian species. Body mass and testicular volume data gathered by Banks and colleagues confirmed the breeding and non-breeding status of LD and SD individuals, respectively (Banks et al., 2016). DNA methyltransferase expression results indicated that the expression of hypothalamic *Dnmt1, 3a* and *3b* enzymes is not driven by photoperiod or T_3 injections. However, since previous studies reported decreased Dnmt expression in SD Siberian hamsters (Stevenson and Prendergast, 2013; Tolla and Stevenson, 2020b), it may be possible that 2 weeks of SD were not sufficient to alter DNA methyltransferase levels in this region of the brain in males. Furthermore, results show that T_3 acts to inhibit *Rfrp3* expression. *Rfrp3* levels were also reduced as an effect of short photoperiod, which has been reported in other studies (Klosen et al., 2013; Henson et al., 2013).

The present data suggest a complex neuroendocrine interaction between thyroid hormones, reproductive hormones such as RFamide-related peptide 3 and DNA methylation in hypothalamus brain regions of the male Siberian hamster. Additional research in the field of epigenetics and neuroendocrinology in mammals is needed to further assess the role and patterns of hormones important for reproduction and relate them to the methods by which environmental pressures act on the physiology of organisms, *i.e.* enzymes that carry out epigenetic modifications.

Chapter 5 – Photoperiod-Induced Changes in Hypothalamic *de novo* DNA Methyltransferase Expression are Independent of Triiodothyronine in Female Siberian Hamsters (*Phodopus sungorus*).

Published Article: Tolla, E., & Stevenson, T. J. (2020). Photoperiod-induced changes in hypothalamic de novo DNA methyltransferase expression are independent of triiodothyronine in female Siberian hamsters (*Phodopus sungorus*). *General and Comparative Endocrinology*, 299, 113604.

Abstract

Many temperate zone animals engage in seasonal reproductive physiology and behaviour as a strategy to maximise the propagation of the species. The hypothalamus integrates environmental cues and hormonal signalling to optimize the timing of reproduction. Recent work has revealed that epigenetic modifications, such as DNA methylation, vary across seasonal reproductive states. Multiple hormones act in the hypothalamus to permit or inhibit reproductive physiology, and the increase in thyroid hormone triiodothyronine (T_3) has been implicated in the initiation of breeding in many species. The objective of this study was to examine the effect of T_3 on the photoperiod-dependent regulation of reproductive physiology and hypothalamic DNA methyltransferase enzyme expression in female Siberian hamsters (*Phodopus sungorus*). The hypothesis that T_3 in short days (SD) would stimulate hypothalamic *Rfrp3* and *de novo* DNA methyltransferase (*Dnmt*) expression in female Siberian hamsters was tested. 10 weeks of SD lengths induced a decrease in body and uterine mass. Hamsters maintained in SD were found to express lower levels of *GnRH, Rfrp3, Dnmt3a* and *Dnmt3b*. Two weeks of daily T_3 injections did not affect body mass, uterine mass, *Gnrh, Rfrp3, Dnmt3a* or *Dnmt3b* expression in neuroendocrine tissues. SD significantly lowered *Tshβ* mRNA expression and T3 reduced *Tshβ* in LD hamsters. The data indicate sex-dependent effects of T_3 for the neuroendocrine regulation of seasonal reproduction in hamsters.

5.1 Introduction

Most temperate species engage in seasonal breeding as a strategy to optimize the timing of reproductive physiology and behaviour and ensure the propagation of the species (Nelson et al., 1990; Tolla et al., 2019). Changes in environmental cues such as temperature, food availability and day lengths (i.e. photoperiod) act on the hypothalamus to regulate the synthesis and secretion of reproductive neuropeptides (Nelson et al., 1990; 1994; Visser et al., 2010; Helm and Stevenson, 2015; Stevenson, et al. 2017a). Photoperiod is considered the primary predictive cue that entrains seasonal reproduction, and supplementary environmental cues, such as temperature, fine-tune the timing of breeding (Paul et al., 2008; Stevenson and Ball, 2011, Wingfield and Kenagy, 1991). Gonadotropin releasing hormone (GnRH) is the final common pathway that integrates photoperiodic and supplementary cues and subsequently governs reproductive physiology and behavior (Lehman et al., 1997; Bentley et al., 2006; Ansel et al., 2011; Stevenson et al., 2012).

In mammals, the annual change in photoperiod is coded via the secretion of melatonin from the pineal gland (Carter and Goldman, 1983; Bartness and Goldman, 1989; Goldman, 2001). Melatonin acts via the primary receptor sub-type Melatonin receptor 1b to trigger gonadal regression in a range of mammalian species that breed during the summer, also referred to as long-day breeders (Yasuo et al., 2009; Prendergast, 2010). Melatonin does not act directly on GnRH cells as these neurons do not express melatonin receptors (Clarke et al., 2009). Instead, melatonin acts via multiple hypothalamic nuclei to regulate the release of GnRH into the pituitary gland (Song and Bartness, 1996). Short day increases in the duration of melatonin trigger a decrease in thyrotropin-stimulating hormone-β (*Tshβ*) expression in the pars tuberalis of hamsters (Watanabe et al., 2004; Klosen et al., 2013; Saenz de Miera et al., 2017) and sheep (Dardente et al., 2010, Wood et al., 2015, Hazlerigg et al., 2018). In birds, melatonin is not necessary for the SD-induced change in reproductive physiology (Juss et al., 1993), yet still exhibit the long-day photoinduced increase in *Tshβ* expression (Nakao et al., 2008; Majumdar et al., 2014). The

current evidence indicates that long-day increases in *Tshβ* pars tuberalis expression is a conserved mechanism that provides a paracrine signal to transiently induce the release of GnRH into the pituitary gland.

Increased *Tshβ* stimulates deiodinase type-2 (*Dio2*) expression in the ependymal layer along the 3rd ventricle (Nakao et al., 2008; Klosen et al., 2013). *Dio2* is a thyroid hormone enzyme that serves to increase the local concentration of triiodothyronine (T_3). In long-day breeding animals, hypothalamic T_3 concentrations are higher in the summer, as it is converted from thyroxine (T_4) to T_3 by *Dio2* (Yoshimura et al., 2003; Yasuo et al., 2005). In the late autumn, T_3 concentrations are proposed to decrease due to the increased expression of deiodinase type-3 (*Dio3*) and the subsequent inactivation of T_3 (Yasuo et al., 2005; Barrett et al., 2007; Stevenson and Prendergast, 2013). Increased hypothalamic T_3 results in the retraction of tanycyte cell innervation from the median eminence and permits GnRH-to-pituitary gland signalling (Yamamura et al., 2004). The T_3 signalling pathway may be evolutionarily conserved as high T_3 concentrations are strongly correlated with reproductive physiology and behaviour during breeding months in both mammals and non-mammalian vertebrates (Wu and Koenig, 2000). Previous work using Siberian hamsters housed in short days and then provided a daily exogenous T_3 injection regimen could induce testicular growth (See Chapter 4; Freeman et al., 2007; Banks et al., 2016). In addition to effects on peripheral physiology, daily T_3 was found to inhibit *Tshβ* expression (Bao et al., 2019) and induce hypothalamic expression of reproductive neuropeptide RF-amide related peptide-3 (*Rfrp3*) (Hansen et al., 2013) but had no effect on *GnRH* expression (Banks et al., 2016). Most research on the neuroendocrine regulation of seasonal reproduction has focused on males, therefore, a greater attention to the role for T_3 in the neuroendocrine control of female reproduction is needed.

Seasonal variation in epigenetic modifications has emerged as a novel mechanism for the long-term timing of reproductive physiology and behaviour (Stevenson, 2018). Epigenetic mechanisms such as DNA methylation is conserved in nature, and found in

plants, invertebrates and vertebrates (Feng et al., 2010). DNA methylation involves the addition of a methyl group to the genomic DNA template, predominantly on cytosine-guanine pairs by DNA methyltransferase (*Dnmt*) enzymes (Jones et al., 2012). Increased promoter DNA methylation prevents transcription factor binding and, therefore represses gene transcription (Jones et al., 2012). In contrast, the removal of methyl groups permits access to the genome template and subsequent gene transcription. There are two classes of *Dnmts*, one isoform is associated with maintaining DNA methylation patterns through cell division (*Dnmt1*) (Bestor et al., 1988), compared to isoforms that are involved in establishing *de novo* methylation patterns (*Dnmt3a and Dnmt3b*) (Okano et al., 1998; Okano et al., 1999). DNA methylation has been demonstrated to oscillate with both daily and seasonal rhythms in multiple species. In the wasp (*Nasonia vitripennis*), a long day breeder, DNA methylation increased in short days and was shown to be essential for the transition into diapause (Pegoraro et al., 2016). In the Thirteen-lined squirrel (*Ictidomys tridecemlineatus*) liver and muscle tissue exhibited a significant increase in *Dnmt3a* expression during non- reproductive winter periods (Alvarado et al., 2015). In the laboratory, short-day photoperiods were found to increase testicular and uterine DNA methylation and *Dnmt3a* and *Dnmt3b* expression in Siberian hamsters (*Phodopus sungorus*) (Lynch et al., 2016). Hypothalamic *Dnmt3a* expression is significantly higher in hamsters maintained in long day conditions (Stevenson and Prendergast, 2013; Stevenson, 2017a), redheaded bunting (*Emberiza bruniceps*) (Sharma et al., 2018) and Japanese quail (*Coturnix japonica*) (Nakao et al., 2008). The increased enzyme expression is paralleled by an increase in global DNA methylation (Stevenson and Prendergast, 2013) and the promoter region for *Dio3* appears to be one genomic motif that exhibits reversible methylation. However, the extent to which hypothalamic T_3 concentrations regulate hypothalamic *Dnmt* expression and a role for the control of female reproduction is not well characterised.

The objective of this study was to determine the effect of T_3 on the photoperiodic regulation of female reproductive physiology and hypothalamic expression of reproductive neuropeptides, *Gnrh, Rfrp3* and epigenetic enzymes *Dnmt1, -3a and 3b* expression. This study used Siberian hamsters due to the well-characterized, robust and reliable reproductive responses to photoperiodic manipulations (Bartness and Goldman, 1989; Prendergast et al, 2013; Stevenson et al., 2017b). The hypothesis that short days would induce reproductive involution across the entire hypothalamo-pituitary gonadal axis was tested. Moreover, it was hypothesized that 2 weeks of daily exogenous T_3 injections in female hamsters housed in short days for 10 weeks would trigger long day-like neuroendocrine and gonadal phenotypes. This study follows the experimental rationale and design described in chapter 4, investigating female Siberian hamsters instead of males.

5.2 Material and Methods

5.2.1 Animals

Adult female hamsters (3-8 months) were obtained from a colony maintained at the University of Aberdeen. Hamsters were housed in polypropylene cages illuminated for 15h/day (15L: 9D). Harlan food and tap water were provided *ad libitum* and each cage was provided cotton-nesting material. All procedures were approved by the University of Aberdeen Animal Welfare and Ethics Committee and Home Office (PPL 70/7017). All procedures were in accordance with the ARRIVE Guidelines for ethical research on animals.

5.2.2 Study design

Adult female hamsters (N=29) were maintained on the colony photoperiod (15L:9D). Hamsters were pseudo-randomly assigned to either long day (LD; 15L:9D) (n=15) or short day (SD; 9L:15D) (n=14) conditions. The transfer to a SD photoperiod

reliably induces reproductive involution in Siberian hamsters (Banks et al., 2016; Bao et al., 2019). After 10 weeks of either LD or SD treatment, body mass was measured (Ohaus Scale) to the nearest 0.1g to confirm photoperiod manipulations. Then, hamsters were divided into saline-treated controls LD+SAL (n=7), SD+SAL (n=6) or females that received exogenous triiodothyronine, LD+T_3 (n=8) and SD+T_3 (n=8). Female hamsters were injected daily with 5 µg T_3 (T2877, Sigma-Aldrich) dissolved in 1M sterile phosphate buffered saline (PBS) subcutaneously for 2-weeks. The T_3 dose selected was to replicate previous work using exogenous injections in male Siberian hamsters (Banks et al., 2016; Onishi et al., 2019; Bao et al., 2019). LD and SD saline controls received the same solution volume during the 2-week period. The injection dose and schedule selected were previously established to induce reproductive development (*i.e.* testicular growth) in SD housed male hamsters (Banks et al., 2016). Baseline pre-treatment body mass were recorded and collected weekly until the termination of the study. Uterine mass was used to confirm the reproductive involution in response to the SD photoperiodic treatment. There were no non-responders identified. At the end of the experiment, females were euthanized by cervical dislocation, the brains were rapidly dissected and frozen in dry ice for approximately 5 minutes. Then, brains were moved to -70°C until RNA extraction.

5.2.3 RNA extraction and cDNA synthesis

Hypothalami and infundibulum (i.e. pars tuberalis) were dissected as previously described (Stevenson and Prendergast 2013; Bao et al., 2019). In brief, the anatomical boundaries for hypothalamus dissection were: the optic chiasm at the anterior border, the mammillary bodies at the posterior border, and laterally at the hypothalamic sulci. Extracted tissue was cut dorsally 3-4 mm from the ventral surface. Tissues were homogenized in Trizol (ThermoFisher Scientific) and RNA extracted as per manufacturers guidelines. RNA concentrations (260/280 ratio) were measured by NanoDrop (ThermoFisher Scientific). cDNA synthesis was carried out using First Strand cDNA

synthesis kit (Invitrogen). RNA concentration was normalized across all samples to 1.2µg/µl made up to 10µl in RNase free H_2O, then 1µl of primer (50 uM oligo dT) and 1µl of annealing buffer were added. RNase-free H_2O was added to take the volume up to 100µl before being stored at -20°C until quantitative PCR (qPCR) assays.

5.2.4 qPCR assay for DNA methyltransferase and photoperiodic genes

To measure mRNA expression, cDNA was assayed using qPCR. Primers for target genes were ordered from Invitrogen and optimised using gel electrophoresis, as described in chapter 4, section 4.2.4. qPCRs were run on a BioRad CFX96 Real time PCR machine in a 20µl reaction. For each well the qPCR mix consisted of 5µl cDNA template, 10µl SYBR green (PrecisionPLUS qPCR Master Mix with SYBR green) 0.5µl (300nM) forward primer, 0.5µl (300nM) reverse primer and 4µl RNase-free H_2O to make up to 20µl. Primers were all ordered from Invitrogen, sequences for *Tshb*, *Gnrh*, *Rfrp3*, *Dnmt1*, *Dnmt3a*, and *Dnmt3b* were optimized and published previously (Stevenson and Prendergast, 2013; Lynch et al., 2016; Bao et al., 2019) as well and the primer sequences for the reference genes glyceraldehyde 3-phosphate dehydrogenase (*Gapdh*) and hypoxanthine phosphoribosyltransferase 1 (*Hprt*) (Lynch et al., 2016). See Table 4.1 for primer information. All samples were run in triplicate in a 96-well plate format under the following cycling conditions; i) initial denaturing at 95°C for 5 min, then 39 cycles of ii) 95°C for 10 secs, iii) 30 secs at annealing temperature dependent on gene of interest (See Table 4.1), then iv) an extension step of 72°C for 30 secs. For each gene analysed, including reference genes, there were no-template H_2O controls included in the plate. Melt curve analysis was carried out to ensure only a single peak was produced for each reaction. PCR Miner (Zhao and Fernald 2005) was used to determine reaction efficiencies (E) and quantification cycle (Ct). According to MIQE guidelines, samples with efficiency values below 0.8 and above 1.2 were excluded from analyses (Bustin et al., 2009). A two-way ANOVA to assess the stability of the reference RNA expression levels across experimental

groups was conducted. Using the average reference Cts, no variation between photoperiod (P=0.34), treatment (P=0.19) or an interaction (P=0.73) was detected. Fold expression of each target gene was measured in relation to the average Ct for two reference genes (*Gapdh* and *Hprt*) and calculated using 2-(ΔΔCt).

5.2.5 Statistical analyses

Statistical analyses were performed using SigmaPlot 13.0. Two-way ANOVA was conducted on uterine and body mass, and hypothalamic mRNA expression. Data were log-transformed in the event of a violation of normality or equal variance. Significance was determined at $p<0.05$. For detailed statistical analysis information, refer to tables A.1 and A.2 in Appendix A.

5.3 Results

5.3.1 Photoperiod but not triiodothyronine regulates uterine and body mass in female hamsters

There was no significant interaction of daily T_3 injections and daylength on uterine mass (F=0.42; P=0.52). Similarly, no effect of daily T_3 injections on uterine mass (F=0.12; P=0.73) was found. However, uterine mass decreased in response to SD (F=14.95; P<0.001) (Fig. 5.1A).

No significant interaction was found between daily T_3 injections and daylength on body mass (F=0.04; P=0.84). Exogenous T_3 did not significantly affect body mass (F=2.85; P=0.10, but there was a significant decrease in body mass in response to SD (F=36.09; P<0.001) (Fig. 5.1B).

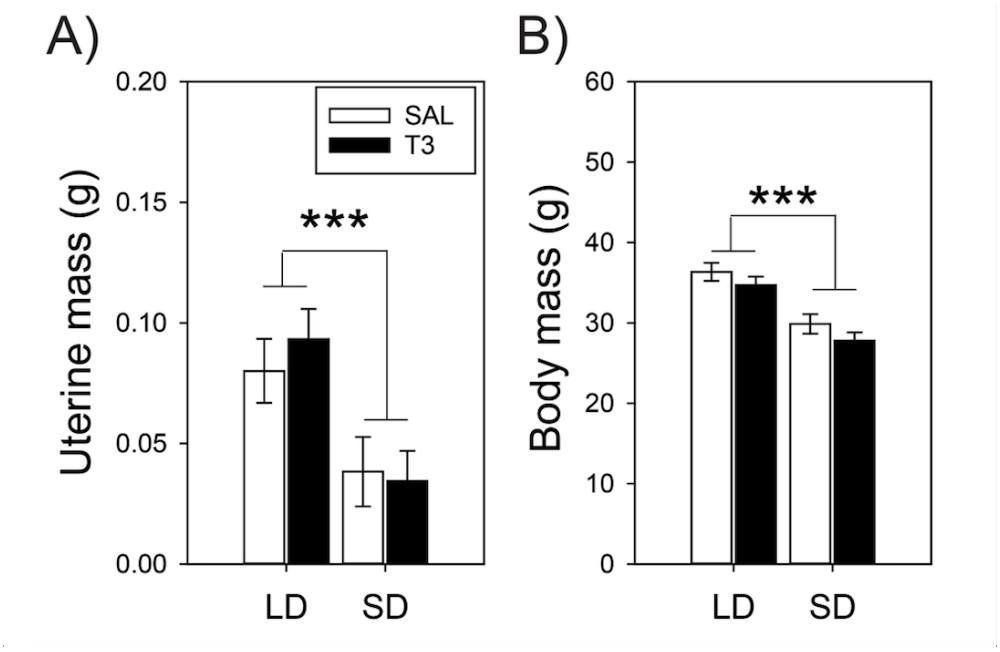

Figure 5.1. Photoperiodic regulation of uterine and body mass in female Siberian hamsters kept under short day (SD) or long day (LD) conditions. Hamsters received either a daily saline (SAL) or triiodothyronine (T3) injection for two weeks. SD induce reproductive involution evidenced by reduced uterine mass (A) and body mass (B). Daily T_3 injections did not significantly affect body mass or uterine mass ($P>0.05$). Data presented as mean ± SEM and asterisks indicate significant difference $P<0.001$. LD+SAL: N=7; SD+SAL: N=6; LD+T3: N=8; SD+T3: N=8.

5.3.2 Exogenous daily T_3 did not augment SD-induced reduction in reproductive neuropeptides.

There was no significant interaction found between daily T_3 injections and daylength on hypothalamic *GnRH* expression ($F=0.42$; $P=0.52$). Exogenous T_3 did not affect *GnRH* expression ($F=0.09$; $P=0.76$). However, female hamsters exposed to SD had significantly lower hypothalamic *GnRH* expression compared to LD animals ($F=15.55$; $P<0.001$) (Fig. 5.2A). These data indicate that *GnRH* expression in females is responsive to photoperiodic manipulations but was not regulated by T_3 signalling.

Next, hypothalamic *Rfrp3* expression was assessed. *Rfrp3* mRNA levels did not vary in response to the interaction between T_3 injections and daylength ($F=0.59$; $P=0.45$). Daily T_3 injections did not affect *Rfrp3* expression ($F=1.85$; $P=0.18$). However, it was confirmed that SD significantly reduced *Rfrp3* expression ($F=4.23$; $P=0.05$) (Fig. 5.2B).

These findings suggest that similar to *GnRH* expression, reproductive neuropeptides in the female hamster hypothalamus are primarily driven by photoperiodic cues independent of T_3 signalling.

Tshβ expression was measured as a means to determine the effectiveness of exogenous T_3 to augment the hypothalamo-thyroid axis. A significant interaction effect of T_3 treatment and daylength was found on *Tshβ* expression ($F=5.72$; $P<0.05$). As expected, SD hamsters had significantly lower *Tshβ* expression compared to LD animals ($F=18.61$; $P<0.001$) (Fig. 5.2C). There was also a main effect of T_3 treatment, with higher *Tshβ* expression in saline treated control hamsters ($F=5.38$; $P<0.05$). These data suggest that *Tshβ* expression is driven by photoperiodic `changes. Furthermore, they suggest that exogenous T_3 injections were sufficient to influence the homeostatic regulation of the neuroendocrine-thyroid axis.

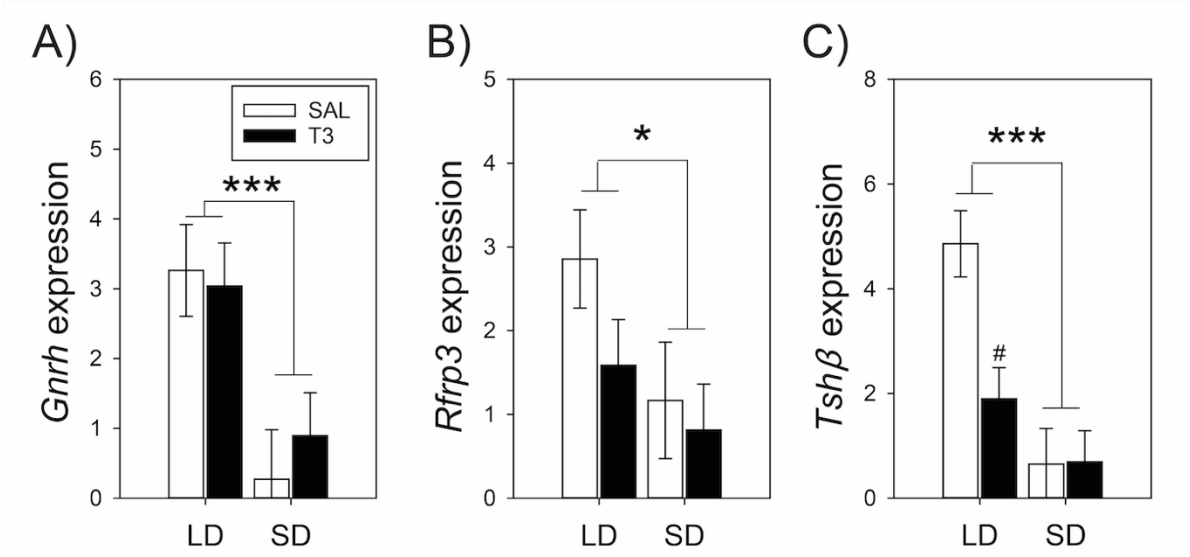

Figure 5.2. Short days induce a significant reduction in photoperiodic and reproductive neuropeptides. Hamsters were kept either under a long day (LD) or short day (SD) condition and received either a daily saline (SAL) or triiodothyronine (T3) injection for two weeks. Prolonged exposure to SD resulted in lower expression of two reproductive neuropeptides: *Gnrh* (A), and *Rfrp3* (B). Decreased photoperiods lowered thyrotrophin-stimulating hormone subunit-β (*Tshβ*) and exogenous T3 significantly reduced expression in LD (C). Data presented as mean ± SEM. Asterisks indicate significant variation between LD and SD *** $P<0.001$ and * $P<0.05$. Hashtag denotes significant T3-induced reduction in LD hamsters # $P<0.05$. LD+SAL: N=7; SD+SAL: N=6; LD+T3: N=8; SD+T3: N=8.

5.3.3 Photoperiod and not T_3 regulates seasonal variation in hypothalamic Dnmt3a/b

There was no significant effect of the interaction between T_3 treatment and photoperiod (F=0.35; P=0.56), or photoperiod alone (F=0.74; P=0.39) (Fig. 5.3A), or daily T_3 injections (F=0.48; P=0.49) on hypothalamic *Dnmt1* expression. There was a non-significant trend for the effect of the interaction between photoperiod and daily T_3 injections on hypothalamic *Dnmt3b* (F=3.56; P=0.07) expression. There was no significant effect of the interaction between daily T_3 injection and photoperiod on hypothalamic *Dnmt3a* (F=2.30; P=0.14). In parallel with the neuroendocrine responses, SD animals showed reduced hypothalamic expression of *Dnmt3a* (F=4.34; P=0.05) and *Dnmt3b* (F=5.71; P=0.05), but T_3 treatments did not significantly impact expression of *Dnmt3a* (F=0.01; P=0.89) (Fig. 5.3B) or *Dnmt3b* (F=2.92; P=0.09) (Fig. 5.3C). These data suggest that LD-induced increases in hypothalamic T_3 concentrations do not regulate *de novo* DNA methyltransferase expression in the hamster hypothalamus.

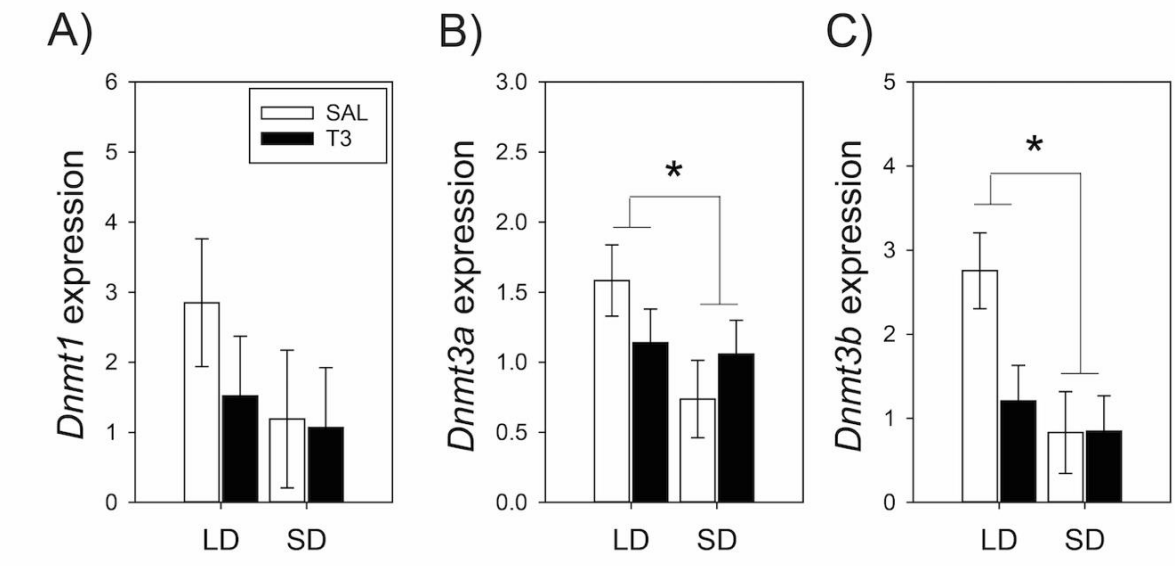

Figure 5.3. Photoperiodic regulation of hypothalamic DNA methyltransferase expression in female hamsters. Hamsters were kept either under a long day (LD) or short day (SD) condition and received either a daily saline (SAL) or triiodothyronine (T3) injection for two weeks. The levels of hypothalamic *Dnmt1* expression were not significantly different across photoperiodic manipulations or T_3 treatment (P>0.05 for all comparisons). Similar to previous reports, SD resulted in reduced hypothalamic *Dnmt3a* (B) and *Dnmt3b* (C) expression. Data presented as mean ± SEM and asterisks indicate significant difference between LD and SD * P<0.05. LD+SAL: N=7; SD+SAL: N=6; LD+T3: N=8; SD+T3: N=8.

5.4 Discussion

The findings presented here confirmed SD-induced reductions in female Siberian hamster body mass and uterine involution. These changes were paralleled by lower neuroendocrine expression of a highly photoperiodic gene, *Tshβ*; and key reproductive neuropeptides *Gnrh* and *Rfrp3*. These findings replicate previous reports in hamsters (Stevenson and Prendergast, 2013; Stevenson, 2016) and redheaded buntings (Sharma et al., 2017) for photoperiod-dependent regulation of hypothalamic *Dnmt3a* and *Dnmt3b*. However, unlike prior studies in male Siberian hamsters (Freeman et al., 2003; Banks et al., 2016), female hamsters housed in SD for 10 weeks did not exhibit gonadal recrudescence, nor a change in neuropeptide expression after 2 weeks of daily T_3 injections. Furthermore, daily T_3 injections did not affect the level of *Dnmt3a* and *Dnmt3b* expression. These data indicate that photoinduced changes in T_3 have sex-specific effects and that females likely require additional supplementary cues for full reproductive development that are independent of T_3 signalling pathways.

Hypothalamic T_3 signalling is conserved across mammalian and avian species and plays a critical role for timing seasonal transitions in reproduction (Yoshimura, 2013). Studies conducted in the 1980s and 1990s illustrated that thyroidectomy disrupted the photoperiodic regulation of reproduction in quail and sheep (Follett and Nicholls, 1985; Parkinson and Follett, 1994). Subsequent work in American Tree sparrows (*Spizella arborea*) indicated that thyroidectomy before LD stimulation inhibited gonadal regression during the onset of photorefractoriness (Wilson and Reinert, 1993). However, thyroidectomy 4 weeks after photostimulation did not impact gonadal involution (Wilson and Reinert, 1995). In combination with similar evidence collected in sheep, these data suggest that thyroid hormones have a window of opportunity to regulate reproductive transitions across photoperiodic states (Thrun et al., 1997). Moreover, the role of T_3 for the regulation of neuroendocrine molecular pathways appears limited, as 49 genes – out of >3000 genes that are differentially expressed between seasons – were observed to be

differentially regulated between intact and thyroidectomised ewes after transfer from SD to LD conditions (Lomet et al., 2018). In hamsters, daily T_3 injections in SD conditions induce testicular growth (Freeman et al., 2007; Hansen et al. 2013; Banks et al., 2016). The T_3 injections regimen does not stimulate the expression of all hypothalamic transcripts identified to exhibit photoperiod-dependent regulation but is instead restricted to a few hypothalamic targets and includes *Pomc* (Bao et al., 2019) and *Rfrp3* (Banks et al., 2016). Other transcripts such as *Npy, Agrp, Cart* (Bao et al., 2019) and *GnRH* (Banks et al., 2016) are not impacted by daily T_3 injections in SD hamsters. Taken together, these studies highlight that thyroid hormone acts during a limited period to regulate the photoperiodic response and only regulates a few hypothalamic transcripts.

The daily T_3 injections regimen significantly decreased *Tshβ* expression in LD hamsters consistent with previous work in male hamsters (Bao et al., 2019). These data are important to establish that the dose of exogenous T_3, mode of administration (i.e. subcutaneous) and injection regimen are sufficient to negatively impact the homeostatic regulation of the hypothalamic-thyroid axis. Moreover, the lower *Tshβ* levels confirm that exogenous T_3 injections can act in key neuroendocrine substrates to regulate gene transcription. It was anticipated that SD *Tshβ* levels are expressed at very low levels and cannot be reduced further in response to exogenous T_3. The dose selected for these studies can mimic physiological responses across several different endocrine and immune systems. For example, adaptive immune responses in SD hamsters (Stevenson et al., 2014), and circulating leukocytes numbers are significantly reduced (Stevenson et al., 2014; Banks et al., 2016). Other work has indicated that hamsters treated with a lower daily dose of T_3 (i.e. 0.5ug) could initiate gonadal recrudescence in SD conditions (Freeman et al., 2007; Hansen et al., 2013). Furthermore, the dose used by Hansen and colleagues (2013) was capable of increasing *Kiss1* immunoreactivity in the anteroventral periventricular nucleus, reducing *Kiss1* immunoreactivity in the arcuate nucleus and increasing *Rfrp3* immunoreactivity in the dorsomedial hypothalamus of SD hamsters. A clear comparison of

the two T_3 doses is challenging as the approach used here examines transcript expression and not protein levels in the hamster hypothalamus. At present, the data indicate T_3 dose-dependent effects on the neuroendocrine regulation of seasonal reproductive physiology.

These findings suggest photoperiod regulation of reproductive physiology can occur independent of T_3 pathways in female hamsters. Sex differences in the environmental regulation of reproduction is widely known and may be driven by resources required for spermatogenesis versus ovulation (Beery et al., 2007) and male-male competition (Prendergast, 2005) to name a few. In birds, photoperiod is sufficient to stimulate reproductive development in males, whereas females, require additional supplementary cues (Wingfield, 2008). In the present study, SD female hamsters that received T_3 injections did not exhibit body mass or uterine growth, nor the hypothesised decrease in hypothalamic *Gnrh* or *Rfrp3* expression. These data indicate that, unlike males, the photoperiodic regulation of reproduction requires additional inputs that are independent of T_3 pathways. In male rats, but not in females, lesions of the medial preoptic area (MPOA) cause a loss of dopamine projections and decreased reproductive behaviour (Hitt et al., 1970; Brackett et al., 1986). Furthermore, the diverse isoforms and functional role of thyroid hormone receptors could contribute to the sex-dependent responses to T_3 injections. Dellovade and colleagues demonstrated that thyroid receptor alpha 1 (TRα1) knockdown in mice results in an inhibition of female reproductive behaviour, whereas thyroid receptor β (TRβ) knockout was able to increase reproductive behaviour (Dellovade et al., 2000). Conversely, TRα1 knockout male mice show an increase in reproductive behaviour compared to wildtype controls, while TRβ knockouts did not change reproductive behaviour (Vasudevan et al., 2013). These studies highlight the fact that thyroid hormone functions are sex-specific and modulating the thyroid hormone pathway at any level is likely to have sex-dependent outcomes on reproductive physiology and behavior.

Daily and seasonal variation in epigenetic enzyme expression has been reported across a range of tissues (Tolla et al., 2019). Hypothalamic *Dnmt3a* levels oscillate across the day with higher expression during the dark phase in hamsters (Stevenson, 2017a). *Dnmt3a* and *Dnmt3b* are expressed in the suprachiasmatic nucleus and the inhibition of *de novo* methyltransferase via zebularine suppressed changes in period length (Azzi et al., 2014). SD photoperiods reduced *Dnmt3a* as well as *Dnmt3b* in a circadian-dependent manner (Stevenson, 2017a). In redheaded buntings, there is a significant reduction in hypothalamic *Dnmt3a* expression in autumn compared to spring conditions (Sharma et al., 2018). The mechanisms that drive greater *de novo* DNA methyltransferase expression in the hypothalamus in LD conditions are not well-characterised. This study tested the hypothesis that T_3 injections would increase hypothalamic *Dnmt3a* and *Dnmt3b* expression in SD hamsters. Contrary to the hypothesis, there was no significant effect of T_3 on hypothalamic *Dnmt1, Dnmt3a,* nor *Dnmt3b* expression. Consistent with previous reports hypothalamic *Dnmt3a* and *Dnmt3b* levels were reduced in SD conditions and occurred independent of exogenous T_3. Therefore, it is possible that (1) an alternative hormonal signal regulates photoperiodic variation in *Dnmt3a* and *Dnmt3b* expression, or (2) the expression levels reflect an endogenous circannual timing system (Stevenson and Lincoln, 2017).

The proximate mechanisms that drive seasonal transitions in growth and reproduction remain less well characterised. The photoperiodic hamster model has been valuable to investigate the sufficiency and necessity of several hormone signalling pathways for the neuroendocrine regulation of seasonal rhythms (Stevenson et al., 2017a). Studying the sufficiency of thyroid hormones for the photoperiodic control of reproductive responses facilitates the ability to identify molecular pathways involved in triggering seasonally-timed changes in physiology and behavior. The present data describe T_3-independent and sex-specific responses in the female Siberian hamster hypothalamus. The data indicate that full reproductive development, measured by uterine mass, requires

additional stimulating input beyond the simple T_3-to-GnRH release pathway. It is likely that several other hormonal pathways (*e.g.* ovarian steroids) and extra-hypothalamic systems (*e.g.* midbrain dopamine) are involved in the integration of supplementary cues that are known to fine-tune female seasonal reproduction. In future studies, it will be necessary to identify which supplementary cues drive the underlying molecular mechanisms involved in triggering full reproductive development in females and how it differs from males.

Chapter 6 – Reversible, Seasonal and Daily Patterns of DNA Methylation and DNA Methyltransferase Enzymes in the Pituitary Gland of Japanese Quail.

6.1 Introduction

6.1.1 Reversible epigenetic mechanisms control seasonal reproduction

In the past 60 years, studies have begun to untangle the role of epigenetic mechanisms such as DNA methylation and histone modifications in the context of a variety of fields, including seasonal biology. By definition, epigenetic alterations do not modify the DNA sequence, and are heritable (Rakyan et al., 2001) and reversible (Herb et al., 2012; Stevenson, 2018). Recently, the role of DNA methylation in the regulation of seasonal rhythms has emerged (see chapter 1). As discussed in previous chapters, Siberian hamsters (*Phodopus sungorus*) have been shown to exhibit plasticity in DNA methylation patterns between breeding and non-breeding seasons in an array of tissues (Stevenson and Prendergast, 2013; Lynch et al., 2016; Tolla and Stevenson, 2020b). To aid in yearly reproductive success and offspring survival, these rhythmic patterns in DNA methylation and DNA methyltransferase expression must be repeatable each season, and therefore reversible. The reversibility of epigenetic modifications is an important concept used in different fields, including cancer research. A range of tumours exhibit elevated DNA methylation, and epigenetic marks are the target in numerous epigenetic therapies (Luczak and Jagodzinski, 2006). By using Dnmt or histone deacetylase (Hdac) inhibitory drugs, it has been possible to develop a number of treatments to reverse aberrant epigenetic patterns in cancer (Luczak and Jagodzinski, 2006), leading to increased patient survival. The reversibility of epigenetic mechanisms has also been shown in human embryonic stem cells (Tompkins et al., 2012).

In birds, much less is known about fluctuating DNA methylation patterns between seasons. Nevertheless, microarray expression profiles in the hypothalamus of Japanese quail have shown that *DNMT3A* is upregulated in long days (Nakao et al., 2008).

6.1.2 DNA methylation and the circadian clock

As mentioned in chapter 1, the circadian clock is a major regulator of gene expression in vertebrates. Studies in mice have found that ~10% of the liver, brain and heart transcriptome is dictated by the circadian cycle (Storch et al., 2002; Ueda et al., 2002; Akhtar et al., 2002). In Siberian hamsters, hypothalamic DNA methyltransferase enzymes *1* and *3a* have been previously shown to oscillate not only between breeding and non-breeding periods, but also during the day (Stevenson, 2017a). In mice, *Dnmt1*, *Dnmt3a*, *Dnmt3b*, ten-eleven translocation enzymes (*Tet*) *1*, *2* and *3* and certain histone demethylase enzymes have all revealed daily patterns of expression (Azzi et al., 2014). In addition, different day lengths have been shown to modify global DNA methylation levels in the suprachiasmatic nucleus (SCN) in mice (Azzi et al., 2014). A study in the barn swallow (*Hirundo rustica*) indicated that exposure to certain pollutants significantly increases *Clock* gene promoter methylation, potentially altering the circadian clock and negatively impacting the life cycle of these birds (Romano et al., 2017). Taken together, these studies suggest a conserved interaction between epigenetic enzymes and the circadian clock in both mammals and birds. However, whether avian DNA methyltransferase enzyme expression varies throughout the day has yet to be explored.

6.1.3 Aims and hypotheses

For this study, two experiments were conducted. Study 1 aimed to investigate the reversibility of DNA methylation patterns between breeding and non-breeding seasons in the Japanese quail, a common bird model. The experimental design of Study 1 allowed for

an exploration of pituitary gland DNA methylation levels in: 1) individuals maintained in a SD condition, 2) individuals maintained under a LD photoperiod, and 3) animals that were moved to a SD condition again after a week of photostimulation. It was proposed that initial SD quail would exhibit a level of DNA methylation in the pituitary gland comparable to individuals that were moved back to a SD condition after being exposed to LD for 1 week. Study 2's objective was to examine the daily variation in expression, if any, of DNA methyltransferases *1*, *3A* and *3B* in the pituitary gland of Japanese quail. Study 2 tested the hypothesis that *Dnmt1, 3A* and *3B* expression varies between the light and dark phase of the day, predicting a peak during the dark phase, as shown by previous studies in other seasonal species (Stevenson, 2017a).

6.2 Materials and Methods

6.2.1 Animals

All procedures were approved by the local ethics committee at the University of Glasgow School of Veterinary Medicine (EA12/19). All procedures were in accordance with the ARRIVE Guidelines for ethical research on animals.

6.2.2 Study 1: Short Day Reversibility Study

6.2.2.1 Experimental Design

Adult male Japanese quail (n=31) were maintained in SD (6L:18D) for 8 weeks and then photostimulated for 7 days by maintaining them in a 18L:6D cycle. After 7 days of LD, the animals were moved back into a SD condition (6L:18D) for an additional 2 weeks. Tissues were collected at the initial SD condition ('SD'; n=8), after 7 days of LD ('LD'; n=8), after being moved again to SD for 1 week ('SD1W'; n=8), and after being kept in SD for 2 weeks ('SD2W'; n=7).

6.2.2.2 DNA extraction

DNA was extracted from the entire pituitary gland using the Qiagen DNeasy Blood and Tissue Kit (Qiagen, UK) according to manufacturer's instructions, and eluted to a final volume of 200 µL. Samples were kept at -20°C until ELISA analysis.

6.2.2.3 Enzyme-linked immunosorbent assay (ELISA)

In order to measure global methylation, an Enzyme-Linked Immunosorbent Assay (ELISA) was run using the pituitary gland (MethylFlash™ Global DNA Methylation ELISA Easy Kit - Colorimetric, Epigentek). The kit was used as per manufacturer's instructions. The preparation of the standard curve consisted in preparing 6 control concentration points. Table 6.1 below describes the contents and volumes of each concentration point.

No.	Control	PC (µL)	Diluted PC (µL)	NC (µL)
1	0.1% PC/well	0	1	9
2	0.2% PC/well	0	1	4
3	0.5% PC/well	0	3	3
4	1% PC/well	1	0	9
5	2% PC/well	1	0	4
6	5% PC/well	3	0	3

Table 6.1. Contents and volumes of each PC concentration point.

For plate setup, negative control wells consisted of 100 µL of binding solution (BS) and 2 µL of negative control (NC; 0.5% 5-mC). For positive control wells, 100 µL of BS and 2 µL of positive control (PC) were added at various concentrations, from 0.1 % to 5 %. 50 ng of DNA (4 µL) and 100 µL of BS were added to each sample well and each sample was run in duplicate. The plate was then shaken gently to ensure each solution covered the bottom of each well. The plate was then sealed with Parafilm and incubated at 37°C for 1 hour. To prepare the 5-mC Detection Complex Solution, the following reagents were added to a tube: 3 ml of diluted wash buffer (WB), 3 ml of 5-mC Antibody (mcAb; 1000X), 3 ml of signal indicator (SI) and 1.5 µL of enhancer solution (ES). After the plate

had finished the incubation period, the BS was removed from each well, and wells were washed 3 times using 150 µL of diluted WB each time. Then, 50 µL of 5-mC Detection Complex Solution were added to each well and the plate was covered with Parafilm and incubated at room temperature for 50 minutes. After the incubation period, the 5-mC Detection Complex Solution was removed and each well was washed again 5 times using 150 µL of diluted WB each time. 100 µL of developer solution (DS) was added to each well and left for 2 minutes, then 100 µL of stop solution (SS) were added to each well. The DS causes the wells to turn a yellow colour, and the SS stops the reaction before measuring absorbance. The plate was then carried to a microplate reader (LT-4500, Labtech) and the absorbance of each well was measured at 450 nm and at 570 nm as a control.

6.2.2.4 5-mC Analysis

In order to calculate the percentage of methylated DNA, a standard curve was generated. To generate the standard curve, the optical density (OD) values obtained by the microplate reader were plotted for each control well (See Table 6.1 for details of control points for standard curve). A polynomial second order regression equation was used on Microsoft Excel to determine the slopes of the standard curve (See Figure 6.1 for curve, equation and slope).

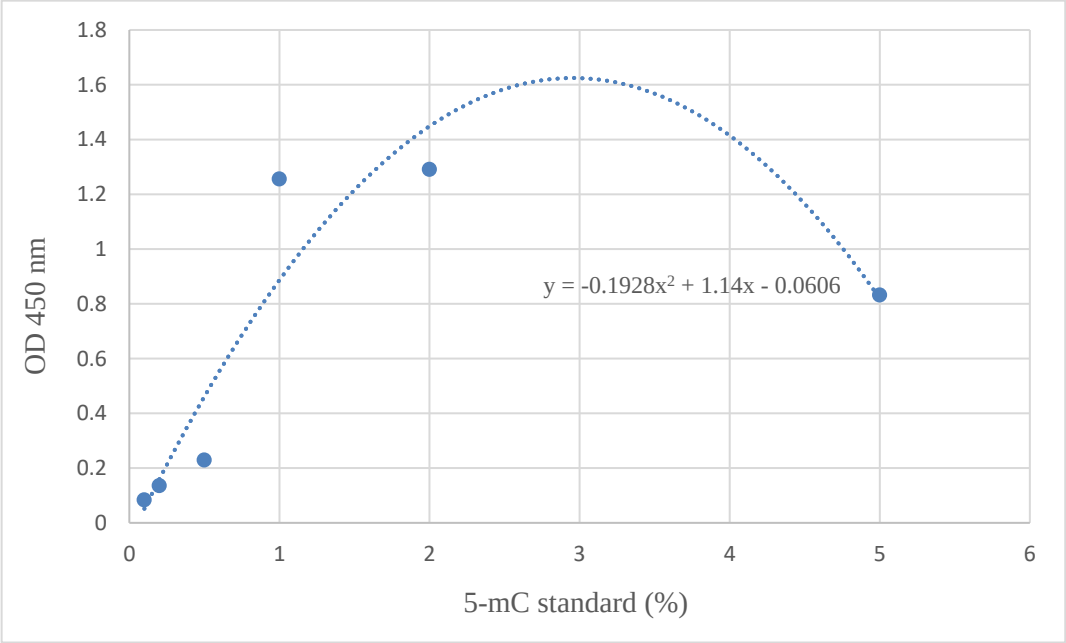

Figure 6.1. Standard curve generated by plotting each control point against their respective optical density (OD) read.

Slope 1 and Slope 2 were determined to be -0.1928 and 1.14, respectively. The 5% PC OD appears reduced compared to the other PCs (Figure 6.1). The reason for this decrease is most likely a saturated signal intensity at high % PCs. However, the highest OD value collected from the samples analysed was 0.62, which indicates that the PC points used for the analysis were 0.1%, 0.2%, 0.5%, and 1% (Table 6.1). The following equation was then used to calculate the 5-mC% of the samples:

$$5\text{-}mC\% = \frac{(b^2 + 4aY)^{0.5} - b}{2a} \div S \times 100\%$$

Figure 6.2. 5-mC% equation. From MethylFlash™ Global DNA Methylation (5-mC) ELISA Easy Kit (Colorimetric) online protocol. Base Catalog # P-1030.

6.2.3 Study 2: Daily Study

6.2.3.1 Experimental Design

Adult male Japanese quail (n=30) were maintained in SD (6L:18D) for 8 weeks and then photostimulated for 1 week by maintaining them in a 18L:6D cycle. In quail kept in

SD condition, tissues were collected 2 hours after light on (SDzt2; n=8) and during the dark phase (SDzt14; n=7). In LD individuals, tissues were collected in the morning (LDzt2; n=7), and in the evening (LDzt14; n=8).

6.2.3.2 RNA Isolation and cDNA Synthesis

RNA was extracted from the entire pituitary gland using TRIzol (ThermoFisher Scientific). 1 mL of TRIzol was added to the tissue and homogenized using Kinematica™ Polytron™ PT1200E handheld homogenizer (Thermo Fisher Scientific). Then, after a 5 min incubation at room temperature, 200 µL of chloroform were added to the homogenized sample and the tubes were incubated for 3 min at room temperature. The samples were centrifuged for 15 min at 12,000 g at 4°C. After centrifugation, the samples separate into an upper aqueous phase, interphase and a lower red phase. The upper aqueous phase was pipetted out of the tube and transferred to a fresh tube. 500 µL of isopropanol were added to the new tubes and incubated for 10 min. The tubes were then centrifuged for 10 min at 12,000 g at 4°C. The supernatant was discarded, and the white RNA pellet was resuspended in 1 mL of 75% ethanol, vortexed and centrifuged for 5 min at 7,500 g at 4°C. The supernatant was discarded, and the tubes were air-dried for 5-10 min. Finally, the pellet was resuspended in 30 µL of RNase-free water. Nucleic acid quality (260/280 ratio) and concentration were determined by using a spectrophotometer (Nanodrop; ThermoFisher Scientific). cDNA was synthesised using Precision nanoScript2 Reverse Transcription Kit (Primerdesign Ltd) (2 µg RNA) and stored at -20 °C until quantitative PCR (qPCR) assays.

6.2.3.3 Real-time PCR (qPCR)

Primers for target genes were ordered from Invitrogen and optimised using gel electrophoresis. See Table 2.1 (chapter 2) for detailed primer information. qPCRs were

performed on a Stratagene Mx3000 Real Time PCR machine in 20 µl reactions. For each well, the qPCR mix consisted of 5 µl cDNA template, 10 µl SYBR green (Primerdesign Ltd), 0.5 µl (300 nM) forward primer, 0.5µl (300nM) reverse primer and 4µl RNase-free H2O. Samples were run in duplicate in a 96-well plate format under the following conditions: i) denaturing at 95°C for 5 min, then 39 cycles of ii) 95°C for 10 secs, iii) 30 secs at annealing temperature dependent on primer (See Table 1), and finally iv) an extension step of 72°C for 30 secs. Melt curves were analysed to ensure the specificity of each reaction through only a single peak. PCR Miner (Zhao and Fernald, 2005) was used to determine reaction efficiencies and quantification cycle (Ct). Fold expression of each gene of interest was measured in relation to the average Ct for two reference genes (*GAPDH* and *B-ACTIN*) and calculated using 2-(ΔΔCt).

6.2.4 Statistical Analysis

All statistical analyses were performed using SigmaPlot 13.0. Log10 transformation was performed when violations of normality or equal variance would occur. Analysis of Variance (ANOVA) on Ranks and Dunn's Method pairwise comparisons were used to analyse results from study 1. Two-way ANOVA was used to analyse the effects of day length and time-of-day in study 2. Significance was determined at $p < 0.05$. For detailed statistical analysis information refer to tables A.1 and A.2 in Appendix A.

6.3 Results

6.3.1 Study 1: Short Day Reversibility Study

6.3.1.1 Peripheral measurements

ANOVA on Ranks analyses revealed a significant effect of treatment on testes mass ($H=17.612$; $p<0.001$). Dunn's post-hoc analyses indicated an increase in testes mass in LD quail compared to SD ($p=0.002$), and in SD1W individuals compared to SD quail ($p=0.001$). No significant difference was detected between the SD and SD2W group ($p=0.084$) (Figure 6.3).

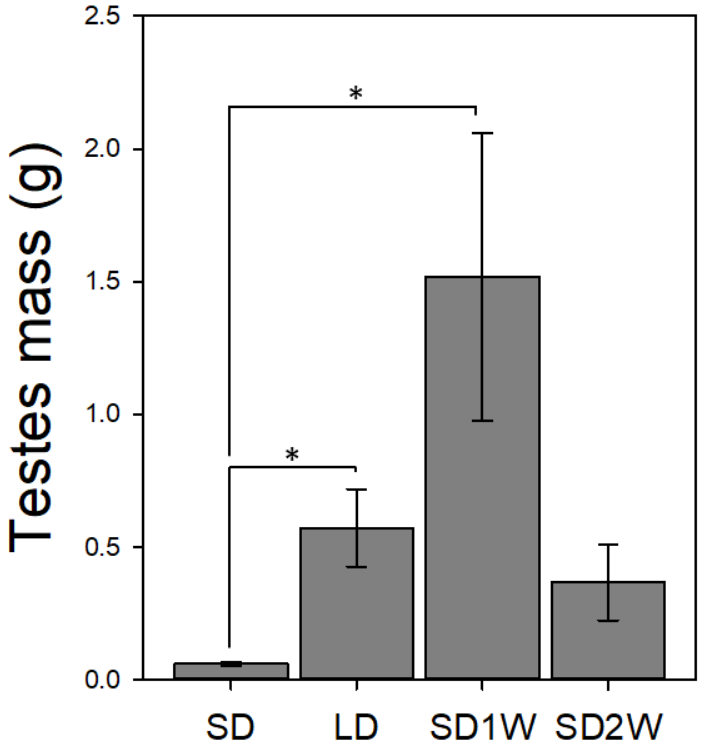

Figure 6.3. Testes mass for quails maintained in an initial short day condition (SD; N=8), long day condition (LD; N=8), or moved back to a short day condition for one (SD1W; N=8) or two weeks (SD2W: N=7). Asterisks (*) represent significance between groups. Results are mean ± SEM.

A significant effect of treatment was found when analysing cloacal gland area (H=11.164; p=0.011). Dunn's post-hoc test revealed no significant difference in cloacal area between SD and LD groups (p=0.074), between SD and SD1W (p=0.443), or between SD and SD2W (p=1.0). A significant decrease was detected in SD2W quails when compared to LD individuals (p=0.031) (Figure 6.4).

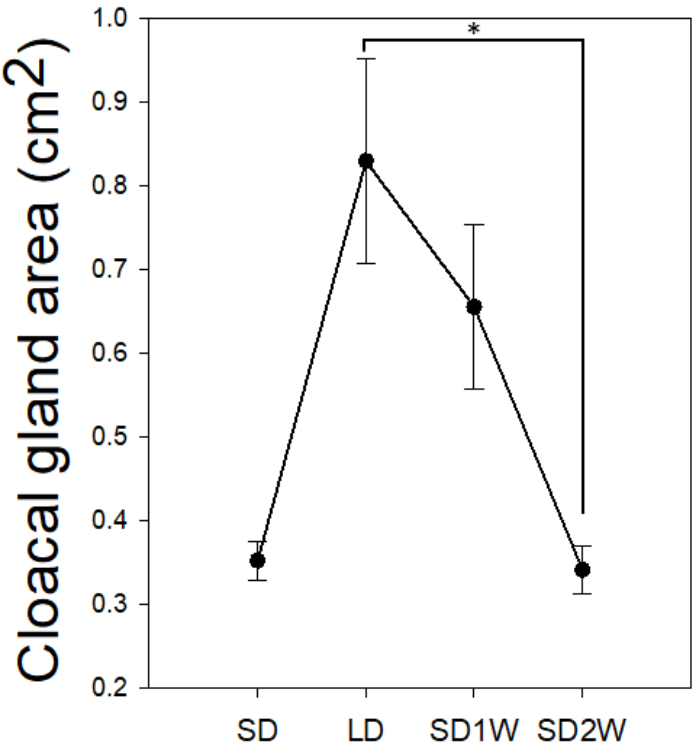

Figure 6.4. Cloacal area for quails maintained in an initial short day condition (SD; N=8), long day condition (LD; N=8), or moved back to a short day condition for one week (SD1W; N=8) or two weeks (SD2W; N=7). Asterisks (*) represent significance between groups. Results are mean ± SEM.

6.3.1.2 DNA methylation levels

A significant effect of treatment was found when analysing methylation levels (5 mC %) (H=13.246; p=0.004). Dunn's post-hoc test determined a significant increase in methylation between the LD and SD group (p=0.009). Methylation was also significantly increased in the pituitary of SD2W individuals compared to SD quail (p=0.012). No significant difference was detected between SD and SD1W animals (p=0.210) (Figure 6.5).

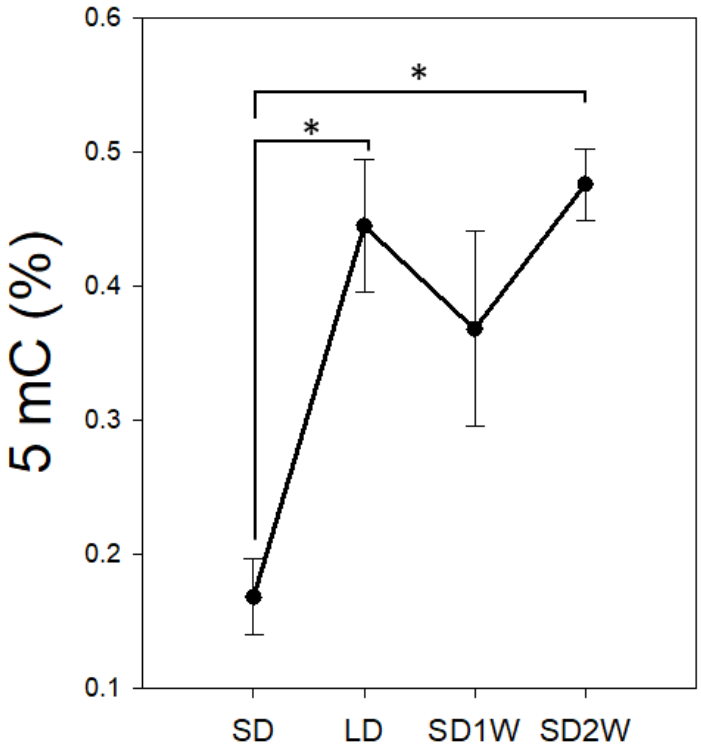

Figure 6.5. DNA methylation percentage (5-mC %) in the pituitary gland of quails maintained in an initial short-day condition (SD; N=8), long day condition (LD; N=8), or moved back to a short day condition for one week (SD1W; N=8) or two weeks (SD2W; N=7). Asterisks (*) represent significance between groups. Results are mean ± SEM.

6.3.2 Study 2: Daily variation in DNA methyltransferase expression

When analysing *DNMT3A* mRNA levels in the pituitary gland, two-way Analysis of Variance did not detect a significant effect of the interaction between time of day and daylength (F=0.254; p=0.619). There was a significant effect of time of day on *DNMT3A* expression (F=6.725; p=0.016), but no effect of daylength (F=3.006; p=0.096) (Figure 6.6).

Similar to *DNMT3A*, *DNMT3B* expression did not change in response to the interaction between time of day and daylength (F=0.715; p=0.406), nor in response to daylength alone (F=0.0235; p=0.879). However, there was a significant effect of time of day on *DNMT3B* expression (F=5.766; p=0.024) (Figure 6.6).

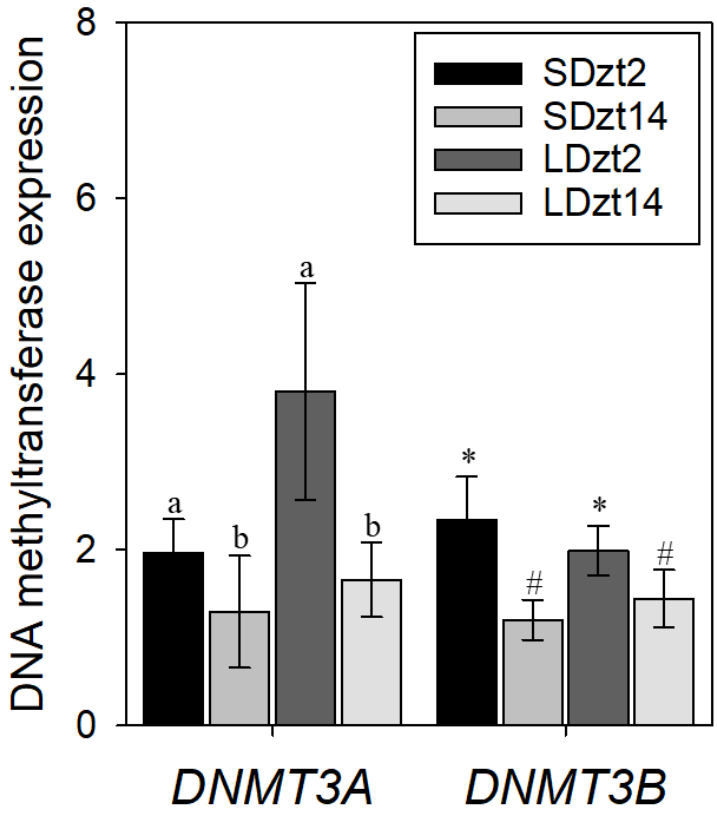

Figure 6.6. DNA methyltransferase 3a (*DNMT3A*) and 3b (*DNMT3B*) expression in the pituitary gland of quail kept in either short day (SD) or long day (LD), and sampled either in the morning (zt2) or in the evening (zt14). For *DNMT3A*, different letters represent statistical significance. For *DNMT3B*, different symbols [either asterisks (*) or hashtag (#)] indicate statistical significance. Results are mean ± SEM. SDzt2: N=8; SDzt14: N=7; LDzt2: N=7; LDzt14: N=8.

6.4 Discussion

6.4.1 Study 1: Short Day Reversibility Study

In study 1, adult quail were maintained in a SD condition ('SD' group), then moved to a LD condition ('LD' group) for 1 week. After 1 week of photostimulation, they were moved back to a SD condition for 1 week ('SD1W' group) or 2 weeks ('SD2W' group). This study sought to explore the concept of the reversibility of epigenetic mechanisms in the context of seasonal reproduction by looking at DNA methylation levels in the pituitary gland. As expected, LD quails exhibited a significant increase in testes mass compared to SD quail. This marked change in gonadal weight between Japanese quail kept under long daylight conditions and quail kept under non-breeding, short day conditions can be considered a hallmark of the activation of the reproductive axis and FSH release, and once more highlights the high phenotypic plasticity between seasons in this species. In SD1W individuals however, testes mass appears to continue to increase, contrary to expected testes mass within the SD paradigm. This absence of testes mass reduction at SD1W could be caused by the insufficiency of 1 week to lower gonadal weight. A study by Robinson and Follett measured testicular mass in Japanese quail transferred to a SD (8L:16D) condition from 14 weeks of LD (16L:8D), and found that testes began to regress just after around 5 days of SD (Robinson and Follett, 1982). However, it is important to note that after 14 weeks of LD, the quails would have been relatively photorefractory (Robinson and Follett, 1982), therefore prone to decrease their testicular mass once exposed to SD. Other reports show testicular regression starting at around 10 days after the transfer from LD to SD (Follett and Farner, 1966). In the present study, SD2W quail did indeed show regressed testes, comparable to testes mass in the SD group. The gonadal data presented here confirms the LD/SD paradigm and phenotypic plasticity in Japanese quail.

During the experiment, an additional indicator of reproduction, *i.e.* cloacal gland area, was measured. LH released from the anterior pituitary gland stimulates the testosterone

production from the testes, and testosterone leads to an increase in cloacal gland size in LD. In the present study, no statistically significant change in cloacal gland area was seen between SD and LD quail. This may be because of high variability in the LD cloacal gland measurement. Indeed, figure 6.4 does show an increase in cloacal area in LD compared to the SD group, but it can only be considered a trend, as it is not significant. However, there was a significant decrease in SD2W cloacal area compared to LD quail. The small cloacal area that can be seen after 2 weeks of SD is comparable to the size of the cloaca in the SD group. These results further confirm the non-breeding status of the animals at SD2W.

Finally, methylation levels were measured in the pituitary gland. In the long day condition, methylation levels significantly increased from ones in SD. This difference in methylation is consistent with the differences in methylation between SD and LD observed in the hypothalamus of the Siberian hamster (Stevenson and Prendergast, 2013; Lynch et al., 2016). However, at SD2W, methylation levels are still significantly higher than SD. Taken together, these data suggest that the confirmatory increase in testes mass in LD individuals reflects not only photostimulated status, but also an increase in DNA methylation in the pituitary gland. Although cloacal area seemingly increased after 1 week of LD, it revealed as just a trend and not as statistically significant. The high levels of DNA methylation following transfer to SD for 2 weeks after 1 week of LD suggest that 14 days may not be sufficient in eliciting the SD-decrease in pituitary methylation. DNA methylation may need to be reduced in SD, as it may be involved in the regulation of molecular processes underlying seasonal reproduction in a similar way to mammals. For instance, *Dio3* expression in Siberian hamsters in the hypothalamus is controlled by differential methylation at the *dio3* promoter region between LD and SD, where more methylation at the site occurs in LD compared to SD, to prepare the individuals for the repression of the HPG axis during the non-breeding period (Stevenson and Prendergast, 2013). Similar processes may be present in the avian pituitary gland, such as genes upstream or downstream of *FSH* and *LH*, *e.g.* oestrogen receptor. Other studies have

analysed epigenetic modulation of specific target genes involved in circannual rhythms in plants (Bastow et al., 2004), insects (Pegoraro et al., 2016), and mammals (Alvarado et al., 2015). In many plant species, flowering occurs following a period of exposure to cold temperatures, called vernalisation. In *Arabidopsis,* it was shown that vernalisation caused increased demethylation within the *FLC* gene, specifically on lysines 9 and 27 of histone 3, leading to flowering (Bastow et al., 2004). The wasp (*Nasonia vitripennis)* exhibits a process called diapause, or offspring developmental arrest in response to short days (Pegoraro et al., 2015). Disruption of *Dnmt1* and *Dnmt3* has been found to inhibit diapause, indicating an essential role of DNA methylation in the regulation of seasonal rhythms in this species (Pegoraro et al., 2015). Bisulfite sequencing assays showed differential methylation of multiple genes, *e.g.* the misshapen (*msn*) gene, a gene involved in insect photoreceptor development. In thirteen-lined ground squirrels (*Ictidomys tridecemlineatus*), a hibernating species, alterations in global skeletal muscle tissue DNA methylation were reported between periods of torpor and arousal (Alvarado et al., 2015). Differential promoter methylation was observed for myocyte enhancer factor 2C (*mef2c*), a gene likely involved in the control of metabolism in skeletal muscle tissue (Alvarado et al., 2015). Taken together, these studies suggest a critical role for DNA methylation and DNA methyltransferases in the regulation of seasonal rhythms in an array of species. Future experiments involving alternative techniques, such as bisulfite sequencing, will be essential for the identification of differentially methylated photoperiodic genes in the quail.

6.4.2 Study 2: Daily variation in DNA methyltransferase expression

The aim of study 2 was to determine whether DNA methyltransferase 3a and 3b expression is altered by photoperiod and/or throughout the day. For this study, Japanese quail were either kept in a LD or SD condition, and the pituitary glands were sampled either in the morning, 2 hours after lights on (zt2), or 14 hours after lights on (zt14). *DNMT3A* and *DNMT3B* expression was found not to be altered by daylength condition.

However, this could be given by the fact that 1 week of LD could not be sufficient to alter *DNMT3A/3B* expression. This is further supported by study 1's finding that suggests that 2 weeks is not sufficient for methylation levels to decrease in SD (Figure 6.5). However, time of day was shown to have an effect in *DNMT3A/3B* expression in SD quail, increasing in the morning and decreasing at night (Figure 6.6). This finding supports the hypothesis that DNA methyltransferase expression in the pituitary gland fluctuates during the day, although showing an opposite pattern of expression from other Dnmt reports. For instance, in the hypothalamus of Siberian hamsters, *Dnmt3a* peaks during the dark phase (Stevenson, 2017a). This could suggest both tissue- and species- specific variation, depending on the Dnmt's downstream target genes.

6.5 Conclusions

In the present study, two experiments were carried out in order to investigate DNA methylation reversibility and the daily regulation of *DNMT3A* and *DNMT3B* expression. It was shown that methylation in the pituitary gland of Japanese quail varies between the breeding and non-reproductive seasons, increasing in the former. It was also revealed that a 2-week transfer from LD to SD is not sufficient to elicit a decrease in methylation levels in this organ. The pituitary gland secretes follicle-stimulating hormone (FSH) and luteinising hormone (LH) to the gonads, stimulating reproductive maturation. In Japanese quail, a 5-fold rise in LH release has been shown just 20 hours after dawn, following transfer from SD to LD (Meddle and Follett, 1997). However, it may be possible that the epigenetic mechanisms that play a role in inhibiting the reproductive axis, perhaps even directly or indirectly interacting with important reproductive components such as LH, require additional time, *i.e.* methylation levels in the pituitary may require a period longer than 2 weeks to decrease to SD standards. The lower methylation found in SD compared to LD is consistent with methylation patterns in the hypothalamus of another highly seasonally plastic species, the Siberian hamster. In the Siberian hamster, one gene that is modulated

by these differences in DNA methylation, more specifically by the DNA methyltransferase enzymes, is *Dio3.* As mentioned in earlier chapters, *Dio3* catalyses the deactivation of triiodothyronine (T_3), an essential reproductive hormone. Differential methylation of the *Dio3* promoter between the breeding and non-breeding seasons underlies the oscillatory expression of *Dio3* (Stevenson and Prendergast, 2013). In future studies it will be useful to examine DNA methylation levels in the hypothalamus of Japanese quail and identify specific *DNMT1/3A/3B* target genes, in order to better understand the molecular processes responsible for seasonal reproduction in the avian brain.

The present study also revealed daily patterns in *DNMT3A* and *DNMT3B* expression in the pituitary gland of Japanese quail, with expression higher in the morning and lower at night, independent of daylength. *Dnmt3a* in the hypothalamus of the Siberian hamster has been shown to follow the opposite pattern of expression (Stevenson, 2017a), indicating that the daily variation in Dnmt expression patterns may be tissue-specific, as well as species-specific. Further studies are required to determine the patterns of Dnmt expression in other quail tissues involved in reproduction, such as the hypothalamus.

Chapter 7 – Summary and Conclusions

This chapter is drawn from the published paper "Tolla, E., & Stevenson, T. J. (2020). Sex differences and the neuroendocrine regulation of seasonal reproduction by supplementary environmental cues. *Integrative and Comparative Biology*.", as it forms part of the discussion and future directions surrounding the findings presented in this thesis.

7.1 The role of VA Opsin and OPN5 in avian reproduction

The thesis aimed to explore the mechanisms underlying the onset of seasonal reproduction in two common seasonal species, the Japanese quail and the Siberian hamster, both summer, long day (LD) breeders. Chapters 2, 3 and 6 described the known processes that control timing of breeding in Japanese quail, *Coturnix japonica.* The way in which the avian brain perceives photoperiod and translates it into a reproductive physiological response is still unclear, largely because the deep-brain photoreceptors (DBPs) responsible for this response have not yet been identified. Based on previous literature and criteria for candidate opsins, I have considered two photoreceptors, Vertebrate-Ancient (VA) Opsin and Neuropsin (OPN5). It was hypothesised that disrupting these two photoreceptors would suppress the reproductive response in LD quail. The expression of these two opsins was silenced via AAV intracerebral injection targeted to the third ventricle (3V) of the hypothalamus. It was found that both opsins may play a role in the stimulation of seasonal reproduction, highlighted by the pattern of gradual increase in testes mass and hypothalamic *GNRH* mRNA expression in KD individuals. However, this pattern must be investigated further, as it was found not to be statistically significant. Increasing sample size may clarify opsin function in future studies. This gradual increase suggests perhaps an inhibitory role for OPN5 and VA Opsin: once removed, a surge in gonadal mass and *GNRH* expression occurred. This hypothesis is supported by studies showing tonic

hyperpolarisation of other photoreceptors, *e.g.* rods and cones (Lamb et al., 2007; Gorman et al., 1971). On the other hand, cloacal growth rate was significantly lower in VA- and 'Both'- RNAi treated birds compared to control individuals, pointing perhaps to a stimulatory role for the two opsins. In addition, FSH receptor expression significantly decreased in OPN5-treated animals, compared to LD controls. This indicates that OPN5 may play a role in increasing testes sensitivity to gonadotropins during breeding months, enabling reproduction. I propose that two distinct mechanisms act on the seasonal reproduction of Japanese quail, one regulating testes growth and hypothalamic *GNRH* expression, and the second one modulating cloacal gland growth. These two mechanisms are likely to involve differential regulation by *LHB* and *FSH*, and, from the data gathered, it is possible that these two processes include both VA Opsin and OPN5. Further statistical tests to explain the results could be used, such as Gamma GLM models, as the distribution of the data is a Gamma distribution. Moreover, low sample size and incomplete protein knockdown were two limitations that may have masked significant results in this study. The pilot data presented in this chapter can be used to power future, larger-scale experiments. Furthermore, the study described in chapter 1 is the first report of timescale effects of VA Opsin and OPN5 silencing via AAV injection in the 3V of the Japanese quail.

DBP expression and the role of stress was also explored during embryonic development of the Japanese quail (chapter 3). Embryonic day 14 (E14) emerged as a critical developmental day, as expression of *GNRH* and *OPN5* increased significantly at this stage, independent of corticosterone (CORT) treatment. *GNRH* then decreased at E17, increasing again postnatally, presumably in preparation of puberty. One hypothesis for the *OPN5* surge at E14 implies a role for *OPN5* in the organisation of pathways that will modulate postnatal physiology, such as embryonic OPN5-dependent dopamine signalling that allows for adult vision in the retina of mice (Nguyen et al., 2019). Adult quail exhibited a reduction, although not significant, in *VA Opsin* and *OPN5* levels in the

hypothalamus in SD, compared to LD, further suggesting a stimulatory role for the opsins in activating the HPG axis. A significant reduction in *VA Opsin/OPN5* in SD may be concealed by sex-differences, as neither embryos or adults were separated by sex, and will need to be addressed in future studies.

7.2 DNA methylation and DNA methyltransferases

In recent years, epigenetic mechanisms, especially DNA methylation, have emerged as important components of the regulation of seasonal breeding in mammals. In Siberian hamsters, a seasonal species, there are marked differences in the seasonal variation in DNA methylation in the testes and uterine tissues. For example, in the short-day non-breeding state, the testes and uterine tissue show elevated levels of *Dnmt3a* expression and global DNA methylation (Lynch et al., 2016). The ovary was not found to show any change in DNA methyltransferase expression, nor global DNA methylation (Lynch et al., 2016). Moreover, two histone deacetylase enzymes (Hdac), testicular *Hdac3* and uterine *Hdac2*, exhibit seasonal changes in expression, suggesting that other epigenetic modifications are involved in sex-specific timing of reproductive function (Lynch et al., 2017). Seasonal rhythmic changes in DNA methylation and/or Dnmt expression have been reported across mammalian and avian species with localized patterns in liver (Alvarado et al., 2015), muscle (Alvarado et al., 2015), leukocytes (Stevenson et al., 2014), and hypothalamus (Sharma et al., 2018, Stevenson et al., 2013; Stevenson, 2017, Coyle et al., 2020). The present thesis aimed to understand whether these epigenetic processes also are involved in the timing and modulation of avian reproduction. It was hypothesised that *DNMT1, 3A* or *3B* expression would decrease in knock-down birds compared to control individuals, to perhaps reflect a SD-induced phenotype. *OPN5* K/D Japanese quail photostimulated for 28 days exhibited a significant reduction in the expression of pituitary *DNMT1*, compared to LD CV. In addition, overall hypothalamic *DNMT3B* levels in *OPN5* K/D birds decreased after 7 days of LD compared to only 2 days of LD, though not significantly. Taken

together, these data confirmed the proposed hypothesis and may indicate an interaction between *OPN5* pathways and epigenetic regulation in the avian brain. However, further molecular analyses, *e.g.* bisulfite sequencing, are required to establish the link between photoreceptor function and DNA methylation involved in seasonal reproduction.

In embryos, *DNMT1, 3A* and *3B* were also upregulated at E14, in a similar fashion to *GNRH* and *OPN5,* independent from CORT treatment. E14 could therefore be an important stage for epigenetic resetting. As outlined in chapter 1, previous studies have suggested that birds may possess a dosage compensation mechanism similar to mammalian X chromosome inactivation, via sex differences in transcription of specific regions, *e.g.* MHM and DMRT1. Further timepoint and RNAi experiments are required in order to fully understand sexual differentiation and dosage compensation in birds, and whether these sex determination mechanisms occur at E14 in the Japanese quail. In adult quail, *DNMT3A* and *DNMT3B* were both reduced in SD, although not significantly. However, this lack of significance may be masked by sex differences, as this particular study (chapter 3, study 2) considered both males and females.

Epigenetic reversibility was also investigated (chapter 6). It was found that global DNA methylation in the pituitary gland of Japanese quail was significantly reduced in SD individuals, compared to LD. These results are consistent with DNA methylation patterns in the hypothalamus of another markedly seasonal species, the Siberian hamster (Stevenson and Prendergast, 2013; Tolla et al., 2020b). However, after 7 days of LD, followed by 2 weeks of SD, pituitary DNA methylation levels did not decrease to initial SD standards. This suggests 2 weeks are not sufficient to reduce methylation levels within this organ. In the Siberian hamster, one gene that is regulated by this LD/SD switch in DNA methylation, is deiodinase 3 (*Dio3*). Decreased methylation of the *Dio3* promoter during non-breeding season allows for the suppression of the reproductive response (Stevenson and Prendergast, 2013). Seasonal changes in DNA methylation or DNA methyltransferase expression have been also reported in *Arabidopsis* (Bastow et al., 2004),

the wasp (*Nasonia vitripennis;* Pegoraro et al., 2015), and thirteen-lined ground squirrels (*Ictidomys tridecemlineatus*; Alvarado et al., 2015). In future studies it will be essential to investigate DNA methylation levels in the hypothalamus of Japanese quail, along with possible target genes, such as *DIO3*. It was also found that pituitary gland *DNMT3A* and *DNMT3B* are expressed at significantly higher levels in the morning, compared to the evening. Previous studies have suggested the opposite daily variation pattern in *Dnmt3a* expression in the hypothalamus of mice and Siberian hamsters (Stevenson, 2017). Further gene quantification and sequencing analyses are required to determine the patterns of Dnmt expression in other quail tissues involved in reproduction, such as the hypothalamus.

7.3 Neuroendocrine regulation of reproduction function in Siberian hamsters

Chapters 4 and 5 provided evidence for sex differences in reproductive neuroendocrine pathways in the Siberian hamster, specifically the role of triiodothyronine (T_3) in the stimulation of breeding. In seasonally breeding mammals and birds, the local synthesis of thyroid hormone in the hypothalamus is an essential component that governs the release of GnRH into the portal vasculature (Dardente et al., 2014). In female mice, silencing the expression of thyroid hormone receptor alpha 1 (THrα1) repressed reproductive behavior, but knocking down receptor β (THrβ) had the opposite effect (Dellovade et al., 2000). In contrast, THrα1 repression in male mice increased breeding behavior, and THrβ knock down resulted in its reduction (Dellovade et al., 2000). Recent data has shown that silencing THrα in male mice specifically suppresses the regulation of *Rfrp3* by melatonin, though not affecting *Tshb* or *Dio2/3* expression (Quignon et al., 2020). These data support the notion for sex differences in the role of thyroid hormones to regulate the neuroendocrine control of reproductive physiology and behaviour. In male Siberian hamsters, daily injections of T_3 in non-breeding animals held in short days trigger a long day breeding phenotype exhibited by increased testicular volume and body weight gain (Banks et al., 2016; Freeman et al., 2007; Bao et al., 2019). Female hamster data

(chapter 5) has revealed that females do not show any significant change in uterine mass, body mass or reproductive neuroendocrine expression in the hypothalamus in response to T_3. In addition, it was hypothesised that T_3 injections in SD hamsters would stimulate the increase in hypothalamic Dnmt expression seen in LD animals. It was found that in males, there was no change in *Dnmt1, 3a* or *3b* expression in response to daylength or exogenous T_3. However, females exhibited a reduction in *Dnmt3a* and *Dnmt3b* levels under SD photoperiod, independent of T_3, suggesting sex-specific variation. These data indicate that T_3 is not involved in the regulation of epigenetic enzymes underlying seasonal reproductive mechanisms in the Siberian hamster. It is possible that (1) a different hormonal signal controls photoperiodic variation in *Dnmt3a* and *Dnmt3b* expression, or (2) the expression levels reflect an endogenous circannual timing system (Stevenson and Lincoln, 2017). Finally, it is likely that additional supplementary cues are required to stimulate gonadal development in females besides photoperiodic induced changes in T_3-mediated GnRH release.

7.4 Supplementary cues and timing seasonal reproduction

As discussed throughout the present thesis, the duration of light has been shown to be the main predictive cue regulating the timing of breeding in both birds and mammals. However, studies have shown fundamental differences in the role that supplementary cues play in the reproductive development of male and female vertebrates (see chapter 1). Sexual differences in brain structure and function arise during a critical period in development and are the result of organizational effect of hormones (Arnold, 2009). Gonadal steroids have recently been identified to organize sex differences in epigenetic modifications in neuroendocrine substrates essential for the control of reproduction (Nugent et al., 2015). Supplementary cues fine tune the timing of seasonal reproduction. In many instances, there are marked sex differences in the reproductive response to supplementary cues. The integration of these environmental cues in the reproductive

neuroendocrine axis occurs in a sex-dependent manner (Ball and Ketterson, 2008). In chapter 1, I highlighted that sex-specific responses to supplementary cues likely develop from organizational effects of sex steroids early in development and that epigenetic modifications could be one factor that regulates the reproductive response to supplementary cues in adulthood (Figure 7.1).

The proposition that epigenetic modifications are central to the impact of supplementary cues has several exciting outstanding questions. First, how do seasonal supplementary cues regulate epigenetic modifications during juvenile development and adulthood? Second, how does sex influence the impact of supplementary cues on seasonal epigenetic modifications in the neuroendocrine axis? And lastly, can alterations in the epigenetic profile in response to supplementary cues be inherited? Until recently, the major limitation for understanding the molecular and genomic basis of seasonal rhythms has been due to a lack of genome sequence information. The role of supplementary cues in regulating genome plasticity can now be unraveled in the Great tit and the Siberian hamster, as their genomes have been sequenced (Laine et al., 2016; Bao et al., 2019). Recent work has shown that DNA methylation patterns in Great tit red blood cells show robust seasonal rhythms and several candidate markers (e.g. *Dio2*) may be consistent genomic markers of internal timing mechanisms (Viitaniemi et al., 2019). These questions are a few that will begin to shed exciting new discoveries for the role of epigenetic modifications in the timing of seasonal reproduction.

7.5 Summary and future directions

The aims of the thesis were to gain a deeper understanding of (1) whether VA Opsin and OPN5 underlie seasonal reproduction in quail, (2) embryonic and adult levels of VA Opsin and OPN5 in quail, and whether stress hormones affect these levels, and (3) oscillating patterns of DNA methylation and DNA methyltransferase enzymes within the HPG axis of both Japanese quail and Siberian hamster.

Overall, the studies presented show that the seasonal increase in photoperiod causes two avian brain photoreceptors, VA Opsin and OPN5, to translate the light signal into a reproductive response, likely through tonic hyperpolarisation. The data also provided evidence for embryonic day 14 as a critical developmental day in Japanese quail, as there was a rise in hypothalamic expression of *GNRH* and *OPN5* at this stage. Oscillating patterns of DNA methylation levels and DNA methyltransferase expression between seasons were found in both Japanese quail and Siberian hamster, suggesting a role for epigenetic processes in modulating breeding in these species. Furthermore, data presented in chapters 4 and 5 indicated sex-differences in T_3 function, as well as regulation by DNA methyltransferases, in the hypothalami of Siberian hamsters. It was proposed that female hamsters require supplementary cues for full sexual maturation. Future studies involving exposing female hamsters to a combination of exogenous T_3 injections and social cues, *e.g.* male presence, are required to delineate the reproductive neuroendocrine pathways in female mammals. Additional experiments are also essential to identify downstream processes of both DBPs and epigenetic processes, in order to untangle the intricate neuroendocrine network that underlies the onset of reproduction.

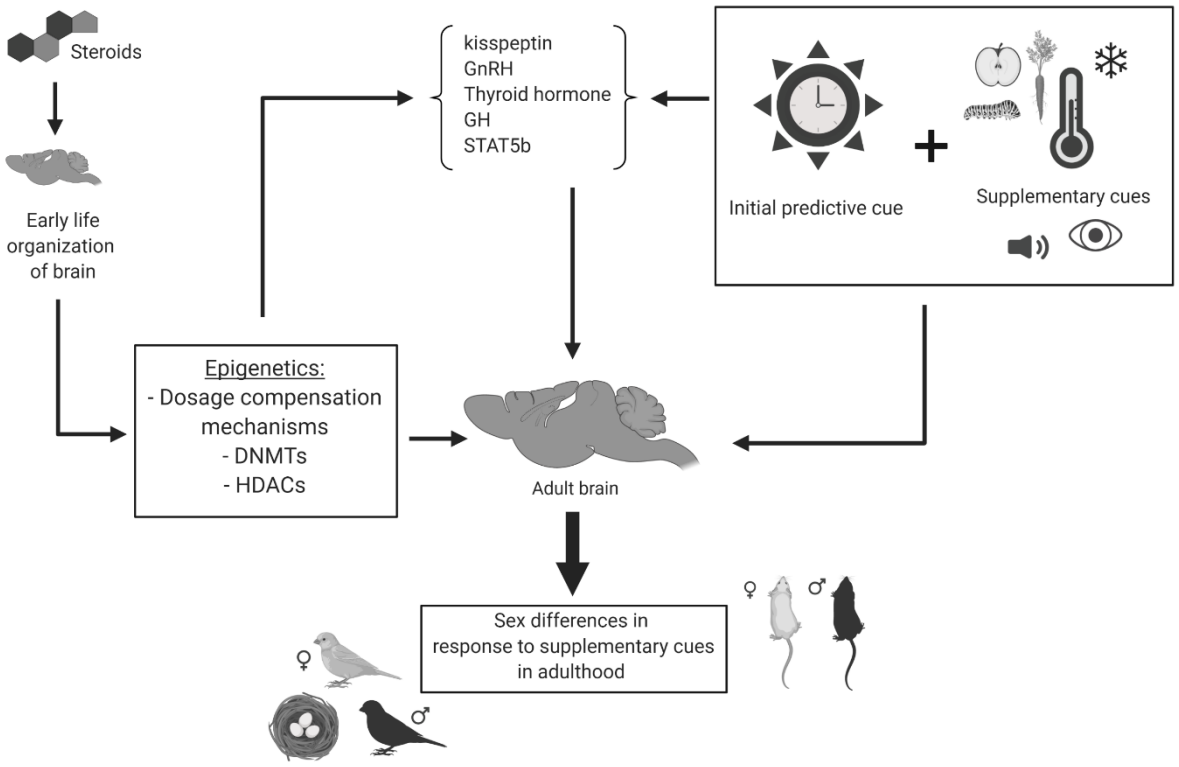

Figure 7.1 - The proposed model of early-life organization of the brain in seasonal species leading to sex differences in response to supplementary cues in adulthood. The organizational effects of sex steroids early during embryonic development in mammals and birds could potentially be mediated by a range of epigenetic mechanisms, such as dosage compensation (*e.g.*, X chromosome silencing in mammals), or modulation of DNA methyltransferase (DNMTs) and histone deacetylase (HDACs) expression. These epigenetic processes persist in the adult brain and affect an array of peptides involved in seasonal reproduction: kisspeptin, gonadotropin releasing hormone (GnRH), thyroid hormone and its receptors, growth hormone (GH) and signal transducer and activator of transcription 5 (STAT5b), all of which have been shown to be directly altered by photoperiod ('initial predictive cue') and supplementary cues such as food availability, nutrient quality, temperature, visual and auditory cues. Epigenetic modifications could be one factor that regulates the reproductive response to supplementary cues in adulthood and male-female differences in this response. From Tolla and Stevenson, 2020.

Appendix A: Supplementary tables

Table A.1. List of statistical tests done per chapter. GNRH= Gonadotrophin-releasing hormone; GNIH= Gonadotrophin-inhibiting hormone; DNMT= DNA methyltransferase; TSHB= Thyroid stimulating hormone beta; LHB= luteinising hormone beta; FSH= follicle-stimulating hormone; GNRH-R= Gonadotrophin-releasing hormone receptor; FSHR= follicle-stimulating hormone receptor; LHR= luteinising hormone receptor; AR= androgen receptor; OPN5= neuropsin; VA Opsin= Vertebrate ancient opsin; N/A= not applicable.

Chapter	Figure #	Transformation	Explanatory variable(s)	Response variable	Test applied	F or H?	F/H	P-value
2	2.3 A	No	Injection	Testes mass	1 way ANOVA	F	1.72	0.199
2	2.3 B	Log10	Injection	Testes mass	1 way ANOVA	F	11.334	<0.001
2	2.3 C	No	Injection	Testes mass	1 way ANOVA	F	0.205	0.892
2	2.4 A	No	Injection	Body mass	Kruskal-Wallis	H	0.317	0.957
2	2.4 B	No	Injection	Body mass	1 way ANOVA	F	0.88	0.487
2	2.4 C	No	Injection	Body mass	1 way ANOVA	F	2.413	0.069
2	2.5	Log10	Injection	Cloacal gland growth rate	2 way ANOVA	F	3.512	0.009
2	2.5	Log10	Week	Cloacal gland growth rate	2 way ANOVA	F	33.636	<0.001
2	2.6 A	Log10	Injection	*GNRH* expression	1 way ANOVA	F	0.237	0.869
2	2.6 B	Log10	Injection	*GNRH* expression	1 way ANOVA	F	3.858	0.012
2	2.7 A	No	Injection	*GNIH* expression	1 way ANOVA	F	0.104	0.957
2	2.7 B	Log10	Injection	*GNIH* expression	Kruskal-Wallis	H	3.237	0.519
2	2.8 A	Log10	Injection	*DNMT1* expression	1 way ANOVA	F	0.214	0.885
2	2.8 B	Log10	Injection	*DNMT3A* expression	1 way ANOVA	F	0.12	0.947
2	2.8 C	Log10	Injection	*DNMT3B* expression	1 way ANOVA	F	0.134	0.939
2	2.9 A	Log10	Injection	*DNMT1 expression*	Kruskal-Wallis	H	4.833	0.305
2	2.9 B	Log10	Injection	*DNMT3A* expression	Kruskal-Wallis	H	8.601	0.072
2	2.9 C	Log10	Injection	*DNMT3B* expression	Kruskal-Wallis	H	4.222	0.377
2	2.9 D	Log10	Injection	*DNMT3B* expression	T-test (1 tailed p-value)	N/A	N/A	0.0536
2	2.10 A	No	Injection	*TSHB* expression	1 way ANOVA	F	1.632	0.219
2	2.10 B	Log10	Injection	*LHB* expression	1 way ANOVA	F	0.663	0.586
2	2.10 C	Log10	Injection	*FSH* expression	1 way ANOVA	F	9.346	<0.001
2	2.11 A	Log10	Injection	*TSHB* expression	Kruskal-Wallis	H	2.129	0.712
2	2.11 B	Log10	Injection	*LHB* expression	Kruskal-Wallis	H	1.865	0.761
2	2.11 C	Log10	Injection	*FSH* expression	1 way ANOVA	F	3.139	0.028
2	2.12 A	Log10	Injection	*TSHB* expression	Kruskal-Wallis	H	5.681	0.128
2	2.12 B	Log10	Injection	*GNRH-R* expression	1 way ANOVA	F	2.899	0.051
2	2.12 C	Log10	Injection	*LHB* expression	Kruskal-Wallis	H	4.372	0.224
2	2.12 D	Log10	Injection	*FSH* expression	Kruskal-Wallis	H	5.943	0.114
2	2.13 A	Log10	Injection	*DNMT1* expression	Kruskal-Wallis	H	9.523	0.023
2	2.13 B	Log10	Injection	*DNMT3A* expression	1 way ANOVA	F	0.988	0.412
2	2.14 A	Log10	Injection	*FSHR* expression	1 way ANOVA	F	0.907	0.458
2	2.14 B	Log10	Injection	*LHR* expression	Kruskal-Wallis	H	5.309	0.151
2	2.14 C	Log10	Injection	*AR* expression	1 way ANOVA	F	0.718	0.555
2	2.15 A	Log10	Injection	*FSHR* expression	Kruskal-Wallis	H	7.395	0.116
2	2.15 B	Log10	Injection	*LHR* expression	Kruskal-Wallis	H	0.554	0.968

Chapter	Figure #	Transformation	Explanatory variable(s)	Response variable	Test applied	F or H?	F/H	P-value
2	2.15 C	Log10	Injection	*AR* expression	Kruskal-Wallis	H	3.527	0.474
2	2.16 A	Log10	Injection	*FSHR* expression	1 way ANOVA	F	3.028	0.044
2	2.16 B	Log10	Injection	*LHR* expression	Kruskal-Wallis	H	1.164	0.762
2	2.16 C	Log10	Injection	*AR* expression	1 way ANOVA	F	1.478	0.24
2	2.17 A	No	Injection	Plasma testosterone	1 way ANOVA	F	0.922	0.451
2	2.17 B	No	Injection	Plasma testosterone	1 way ANOVA	F	31.693	<0.001
2	2.17 C	Log10	Injection	Plasma testosterone	1 way ANOVA	F	8.105	<0.001
3	3.1	Log10	Age	*GNRH* expression	2 way ANOVA	F	6.242	0.001
3	3.1	Log10	Hormone	*GNRH* expression	2 way ANOVA	F	0.031	0.861
3	3.1	Log10	Age x hormone	*GNRH* expression	2 way ANOVA	F	0.397	0.756
3	3.2 A	Log10	Age	*DNMT1* expression	2 way ANOVA	F	18.392	<0.001
3	3.2 A	Log10	Hormone	*DNMT1* expression	2 way ANOVA	F	8.594	0.005
3	3.2 A	Log10	Age x hormone	*DNMT1* expression	2 way ANOVA	F	0.655	0.584
3	3.2 B	Log10	Age	*DNMT3A* expression	2 way ANOVA	F	3.824	0.016
3	3.2 B	Log10	Hormone	*DNMT3A* expression	2 way ANOVA	F	0.858	0.359
3	3.2 B	Log10	Age x hormone	*DNMT3A* expression	2 way ANOVA	F	1.345	0.271
3	3.2 C	Log10	Age	*DNMT3B* expression	2 way ANOVA	F	16.248	<0.001
3	3.2 C	Log10	Hormone	*DNMT3B* expression	2 way ANOVA	F	0.256	0.615
3	3.2 C	Log10	Age x hormone	*DNMT3B* expression	2 way ANOVA	F	4.683	0.006
3	3.3 A	Log10	Age	*VA Opsin* expression	2 way ANOVA	F	1.692	0.191
3	3.3 A	Log10	Hormone	*VA Opsin* expression	2 way ANOVA	F	0.0632	0.803
3	3.3 A	Log10	Age x hormone	*VA Opsin* expression	2 way ANOVA	F	0.693	0.564
3	3.3 B	Log10	Age	*OPN5* expression	2 way ANOVA	F	7.103	0.004
3	3.3 B	Log10	Hormone	*OPN5* expression	2 way ANOVA	F	3.726	0.066
3	3.3 B	Log10	Age x hormone	*OPN5* expression	2 way ANOVA	F	3.01	0.069
3	3.4 A	Log10	Daylength	*GNRH* expression	T-test (1 tailed p-value)	N/A	N/A	0.159
3	3.4 B	Log10	Daylength	*GNIH* expression	T-test (1 tailed p-value)	N/A	N/A	0.14
3	3.4 C	Log10	Daylength	*TSHB* expression	T-test (1 tailed p-value)	N/A	N/A	0.0000041
3	3.5 A	Log10	Daylength	*DNMT1* expression	T-test (2 tailed p-value)	N/A	N/A	0.727
3	3.5 B	Log10	Daylength	*DNMT3A* expression	T-test (2 tailed p-value)	N/A	N/A	0.436
3	3.5 C	Log10	Daylength	*DNMT3B* expression	T-test (2 tailed p-value)	N/A	N/A	0.334
3	3.6 A	Log10	Daylength	*VA Opsin* expression	T-test (2 tailed p-value)	N/A	N/A	0.475
3	3.6 B	Log10	Daylength	*OPN5* expression	T-test (2 tailed p-value)	N/A	N/A	0.194
4	4.2 A	Log10	Daylength	*DNMT1* expression	2 way ANOVA	F	0.0000616	0.994
4	4.2 A	Log10	Injection	*DNMT1* expression	2 way ANOVA	F	0.189	0.667
4	4.2 A	Log10	Daylength x Injection	*DNMT1* expression	2 way ANOVA	F	0.42	0.522

Chapter	Figure #	Transformation	Explanatory variable(s)	Response variable	Test applied	F or H?	F/H	P-value
4	4.2 B	Log10	Daylength	*DNMT3A* expression	2 way ANOVA	F	0.129	0.722
4	4.2 B	Log10	Injection	*DNMT3A* expression	2 way ANOVA	F	0.203	0.656
4	4.2 B	Log10	Daylength x Injection	*DNMT3A* expression	2 way ANOVA	F	0.233	0.633
4	4.2 C	Log10	Daylength	*DNMT3B* expression	2 way ANOVA	F	0.0937	0.762
4	4.2 C	Log10	Injection	*DNMT3B* expression	2 way ANOVA	F	0.35	0.559
4	4.2 C	Log10	Daylength x Injection	*DNMT3B* expression	2 way ANOVA	F	0.0000678	0.993
5	5.1 A	No	Daylength	Uterine mass	2 way ANOVA	F	14.592	<0.001
5	5.1 A	No	Injection	Uterine mass	2 way ANOVA	F	0.121	0.731
5	5.1 A	No	Daylength x Injection	Uterine mass	2 way ANOVA	F	0.421	0.522
5	5.1 B	No	Daylength	Body mass	2 way ANOVA	F	36.097	<0.001
5	5.1 B	No	Injection	Body mass	2 way ANOVA	F	2.851	0.104
5	5.1 B	No	Daylength x Injection	Body mass	2 way ANOVA	F	0.0409	0.841
5	5.2 A	No	Daylength	*Gnrh* expression	2 way ANOVA	F	15.552	<0.001
5	5.2 A	No	Injection	*Gnrh* expression	2 way ANOVA	F	0.0956	0.76
5	5.2 A	No	Daylength x Injection	*Gnrh* expression	2 way ANOVA	F	0.421	0.522
5	5.2 B	No	Daylength	*Rfrp3* expression	2 way ANOVA	F	4.237	0.051
5	5.2 B	No	Injection	*Rfrp3* expression	2 way ANOVA	F	1.852	0.186
5	5.2 B	No	Daylength x Injection	*Rfrp3* expression	2 way ANOVA	F	0.59	0.45
5	5.2 C	No	Daylength	*Tshb* expression	2 way ANOVA	F	18.613	<0.001
5	5.2 C	No	Injection	*Tshb* expression	2 way ANOVA	F	5.387	0.029
5	5.2 C	No	Daylength x Injection	*Tshb* expression	2 way ANOVA	F	5.726	0.025
5	5.3 A	Log10	Daylength	*Dnmt1* expression	2 way ANOVA	F	0.744	0.397
5	5.3 A	Log10	Injection	*Dnmt1* expression	2 way ANOVA	F	0.489	0.491
5	5.3 A	Log10	Daylength x Injection	*Dnmt1* expression	2 way ANOVA	F	0.349	0.56
5	5.3 B	Log10	Daylength	*Dnmt3a* expression	2 way ANOVA	F	4.342	0.048
5	5.3 B	Log10	Injection	*Dnmt3a* expression	2 way ANOVA	F	0.0189	0.892
5	5.3 B	Log10	Daylength x Injection	*Dnmt3a* expression	2 way ANOVA	F	2.62	0.118
5	5.3 C	Log10	Daylength	*Dnm3b* expression	2 way ANOVA	F	5.716	0.025
5	5.3 C	Log10	Injection	*Dnm3b* expression	2 way ANOVA	F	2.927	0.099
5	5.3 C	Log10	Daylength x Injection	*Dnm3b* expression	2 way ANOVA	F	3.561	0.071
6	6.3	Log10	Daylength	Testes mass	Kruskal-Wallis	H	17.612	<0.001
6	6.4	Log10	Daylength	Cloacal gland area	Kruskal-Wallis	H	11.164	0.011
6	6.5	Log10	Daylength	5 mC (%)	Kruskal-Wallis	H	13.246	0.004
6	6.6	Log10	Daylength	*DNMT3A* expression	2 way ANOVA	F	3.006	0.096
6	6.6	Log10	Time (zeitenberg)	*DNMT3A* expression	2 way ANOVA	F	6.725	0.016
6	6.6	Log10	Daylength x Time	*DNMT3A* expression	2 way ANOVA	F	0.254	0.619
6	6.6	Log10	Daylength	*DNMT3B* expression	2 way ANOVA	F	0.0235	0.879
6	6.6	Log10	Time (zeitenberg)	*DNMT3B* expression	2 way ANOVA	F	5.766	0.024
6	6.6	Log10	Daylength x Time	*DNMT3B* expression	2 way ANOVA	F	0.715	0.406

Table A.2. List of post-hoc tests done per chapter. LD= long-day; SD= short-day; GNRH= Gonadotrophin-releasing hormone; GNIH= Gonadotrophin-releasing hormone; DNMT= DNA methyltransferase; TSHB= Thyroid stimulating hormone beta; LHB= luteinising hormone beta; FSH= follicle-stimulating hormone; GNRH-R= Gonadotrophin-releasing hormone receptor; FSHR= follicle-stimulating hormone receptor; LHR= luteinising hormone receptor; AR= androgen receptor; OPN5= neuropsin; VA Opsin= Vertebrate ancient opsin; wk= week; 7d= 7-day photostimulation; E11= embryonic day 11; E14= embryonic day 14; E17= embryonic day 17; P10= postanal day 10; CORT= corticosterone-injected; SD1W; 1 week short-day group; SD2W= 2 week short-day group; 5mC %= 5 methylcytosine percentage; N/A= not applicable.

Chapter	**Figure #**	**Post-Hoc test**	**Comparison factor**	**Response variable**	**Comparison**	**P-value**
2	2.3 B	Tukey Test	Injection	Testes mass	Both vs. SD	<0.001
2	2.3 B	Tukey Test	Injection	Testes mass	VA vs. SD	<0.001
2	2.3 B	Tukey Test	Injection	Testes mass	OPN5 vs. SD	<0.001
2	2.3 B	Tukey Test	Injection	Testes mass	CV vs. SD	0.004
2	2.5	Fisher LSD	Injection	Cloacal gland growth rate	CV vs. VA	0.004
2	2.5	Fisher LSD	Injection	Cloacal gland growth rate	CV vs. Both	0.001
2	2.5	Fisher LSD	Week	Cloacal gland growth rate	1 wk vs. 4 wk	<0.001
2	2.5	Fisher LSD	Week	Cloacal gland growth rate	1 wk vs. 3 wk	<0.001
2	2.5	Fisher LSD	Week	Cloacal gland growth rate	1 wk vs. 2 wk	0.003
2	2.5	Fisher LSD	Week	Cloacal gland growth rate	2 wk vs. 4 wk	<0.001
2	2.5	Fisher LSD	Week	Cloacal gland growth rate	2 wk vs. 3 wk	0.003
2	2.5	Fisher LSD	Week	Cloacal gland growth rate	3 wk vs. 4 wk	0.006
2	2.6 B	Tukey Test	Injection	*GNRH* expression	SD vs. VA	0.018
2	2.10 C	Tukey Test	Injection	*FSH* expression	CV vs. SD	<0.001
2	2.10 C	Tukey Test	Injection	*FSH* expression	OPN5 vs. SD	0.007
2	2.10 C	Tukey Test	Injection	*FSH* expression	VA vs. SD	0.023
2	2.11 C	Tukey Test	Injection	*FSH* expression	Both 7d vs. SD	0.023
2	2.13 A	Tukey Test	Injection	*DNMT1* expression	CV vs. VA	0.028
2	2.16 A	Tukey Test	Injection	*FSHR* expression	CV vs. OPN5	0.035
2	2.17 B	Tukey Test	Injection	Plasma testosterone	VA vs. SD	<0.001
2	2.17 B	Tukey Test	Injection	Plasma testosterone	Both vs. SD	<0.001
2	2.17 B	Tukey Test	Injection	Plasma testosterone	OPN5 vs. SD	<0.001
2	2.17 B	Tukey Test	Injection	Plasma testosterone	CV vs. SD	<0.001
2	2.17 C	Tukey Test	Injection	Plasma testosterone	CV vs. SD	<0.001
2	2.17 C	Tukey Test	Injection	Plasma testosterone	OPN5 vs. SD	<0.001
2	2.17 C	Tukey Test	Injection	Plasma testosterone	VA vs. SD	0.01
3	3.1	Fisher LSD	Age	*GNRH* expression	E14 vs.E11	<0.001
3	3.2 A	Fisher LSD	Age	*DNMT1* expression	E14 VS.E17	0.017
3	3.2 A	Fisher LSD	Age	*DNMT1* expression	P10 vs.E11	<0.001
3	3.2 A	Fisher LSD	Age	*DNMT1* expression	E17 vs. E11	0.002
3	3.2 A	Fisher LSD	Hormone	*DNMT1* expression	Control vs. CORT	0.005
3	3.2 B	Fisher LSD	Age	*DNMT3A* expression	E14 vs.E11	0.004
3	3.2 B	Fisher LSD	Age	*DNMT3A* expression	P10 vs.E11	0.006
3	3.2 C	Fisher LSD	Hormone within E11	*DNMT3B* expression	Control vs. CORT	0.003
3	3.2 C	Fisher LSD	Age within CORT	*DNMT3B* expression	E14 vs.E11	<0.001
3	3.2 C	Fisher LSD	Age within CORT	*DNMT3B* expression	E14 VS.E17	0.038

Chapter	Figure #	Post-Hoc test	Comparison factor	Response variable	Comparison	P-value
3	3.2 C	Fisher LSD	Age within CORT	*DNMT3B* expression	PND10 vs.E11	<0.001
3	3.2 C	Fisher LSD	Age within CORT	*DNMT3B* expression	E17 vs. E11	<0.001
3	3.2 C	Fisher LSD	Age within Control	*DNMT3B* expression	E14 vs.E11	0.031
3	3.3 B	Fisher LSD	Age	*OPN5* expression	E14 vs. P10	0.005
3	3.3 B	Fisher LSD	Age	*OPN5* expression	E14 vs. E11	0.013
5	5.1 A	Tukey Test	Daylength	Uterine mass	LD vs. SD	<0.001
5	5.1 A	Tukey Test	Daylength within Saline	Uterine mass	LD vs. SD	0.043
5	5.1 A	Tukey Test	Daylength within T3	Uterine mass	LD vs. SD	0.003
5	5.1 B	Tukey Test	Daylength	Body mass	LD vs. SD	<0.001
5	5.1 B	Tukey Test	Daylength within Saline	Body mass	LD vs. SD	<0.001
5	5.1 B	Tukey Test	Daylength within T3	Body mass	LD vs. SD	<0.001
5	5.2 A	Tukey Test	Daylength	*Gnrh* expression	LD vs. SD	<0.001
5	5.2 A	Tukey Test	Daylength within Saline	*Gnrh* expression	LD vs. SD	0.005
5	5.2 A	Tukey Test	Daylength within T3	*Gnrh* expression	LD vs. SD	0.021
5	5.2 C	Tukey Test	Daylength	*Tshb* expression	LD vs. SD	<0.001
5	5.2 C	Tukey Test	Injection	*Tshb* expression	Saline vs. T3	0.029
5	5.2 C	Tukey Test	Injection within LD	*Tshb* expression	Saline vs. T3	0.002
5	5.2 C	Tukey Test	Daylength within Saline	*Tshb* expression	LD vs. SD	<0.001
5	5.3 B	Tukey Test	Daylength	*Dnmt3a* expression	LD vs. SD	0.048
5	5.3 B	Tukey Test	Daylength within Saline	*Dnmt3a* expression	LD vs. SD	0.02
5	5.3 C	Tukey Test	Daylength	*Dnmt3b* expression	LD vs. SD	0.025
5	5.3 C	Tukey Test	Injection within LD	*Dnmt3b* expression	Saline vs. T3	0.016
5	5.3 C	Tukey Test	Daylength within Saline	*Dnmt3b* expression	LD vs. SD	0.008
6	6.3	Dunn's method	Daylength	Testes mass	SD1W vs. SD	0.001
6	6.3	Dunn's method	Daylength	Testes mass	LD vs. SD	0.002
6	6.3	Dunn's method	Daylength	Testes mass	SD2W vs. SD	0.084
6	6.4	Dunn's method	Daylength	Cloacal gland area	LD vs. SD2W	0.031
6	6.4	Dunn's method	Daylength	Cloacal gland area	SD2W vs. SD	0.012
6	6.5	Dunn's method	Daylength	5 mC (%)	LD vs. SD	0.009

Table A.3. Summary of genes/proteins analysed. LD= long-day; SD= short-day; GNRH= Gonadotrophin-releasing hormone; GNIH= Gonadotrophin-releasing hormone; DNMT= DNA methyltransferase; TSHB= Thyroid stimulating hormone beta; LHB= luteinising hormone beta; FSH= follicle-stimulating hormone; GNRH-R= Gonadotrophin-releasing hormone receptor; FSHR= follicle-stimulating hormone receptor; LHR= luteinising hormone receptor; AR= androgen receptor; OPN5= neuropsin; VA Opsin= Vertebrate ancient opsin; w= week; 2d= 2-day photostimulation; 7d= 7-day photostimulation; 28d= 28-day photostimulation; 12d= 12 days; E11= embryonic day 11; E14= embryonic day 14; E17= embryonic day 17; P10= postanal day 10; CORT= corticosterone-injected; SAL= saline-injected; T3= triiodothyronine-injected; SD1W; 1 week short-day group; SD2W= 2 week short-day group; 5mC %= 5 methylcytosine percentage; zt= zeiteberg time (2: 2 hours after lights on; 14: 14 hours after lights on; N/A= not applicable.

Chapter	Figure #	Species	Sex	Tissue	Timepoint	mRNA/protein?	Name of gene/protein
2	2.2 A	Japanese quail	Male	Hypothalamus	2d and 7d	mRNA	*OPN5* and VA *Opsin*
2	2.2 B	Japanese quail	Male	Hypothalamus	2d and 7d	protein	OPN5 and VA Opsin
2	2.6 A	Japanese quail	Male	Hypothalamus	2d	mRNA	*GNRH*
2	2.6 B	Japanese quail	Male	Hypothalamus	7d	mRNA	*GNRH*
2	2.7 A	Japanese quail	Male	Hypothalamus	2d	mRNA	*GNIH*
2	2.7 B	Japanese quail	Male	Hypothalamus	7d	mRNA	*GNIH*
2	2.8 A	Japanese quail	Male	Hypothalamus	2d	mRNA	*DNMT1*
2	2.8 B	Japanese quail	Male	Hypothalamus	2d	mRNA	*DNMT3A*
2	2.8 C	Japanese quail	Male	Hypothalamus	2d	mRNA	*DNMT3B*
2	2.9 A	Japanese quail	Male	Hypothalamus	7d	mRNA	*DNMT1*
2	2.9 B	Japanese quail	Male	Hypothalamus	7d	mRNA	*DNMT3A*
2	2.9 C	Japanese quail	Male	Hypothalamus	7d	mRNA	*DNMT3B*
2	2.9 D	Japanese quail	Male	Hypothalamus	2d and 7d	mRNA	*DNMT3B*
2	2.10 A	Japanese quail	Male	Pituitary gland	2d	mRNA	*TSHB*
2	2.10 B	Japanese quail	Male	Pituitary gland	2d	mRNA	*LHB*
2	2.10 C	Japanese quail	Male	Pituitary gland	2d	mRNA	*FSH*
2	2.11 A	Japanese quail	Male	Pituitary gland	7d	mRNA	*TSHB*
2	2.11 B	Japanese quail	Male	Pituitary gland	7d	mRNA	*LHB*
2	2.11 C	Japanese quail	Male	Pituitary gland	7d	mRNA	*FSH*
2	2.12 A	Japanese quail	Male	Pituitary gland	28d	mRNA	*TSHB*
2	2.12 B	Japanese quail	Male	Pituitary gland	28d	mRNA	*GNRH-R*
2	2.12 C	Japanese quail	Male	Pituitary gland	28d	mRNA	*LHB*
2	2.12 D	Japanese quail	Male	Pituitary gland	28d	mRNA	*FSH*
2	2.13 A	Japanese quail	Male	Pituitary gland	28d	mRNA	*DNMT1*
2	2.13 B	Japanese quail	Male	Pituitary gland	28d	mRNA	*DNMT3A*
2	2.14 A	Japanese quail	Male	Testes	2d	mRNA	*FSH-R*
2	2.14 B	Japanese quail	Male	Testes	2d	mRNA	*LH-R*
2	2.14 C	Japanese quail	Male	Testes	2d	mRNA	*AR*
2	2.15 A	Japanese quail	Male	Testes	7d	mRNA	*FSH-R*
2	2.15 B	Japanese quail	Male	Testes	7d	mRNA	*LH-R*
2	2.15 C	Japanese quail	Male	Testes	7d	mRNA	*AR*
2	2.16 A	Japanese quail	Male	Testes	28d	mRNA	*FSH-R*
2	2.16 B	Japanese quail	Male	Testes	28d	mRNA	*LH-R*
2	2.16 C	Japanese quail	Male	Testes	28d	mRNA	*AR*
2	2.17 A	Japanese quail	Male	Plasma	2d	protein	Testosterone
2	2.17 B	Japanese quail	Male	Plasma	7d	protein	Testosterone

Chapter	Figure #	Species	Sex	Tissue	Timepoint	mRNA/protein?	Name of gene/protein
2	2.17 C	Japanese quail	Male	Plasma	28d	protein	Testosterone
3	3.1	Japanese quail	Male	Hypothalamus	E11, E14, E17, P10	mRNA	*GNRH*
3	3.2 A	Japanese quail	Male	Hypothalamus	E11, E14, E17, P10	mRNA	*DNMT1*
3	3.2 B	Japanese quail	Male	Hypothalamus	E11, E14, E17, P10	mRNA	*DNMT3A*
3	3.2 C	Japanese quail	Male	Hypothalamus	E11, E14, E17, P10	mRNA	*DNMT3B*
3	3.3 A	Japanese quail	Male	Hypothalamus	E11, E14, E17, P10	mRNA	*VA Opsin*
3	3.3 B	Japanese quail	Male	Hypothalamus	E11, E14, E17, P10	mRNA	*OPN5*
3	3.4 A	Japanese quail	Male	Hypothalamus	LD (12d), SD (12d)	mRNA	*GNRH*
3	3.4 B	Japanese quail	Male	Hypothalamus	LD (12d), SD (12d)	mRNA	*GNIH*
3	3.4 C	Japanese quail	Male	Hypothalamus	LD (12d), SD (12d)	mRNA	*TSHB*
3	3.5 A	Japanese quail	Male	Hypothalamus	LD (12d), SD (12d)	mRNA	*DNMT1*
3	3.5 B	Japanese quail	Male	Hypothalamus	LD (12d), SD (12d)	mRNA	*DNMT3A*
3	3.5 C	Japanese quail	Male	Hypothalamus	LD (12d), SD (12d)	mRNA	*DNMT3B*
3	3.6 A	Japanese quail	Male	Hypothalamus	LD (12d), SD (12d)	mRNA	*VA Opsin*
3	3.6 B	Japanese quail	Male	Hypothalamus	LD (12d), SD (12d)	mRNA	*OPN5*
4	4.2 A	Siberian hamster	Male	Hypothalamus	LD SAL (2w), SD SAL (2w), LD T3 (2w), SD T3 (2w)	mRNA	*DNMT1*
4	4.2 B	Siberian hamster	Male	Hypothalamus	LD SAL (2w), SD SAL (2w), LD T3 (2w), SD T3 (2w)	mRNA	*DNMT3A*
4	4.2 C	Siberian hamster	Male	Hypothalamus	LD SAL (2w), SD SAL (2w), LD T3 (2w), SD T3 (2w)	mRNA	*DNMT3B*
5	5.2 A	Siberian hamster	Female	Hypothalamus	LD SAL (2w), SD SAL (2w), LD T3 (2w), SD T3 (2w)	mRNA	*Gnrh*
5	5.2 B	Siberian hamster	Female	Hypothalamus	LD SAL (2w), SD SAL (2w), LD T3 (2w), SD T3 (2w)	mRNA	*Rfrp3*
5	5.2 C	Siberian hamster	Female	Hypothalamus	LD SAL (2w), SD SAL (2w), LD T3 (2w), SD T3 (2w)	mRNA	*Tshb*
5	5.3 A	Siberian hamster	Female	Hypothalamus	LD SAL (2w), SD SAL (2w), LD T3 (2w), SD T3 (2w)	mRNA	*Dnmt1*
5	5.3 B	Siberian hamster	Female	Hypothalamus	LD SAL (2w), SD SAL (2w), LD T3 (2w), SD T3 (2w)	mRNA	*Dnmt3a*
5	5.3 C	Siberian hamster	Female	Hypothalamus	LD SAL (2w), SD SAL (2w), LD T3 (2w), SD T3 (2w)	mRNA	*Dnmt3b*
6	6.6	Japanese quail	Male	Pituitary gland	zt2, zt14	mRNA	*DNMT3A* and *DNMT3B*

Appendix B: Published papers

Bao R, Onishi K, **Tolla E**, Ebling F, Lewis J, Anderson R, Barrett PJ, Prendergast B, Stevenson TJ. (2019). Genome sequencing and transcriptome analyses of the Siberian hamster hypothalamus identify mechanisms for seasonal energy balance. *Proceedings of the National Academy of Sciences*, 116(26), pp.13116-13121.

Coyle CS, **Tolla E**, Stevenson TJ. (2020). Rhythmic epigenetics in neuroendocrine and immune systems. In *Developmental Neuroendocrinology* (pp. 295-314). Springer, Cham.

Tolla E, Pérez J, Dunn I, Meddle S, & Stevenson TJ. (2019). Neuroendocrine regulation of seasonal reproduction. In *Oxford Research Encyclopedia of Neuroscience*. Oxford University Press.

Pérez J, **Tolla E**, Dunn I, Meddle S and Stevenson TJ. (2019). A Comparative Perspective on Extra-retinal Photoreception. *Trends in Endocrinology & Metabolism*, 30(1), pp.39-53.

Tolla E, Stevenson TJ. (2020). Sex differences and the neuroendocrine regulation of seasonal reproduction by supplementary environmental cues. *Integrative and Comparative Biology*.

Tolla E, Stevenson TJ. (2020). Photoperiod-induced changes in hypothalamic de novo DNA methyltransferase expression are independent of triiodothyronine in female Siberian hamsters. *General and Comparative Endocrinology*.

Coyle CS, Caso F, **Tolla E**, Barrett PJ, Onishi KG, Tello JA, Stevenson TJ. (2019). Ovarian hormones induce de novo DNA methyltransferase expression in the Siberian hamster suprachiasmatic nucleus. *Journal of Neuroendocrinology*.

Published paper: Bao et al., 2019

PNAS

Genome sequencing and transcriptome analyses of the Siberian hamster hypothalamus identify mechanisms for seasonal energy balance

Riyue Bao[a,b], Kenneth G. Onishi[c], Elisabetta Tolla[d], Fran J. P. Ebling[e], Jo E. Lewis[f], Richard L. Anderson[g], Perry Barrett[g], Brian J. Prendergast[c,h], and Tyler J. Stevenson[d,1]

[a]Center for Research Informatics, University of Chicago, Chicago, IL 60637; [b]Department of Pediatrics, University of Chicago, Chicago, IL 60637; [c]Institute for Mind and Biology, University of Chicago, Chicago, IL 60637; [d]Institute for Biodiversity, Animal Health and Comparative Medicine, University of Glasgow, Glasgow G61 1QH, United Kingdom; [e]School of Life Sciences, University of Nottingham, Nottingham NG7 2UH, United Kingdom; [f]Institute of Metabolic Sciences, University of Cambridge, Cambridge CB2 0QQ, United Kingdom; [g]Rowett Institute, University of Aberdeen, Aberdeen AB25 2ZD, United Kingdom; and [h]Department of Psychology, University of Chicago, Chicago, IL 60637

Edited by Donald Pfaff, The Rockefeller University, New York, NY, and approved May 13, 2019 (received for review February 18, 2019)

Synthesis of triiodothyronine (T_3) in the hypothalamus induces marked seasonal neuromorphology changes across taxa. How species-specific responses to T_3 signaling in the CNS drive annual changes in body weight and energy balance remains uncharacterized. These experiments sequenced and annotated the Siberian hamster (*Phodopus sungorus*) genome, a model organism for seasonal physiology research, to facilitate the dissection of T_3-dependent molecular mechanisms that govern predictable, robust, and long-term changes in body weight. Examination of the *Phodopus* genome, in combination with transcriptome sequencing of the hamster diencephalon under winter and summer conditions, and in vivo-targeted expression analyses confirmed that proopiomelanocortin (*pomc*) is a primary genomic target for the long-term T_3-dependent regulation of body weight. Further in silico analyses of *pomc* promoter sequences revealed that thyroid hormone receptor 1β-binding motif insertions have evolved in several genera of the Cricetidae family of rodents. Finally, experimental manipulation of food availability confirmed that hypothalamic *pomc* mRNA expression is dependent on longer-term photoperiod cues and is unresponsive to acute, short-term food availability. These observations suggest that species-specific responses to hypothalamic T_3, driven in part by the receptor-binding motif insertions in some cricetid genomes, contribute critically to the long-term regulation of energy balance and the underlying physiological and behavioral adaptations associated with the seasonal organization of behavior.

triiodothyronine | proopiomelanocortin | seasonal | obesity

Rheostatic regulation of physiological processes is pervasive (1), and naturally occurring, long-term programmed seasonal reproduction and energy balance is one salient example. High-amplitude seasonal cycles in energy balance and somatic growth are common in nature and provide a unique and valuable opportunity to identify the genomic and molecular pathways involved in rheostatic control of physiology (2–5). Siberian hamsters (*Phodopus sungorus*) exhibit marked changes in energy balance as they adapt from a summer to a winter environment in nature: a decrease in day length (i.e., photoperiod) below ∼13 h light/day triggers seasonal infertility, anorexia, and a dramatic decrease in body fat (2). Consequently, *Phodopus* provide a unique and important model for neuroendocrine, physiological, and behavioral mechanisms that govern long-term seasonal regulation of body weight and reproduction (2, 5); these robust phenotypic changes in physiology and behavior can be recapitulated in the laboratory with manipulations of day length (photoperiod) alone.

Triiodothyronine (T_3)-responsive neuro-glial substrates figure prominently in the transduction of photoperiod signals into the neuroendocrine system. T_3-responsive targets in the central nervous system (CNS) constitute an evolutionarily conserved system that orchestrates morphological brain plasticity in the service of timing seasonal biology (6, 7). Enzymes that act on thyroid hormones, in particular the iodothyronine deiodinases (type 2 and 3; DIO2 and DIO3, respectively) respond to seasonal changes in photoperiod-driven melatonin secretion and govern peri-hypothalamic catabolism of the prohormone thyroxine (T_4), which limits T_3-driven changes in neuroendocrine activity. T_3 induces ligand-dependent rearrangement of the thyroid hormone receptor (TR), and T_3 drives the vast majority of TR-induced gene expression (8). Increased hypothalamic T_3 production in long summer days, driven in most amniotes by peri-hypothalamic DIO2-mediated conversion of T_4 to the biologically active hormone T_3, activates anabolic neuroendocrine pathways that maintain reproductive competence and increase body weight. Decreased T_3 signaling is afforded by peri-hypothalamic DIO3 expression, which catabolizes T_4 and T_3 into receptor-inactive amines, and is associated with adaptation to reproductively inhibitory photoperiods (9–12). In diverse taxa, DIO2

Significance

The genome and hypothalamic transcriptome of the Siberian hamster were sequenced and annotated to identify transcriptional pathways that exhibit seasonal plasticity in energy balance. Adaptation to short winter days reversed seasonal obesity and down-regulated hypothalamic proopiomelanocortin, and exogenous triiodothyronine reinstated weight gain and proopiomelanocortin expression. In silico analyses identified the evolution of thyroid hormone receptor binding motifs in the proximal promoter of the proopiomelanocortin gene of hamsters and other Cricetidae. Energetic challenges imposed by food restriction elicited orexigenic and anorexigenic neuropeptide responses in the hypothalamus, but did not affect proopiomelanocortin, which was regulated only by photoperiod. Hypothalamic proopiomelanocortin is maintained by photoperiod-driven triiodothyronine signaling and thereby affords adaptive long-term temporal organization of physiological systems that regulate energy balance.

Author contributions: R.B., E.T., F.J.P.E., P.B., B.J.P., and T.J.S. designed research; R.B., K.G.O., E.T., J.E.L., R.L.A., and T.J.S. performed research; R.B., K.G.O., E.T., F.J.P.E., J.E.L., R.L.A., P.B., and T.J.S. analyzed data; and R.B., B.J.P., and T.J.S. wrote the paper.

The authors declare no conflict of interest.

This article is a PNAS Direct Submission.

Data deposition: The Siberian hamster genome is available in GenBank (https://www.ncbi.nlm.nih.gov/nuccore/1056038647).

[1]To whom correspondence may be addressed. Email: tyler.stevenson@glasgow.ac.uk.

This article contains supporting information online at www.pnas.org/lookup/suppl/doi:10.1073/pnas.1902896116/-/DCSupplemental.

Published online June 12, 2019.

and DIO3 responses to environmental cues (e.g., photoperiod, or hours of light per day) have established links between tissue-specific patterns of T_3 signaling and seasonal changes in reproduction and ponderal growth/regression (2, 6). Conspicuously absent are insights into how T_3 signaling impacts hypothalamic orexigenic/anorexigenic neuropeptide systems that govern changes in energy balance mandatory to support these seasonal cycles of reproduction and life history.

Results and Discussion

Characterization of the Siberian Hamster Genome and Photoperiodic Diencephalon. Seasonal changes in day length are sufficient to induce a constellation of changes in Siberian hamster physiology that support adaptation to and survival of winter: exposure to a short-day photoperiod (SD) causes molt to a more insulative fur (Fig. 1*A*) and gonadal involution ($P < 0.001$; Fig. 1*B*), body weight is strikingly reduced in SD, white adipose tissue is depleted ($P < 0.001$; Fig. 1*C*), and brown adipose tissue thermogenic capacity is augmented (13). Nocturnal foraging persists throughout the winter months, but metabolic rate is decreased through daily torpor, which conserves energy (14). The absence of comprehensive genomic information for *Phodopus* has limited molecular insights into the physiological processes that regulate these seasonal adaptations in energy balance. To address this deficiency, we used Illumina sequencing to draft the Siberian hamster genome (*SI Appendix*, Table S1 and Fig. S1; ref. 15). To complement genome annotation and to identify molecular pathways involved in energy balance, a seasonal hypothalamic transcriptome was also sequenced and annotated. Transcriptomic analyses were performed on hypothalamic RNA from adult male hamsters following adaptation to long-day (LD) and SD photoperiods. Over 5,000 unique transcripts were identified, and 32 exhibited significant expression changes between the photoperiods [false discovery rate (FDR) < 0.05-corrected; *SI Appendix*, Table S2] with the top differentially expressed protein-coding transcripts shown (Fig. 1*D*). Multiple RNAs that have previously been implicated individually in the long-term, neuroendocrine control of reproductive physiology were identified, including thyrotropin-stimulating hormone subunit-β (*tshβ*), neuropeptide VF precursor (*npvf*), and iodothyronine deiodinase type III (*dio3*; Fig. 1*E* and *SI Appendix*, Fig. S2). Gene

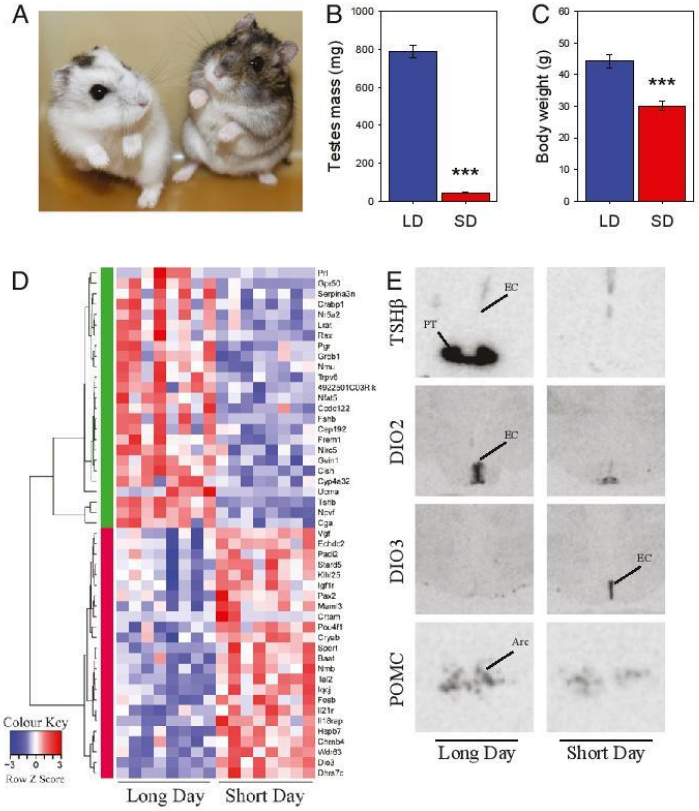

Fig. 1. Seasonal hypothalamic transcriptome in Siberian hamsters. Compared with long-day photoperiod (LD; > 13 h light/day), adaptation to short-day photoperiod (SD) induces multiple physiological adaptations including (*A*) pelage molt, from agouti (*Right*) to white (*Left*) fur, (*B*) gonadal regression, and (*C*) decreased body mass (*B* and *C* depict mean ± SEM; ***$P < 0.001$). (*D*) RNA-seq analyses revealed extensive plasticity in RNA expression for transcripts associated with neuroendocrine function. Rows indicate individual transcripts identified at a group level to be significantly (FDR < 0.05) up-regulated (red) or down-regulated (blue) by SD photoperiod. Columns indicate individual hamsters (biological replicates; LD: $n = 8$; SD: $n = 8$). (*E*) Following adaptation to LD or SD photoperiods, expression of multiple transcripts associated with energy balance, food intake, and neuroendocrine function changed in dissected hypothalamic tissue: thyrotrophin-stimulating hormone β (*tshβ*), iodothyronine deiodinase type II (*dio2*) and type III (*dio3*), and proopiomelanocortin (*pomc*). These mRNAs are anatomically localized to the pars tuberalis (PT, *tshβ*), the ependymal cells (EC, *dio2*, *dio3*) lining the third ventricle, or the arcuate nucleus (Arc, *pomc*).

ontology (GO) analyses identified a photoperiodic transcriptome strikingly enriched (FDR-corrected $P < 0.05$) for cellular activity related to hormone secretion and neuropeptide signaling (*SI Appendix*, Table S3 and Figs. S3 and S4). Common to many ($n = 10$) GO terms enriched by photoperiod in the hypothalamic transcriptome was proopiomelanocortin (*pomc*), a neuropeptide that is centrally implicated in energy balance, suggesting that *pomc* may be a first-order neuropeptide in the rheostatic regulation of body weight by seasonal changes in photoperiod.

Role of T_3 in Hypothalamic *pomc* Regulation. Across diverse taxa thyroid hormone signaling plays a central role in regulating seasonal physiology via actions in the brain and in the periphery (4, 5). To further examine how thyroid hormone signaling interacts with *pomc* in the regulation of seasonal energy balance, hypothalamic expression of *pomc*, along with other genes, the protein products of which participate in CNS regulation of food intake and energy balance (*npy*, *agrp*, *cart*), was quantified in LD and SD hamsters following 2 wk of daily T_3 treatment (5 μg; s.c.). Adaptation to SD decreased (Fig. 2*A* and *SI Appendix*, Fig. S5*A*), and T_3 injections increased (Fig. 2*A*) body weight. Adaptation to SD also significantly down-regulated expression of *pomc*, consistent with prior reports (16–18) Moreover in SD, T_3 increased hypothalamic *pomc* expression to a level indistinguishable from that exhibited in LD ($P < 0.05$; Fig. 2*B*). Photoperiod did not alter *npy*, *agrp* or *cart* expression ($P > 0.05$, all comparisons; *SI Appendix*, Fig. S5), and T_3 was likewise without effect on *npy* or *agrp* ($P > 0.05$, both comparisons; *SI Appendix*, Fig. S5), but did up-regulate *cart* expression in SD (*SI Appendix*, Fig. S5). Taken together, these data suggest, among hypothalamic appetitive neuropeptides, a relatively selective effect of T_3 on *pomc*.

Regulation of gene expression by T_3 occurs via binding to the TRs, which in turn bind to thyroid hormone response elements (TREs) in the DNA sequence. TREs are composed of half-sites, the spacing and orientation of which can affect their regulatory ability (19, 20). In silico analyses of the *pomc* proximal promoter sequence using PROMO (21, 22) identified two thyroid-receptor 1b (*Thrb*) half-sites: TCC-TGG-TGA and TCA-CCT-GGA (*SI Appendix*, Table S4), indicating that T_3 may be capable of directly regulating *pomc* transcription. These specific binding motifs were not identified in the proximal promoter for *npy*, *agrp*, or *cart*, consistent with the relative specificity and selectivity illustrated in Fig. 2 (*SI Appendix*, Fig. S5) and suggesting a privileged role for *pomc* among the hypothalamic targets of T_3 in signal transduction relevant to seasonal changes energy balance. Indeed, a phylogenic analysis of *pomc* proximal promoters across a range of species revealed that this specific *Thrb* motif has evolved in the Cricetidae family (Fig. 2*C*). To further evaluate responsiveness of the hamster-specific *Thrb* motif in the regulation of *pomc*, GH3 cells were transfected with a Siberian hamster or the mouse *pomc* proximal promoter sequence upstream of a luciferase reporter gene, and the ability of T_3 to drive luciferase activity was evaluated; however, this assay indicated that T_3 was no more effective than hormone-free vehicle in driving

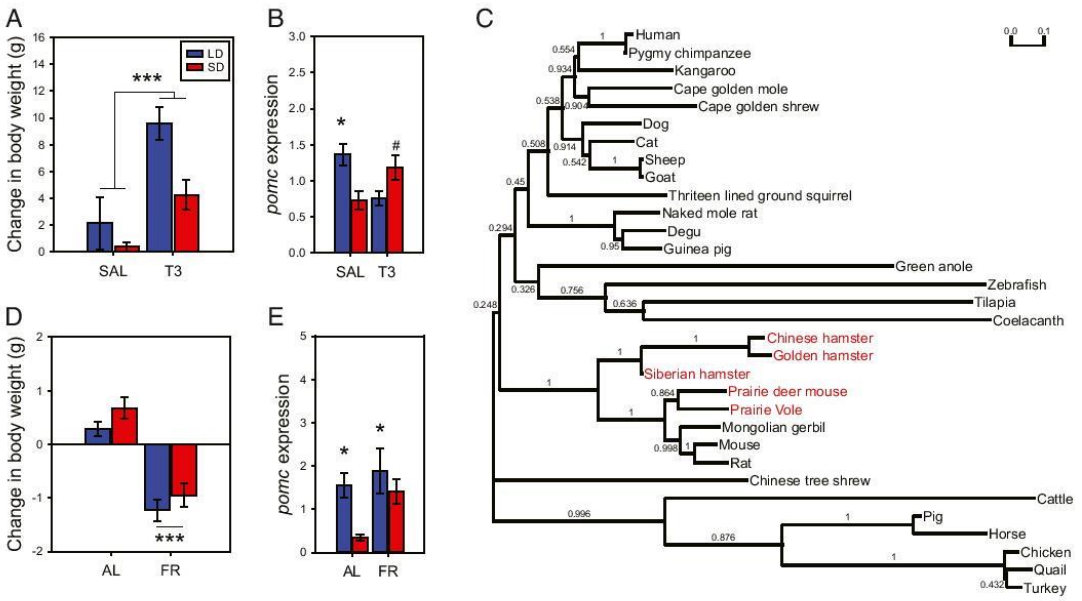

Fig. 2. Long-term photoperiodic regulation of hypothalamic *pomc* expression. Mean ± SEM (*A*) change in body mass and (*B*) hypothalamic *pomc* mRNA expression in adult male Siberian hamsters following 8 wk of exposure to LD (blue bars) or SD (red bars) and 2 wk of daily treatment with T_3 (5 μg; s.c.). (*A*) T_3 treatment increased body mass in LD and in SD (***$P < 0.001$). (*B*) SD inhibited hypothalamic *pomc* expression in saline-treated controls (*$P < 0.01$ vs. LD saline). T_3 suppressed *pomc* expression in LD-treated hamsters ($P < 0.05$) but increased *pomc* expression in SD (#$P < 0.05$). (*C*) PROMO analysis identified thyroid hormone receptor 1b (*Thrb*)-binding motifs in the Siberian hamster *pomc* proximal promoter, and phylogenetic analyses of the *pomc* proximal promoter indicated that the hamster-specific *Thrb* motif has evolved multiple times in the Cricetidae family (indicated by red font). Mean ± SEM (*D*) change in body mass and (*E*) hypothalamic *pomc* mRNA expression in adult male and female Siberian hamsters subjected to a 16-h interval of food deprivation (FR) or maintained on ad libitum feeding (AL) after 12 wk of exposure to LD (blue bars) or SD (red bars). (*D*) FR decreased body mass in both LD and SD (***$P < 0.001$ vs. AL). (*E*) SD significantly reduced hypothalamic *pomc* (*$P < 0.05$) but FR did not significantly affect hypothalamic *pomc* mRNA expression (*$P = 0.54$ within LD; $P = 0.07$ within SD).

transcriptional activity (P >0.30; *SI Appendix*, Fig. S6). The inadequacy of T_3 alone in driving luciferase activity in this assay may indicate that additional intracellular signaling pathways are required, or that functional T_3-driven transcriptional regulation at the *pomc* proximal promoter requires distal enhancer elements.

Regulation of Hypothalamic *pomc* Expression by Photoperiod vs. Food. POMC per se is functionally inert, but it is cleaved into multiple peptides, one of which, α-melanocyte–stimulating hormone, is a potent inhibitor of food intake (23). The *pomc*-knockout mice are obese (24), and acute starvation markedly down-regulates *pomc* expression, indicative of its central role in energy homeostasis (25). Therefore, we assessed the impact of acute food restriction on body weight and responses of hypothalamic neuropeptides related to energy homeostasis (*pomc*, *cart*, *npy*, and *agrp*). Male and female hamsters were acutely (16 h) food-restricted (FR) after 12 wk of adaptation to LD or SD photoperiods. Again, hamsters weighed less in SD ($P < 0.001$; *SI Appendix*, Fig. S7) and acute FR further reduced body weight in both photoperiods ($P < 0.001$; Fig. 2*D*), suggesting a comparable challenge to energy homeostasis in both groups. FR also significantly up-regulated hypothalamic expression of neuropeptides that play key roles in food intake and energy balance: *npy*, *agrp*, and *cart* ($P < 0.05$, all comparisons; *SI Appendix*, Fig. S7), but failed to significantly inhibit *pomc* expression ($P > 0.05$; Fig. 2*E*), consistent with prior reports (16–18). Taken together, these data indicate that hypothalamic *pomc* is not inhibited by acute negative energy balance in Siberian hamsters but support the hypothesis that *pomc* expression is instead associated with longer-term (seasonal) states of metabolic change, specifically those linked to predictive changes in body weight and metabolism associated with seasonal/photoperiodic adjustments.

General Discussion

Here we present the sequencing and annotation of the Siberian hamster genome, a model organism for seasonal biology. The availability of well-described intergenic regions facilitated the identification of TR-binding motifs in a key neuropeptide involved in the regulation of energy balance, *pomc*. These hypothalamic transcriptomic analyses also identified several other well-described molecular markers that are regulated by photoperiodic cues: RNA-seq analyses identified changes in transcripts associated with the neuroendocrine control of reproduction, including follicle-stimulating hormone subunit-β (*fshβ*), prolactin (*prl*), and progesterone receptor (*pgr*). Moreover, we identified several previously uncharacterized transcripts involved in neuronal communication such as Glutamate metabotropic receptors (*grm*) and Gamma-aminobutyric acid type A receptor (*gabr*). Several noncoding RNA (e.g., *mir133b*) were also observed to exhibit photoperiodic variation in expression and suggest that a complex level of molecular plasticity is involved in the seasonal neuroendocrine regulation of energy balance yet to be uncovered. Mechanistic assessments confirmed that *dio3* and *pomc* were transcriptionally controlled by photoperiod in a manner that effects a down-regulation of T_3 and POMC-mediated signaling in winter. Importantly, seasonal changes in *pomc* are not merely a consequence of changes in appetite or food intake (16–18). Enhancing T_3 signaling counteracted the short-day photoperiodic inhibition of *pomc*, suggesting that interactions between T_3 and *pomc* may be in a superordinate position to drive seasonal energetic transitions.

Siberian hamsters have emerged as a key model species for investigations of biological rhythms on an annual timescale (26, 27). The hamster genome elaborated in this paper, combined with the prevalence of enrichment for POMC signaling in the RNA-seq data, directly facilitated identification of the insertions of *Thrb*-binding motifs in the *pomc* proximal promoter, which was subsequently also identified in seasonally breeding Syrian hamsters, deer mice, and prairie voles. One noteworthy pattern was increased *pomc* expression in LD hamsters, which defend a higher body weight set point and classify as obese. An observation based on common biomedical mammalian models, e.g., mice and humans, is that *pomc* has anorexigenic effects on food intake and appetite because of RNA splicing directed to the production of α-MSH as the principal neuropeptide. In Siberian hamsters, however, the actions of *pomc* may be driven by post-translational modifications such as increased carboxypeptidase E expression to drive alternative *pomc* slicing and neuropeptide synthesis (28).

The present study replicates multiple prior reports in Siberian hamsters, which exhibit decreases in body mass after ∼4 wk of exposure to SD (9–12), a winter decrease in body weight typical of other Cricetidae such as deer mice and prairie voles (28), which exhibit *Thrb* motifs in the *pomc* promoter. *Thrb* half-sites are also found in the *pomc* promoter of Syrian hamsters, which, unlike voles, deer mice, and *Phodopus*, initially exhibit modest increases in body mass and later decreases in body mass over the course of prolonged exposure to SD (30, 31). We suspect that neuroendocrine pathways other than TREs in the *pomc* promoter may explain these differences. Indeed, paralleling these species differences in body mass responses to SD are notable differences in the temporal regulation of *dio3* expression in the hypothalamus. Syrian hamsters exhibit little-to-no *dio3* expression in the hypothalamus for the first 10 wk in SD (32), an interval during which body mass responses are presumably being initiated. A delayed *dio3* response to SD would be predicted to allow elevated, LD-like, T_3 signaling to persist in the hypothalamus over the initial interval of exposure to SD and perhaps allow this species to exhibit transient weight gain. This would be consistent with the temporal expression of *dio3* and body weight change seen under natural photoperiod conditions in Siberian hamsters (33). Additionally, Syrian and Siberian hamsters may differ in the extent to which the abrupt square-wave photoperiod transitions deployed in laboratory investigations synchronize changes in body weight, compared with timing under natural photoperiodic cycles.

The results of experiment 4 provide convergent evidence in support of *pomc* as a prime candidate for long-term photoperiodic regulation of energy balance, independent of short-term energetic cues. FR elicited the expected increases in *npy* and *agrp*, but was completely ineffective in inhibiting *pomc*, confirming other reports in this species (16–18). Indeed, a nonsignificant paradoxical increase in *pomc* was observed in SD hamsters, which may reflect an additional layer of photoperiodic modulation of the response to food deprivation. Prior work indicated a relative insensitivity of hypothalamic *pomc*, body mass, luteinizing hormone, or follicle-stimulating hormone to leptin in LD hamsters (16). Collectively, these data indicate that hypothalamic *pomc* expression is regulated by longer-term predictive cues such as photoperiod (likely via T_3 signaling) independent of more proximal energetic cues such as those that reference short-term food availability (e.g., FR) or adiposity (i.e., leptin).

Finally, the availability of an annotated genome and hypothalamic transcriptome of a highly seasonal mammal may permit deeper understanding of the molecular signaling pathways that translate environmental cues into seasonal biological signals, which is relevant for understanding and mitigating the impact of seasonal disruption on health and well-being in human and nonhuman animals (34).

Methods and Materials

Additional details of experimental protocols are described in *SI Appendix*.

Animal Use and Ethics. All procedures were approved by the Animal Care and Use Committee at the University of Chicago, the National Institutes of Health *Guide for the Care and Use of Laboratory Animals* (35), or the Animal Welfare and Ethics Review Board at the University of Aberdeen, and were

conducted under the Home Office license (PPL 70/7917). All procedures were in accordance with the ARRIVE guidelines. Siberian hamsters (*P. sungorus*) were used in these studies. Hamsters were housed in polypropylene cages illuminated for 15 h or 9 h per day (LD or SD, respectively; lights off at 1700 hours CST). Food [Teklad (formerly Harlan)] and filtered tap water were provided ad libitum.

Genome Sequencing, De Novo Assembly, and Transcriptome Analyses. The data analysis workflow for genome assembly and annotation is outlined in *SI Appendix*, Fig. S1. Genomic DNA was extracted from liver tissue of two adult male hamsters using DNeasy (Qiagen; catalog #69504), and the quantity was determined using Nanodrop spectrophotometry (ThermoFisher Scientific). One paired-end library with a 250-bp insert size were prepared and sequenced on an Illumina HiSeq2000 instrument at The University of Chicago Genomic Facility. A total of 918 million 100-bp paired-end reads were generated achieving a depth of 37× (*SI Appendix*, Table S1). Hypothalamic RNA was extracted using Qiagen RNeasy (catalog #74104), and quantity was assessed using Nanodrop. Paired-end libraries were prepared and sequenced on an Illumina HiSeq 2000 instrument at The University of Chicago Genomic Facility. The transcriptome was reconstructed using a Trinity de novo assembly pipeline (v2013-02-25) (36). Transcripts differentially expressed between groups were identified at both gene and isoform level using the Bioconductor package edgeR (37), with samples of the same group as biological replicates within the group. See *SI Appendix*, Table S2 for expression fold change and FDR-corrected *P* values.

Quantification of Hypothalamic RNA Expression. The hypothalamus was dissected and expression of *tshβ*, deiodinase type II (*dio2*), and deiodinase type III (*dio3*) were measured to confirm photoperiod manipulation (*SI Appendix*). Hypothalamic RNA was extracted from tissues using TRIzol (ThermoFisher Scientific). cDNA was synthesized using SuperScript III (Invitrogen), and cDNA was stored at −20 °C. qPCRs for mRNA expression in hypothalamic tissue were performed using Bio-Rad CFX96. *SI Appendix*, Table S5, describes the qPCR parameters for each target and reference transcript. We used PCR Miner (38) to calculate reaction efficiencies and cycle thresholds, and samples were evaluated based on the Minimum Information for Publication of Quantitative Real-Time PCR guidelines (39).

In Situ Hybridization of Select Photoperiodic Genes. mRNA distribution of select photoperiodic genes (*tshβ*, *dio2*, *dio3*, *pomc*) were examined in coronal hypothalamic sections by radioactive in situ hybridization. Twenty-micron–thick sections of the hypothalamus were cut and mounted onto poly-L-lysine–coated slides. Riboprobes were generated from cloned PCR-generated fragments as previously described (33). In situ hybridization was carried out as previously described (40).

Photoperiodic and Triiodothyronine Regulation of *pomc*. Hamsters were group-housed in LD ($n = 15$) or transferred to SD (9L:15D; $n = 16$) cabinets for 8 wk (Arrowmight). LD and SD hamsters were then divided into two treatment groups that received daily saline control (LD+S and SD+S) or 5-μg T3 injections (LD+T_3 and SD+T_3). The final treatment group sample sizes were LD+S ($n = 9$), LD+T_3 ($n = 6$), SD+S ($n = 8$), and SD+T_3 ($n = 8$). These dose and injection regimens were selected based on previous work (41–43).

Impact of Food Restriction on *pomc* Expression. This experiment used adult (~6 mo of age; $n = 23$) male and female Siberian hamsters. Hamsters were housed in LD ($n = 12$) or transferred to SD for 12 wk. Body weights were measured before photoperiodic treatment (0 wk) and then at 2-wk intervals through week 12, shortly before lights off. On the last day of the experiment, a subset of LD and SD hamsters was kept on food ad libitum ($n = 10$) or had food completely removed (i.e., food restriction; FR, $n = 13$). FR started just before lights-out on the final night. Overall, there were four experimental groups: ad libitum-fed LD ($n = 5$), ad libitum-fed SD ($n = 5$), LD-FR ($n = 7$), and SD-FR ($n = 6$).

Statistical Analyses. Sigmaplot was used for all statistical analyses unless stated otherwise. For experiments 2 and 4, we conducted repeated two-way ANOVAs to examine the impact of SD treatment on body weight. We conducted two-way ANOVAs for experiment 2 (factors: photoperiod vs. T_3 injection) and experiment 4 (factors: photoperiod and food restriction) to analyze the effect of daily T_3 injections or food restriction on the change in body weight and hypothalamic gene expression. Significance was determined at $P < 0.05$.

ACKNOWLEDGMENTS. We thank the manuscript reviewers for constructive feedback; David G. Hazlerigg, Cristina Saenz de Miera, and Valerie Simonneaux for genome sequence contributions; Nicolas Scrutton and Lindsey Duguid for expert technical assistance; and Michael Jarsulic for technical assistance on the high-performance computing clusters. This project was supported by a project research grant from The British Society for Neuroendocrinology (to T.J.S.); Grants BB/M021629/1 and BB/M001555/1 (to F.J.P.E.) from the Biotechnology and Biological Sciences Research Council, and Grants UL1-TR000430 (to T.J.S. and B.J.P.) and R01-AI067406 (to B.J.P.) from the National Institutes of Health. T.J.S. is funded by The Leverhulme Trust. The Center for Research Informatics was supported by the Biological Sciences Division at the University of Chicago with additional support provided by the Institute for Translational Medicine/Clinical and Translational award (NIH 5UL1TR002389-02) and the University of Chicago Comprehensive Cancer Center Support Grant (NIH Grant P30CA014599). The bioinformatics analysis was performed on high-performance computing clusters at the Center for Research Informatics, Biological Sciences Division. P.B. was funded by the Scottish Government Rural and Environment Science and Analytical Services Division grant to the Rowett Institute.

1. N. Mrosovksy, *Rheostasis: The Physiology of Change* (Oxford University Press, 1990).
2. F. J. P. Ebling, Hypothalamic control of seasonal changes in food intake and body weight. *Front. Neuroendocrinol.* **37**, 97–107 (2015).
3. T. J. Stevenson, G. F. Ball, Information theory and the neuropeptidergic regulation of seasonal reproduction in mammals and birds. *Proc. Biol. Sci.* **278**, 2477–2485 (2011).
4. Y. Nakane, T. Yoshimura, Universality and diversity in the signal transduction pathway that regulates seasonal reproduction in vertebrates. *Front. Neurosci.* **8**, 115 (2014).
5. T. J. Stevenson, B. J. Prendergast, R. J. Nelson, "Mammalian seasonal rhythms: Behavior and neuroendocrine substrates" in *Hormones, Brain, and Behavior*, D. Pfaff *et al.*, Eds. (Elsevier Press, ed. 3, 2016).
6. T. Nishiwaki-Ohkawa, T. Yoshimura, Molecular basis for regulating seasonal reproduction in vertebrates. *J. Endocrinol.* **229**, R117–R127 (2016).
7. T. Yoshimura *et al.*, Light-induced hormone conversion of T4 to T3 regulates photoperiodic response of gonads in birds. *Nature* **426**, 178–181 (2003).
8. A. C. Bianco, D. Salvatore, B. Gereben, M. J. Berry, P. R. Larsen, Biochemistry, cellular and molecular biology, and physiological roles of the iodothyronine selenodeiodinases. *Endocr. Rev.* **23**, 38–89 (2002).
9. J. E. Lewis, F. J. P. Ebling, Tanycytes as regulators of seasonal cycles in neuroendocrine function. *Front. Neurol.* **8**, 79 (2017).
10. T. J. Stevenson, B. J. Prendergast, Reversible DNA methylation regulates seasonal photoperiodic time measurement. *Proc. Natl. Acad. Sci. U.S.A.* **110**, 16651–16656 (2013).
11. B. J. Prendergast, L. M. Pyter, A. Kampf-Lassin, P. N. Patel, T. J. Stevenson, Rapid induction of hypothalamic iodothyronine deiodinase expression by photoperiod and melatonin in juvenile Siberian hamsters (*Phodopus sungorus*). *Endocrinology* **154**, 831–841 (2013).
12. P. Barrett *et al.*, Hypothalamic thyroid hormone catabolism acts as a gatekeeper for the seasonal control of body weight and reproduction. *Endocrinology* **148**, 3608–3617 (2007).
13. G. Heldmaier, S. Steinlechner, J. Rafael, Nonshivering thermogenesis and cold resistance during seasonal acclimatization in the Djungarian hamster. *J. Comp. Physiol.* **149**, 1–9 (1982).
14. T. Ruf, G. Heldmaier, The impact of daily torpor on energy requirements in the Djungarian hamster (*Phodopus sungorus*). *Physiol. Zool.* **65**, 994–1010 (1992).
15. R. Bao, D. Hazlerigg, B. Prendergast, T. J. Stevenson, The sequence and de novo assembly of the Siberian hamster genome (*Phodopus sungorus*). GenBank. https://www.ncbi.nlm.nih.gov/nuccore/1056038647. Deposited 18 August 2016.
16. K. Rousseau *et al.*, Photoperiodic regulation of leptin resistance in the seasonally breeding Siberian hamster (*Phodopus sungorus*). *Endocrinology* **143**, 3083–3095 (2002).
17. A. B. Reddy, A. S. Cronin, H. Ford, F. J. Ebling, Seasonal regulation of food intake and body weight in the male siberian hamster: Studies of hypothalamic orexin (hypocretin), neuropeptide Y (NPY) and pro-opiomelanocortin (POMC). *Eur. J. Neurosci.* **11**, 3255–3264 (1999).
18. J. G. Mercer, K. M. Moar, A. W. Ross, P. J. Morgan, Regulation of leptin receptor, POMC and AGRP gene expression by photoperiod and food deprivation in the hypothalamic arcuate nucleus of the male Siberian hamster (*Phodopus sungorus*). *Appetite* **34**, 109–111 (2000).
19. M. Harbers, G. M. Wahlström, B. Vennström, Transactivation by the thyroid hormone receptor is dependent on the spacer sequence in hormone response elements containing directly repeated half-sites. *Nucleic Acids Res.* **24**, 2252–2259 (1996).
20. L. F. Velasco *et al.*, Thyroid hormone response element organization dictates the composition of active receptor. *J. Biol. Chem.* **282**, 12458–12466 (2007).
21. X. Messeguer *et al.*, PROMO: Detection of known transcription regulatory elements using species-tailored searches. *Bioinformatics* **18**, 333–334 (2002).
22. D. Farré *et al.*, Identification of patterns in biological sequences at the ALGGEN server: PROMO and MALGEN. *Nucleic Acids Res.* **31**, 3651–3653 (2003).
23. D. Huszar *et al.*, Targeted disruption of the melanocortin-4 receptor results in obesity in mice. *Cell* **88**, 131–141 (1997).
24. B. G. Challis *et al.*, Mice lacking pro-opiomelanocortin are sensitive to high-fat feeding but respond normally to the acute anorectic effects of peptide-YY(3-36). *Proc. Natl. Acad. Sci. U.S.A.* **101**, 4695–4700 (2004).
25. T. M. Mizuno *et al.*, Hypothalamic pro-opiomelanocortin mRNA is reduced by fasting and [corrected] in ob/ob and db/db mice, but is stimulated by leptin. *Diabetes* **47**, 294–297 (1998).
26. F. J. Ebling, On the value of seasonal mammals for identifying mechanisms underlying the control of food intake and body weight. *Horm. Behav.* **66**, 56–65 (2014).
27. T. J. Stevenson *et al.*, The value of comparative animal research: Krogh's principle facilitates scientific discoveries. *Policy Insights Behav. Brain Sci.* **5**, 118–125 (2018).
28. M. Helwig *et al.*, Photoperiod-dependent regulation of carboxypeptidase E affects the selective processing of neuropeptides in the seasonal Siberian hamster (*Phodopus sungorus*). *J. Neuroendocrinol.* **25**, 190–197 (2013).
29. C. A. Moffatt, A. C. DeVries, R. J. Nelson, Winter adaptations of male deer mice (*Peromyscus maniculatus*) and prairie voles (*Microtus ochrogaster*) that vary in reproductive responsiveness to photoperiod. *J. Biol. Rhythms* **8**, 221–232 (1993).
30. T. J. Bartness, G. N. Wade, Photoperiodic control of seasonal body weight cycles in hamsters. *Neurosci. Biobehav. Rev.* **9**, 599–612 (1985).
31. J. E. Larkin, J. Jones, I. Zucker, Temperature dependence of gonadal regression in Syrian hamsters exposed to short day lengths. *Am. J. Physiol. Regul. Integr. Comp. Physiol.* **282**, R744–R752 (2002).
32. S. Milesi, V. Simonneaux, P. Klosen, Downregulation of Deiodinase 3 is the earliest event in photoperiodic and photorefractory activation of the gonadotropic axis in seasonal hamsters. *Sci. Rep.* **7**, 17739 (2017).
33. I. Petri *et al.*, Orchestration of gene expression across the seasons: Hypothalamic gene expression in natural photoperiod throughout the year in the Siberian hamster. *PLoS One* **9**, e90253 (2016).
34. T. J. Stevenson *et al.*, Disrupted seasonal biology impacts health, food security and ecosystems. *Proc. Biol. Sci.* **282**, 20151453 (2015).
35. National Research Council, *Guide for the Care and Use of Laboratory Animals* (National Academies Press, Washington, DC, ed. 8, 2011).
36. M. G. Grabherr *et al.*, Full-length transcriptome assembly from RNA-Seq data without a reference genome. *Nat. Biotechnol.* **29**, 644–652 (2011).
37. M. D. Robinson, D. J. McCarthy, G. K. Smyth, edgeR: A Bioconductor package for differential expression analysis of digital gene expression data. *Bioinformatics* **26**, 139–140 (2010).
38. S. Zhao, R. D. Fernald, Comprehensive algorithm for quantitative real-time polymerase chain reaction. *J. Comput. Biol.* **12**, 1047–1064 (2005).
39. S. A. Bustin *et al.*, MIQE: A step toward more robust and reproducible quantitative PCR. *Clin. Chem.* **55**, 611–622 (2009).
40. A. Herwig *et al.*, Photoperiod and acute energy deficits interact on components of the thyroid hormone system in hypothalamic tanycytes of the Siberian hamster. *Am. J. Physiol. Regul. Integr. Comp. Physiol.* **296**, R1307–R1315 (2009).
41. R. Banks, M. Delibegovic, T. J. Stevenson, Photoperiod- and triiodothyronine-dependent regulation of reproductive neuropeptides, proinflammatory cytokines, and peripheral physiology in Siberian hamsters (*Phodopus sungorus*). *J. Biol. Rhythms* **31**, 299–307 (2016).
42. D. A. Freeman, B. J. W. Teubner, C. D. Smith, B. J. Prendergast, Exogenous T3 mimics long day lengths in Siberian hamsters. *Am. J. Physiol. Regul. Integr. Comp. Physiol.* **292**, R2368–R2372 (2007).
43. T. J. Stevenson, K. G. Onishi, S. P. Bradley, B. J. Prendergast, Cell-autonomous iodothyronine deiodinase expression mediates seasonal plasticity in immune function. *Brain Behav. Immun.* **36**, 61–70 (2014).

References

Ahmed AA, Ma W, Ni Y, Wang S, Zhao R. (2014). Corticosterone in ovo modifies aggressive behaviors and reproductive performances through alterations of the hypothalamic-pituitary-gonadal axis in the chicken. *Anim Reprod Sci*, 146(3-4), pp.193-201.

Akhtar RA, Reddy AB, Maywood ES, Clayton JD, King VM, Smith AG, Gant TW, Hastings MH, Kyriacou CP. (2002). Circadian cycling of the mouse liver transcriptome, as revealed by cDNA microarray, is driven by the suprachiasmatic nucleus. *Curr Biol*, 12(7), pp.540-550.

Alikhani-Koopaei R, Fouladkou F, Frey FJ, Frey BM. (2004). Epigenetic regulation of 11β-hydroxysteroid dehydrogenase type 2 expression. *J Clin Invest*, 114(8), 1146-1157.

Alvarado S, Mak T, Liu S, Storey KB, Szyf M. (2015). Dynamic changes in global and gene specific DNA methylation during hibernation in adult thirteen-lined ground squirrels, Ictidomys tridecemlineatus. *J Exp Biol*, 218, 1787–1795.

Ancel C, Bentsen A, Sébert M, Tena-Sempere M, Mikkelsen J, Simonneaux V. (2012). Stimulatory Effect of RFRP-3 on the Gonadotrophic Axis in the Male Syrian Hamster: The Exception Proves the Rule. *Endocrinol*, 153(3), pp.1352- 1363.

Anderson DM, Keafer BA. (1987). An endogenous annual clock in the toxic marine dinoflagellate Gonyaulax tamarensis. *Nature*, 325, 616–617.

Ansel L, Bentsen AH, Ancel C, Bolborea M, Klosen P, Mikkelsen JD, Simmonneaux V. (2011). Peripheral kisspeptin reverses short photoperiod-induced gonadal regression in Syrian hamsters by promoting GNRH release. *Reproduction* (Cambridge, England) 142 (3), 417–425.

Araki M, Fukada Y, Shichida Y, Yoshizawa T. (1990). Localization of iodopsin in the chick retina during in vivo and in vitro cone differentiation. *Invest Ophthalmol Vis Sci* 31:1466–1473

Araki M, Fukada Y, Shichida Y, Yoshizawa T, Tokunaga F. (1992). Differentiation of both rod and cone types of photoreceptors in the in vivo and in vitro developing pineal glands of the quail. *Dev Brain Res*, 65(1), pp.85-92.

Archer SN, Djamgoz MBA, Loew ER, Partridge JC, Vallerga S, Shand J, Foster RG. (1999). The extraretinal photoreceptors of non-mammalian vertebrates. In *Adaptive mechanisms in the ecology of vision.*

Arnold AP, Gorski RA. (1984). Gonadal steroid induction of structural sex differences in the central nervous system. *Ann Rev Neurosci* 7:413-442.

Arnold AP. (2009). The organizational–activational hypothesis as the foundation for a unified theory of sexual differentiation of all mammalian tissues. *Horm Behav* 55:570-578.

Avner P Heard E. (2001). X-chromosome inactivation: counting, choice and initiation. *Nat Rev Genetics* 2:59–67.

Azzi A, Dallmann R, Casserly A, Rehrauer H, Patrignani A, Maier B, Kramer A, Brown SA. (2014). Circadian behavior is light-reprogrammed by plastic DNA methylation. *Nat Neurosci*, 17(3), pp.377-382.

Badyaev AV, Hill GE, Beck ML, Dervan AA, Duckworth RA, McGraw KJ, Nolan PM, Whittingham LA. (2002). Sex-biased hatching order and adaptive population divergence in a passerine bird. *Science*, *295*(5553), pp.316-318.

Baker JR. (1938). The evolution of breeding seasons. In *Evolution: Essays on aspects of evolutionary biology* (pp. 161–177).

Bakker J, De Mees C, Douhard Q, Balthazart J, Gabant P, Szpirer J, Szpirer C. (2006). Alpha-fetoprotein protects the developing female mouse brain from masculinization and defeminization by estrogens. *Nat Neurosci*, 9:220-226.

Ball GF, Balthazart J. (2010). Japanese quail as a model system for studying the neuroendocrine control of reproductive and social behaviors. *ILAR J*, *51*(4), pp.310-325.

Ball GF, Ketterson ED. (2008). Sex differences in the response to environmental cues regulating seasonal reproduction in birds. *Philos Trans Roy Soc B: Biol Sci*, 363:231-246.

Balthazart J, Tlemçani O, Ball GF. (1996). Do sex differences in the brain explain sex differences in the hormonal induction of reproductive behavior? What 25 years of research on the Japanese quail tells us. *Horm Behav* 30:627-661.

Banks R, Delibegovic M, Stevenson TJ. (2016). Photoperiod-and triiodothyronine-dependent regulation of reproductive neuropeptides, proinflammatory cytokines, and peripheral physiology in Siberian hamsters (Phodopus sungorus). *J Biol Rhythm*, *31*(3), pp.299-307.

Bao R, Onishi KG, Tolla E, Ebling FJ, Lewis JE, Anderson RL, Barrett P, Prendergast BJ, Stevenson TJ. (2019). Genome sequencing and transcriptome analyses of the Siberian hamster hypothalamus identify mechanisms for seasonal energy balance. *PNAS*, *116*(26), pp.13116-13121.

Barrett P, Ebling FJ, Schuhler S, Wilson D, Ross AW, Warner A, Jethwa P, Boelen A, Visser TJ, Ozanne DM. (2007) Hypothalamic thyroid hormone catabolism acts as a gatekeeper for the seasonal control of body weight and reproduction. *Endocrinol*, 148:3608-3617.

Bartness TJ, Wade GN. (1984). Photoperiodic control of body weight and energy metabolism in Syrian hamsters (Mesocricetus auratus): Role of pineal gland, melatonin, gonads, and diet. *Endocrinol*, 114(2), 492–498.

Bartness TJ, Wade GN. (1985). Photoperiodic control of seasonal body weight cycles in hamsters. *Neurosci Biobehav R*, *9*(4), pp.599-612.

Bartness TJ, Goldman BD. (1989). Mammalian pineal melatonin: a clock for all seasons. *Experientia* 45:939-945.

Bartness TJ, Powers JB, Hastings MH, Bittman EL, Goldman BD. (1993). The timed infusion paradigm for melatonin delivery: What has it taught us about the melatonin signal, its reception, and the photoperiodic control of seasonal responses? *J Pineal Res*, 15, 161–190.

Bastow R, Mylne JS, Lister C, Lippman Z, Martienssen RA, Dean C. (2004). Vernalization requires epigenetic silencing of FLC by histone methylation. *Nature*, 427(6970), pp.164-167.

Beatty WW. (1984). Hormonal organization of sex differences in play fighting and spatial behavior. In *Progress in brain research* (Vol. 61, pp. 315-330). Elsevier.

Bédécarrats GY, Shimizu M, Guémené D. (2006). Gonadotropin releasing hormones and their receptors in avian species. *J Poult Sci*, *43*(3), pp.199-214.

Beery AK, Trumbull JJ, Tsao JM, Costantini RM, Zucker I. (2006). Sex differences in the onset of seasonal reproductive quiescence in hamsters. *Proc Roy Soc B*, 274:281-286.

Benoit J. (1935). Le role des yeux dans l'action stimulante de la lumiere sure le developement testiculaire chez le canard. *CR Soc Biol*, 118, 669–671.

Benoit JD, Rakic P, Frick KM. (2015). Prenatal stress induces spatial memory deficits and epigenetic changes in the hippocampus indicative of heterochromatin formation and reduced gene expression. *Behav Brain Res*, *281*, pp.1-8.

Bentley GE, Wingfield JC, Morton ML, Ball GF. (2000). Stimulatory effects on the reproductive axis in female songbirds by conspecific and heterospecific male song. *Horm Behav*, 37:179–189.

Bentley GE, Perfito N, Ukena K, Tsutsui K, Wingfield JC. (2003). Gonadotropin-inhibitory peptide in song sparrows (Melospiza melodia) in different reproductive conditions, and in house sparrows (Passer domesticus) relative to chicken-gonadotropin-releasing hormone. *J Neuroendocrinol*, 15, 794–802.

Bentley GE, Kriegsfeld LJ, Osugi T, Ukena K, O'Brien S, Perfito N, Moore IT, Tsutsui K, Wingfield JC. (2006). Interactions of gonadotropin-releasing hormone (GnRH) and gonadotropin-inhibitory hormone (GnIH) in birds and mammals. *J Exp Zool A Exp Biol*, 305:807-814.

Bestor T, Laudano A, Mattaliano R, Ingram V. (1988). Cloning and sequencing of a cDNA encoding DNA methyltransferase of mouse cells. *J Mol Biol*, 203, 971–983.

Bianco AC, Salvatore D, Gereben B, Berry MJ, Larsen PR. (2002). Biochemistry, cellular and molecular biology, and physiological roles of the iodothyronine selenodeiodinases. *Endo Rev*, 23, 38–89.

Bianco A, Kim B. (2006). Deiodinases: Implications of the local control of thyroid hormone action. *J Clin Investigat*, 116, 2571–2579.

Bird A, Wolffe A. (1999). Methylation-induced repression—belts, braces, and chromatin. *Cell*, 99, 451–454.

Bissonnette TH. (1941). Experimental modification of breeding cycles in goats. *Physiol Zool*, 14:379-383

Bittman EL, Karsch FJ. (1984). Nightly duration of pineal melatonin secretion determines the reproductive response to inhibitory day length in the ewe. *Biol Reprod*, 30, 585–593.

Blackshaw S, Snyder SH. (1999). Encephalopsin: A novel mammalian extraretinal opsin discretely localized in the brain. *J Neurosci*, 19, 3681.

Bolborea M, Dale N. (2013). Hypothalamic tanycytes: Potential roles in the control of feeding and energy balance. *Trends Neurosci*, 36, 91–100.

Boyes J, Bird A. (1991). DNA methylation inhibits transcription indirectly via a methyl-CpG binding protein. *Cell*, 64, 1123–1134.

Brackett NL, Iuvone PM, Edwards DA. (1986). Midbrain lesions, dopamine and male sexual behavior. *Behav Brain Res*, 20:231-240.

Bronson FH. (1989). Mammalian reproductive biology. University of Chicago Press.

Brown NL, Follett BK. (1977). Effects of androgens on the testes of intact and hypophysectomized Japanese quail. *Gen Comp Endocr*, *33*(2), pp.267-277.

Burmeister SS, Wilczynski W. (2005). Social signals regulate gonadotropin-releasing hormone neurons in the green treefrog. *Brain Behav Evolut*, 65(1), 26-32.

Bustin SA, Benes V, Garson JA, Hellemans J, Huggett J, Kubista M, Mueller R, Nolan T, Pfaffl MW, Shipley GL, Vandesompele J, Wittwer CT. (2009). The MIQE guidelines: minimum information for publication of quantitative real-time PCR experiments. *Clin Chem*, 55:611-622.

Carter D, Goldman B. (1983). Antigonadal Effects of Timed Melatonin Infusion in Pinealectomized Male Djungarian Hamsters (Phodopus sungorus): Duration is the Critical Parameter. *Endocrinol*, 113:1261-1267.

Casagrande S, Zsolt Garamszegi L, Goymann W, Donald J, Francis CD, Fuxjager MJ, Husak JF, Johnson MA, Kircher B, Knapp R, Martin LB. (2018). Do seasonal glucocorticoid changes depend on reproductive investment? A comparative approach in birds. *Integr Comp Biol*, *58*(4), pp.739-750.

Castellano JM, Navarro VM, Fernández-Fernández R, Nogueiras R, Tovar S, Roa J, Vazquez MJ, Vigo E, Casanueva FF, Aguilar E, Pinilla L, Dieguez C, Tena-Sempere M. (2005). Changes in hypothalamic KiSS-1 system and restoration of pubertal activation of the reproductive axis by kisspeptin in undernutrition. *Endocrinol.* 146:3917–25.

Champagne FA, Weaver ICG, Diorio J, Dymov S, Szyf M, Meaney MJ. (2006). Maternal Care Associated with Methylation of the Estrogen Receptor-α1b Promoter and Estrogen Receptor-α Expression in the Medial Preoptic Area of Female Offspring. *Endocrinol.* 147:2909–15.

Chen X, Watkins R, Delot E, Reliene R, Schiestl RH, Burgoyne PS, Arnold AP. (2008). Sex difference in neural tube defects in p53‐null mice is caused by differences in the complement of X not Y genes. *Develop Neurobiol*, 68:265-273.

Clarke LJ, Qi Y, Sari IP, Smith JT. (2009). Evidence that RF-amide related peptides are inhibitors of reproduction in mammals. *Fron Neuroendocrinol*, 30:371-378.

Clarke IJ, Caraty A. (2013). Kisspeptin and seasonality of reproduction. *Adv Exp Med Biol*, 784:411-430.

Clarkson J, Herbison AE. (2006). Oestrogen, Kisspeptin, GPR54 and the Pre-Ovulatory Luteinising Hormone Surge. *J Neuroendocrinol*, 21:305–11.

Cortijo S, Wardenaar R, Colomé-Tatché M, Gilly A, Etcheverry M, Labadie K, Caillieux E, Aury JM, Wincker P, Roudier F, Jansen RC. (2014). Mapping the epigenetic basis of complex traits. *Science*, *343*(6175), pp.1145-1148.

Costantini D, Metcalfe NB, Monaghan P. (2010). Ecological processes in a hormetic framework. *Ecol Lett*, *13*(11), pp.1435-1447.

Cottrell EC, Seckl J. (2009). Prenatal stress, glucocorticoids and the programming of adult disease. *Fron Behav Neurosci*, *3*, p.19.

Crudo A, Petropoulos S, Moisiadis VG, Iqbal M, Kostaki A, Machnes Z, Moshe S, Matthews SG. (2012). Prenatal synthetic glucocorticoid treatment changes DNA methylation states in male organ systems: multigenerational effects. *Endocrinol*, 153(7), 3269-3283.

Cubuk C, Kemmling J, Fabrizius A, Herwig A. (2017). Transcriptome analysis of hypothalamic gene expression during daily torpor in Djungarian hamsters (Phodopus sungorus). *Front Neurosci*, 11, 122.

Cunha C, Brambilla R, Thomas KL. (2010). A simple role for BDNF in learning and memory?. *Front Mol Neurosci*, 3, 1.

Dahl GE, Evans NP, Moenter SM, Karsch FJ. (1994). The thyroid gland is required for reproductive neuroendocrine responses to photoperiod in the ewe. *Endocrinol*, 135(1), 10–15.

Dardente H, Wyse CA, Birnie MJ, Dupre SM, Loudon AS, Lincoln GA, Hazlerigg DG. (2010). A molecular switch for photoperiod responsiveness in mammals. *Curr Biol*, 24:2193-2198.

Dardente H, Hazlerigg DG, Ebling FJ. (2014). Thyroid hormone and seasonal rhythmicity. *Front Endocrinol*, 5:19.

Dark J, Pickard GE, Zucker I. (1985). Persistence of circannual rhythms in ground squirrels with lesions of the suprachiasmatic nuclei. *Brain Res*, 332, 201–207.

Davies WI, Turton M, Peirson SN, Follett BK, Halford S, Garcia-Fernandez JM, Sharp PJ, Hankins MW, Foster RG. (2011) Vertebrate ancient opsin photopigment spectra and the avian photoperiodic response. *Biol Lett*, 8, 291–294

Davies S, Cros T, Richard D, Meddle SL, Tsutsui K, Deviche P. (2015). Food availability, energetic constraints and reproductive development in a wild seasonally breeding songbird. *Funct Ecol*, 29:1421-1434.

Dawson A. (2015). Annual gonadal cycles in birds: Modeling the effects of photoperiod on seasonal changes in GnRH-1 secretion. *Front Neuroendocrinol*, 37, 52–64.

Dawson A, King VM, Bentley GE, Ball GF. (2001) Photoperiodic control of seasonality in birds. *J Biol Rhythms*, 16, 365–380

Dawson A, Goldsmith AR. (1997). Changes in gonadotrophin-releasing hormone (GnRH-I) in the pre-optic area and median eminence of starlings (Sturnus vulgaris) during the recovery of photosensitivity and during photostimulation. *Reproduction*, 111(1), 1-6.

De Seranno S, d'Anglemont de Tassigny X, Estrella C, Loyens A, Kasparov S, Leroy D, Ojeda SR, Beauvillain JC, Prevot V. (2010). Role of estradiol in the dynamic control of

tanycyte plasticity mediated by vascular endothelial cells in the median eminence. *Endocrinol*, 151, 1760–1772.

Decourt C, Anger K, Robert V, Lomet D, Bartzen-Sprauer J, Caraty A, Dufourny L, Anderson G, Beltramo M. (2016). No evidence that Rfamide-Related Peptide 3 directly modulates LH secretion in the ewe. *Endocrinol*, 157, 1566–1575.

De la Cruz LF, Illera M, Mataix FJ. (1987). Developmental changes induced by glucocorticoids treatment in breeder quail (Coturnix coturnix japonica). *Horm Metabol Res, 19*(03), pp.101-104.

Dellovade TL, Chan J, Vennstrom B, Forrest D, Pfaff DW. (2000). The two thyroid hormone receptor genes have opposite effects on estrogen-stimulated sex behaviors. *Nat Neurosci*, 3:472-475.

Ding Y, Wang X, Su L, Zhai J, Cao S, Zhang D, Liu C, Bi Y, Qian Q, Cheng Z, Chu C. (2007). SDG714, a histone H3K9 methyltransferase, is involved in Tos17 DNA methylation and transposition in rice. *Plant Cell*, 19, 9–22.

Dunn IC, Sharp PJ. (1999). Photo-induction of hypothalamic gonadotrophin releasing hormone 1 mRNA in the domestic chicken: a role for oestrogen? *J Neuroendocrinol*, 11, 371–371.

Dunn IC, Wilson PW, Shi Y, Burt DW, Loudon ASI, Sharp PJ. (2017). Diurnal and photoperiodic changes in thyrotrophin‐stimulating hormone β expression and associated regulation of deiodinase enzymes (DIO 2, DIO 3) in the female juvenile chicken hypothalamus. *J Neuroendocrinol*, 29(12), p.e12554.

Duston J, Bromage N. (1991). Circannual rhythms of gonadal maturation in female rainbow trout (Oncorhynchus mykiss). *J Biol Rhythms*, 6, 49–53.

Ebling FJP. (2015). Hypothalamic control of seasonal changes in food intake and body weight. *Front Neuroendocrinol*, 37, 97–107.

El Halawani ME, Kang SW, Leclerc B, Kosonsiriluk S, Chaiseha Y. (2009). Dopamine–melatonin neurons in the avian hypothalamus and their role as photoperiodic clocks. *Gen Comp Endocrinol, 163*(1-2), pp.123-127.

Farinelli P, Perera A, Arango-Gonzalez B, Trifunovic D, Wagner M, Carell T, Ekström PAR. (2014). DNA methylation and differential gene regulation in photoreceptor cell death. *Cell Death Dis*, 5(12), e1558.

Farner DS, Lewis RA. (1971). Photoperiodism and reproductive cycles in birds. In *Photophysiology: current topics in photobiology and photochemistry* Vol VI eds. Giese, A.C., Academic Press, New York. Pg. 325-370.

Feng S, Cokus SJ, Zhang X, Chen PY, Bostick M, Goll MG, Hetzel J, Jain J, Strauss SH, Halpern ME, Ukomadu C, Sadler KC, Pradhan S, Pellegrini M, Jacobsen SE. (2010). Conservation and divergence of methylation patterning in plants and animals. *Proc Natl Acad Sci*, 107:8689-8694.

Finley CM, Gorman MR, Tuthill CR, Zucker I. (1995). Long-term reproductive effects of a single long day in the Siberian hamster (Phodopus sungorus). *J Biol Rhythms, 10*(1), pp.33-41.

Follett BK. (2015). Seasonal changes in the neuroendocrine system: some reflections. *Front Neuroendocrinol,* 3-12.

Follett BK. (1976). Plasma follicle-stimulating hormone during photoperiodically induced sexual maturation in male Japanese quail. *J Endocrinol*, *69*(1), pp.117-126.

Follett BK, Farner DS. (1966). The effects of the daily photoperiod on gonadal growth, neurohypophysial hormone content, and neurosecretion in the hypothalamo-hypophysial system of the Japanese quail (Coturnix coturnix japonica). *Gen Comp Endocrinol*, *7*(1), pp.111-124.

Follett BK, Maung SL. (1978). Rate of testicular maturation, in relation to gonadotrophin and testosterone levels, in quail exposed to various artificial photoperiods and to natural daylengths. *J Endocrinol*, *78*(2), pp.267-280.

Follett BK, Nicholls T. (1985). Influences of thyroidectomy and thyroxine replacement on photoperiodically controlled reproduction in quail. *J Endocrinol*, 107, 211–221

Follett BK, Nicholls TJ. (1988). Acute effect of thyroid hormones in mimicking photoperiodically induced release of gonadotropins in Japanese quail. *J Comp Physiol B*, 157, 837–843.

Follett BK, Nicholls TJ, Mayes CR. (1988). Thyroxine can mimic photoperiodically induced gonadal growth in Japanese quail. *J Comp Physiol B, 157*(6), pp.829-835.

Foster RG, Follett BK. (1985). The involvement of a rhodopsin-like photopigment in the photoperiodic response of the Japanese quail. *J Comp Physiol*, 157, 519–528.

Foster RG, Timmers AM, Schalken JJ, De Grip WJ. (1989). A comparison of some photoreceptor characteristics in the pineal and retina: II. The Djungarian hamster (Phodopus sungorus). *J Comp Physiol A*, 165, 565–572.

Free MJ, Tillson SA. (1973). Secretion rate of testicular steroids in the conscious and halothane-anesthetized rat. *Endocrinol*, *93*(4), pp.874-879.

Freeman DA, Teubner BJW, Smith CD, Prendergast BJ. (2007). Exogenous T3 mimics long day lengths in Siberian hamsters. *Am J Physiol* 292:R2368-R2372.

Friedman MB. (1977). Interactions between visual and vocal courtship stimuli in the neuroendocrine response of female doves. *J Comp Physiol Psych*, 91:1408.

Fuks F. (2005). DNA methylation and histone modifications: Teaming up to silence genes. *Curr Opin Genet Develop*, 15, 490–495.

García-Fernández JM, Cernuda-Cernuda R, Davies WI, Rodgers J, Turton M, Peirson SN, Follett BK, Halford S, Hughes S, Hankins MW, Foster RG. (2015). The hypothalamic photoreceptors regulating seasonal reproduction in birds: a prime role for VA opsin. *Front Neuroendocrinol*, 37, 13–28.

Gentner TQ, Hulse SH. (2000). Female European starling preference and choice for variation in conspecific male song. *Ani Behav*, 59:443–458.

Gluckman PD, Hanson MA. (2004). The developmental origins of the metabolic syndrome. *Trends Endocrinol Metabol*, *15*(4), pp.183-187.

Goldman BD, Nelson RJ. (1993). Melatonin and seasonality in mammals. In H. S. Yu & R. J. Reiters (Eds.), *Melatonin: Biosynthesis, physiological effects and clinical applications* (pp. 225–252).

Goldman B. (2001). Mammalian Photoperiodic System: Formal Properties and Neuroendocrine Mechanisms of Photoperiodic Time Measurement. *J Biol Rhythms,* 16:283-301.

Goldsmith AR, Nicholls TJ. (1984). Thyroidectomy prevents the development of refractoriness and the associated rise in plasma prolactin in starlings. *Gen Comp Endocrinol*, 54, 256–293.

Goodman RL, Lehman MN. (2012). Kisspeptin neurons from mice to men: similarities and differences. *Endocrinol*, 153:5105-5118.

Gorman ALF, McReynolds JS, Barnes SN. (1971). Photoreceptors in primitive chordates: fine structure, hyperpolarizing receptor potentials, and evolution. *Science*, 172(3987), pp.1052-1054.

Gorski RA, Gordon JH, Shryne JE, Southam AM. (1978). Evidence for a morphological sex difference within the medial preoptic area of the rat brain. *Brain Res*, 148:333-346.

Grant-Downton R, Dickinson HG. (2005). Epigenetics and its implications for plant biology. 1. The epigenetic network in plants. *Annals Botany,* 96:1143-1164.

Greives TJ, Humber SA, Goldstein AN, Scotti MAL, Demas GE, Kriegsfeld LJ. (2008). Photoperiod and testosterone interact to drive seasonal changes in kisspeptin expression in Siberian hamsters (Phodopus sungorus). *J Neuroendocrinol*, 20, 1339–1347.

Greives TJ, Mason AO, Scotti MAL, Levine J, Ketterson ED, Kriegsfeld LJ. (2007). Environmental control of kisspeptin: Implications for seasonal reproduction. *Endocrinol*, 148, 1158–1166.

Gwinner E. (1996). Circannual clocks in avian reproduction and migration. *Ibis*, 1, 47–63.

Haakenson CM, Madison FN, Ball GF. (2019). Effects of song experience and song quality on immediate early gene expression in female canaries (Serinus canaria). *Develop Neurobiol*, 79:521-535.

Halford S, Pires SS, Turton M, Zheng L, González-Menéndez I, Davies WL, Peirson SN, García-Fernández JM, Hankins MW, Foster RG. (2009). VA Opsin-Based Photoreceptors in the Hypothalamus of Birds. *Curr Biol*, 19(16), 1396-1402

Hang CY, Moriya S, Ogawa S, Parhar IS. (2016). Deep brain photoreceptor (val-opsin) gene knockout using CRISPR/Cas affects chorion formation and embryonic hatching in the zebrafish. *PloS one*, 11(10), p.e0165535.

Hankins MW, Peirson SN, Foster RG. (2008). Melanopsin: An exciting photopigment. *Trends Neurosci*, 31, 27–36.

Hanon EA, Lincoln GA, Fustin JM, Dardente H, Masson-Pévet M, Morgan PJ, Hazlerigg DG. (2008). Ancestral TSH mechanism signals summer in a photoperiodic mammal. *Curr Biol*, 18, 1147–1152.

Harony H, Ankri S. (2008). What do unicellular organisms teach us about DNA methylation? *Trends Parasitol*, 24, 205–209.

Hastings MH, Maywood ES, Brancaccio M. (2018). Generation of circadian rhythms in the suprachiamatic nucleus. *Nat Rev Neurosci,* 19, 453–469.

Hau M. (2001). Timing of breeding in variable environments: Tropical birds as model systems. *Horm Behav*, 40, 281–290.

Hayward LS, Satterlee DG, Wingfield JC. (2005). Japanese quail selected for high plasma corticosterone response deposit high levels of corticosterone in their eggs. *Physiol Biochem Zool*, *78*(6), pp.1026-1031.

Hayward LS, Wingfield JC. (2004). Maternal corticosterone is transferred to avian yolk and may alter offspring growth and adult phenotype. *Gen Comp Endocrinol 135*(3), pp.365-371.

Hazlerigg DF, Lincoln GA. (2011). Hypothesis: Cyclical histogenesis is the basis of circannual timing. *J Biol Rhythms*, 26, 471–485.

Halzerigg DH, Lomet D, Lincoln G, Dardente H. (2018). Neuroendocrine correlates of the critical day length response in the Soay sheep. *J Neuroendocrinol*, 30:e12631.

Heideman PD, Bronson FH. (1992). A pseudoseasonal reproductive strategy in a tropical rodent, Peromyscus nudipes. *Reproduction*, 95:57-67.

Helm B, Stevenson, TJ. (2015). Circannual rhythms: History, present challenges, future directions. In H. Numata & B. Helm (Eds.), *Annual, lunar and tidal clocks: Patterns and mechanisms of nature's enigmatic rhythms* (pp. 213–225).

Henriksen R, Rettenbacher S, Groothuis TG. (2011). Prenatal stress in birds: pathways, effects, function and perspectives. *Neurosci Biobehav Rev*, *35*(7), pp.1484-1501.

Henson J, Carter S, Freeman D. (2013). Exogenous T3 Elicits Long Day-Like Alterations in Testis Size and the RFamides Kisspeptin and Gonadotropin-Inhibitory Hormone in Short-Day Siberian Hamsters. *J Biol Rhythms*, 28(3), pp.193-200.

Herb BR, Wolschin F, Hansen KD, Aryee MJ, Langmead B, Irizarry R, Amdam GV, Feinberg AP. (2012). Reversible switching between epigenetic states in honeybee behavioral subcastes. *Nat Neurosci*, *15*(10), pp.1371-1373.

Herbison AE. (2016). Control of puberty onset and fertility by gonadotropin-releasing hormone neurons. *Nat Rev Endocrinol*, 12, 452–466.

Hernandez AM, MacDougall-Shackleton SA. (2004). Effects of early song experience on song preferences and song control and auditory brain regions in female house finches (Carpodacus mexicanus). *J Neurobiol*, 59:247–258.

Hinde RA, Steel E. (1976). The effect of male song on an estrogen-dependent behavior pattern in the female canary (Serinus canarius). *Horm Behav*, 7:293-304.

Hitt JC, Hendricks SE, Ginsberg SI, Lewis JH. (1970). Disruption of male, but not female, sexual behavior in rats by medial forebrain bundle lesions. *J Comp Physiol Psych, 73*(3), p.377.

Hoffmann I, Roatsch M, Schmitt ML, Carlino L, Pippel M, Sippl W, Jung M. (2012). The role of histone demethylases in cancer therapy. *Mol Oncol*, 6, 683–703.

Holliday R, Pugh J. (1975). DNA modification mechanisms and gene activity during development. *Science*, 187, 226–232.

Hulet CV, Shupe WL, Ross T, Richards W. (1986). Effects of nutritional environment and ram effect on breeding season in range sheep. *Theriogenol*, 25:317–323.

Husby A, Nussey DH, Visser ME, Wilson AJ, Sheldon BC, Kruuk LE. (2010). Contrasting patterns of phenotypic plasticity in reproductive traits in two great tit (Parus major) populations. *Evolution*, 64(8):2221-37.

Huss D, Poynter G, Lansford R. (2008). Japanese quail (Coturnix japonica) as a laboratory animal model. *Lab animal*, *37*(11), pp.513-519.

Hut RA, Paolucci S, Dor R, Kyriacou CP, Daan S. (2013). Latitudinal clines: An evolutionary view on biological rhythms. *Proc Roy Soc B*, 280, 20130433.

Jones P, Laird P. (1999). Cancer-epigenetics comes of age. *Nat Genet*, 21, 163–167.

Jones PA. (2012). Functions of DNA methylation: islands, start sites, gene bodies and beyond. *Nat Rev Genet*, *13*(7), 484-492.

Juraska JM. (1991). Sex differences in "cognitive" regions of the rat brain. *Psychoneuroendocrinol*. 16:105-119.

Juss TS, Meddle SL, Servant RS, King VM. (1993). Melatonin and photoperiodic time measurement in Japanese quail (Coturnix coturnix japonica). *Proc Biol Sci B*, 254, 21–28.

Kang SW, Madkour M, Kuenzel WJ. (2017). Tissue-specific expression of DNA methyltransferases involved in early-life nutritional stress of chicken, Gallus gallus. *Front Genet*, 8, 204.

Karsch FJ, Bittman EL, Foster DL, Goodman RL, Legan SJ, Robinson JE. (1984). Neuroendocrine basis of seasonal reproduction. *Recent Prog Horm Res.* 40, 185–232.

Kato M., Konishi T. (1968). The effect of light and temperature on the testicular growth of the Japanese quail. *Poultry Sci*, *47*(4), pp.1052-1056.

Ketterson ED, Nolan Jr V, Wolf L, Ziegenfus C, Dufty Jr AM, Ball GF, Johnsen TS. (1991). Testosterone and avian life histories: the effect of experimentally elevated testosterone on corticosterone and body mass in dark-eyed juncos. *Horm Behav*, *25*(4), pp.489-503.

Kim DK, Cho EB, Moon MJ, Hwang JI, Do-Rego JL, Vaudry H, Seong JY. (2012). Molecular coevulation of neuropeptides gonadotropin-releasing hormone and kisspeptin with their cognate G protein-coupled receptors. *Front Neurosci*, 6, 3.

Klosen P, Sébert ME, Rasri K, Laran-Chich MP, Simonneaux V. (2013). TSH restores a summer phenotype in photoinhibited mammals via the RF-amides RFRP3 and kisspeptin. *FASEB J*., 27, 2677–2686.

Korn H, Taitt MJ. (1987). Initiation of early breeding in a population of Microtus townsendii (Rodentia) with the secondary plant compound 6-MBOA. *Oecologia*. 1;71(4):593-6.

Kosten TA, Huang W, Nielsen DA. (2014). Sex and litter effects on anxiety and DNA methylation levels of stress and neurotrophin genes in adolescent rats. *Dev Psychobiol*, 56(3), 392-406.

Kriegsfeld LJ, Mei DF, Bentley GE, Ubuka T, Mason AO, Inoue K, Ukena K, Tsutsui K, Silver R. (2006). Identification and characterization of a gonadotropin-inhibitory system in the brains of mammals. *Proc Natl Acad Sci*, 103(7), 2410-2415.

Kriegsfeld LJ, Ubuka T, Bentley GE, Tsutsui K. (2015). Seasonal control of gonadotropin-inhibitory (GnIH) in birds and mammals. *Front Neuroendocrinol*, 37, 65–75.

Kumar V, Wingfield JC, Dawson A, Ramenofsky M, Rani S, Bartell P. (2010). Biological clocks and regulation of seasonal reproduction and migration in birds. *Physiol Biochem Zool*, *83*(5), pp.827-835.

Lachner M, Jenuwein T. (2002). The many faces of histone lysine methylation. *Curr Open Cell Biol*, 14, 286–298.

Laine VN, Gossmann TI, Schachtschneider KM, Garroway CJ, Madsen O, Verhoeven KJF, de Jager V, Megens HJ, Warren WC, Minx P, Crooijmans RPMA, Corcoran P, The Great tit HapMap Consortium, Sheldon BC, Slate J, Zeng Kai, van Oers K, Visser ME, Groenen MAM. (2016). Evolutionary signals of selection on cognition from the great tit genome and methylome. *Nat Commun*, 7:10474.

Lamb TD, Collin SP, Pugh EN. (2007). Evolution of the vertebrate eye: opsins, photoreceptors, retina and eye cup. *Nat Rev Neurosci*, 8(12), pp.960-976.

Lechan RM, Fekete C. (2007). Infundibular tanycytes as modulators of neuroendocrine function: hypothetical role in the regulation of the thyroid and gonadal axis. *Acta Biomed*, 78, 84–98.

Lee DA, Bedont JL, Pak T, Wang H, Song J, Miranda-Angulo A, Takiar V, Charubhumi V, Balordi F, Takebayashi H, Aja S. (2012). Tanycytes of the hypothalamic median eminence form a diet-responsive neurogenic niche. *Nat Neurosci*, 15, 700.

Lehman MN, Goodman RL, Karsch FJ, Jackson GL, Berriman SJ, Jansen HT. (1997). The GnRH system of seasonal breeders: Anatomy and plasticity. *Brain Res Bull*, 44, 445–457.

Lehrman DS. (1965). Interaction between internal and external environments in the regulation of the reproductive cycle of the ring dove. *Sex Behav*, 355.

Lewis JE, Ebling, FJP. (2017). Tanycytes as regulators of seasonal cycles in neuroendocrine function. *Front Neurosci*, 8, 79.

Li E, Bestor T, Jaenisch R. (1992). Targeted mutation of the DNA methyltransferase gene results in embryonic lethality. *Cell*, 69, 915–926.

Lincoln GA, Andersson H, Hazlerigg DG. (2003). Clock genes and the long-term regulation of prolactin secretion: Evidence for a photoperiod/circannual timer in the Pars tuberalis. *J Neuroendocrinol*, 15, 390–397.

Lomet D, Cognie J, Chesneau D, Dubois E, Hazlerigg DG, Dardente H. (2018). The impact of thyroid hormone in seasonal breeding has a restricted transcriptional signature. *Cell Mole Life Sci*, 75, 905–919.

Love OP, Chin EH, Wynne-Edwards KE, Williams TD. (2005). Stress hormones: a link between maternal condition and sex-biased reproductive investment. *The American Naturalist*, *166*(6), pp.751-766.

Love OP, Williams TD. (2008). Plasticity in the adrenocortical response of a free-living vertebrate: the role of pre-and post-natal developmental stress. *Horm Behav*, 54(4), pp.496-505.

Luczak MW, Jagodziński PP. (2006). The role of DNA methylation in cancer development. *Folia histochemica et cytobiologica*, 44(3), 143-154.

Lynch EW, Coyle CS, Lorgen M, Campbell EM, Bowman AS, Stevenson TJ. (2016). Cyclical DNA Methyltransferase 3a expression is a seasonal and Estrus timer in reproductive tissues. *Endocrinol*, 157, 2469–2478.

MacDougall-Shackleton SA, Deviche PJ, Crain RD, Ball GF, Hahn TP. (2001). Seasonal changes in brain GnRH immunoreactivity and song-control nuclei volumes in an opportunistically breeding songbird. *Brain Behav Evol*, 58:38-48.

MacDougall-Shackleton SA, Stevenson TJ, Watts HE, Pereyra M, Hahn TP. (2009). The evolution of photoperiod response systems and seasonal GnRH plasticity in birds. *Inte Comp Biol*, 49, 580–589.

MacLusky NJ, Naftolin F. (1981). Sexual differentiation of the central nervous system. *Science*, 1294-1303.

Majumdar G, Yadav G, Rani S, Kumar V. (2014). A photoperiodic molecular response in migratory redheaded bunting exposed to a single long day. *Gen Comp Endocrinol*, 204, 104–113.

Maney DL, MacDougall-Shackleton EA, MacDougall-Shackleton SA, Ball GF, Hahn TP. (2003). Immediate early gene response to hearing song correlates with receptive behavior and depends on dialect in a female songbird. *J Comp Physiol A: Neuroethol Sens Neur Behav Physiol*, 189:667–674.

Mason AO, Duffy S, Zhao S, Ubuka T, Bentley GE, Tsutsui K, Silver R, Kriegsfeld LJ. (2010). Photoperiod and reproductive condition are associated with changes in RFamide-related peptide expression in Syrian hamsters (Mesocricetus auratus). *J Biol Rhythms*, 25, 176–185.

McCarthy MM. (2008). Estradiol and the developing brain. *Physiol Rev*, 88:91-134.

McCarthy MM, Auger AP, Bale TL, De Vries GJ, Dunn GA, Forger NG, Wilson ME. (2009). The epigenetics of sex differences in the brain. *J Neurosci*, 29:12815-12823.

McGuire NL, Kangas K, Bentley GE. (2011). Effects of melatonin on peripheral reproductive function: Regulation of testicular GnIH and testosterone. *Endocrinol*, 152, 3461–3470.

Meddle SL, Follet BK. (1997). Photoperiodically driven changes in Fos expression within the basal tuberal hypothalamus and median eminence of Japanese quail. *J Neurosci*, 17, 8909–8918.

Meddle SL, Bush S, Sharp PJ, Millar RP, Wingfield JC. (2006). Hypothalamic pro-GnRH-GAP, GnRH-I and GnRH-II during the onset of photorefractoriness in the white-crowned sparrow (Zonotrichia leucophrys gambelii). *J Neuroendocrinol* 18, 217–226.

Menaker M, Keatts H. (1968). Extraretinal light perception in the sparrow. II. Photoperiodic stimulation of testis growth. *Proc Natl Acad Sci*, 60, 146–151.

Menaker M, Underwood H. (1976). Extraretinal photoreception in birds. *Photophysiol*, 23, 299–306.

Mishra I, Bhardwaj SK, Malik S, Kumar V. (2017). Concurrent hypothalamic gene expression under acute and chronic long days: Implications for initiation and maintenance of photoperiodic response in migratory songbirds. *Mol Cell Endocrinol*, 439, 81-94.

Moenter SM, Woodfill CJ, Karsch FJ. (1991). Role of the thyroid gland in seasonal reproduction: Thyroidectomy blocks seasonal suppression of reproductive neuroendocrine activity in ewes. *Endocrinol*, 128, 1337–13344.

Mueller BR, Bale TL. (2008). Sex-specific programming of offspring emotionality after stress early in pregnancy. *J Neurosci*, 28(36), 9055-9065.

Mukai M, Replogle K, Drnevich J, Wang G, Wacker D, Band M, Clayton DF, Wingfield JC. (2009). Seasonal differences of gene expression profiles in song sparrow (Melospiza melodia) hypothalamus in relation to territorial aggression. *PloS one*, *4*(12), p.e8182.

Naftolin F Ryan KJ. (1975). The metabolism of androgens in central neuroendocrine tissues. *J Steroid Biochem* 6:993–7.

Nakane Y, Ikegami K, Ono H, Yamamoto N, Yoshida S, Hirunagi K, Ebihara S, Kubo Y, Yoshimura T. (2010) A mammalian neural tissue opsin (Opsin 5) is a deep brain photoreceptor in birds. *Proc Natl Acad Sci USA*, 107, 15264–15268

Nakane Y, Yoshimura T. (2010). Deep brain photoreceptors and a seasonal signal transduction cascade in birds. *Cell Tissue Res*, 342, 341–344.

Nakane Y, Simmura T, Abe H, Yoshimura T. (2014). Intrinsic photosensitivity of a deep brain photoreceptor. *Curr Biol*, 24, 596–597.

Nakao N, Ono H, Yamamura T, Anraku T, Takagi T, Higashi K, Yasuo S, Katou Y, Kageyama S, Uno Y, Kasukawa T. (2008) Thyrotrophin in the pars tuberalis triggers photoperiodic response. *Nature*, 452, 317–322

Nasonkin IO, Hambright D, Lazo K, Fariss R, Rachel R, Bharti K, Swaroop A. (2010). Role of Epigenetics (DNA Methylation) in RPE and Photoreceptor Development. *Invest Ophth Vis Sci*, 51(13), 4304-4304.

Nelson RJ, Dark J, Zucker I. (1983). Influence of photoperiod, nutrition and water availability on reproduction of male California voles (Microtus californicus). *Reproduction*, 69:473-477.

Nelson RJ, Badura LL, Goldman BD. (1990). Mechanisms of seasonal cycles of behaviour. *Annu Rev Psychol*, 41:81-108.

Nguyen MTT, Vemaraju S, Nayak G, Odaka Y, Buhr ED, Alonzo N, Tran U, Batie M, Upton BA, Darvas M, Kozmik Z. (2019). An opsin 5–dopamine pathway mediates light-dependent vascular development in the eye. *Nat Cell Biol*, *21*(4), pp.420-429.

Nicholls TJ, Goldsmith AR, Dawson A. (1988). Photorefractoriness in birds and comparison with mammals. *Physiol Rev*, 68, 133–176.

Noguera JC, Velando A. (2019). Bird embryos perceive vibratory cues of predation risk from clutch mates. *Nat Ecol Evolut*, 3(8), 1225-1232.

Nottebohm F, Arnold AP. (1976). Sexual dimorphism in vocal control areas of the songbird brain. *Science,* 194:211-213.

Nugent BM, Wright CL, Shetty AC, Hodes GE, Lenz KM, Mahurkar A, McCarthy MM. (2015). Brain feminization requires active repression of masculinization via DNA methylation. *Nat Neurosci*, 18:690.

Oberlander TF, Bonaguro RJ, Misri S, Papsdorf M, Ross CJD, Simpson EM. (2008). Infant serotonin transporter (SLC6A4) promoter genotype is associated with adverse neonatal outcomes after prenatal exposure to serotonin reuptake inhibitor medications. *Mol Psych*, 13(1), 65-73.

Okano M, Bell DW, Haber DA, Li E. (1999). DNA methyltransferases Dnmt3a and Dnmt3b are essential for de novo methylation and mammalian development. *Cell*, 99, 247–257.

Okano M, Xie S, Li E. (1998). Cloning and characterization of a family of novel mammalian DNA (cytosine-5) methyltransferases. *Nat Genet*, 19, 219–220.

Okano T, Yoshizawa T, Fukada Y (1994) Pinopsin is a chicken pineal photoreceptive molecule. *Nature*, 372, 94–97

Oliver J, Jallageas M, Bayle JD. (1979). Plasma testosterone and LH levels in male quail bearing hypothalamic lesions or radioluminous implants. *Neuroendocrinol*, 28, 114–122.

Ottinger MA, Kubakawa K, Kikuchi M, Thompson N, Ishii S. (2002). Effects of exogenous testosterone on testicular luteinizing hormone and follicle-stimulating hormone receptors during aging. *Exp Biol Med*, *227*(9), pp.830-836.

Panzica GC, Viglietti-Panzica C, Balthazart J. (1996). The sexually dimorphic medial preoptic nucleus of quail: a key brain area mediating steroid action on male sexual behavior. *Front Neuroendocrinol*, 17:51-125.

Parkinson TJ, Douthwaite JA, Follett BK. (1995). Responses of pre-pubertal and mature rams to thyroidectomy. *J Reprod Fertil*, 104, 51–56.

Parkinson TJ, Follett BK. (1994). Effect of thyroidectomy upon seasonality in rams. *J Reprod Fertil*, 101:51-58.

Paul MJ, Zucker I, Schwartz WJ. (2008). Tracking the seasons: The internal calendars of vertebrates. *Phil Trans Roy Soc B,* 363, 341–361.

Paul MJ, Pyter LM, Freeman DA, Galang J, Prendergast BJ. (2009). Photic and nonphotic seasonal cues differentially engage hypothalamic kisspeptin and RFamide-related peptide mRNA expression in Siberian hamsters. *J Neuroendocrinol*, 21:1007-1014.

Pegoraro M, Bafna A, Davies NJ, Shuker DM, Tauber E. (2015). DNA methylation changes induced by long and short photoperiods in Nasonia. *Genome Res*, 26, 203–210.

Pike TW, Petrie M. (2006). Experimental evidence that corticosterone affects offspring sex ratios in quail. *Proc Roy Soc B Biol Sci*, *273*(1590), pp.1093-1098.

Pérez J, Tolla E, Dunn I, Meddle S, Stevenson T. (2019). A Comparative Perspective on Extra-retinal Photoreception. *Trends Endocrinol Metabol*, 30(1), 39-53.

Pérez JH, Meddle SL, Wingfield JC, Ramenofsky M. (2018) Effects of thyroid hormone manipulation on pre-nuptial molt, luteinizing hormone and testicular growth in male white-

crowned sparrows (Zonotrichia leuchophrys gam- belii). *Gen Comp Endocrinol*, 255, 12–18

Perfito N, Zann R, Ubuka T, Bentley G, Hau M. (2011). Potential roles for GNIH and GNRH-II in reproductive axis regulation of an opportunistically breeding songbird. *Gen Comp Endocrinol*, *173*(1), pp.20-26.

Phoenix CH, Goy RW, Gerall AA, Young WC. (1959). Organizing action of prenatally administered testosterone propionate on the tissues mediating mating behavior in the female guinea pig. *Endocrinol*, 65:369-382.

Pitk M, Tilgar V, Kilgas P, Mänd R. (2012). Acute stress affects the corticosterone level in bird eggs: A case study with great tits (Parus major). *Horm Behav*. 62, 475–479.

Prendergast BJ. (2005). Internalization of seasonal time. *Horm Behav*, 48:503-511.

Prendergast BJ. (2010). MT1 melatonin receptor mediate somatic, behavioural and reproductive neuroendocrine responses to photoperiod and melatonin in Siberian hamsters (Phodopus sungorus). *Endocrinol*, 151, 714–721.

Prendergast BJ, Pyter LM, Patel PN, Stevenson TJ. (2013). Rapid induction of hypothalamic iodothyronine mRNA by photoperiod and melatonin in juvenile male Siberian hamsters (Phodopus sungorus). *Endocrinol*, 154, 831–841.

Quignon C, Beymer M, Gauthier K, Gauer F, Simonneaux V. (2020). Thyroid hormone receptors are required for the melatonin‐dependent control of Rfrp gene expression in mice. *FASEB J*, 34(9), pp.12072-12082.

Raisman G, Field PM. (1973). Sexual dimorphism in the neurophil of the preoptic area of the rat and its dependence on neonatal androgen. *Brain Res*, 54:1-29.

Rakyan VK, Preis J, Morgan HD, Whitelaw E. (2001). The marks, mechanisms and memory of epigenetic states in mammals. *Biochem J*, *356*(1), pp.1-10.

Rao RC, Tchedre KT, Malik MTA, Coleman N, Fang Y, Marquez VE, Chen DF. (2010). Dynamic patterns of histone lysine methylation in the developing retina. *Invest Ophth Vis Sci*, 51(12), 6784- 6792.

Reinert BD, Wilson FE. (1996). The thyroid and the hypothalamus–pituitary–ovarian axis in American tree sparrows (Spizella arborea). *Gen Comp Endocrinol*, 103(1), 60-70.

Reiter RJ. (1991). Pineal melatonin: Cell biology of its synthesis and of its physiological interactions. *Endo Rev*, 12, 151–180.

Revel FG, Saboureau M, Masson-Pevet M, Pevet P, Mikkelsen JD, Simonneaux V. (2006). Kisspeptin mediates the photoperiodic control of reproduction in hamsters. *Curr Biol*, 16, 1730–1735.

Revel FG, Saboureau M, Pevet P, Simonneaux V, Mikkelson JD. (2008). RFamide-related peptide gene is a melatonin-driven photoperiodic gene. *Endocrinol*, 149, 902–912.

Rhee KD, Yu J, Zhao CY, Fan G, Yang XJ. (2012). Dnmt1-dependent DNA methylation is essential for photoreceptor terminal differentiation and retinal neuron survival. *Cell Death Dis*, 3(11), e427.

Riggs AD. (1975). X inactivation, differentiation, and DNA methylation. *Cytogen Genome Res*, 14, 9–25.

Riley GM, Witschi E. (1938). Comparative effects of light stimulation and administration of gonadotropic hormones on female sparrows. *Endocrinol*, 23:618-624.

Rios MN, Marchese NA, Guido ME. (2019). Expression of non-visual opsins Opn3 and Opn5 in the developing inner retinal cells of birds. Light-responses in Muller glial cells. *Front Cell Neurosci*, 13, p.376.

Robinson JE, Follett BK. (1982). Photoperiodism in Japanese quail: the termination of seasonal breeding by photorefractoriness. *P R Soc London B Bio*, *215*(1198), pp.95-116.

Romano A, De Giorgio B, Parolini M, Favero C, Possenti CD, Iodice S, Caprioli M, Rubolini D, Ambrosini R, Gianfranceschi L, Saino N. (2017). Methylation of the circadian Clock gene in the offspring of a free-living passerine bird increases with maternal and individual exposure to PM10. *Environ Pollut*, *220*, pp.29-37.

Romero LM, Wingfield JC. (1999). Alterations in hypothalamic–pituitary–adrenal function associated with captivity in Gambel's white-crowned sparrows (Zonotrichia leucophrys gambelii). *Comp Biochem Phys B*, *122*(1), pp.13-20.

Romero LM. (2002). Seasonal changes in plasma glucocorticoid concentrations in free-living vertebrates. *Gen Comp Endocrinol*, *128*(1), pp.1-24.

Rowan W. (1926). On photoperiodism, reproductive periodicity and the annual migration of birds and certain fishes. *Proc Boston Soc Nat History*, 38, 147–189.

Ruby NF, Dark J, Heller HC, Zucker I. (1998). Suprachiasmatic nucleus: Role in circannual body mass and hibernation rhythms of ground squirrels. *Brain Res*, 782, 63–72.

Saenz de Miera C, Bothorel B, Jaeger C, Simonneaux V, Hazlerigg DG. (2017). Maternal photoperiod programs hypothalamic thyroid status via the fetal pituitary gland. *Proc Natl Acad Sci USA*, 31:8408-8413.

Santoro R, Grummt I. (2005). Epigenetic mechanism of rRNA gene silencing: Temporal order of NoRC-mediated histone modification, chromatin remodeling, and DNA methylation. *Mol Cell Biol*, 25, 2539–2546.

Sapolsky, R., Armanini, M., Packan, D. and Tombaugh, G., 1987. Stress and glucocorticoids in aging. *Endocrin Metab Clin*, *16*(4), pp.965-980.

Satterlee DG, Cole CA, Castille SA. (2007). Maternal corticosterone further reduces the reproductive function of male offspring hatched from eggs laid by quail hens selected for exaggerated adrenocortical stress responsiveness. *Poultry Sci*, *86*(3), pp.572-581.

Schadler MH, Butterstein GM, Faulkner BJ, Rice SC, Weisinger LA. (1988). The plant metabolite, 6-methoxybenzoxazolinone, stimulates an increase in secretion of follicle-stimulating hormone and size of reproductive organs in Microtuspinetorum. *Biol Reprod*, 1;38(4):817-20.

Schweizer U, Schlicker C, Braun D, Kohrle J, Steegborn C. (2014). Crystal structure of mammalian selenocysteine-dependent iodothyronine deiodinase suggests a peroxiredoxin-like catalytic mechanism. *Proc Natl Acad Sci*, 111, 10526–10531.

Schumacher M, Balthazart J. (1983). The effects of testosterone and its metabolites on sexual behavior and morphology in male and female Japanese quail. *Physiol Behav*, *30*(3), 335-339.

Sharif J, Muto M, Takebayashi SI, Suetake I, Iwamatsu A, Endo TA, Shinga J, Mizutani-Koseki Y, Toyoda T, Okamura K, Tajima S. (2007). The SRA protein Np95 mediates epigenetic inheritance by recruiting Dnmt1 to methylated DNA. *Nature*, 450, 908–912.

Sharma SA, Singh D, Malik S, Gupta NJ, Rani S, Kumar V. (2018). Difference in control between spring and autumn migration in birds: insight from seasonal changes in hypothalamic gene expression in captive buntings. *Proc Bio Sci*, 285:1885

Shelton M. (1960). Influence of the presence of a male goat on the initiation of estrous cycling and ovulation of Angora does. *J Anim Sci*, 19:368-375.

Shimakura K. (1940). Notes on the genetics of the Japanese quail. I. The simple, Mendelian, autosomal, recessive character" brown-splashed white," of its plumage. *Idengahu Zasshi= Japanese Journal of Genetics*, *16*, pp.106-112.

Simonneaux V. (2020). A kiss to drive rhythms in reproduction. *Eur J Neurosci*. 51:509-530.

Smith CA, Roeszler KN, Ohnesorg T, Cummins DM, Farlie PG, Doran TJ, Sinclair AH. (2009). The avian Z-linked gene DMRT1 is required for male sex determination in the chicken. *Nature*. 461(7261):267-71.

Snowden A, Gregory P, Case C, Pabo C. (2002). Gene-specific targeting of H3K9 methylation is sufficient for initiating repression in vivo. *Curr Biol*, 12, 2159–2166.

Song CK, Bartness TJ. (1996). The effects of anterior hypothalamic lesions on short-day responses in Siberian hamsters given timed melatonin infusions. *J Biol Rhythms*, 11:14-26.

Soni BG, Foster RG. (1997). A novel and ancient vertebrate opsin. *FEBS Lett*, 406, 279–283.

Stephan FK. (2001). Food-entrainable oscillators in mammals. In *Circadian clocks* (pp. 223-246). Springer, Boston, MA.

Stevenson TJ. (2018). Epigenetic regulation of biological rhythms: An evolutionary ancient molecular timer. *Trends Genet*, 34, 90–100.

Stevenson TJ, Ball GF. (2011). Information theory and the neuropeptidergic regulation of seasonal reproduction in mammals and birds. *Proc Roy Soc B*, 278, 2477–2485.

Stevenson TJ, Ball GF. (2012). Disruption of neuropsin mRNA expression via RNA interference facilitates the photoinduced increase in thyrotropin-stimulating subunit β in birds. *Eur J Neuro*, 36, 2859–2865.

Stevenson TJ, MacDougall-Shackleton SA, Hahn TP, Ball GF. (2012a). Gonadotropin-releasing hormone plasticity: A comparative perspective. *Front Neuroendocrinol*, 33, 287–300.

Stevenson TJ, Hahn TP, Ball GF. (2012b). Variation in gonadotropin releasing-hormone-1 gene expression in the preoptic area predicts transitions in seasonal reproductive state. *J Neuroendocrinol*, 24, 267–274.

Stevenson TJ, Replogle K, Drnevich J, Clayton DF, Ball GF. (2012c). High throughput brain analysis reveals dissociable gene expression profiles from two independent neural systems involved in regulating social behavior. *BMC Neurosci*, 13, 126.

Stevenson TJ, Lincoln GA. (2017). Epigenetic mechanisms regulating circannual rhythms. In V. Kumar (Ed.), *Biological timekeeping: Clocks, rhythms and behaviour*. India: Springer.

Stevenson TJ. (2017a). Circannual and circadian rhythms of hypothalamic DNA methyltransferase and histone deacetylase expression in male Siberian hamsters (*Phodopus sungorus*). *Gen Comp Endocrinol*, 243:130-137

Stevenson TJ. (2017b). Environmental and hormone regulation of epigenetic enzymes in the hypothalamus. *J Neuroendocrinol*, 29(5).

Stevenson TJ, Lynch KS, Ball GF, Bernard DJ. (2009). Cloning of the gonadotropin releasing-hormone I complementary DNAs in songbirds facilitates dissection of mechanisms mediating seasonal changes in reproduction. *Endocrinol*, 150, 1826–1833.

Stevenson TJ, Prendergast BJ, Nelson RJ. (2017). Mammalian seasonal rhythms: behavior and neuroendocrine substrates. In Pfaff & Joels (Eds.), *Hormone, brain behavior* (Vol. 3). Elsevier Science.

Stevenson TJ, Prendergast BJ. (2013) Reversible DNA methylation regulates seasonal photoperiodic time measurement. *Proc Natl Acad Sci USA*, 110, 16651–16656

Stevenson TJ, Onishi KG, Bradley SP, Prendergast BJ. (2014). Cell-autonomous iodothyronine deiodinase expression mediates seasonal plasticity in immune function. *Brain Behav Immun*, 36:61-70.

Storch KF, Lipan O, Leykin I, Viswanathan N, Davis FC, Wong WH, Weitz CJ. (2002). Extensive and divergent circadian gene expression in liver and heart. *Nature*, 417(6884), pp.78-83.

Struhl K. (1998). Histone acetylation and transcriptional regulatory mechanisms. *Genes Develop*, 12, 599–660.

Sweatt JD. (2009). Experience-dependent epigenetic modifications in the central nervous system. *Biol Psych*, 65(3), 191-197.

Szele FG, Szuchet S. (2003). Cells lining the ventricular system: Evolving concepts underlying developmental events in the embryo and adult. *Adv Mole Cell Biol*, 31, 127–146.

Tarttelin EE, Bellingham J, Hankins MW, Foster RG, Lucas RJ. (2003). Neuropsin (Opn5) a novel opsin identified in mammalian neural tissue. *FEBS Lett*, 554, 410–416.

Tena-Sempere M, Felip A, Gomez A, Zanuy S, Carrillo, M. (2012). Comparative insights of the kisspeptin/kisspeptin receptor system: Lessons from non-mammalian vertebrates. *Gen Comp Endocrinol*, 175, 234–243.

Teranishi M, Shimada Y, Hori T, Nakabayashi O, Kikuchi T, Macleod T, Pym R, Sheldon B, Solovei I, Macgregor H, Mizuno S. (2001). Transcripts of the MHM region on the chicken Z chromosome accumulate as non-coding RNA in the nucleus of female cells adjacent to the DMRT1 locus. *Chromosome Res*, 1;9(2):147-65.

Thomassin H, Flavin M, Espinàs ML, Grange T. (2001). Glucocorticoid-induced DNA demethylation and gene memory during development. *EMBO J*, 20(8), 1974-1983.

Thrun LA, Dahl GE, Evans NP, Karsch FJ. (1997). A critical period for thyroid hormone action on seasonal changes in reproductive neuroendocrine function in the ewe. *Endocrinol*, 138:3402-3409.

Tobari Y, Son YL, Ubuka T, Hasegawa Y, Tsutsui K. (2014). A new pathway mediating social effects on the endocrine system: female presence acting via norepinephrine release stimulates gonadotropin-inhibitory hormone in the paraventricular nucleus and suppresses luteinizing hormone in quail. *J Neurosci*, *34*(29), pp.9803-9811.

Tomasi T, Hellgren E, Tucker T. (1998). Thyroid Hormone Concentrations in Black Bears (Ursus americanus): Hibernation and Pregnancy Effects. *Gen Comp Endocrinol*, 109(2), pp.192-199.

Tomonari S, Takagi A, Noji S, Ohuchi H. (2007). Expression pattern of the melanopsin-like (cOpn4m) and VA opsin-like genes in the developing chicken retina and neural tissues. *Gene Expr Patterns*, 7(7), 746-753.

Tompkins JD, Hall C, Chen VCY, Li AX, Wu X, Hsu D, Couture LA, Riggs AD. (2012). Epigenetic stability, adaptability, and reversibility in human embryonic stem cells. *Proc Natl Acad Sci*, *109*(31), pp.12544-12549.

Tolla E, Pérez JH, Dunn IC, Meddle SL, Stevenson TJ. (2019). Neuroendocrine Regulation of Seasonal Reproduction. In *Oxford Research Encyclopedia of Neuroscience*.

Tolla E, Stevenson TJ. (2020a). Sex differences and the neuroendocrine regulation of seasonal reproduction by supplementary environmental cues. *Integr Comp Biol*.

Tolla E, Stevenson TJ. (2020b). Photoperiod-induced changes in hypothalamic de novo DNA methyltransferase expression are independent of triiodothyronine in female Siberian hamsters (Phodopus sungorus). *Gen Comp Endocrinol*, *299*, p.113604.

Trivedi AK, Sur S, Sharma A, Taufique ST, Gupta NJ, Kumar V. (2019). Temperature alters the hypothalamic transcription of photoperiod responsive genes in induction of seasonal response in migratory redheaded buntings. *Mol Cell Endocrinol* 493:110454.

Tsutsui K, Ishii S. (1978). Effects of follicle-stimulating hormone and testosterone on receptors of follicle-stimulating hormone in the testis of the immature Japanese quail. *Gen Comp Endocrinol*, *36*(2), pp.297-305.

Tsutsui K. (2009). A new key neurohormone controlling reproduction, gonadotropin-inhibitory hormone (GnIH): Biosynthesis, mode of action and functional significance. *Prog Neurobiol*, *88*(1), pp.76-88.

Tsutsui K, Ubuka T, Bentley GE, Kriegsfeld L. (2013). regulatory mechanisms of gonadotropin-inhibitory hormone (GnIH) synthesis and release in photoperiodic animals. *Front Neurosci*, *7*, p.60.

Ubuka T, McGuire NL, Calisi RM, Perfito N, Bentley GE. (2008). The control of reproductive physiology and behavior by gonadotropin-inhibitory hormone. *Integr Comp Biol*, 48(5), 560-569.

Ubuka T, Inoue K, Fukuda Y, Mizuno T, Ukena K, Kriegsfeld LJ, Tsutsui K. (2012). Identification, expression, and physiological functions of Siberian hamster gonadotropin-inhibitory hormone. *Endocrinol*, *153*(1), pp.373-385.

Ubuka T, Son YL, Bentley GE, Millar RP, Tsutsui K. (2013). Gonadotropin-inhibitory hormone (GnIH), GnIH receptor and cell signalling. *Gen Comp Endocrinol*, 190, 10–17.

Udy GB, Towers RP, Snell RG, Wilkins RJ, Park SH, Ram PA, Davey HW. (1997). Requirement of STAT5b for sexual dimorphism of body growth rates and liver gene expression. *Proc Natl Acad Sci*, 94:7239-7244.

Ueda HR, Chen W, Adachi A, Wakamatsu H, Hayashi S, Takasugi T, Nagano M, Nakahama KI, Suzuki Y, Sugano S, Iino M. (2002). A transcription factor response element for gene expression during circadian night. Nature, 418(6897), pp.534-539.

Underwood H., Menaker M. (1976) Extraretinal photoreception in lizards. *Photochem Photobiol*, 23, 227–243

Valle S, Carpentier E, Vu B, Tsutsui K, Deviche P. (2015). Food restriction negatively affects multiple levels of the reproductive axis in male house finches, Haemorhous mexicanus. *J Exp Biol*, 218:2694-2704.

Van Ruijssevelt L, Chen Y, von Eugen K, Hamaide J, De Groof G, Verhoye M, Gunturkun O, Woolley SC, Van der Linden A. (2018). fMRI reveals a novel region for evaluating acoustic information for mate choice in a female songbird. *Curr Biol*, 28:711–721.

Vasudevan N, Morgan M, Pfaff D, Ogawa S. (2013). Distinct behavioral phenotypes in male mice lacking the thyroid hormone receptor α1 or β isoforms. *Horm Behav*, 63:742-51.

Vaugien L. (1951). Ponte induite chez la Perruche ondulee maintenue à l'obscurité et dans l'ambience des volières. *Comptes Rendus Hebdomadaires des Seances de l'Academie des Sciences*, 232:1706-1708.

Vézina F, Gustowska A, Jalvingh K, Chastel O, Piersma T. (2009). Hormonal Correlates and Thermoregulatory Consequences of Molting on Metabolic Rate in a Northerly Wintering Shorebird. *Physiol Biochem Zool*, 82(2), pp.129-142.

Viitaniemi HM, Verhagen I, Visser ME, Honkela A, van Oers K, Husby A. (2019). Seasonal variation in genome-wide DNA methylation patterns and the onset of seasonal timing of reproduction in great tits. *Genome Biol Evolut*, 11(3), 970-983.

Visser ME, Caro SP, van Oers K, Schaper SV, Helm B. (2010). Phenology, seasonal timing and circannual rhythms: towards a unified framework. *Phil Trans Roy Soc B Bio Sci*, 365:3113-3127.

Von Frisch K. (1911) Beitrage zur Physiologie der Pigmentzellan in der Fischhaut. *Pflugers Arch*. 138, 319–387

Walkden-Brown SW, Restall BJ, Norton BW, Scaramuzzi RJ, Martin GB. (1994). Effect of nutrition on seasonal patterns of LH, FSH and testosterone concentration, testicular mass, sebaceous gland volume and odour in Australian cashmere goats. *Reproduction*. 102:351-360.

Walkden-Brown SW, Restall BJ, Scaramuzzi RJ, Martin GB, Blackberry MA. (1997). Seasonality in male Australian cashmere goats: long term effects of castration and

testosterone or oestradiol treatment on changes in LH, FSH and prolactin concentrations, and body growth. *Small Rum Res*, 26:239-252.

Watanabe M, Yasuo S, Watanabe T, Yamamura T, Nakao N, Ebihara S, Yoshimura T. (2004). Photoperiodic regulation of type 2 deiodinase gene in Djungarian hamster: possible homologies between avian and mammalian photoperiodic regulation of reproduction. *Endocrinol*. 145:1546-1549.

Watanabe T, Yamamura T, Watanabe M, Yasuo S, Nakao N, Dawson A, Ebihara S, Yoshimura T. (2007) Hypothalamic expression of thyroid hormone-activating and-inactivating enzyme genes in relation to photorefractoriness in birds and mammals. *Am J Physiol Regul Integr Comp Physiol*, 292, R568–R572

Waxman DJ, Ram PA, Park SH, Choi HK. (1995). Intermittent plasma growth hormone triggers tyrosine phosphorylation and nuclear translocation of a liver-expressed, Stat 5-related DNA binding protein. Proposed role as an intracellular regulator of male-specific liver gene transcription. *J Biol Chem*, 270:13262-13270.

Waxman DJ. (2000). Growth hormone pulse-activated STAT5 signalling: a unique regulatory mechanism governing sexual dimorphism of liver gene expression. In *Novartis Foundation symposium* (Vol. 227, p. 61).

Weaver IC, Cervoni N, Champagne FA, D'Alessio AC, Sharma S, Seckl JR, Dymov S, Szyf M, Meaney MJ. (2004). Epigenetic programming by maternal behavior. *Nat Neurosci*, 7(8), 847-854.

Webster JR, Moenter SM, Woodfill CJ, Karsch FJ. (1991). Role of the thyroid gland in seasonal reproduction. II. Thyroxine allows a season-specific suppression of gonadotropin secretion in sheep. *Endocrinology*, 129, 176–183.

Weems PW, Goodman RL, Lehman MN. (2015). Neural mechanisms controlling seasonal reproduction: principles derived from the sheep model and its comparison with hamsters. *Front Neuroendocrinol*, 37, 43–51.

Wehr TA. (1991). The durations of human melatonin secretion and sleep respond to changes in daylength (photoperiod). *J Clin Endocrinol Metab*, 73, 1276–1280.

White SA, Nguyen T, Fernald RD. (2002). Social regulation of gonadotropin-releasing hormone. *J Exp Biol* 205:2567–81.

Whitlock KE. (2005). Origin and development of GnRH neurons. *Trends Endocrinol Metab*, 16, 145–151.

Wilschut RA, Oplaat C, Snoek LB, Kirschner J, Verhoeven KJ. (2016). Natural epigenetic variation contributes to heritable flowering divergence in a widespread asexual dandelion lineage. *Mol Ecol*, *25*(8), pp.1759-1768.

Williams LM, Morgan PJ. (1988). Demonstration of melatonin-binding sites on the pars tuberalis of the rat. *J Endocrinol*, 119, R1–R3.

Wilson F, Reinert B. (2000) Thyroid hormone acts centrally to programme photostimulated male American tree sparrows (Spizella arborea) for vernal and autumnal components of sea- sonality. *J. Neuroendocrinol*, 12, 87–96

Wilson FE, Donham RS. (1988). Daylength and control of seasonal reproduction in male birds. In *Processing of environmental information in vertebrates* (pp. 101–119). New York, NY: Springer.

Wilson FE, Reinert BD. (1995). A one-time injection of thyroxine programmed seasonal reproduction and postnuptial molt in chronically thyroidectomized male American tree sparrows Spizella arborea exposed to long days. *J Avian Biol*, 225-233.

Wilson FE, Reinert BD. (1999). Long days and thyroxine program American tree sparrows for seasonality: evidence for temporal flexibility of the breeding season of euthyroid females. *Gen Comp Endocrinol*, 113(1), 136-145.

Wingfield JC. (2008). Organization of vertebrate annual cycles: implications for control mechanisms. *Philos Trans R Soc London B,* 363:425-441.

Wingfield JC, Kenagy GJ. (1991). Natural regulation of reproductive cycles. In P. K. T. Pawg & M. P. Schreibruan (Eds.)., *Vertebrate endocrinology: Fundamentals and biomedical implications* (Vol. 5, pp. 181–241). San Diego, CA: Academic Press.

Wingfield JC, Hahn TP, Levin R, Honey P. (1992). Environmental predictability and control of gonadal cycles in birds. *J Exp Zool*, 261:214-231.

Wolffe AP, Matzke MA. (1999). Epigenetics: regulation through repression. *Science*, 286:481-486.

Wood S, Loudon A. (2014). Clocks for all seasons: Unwinding the roles and mechanisms of circadian and interval timers in the hypothalamus and pituitary. *J Endocrinol*, 222, R39–R59.

Wood SH, Christian HC, Miedzinska K, Saer BR, Johnson M, Paton B, Yu L, McNeilly J, Davis JR, McNeilly AS, Burt DW, Loudon AS. (2015). Binary switching of calendar cells in the pituitary defines the phase of the circannual cycle in mammals. *Curr Biol*, 20:2651-2662.

Wu Y, Koenig RJ. (2000). Gene regulation by thyroid hormone. *Trends Endocrinol Metab*, 11, 207–211.

Yamamura T, Hirunangi K, Ebihara S, Yoshimura T. (2004). Seasonal morphological changes in the neuro-glial interaction between gonadotropin-releasing hormone nerve terminals and glial end-feet in Japanese quail. *Endocrinol*, 145, 4264–4267.

Yamao M, Araki M, Okano T, Fukada Y, Oishi T. (1999). Differentiation of pinopsin-immunoreactive cells in the developing quail pineal organ: an in-vivo and in-vitro immunohistochemical study. *Cell Tissue Res*, 296(3), pp.667-671.

Yamashita T, Ohuchi H, Tomonari S, Ikeda K, Sakai K, Shichida Y. (2010). Opn5 is a UV-sensitive bistable pigment that couples with Gi subtype of G protein. *Proc Natl Acad Sci*, 107, 22084–22089.

Yamazaki S, Goto M, Menaker M. (1999). No evidence for extraocular photoreceptors in the circadian system of the Syrian hamster. *J Biol Rhythms*, 14, 197–201.

Yasuo S, Watanabe M, Nakao N, Takagi T, Follett BK, Ebihara S, Yoshimura T. (2005) The reciprocal switching of two thyroid hormone-activating and inactivating enzyme genes is involved in the photoperiodic gonadal response of Japanese quail. *Endocrinol*, 146, 2551–2554

Yasuo S, Yoshimura T, Ebihara S, Korf HW. (2009). Melatonin transmits photoperiodic signals through the MT1 melatonin receptor. *J Neurosci,* 29:2885-2889.

Yeo SH, College WH. (2018). The role of kiss1 neurons as integrators of endocrine, metabolic and environmental factors in the hypothalamic-pituitary-gonadal axis. *Front Endocrinol*, 9, 188.

Yoshimura T, Yasuo S, Watanabe M, Iigo M, Yamamura T, Hirunagi K, Ebihara S. (2003) Light-induced hormone conversion of T4 to T3 regulates photoperiodic response of gonads in birds. *Nature*, 426, 178–181

Yoshimura T. (2013). Thyroid hormone and seasonal regulation of reproduction. *Front Neuroendocrinol,* 34:157-166.

Young JZ. (1935). The photoreceptors of lampreys: II. The functions of the pineal complex. *J Exp Biol*, 12, 254–270.

Zhang X, Yazaki J, Sundaresan A, Cokus S, Chan SW, Chen H, Henderson IR, Shinn P, Pellegrini M, Jacobsen SE, Ecker JR. (2006). Genome-wide high-resolution mapping and functional analysis of DNA methylation in Arabidopsis. *Cell*, 126, 1189–1201.

Zhang Y. (2001). Transcription regulation by histone methylation: Interplay between different covalent modifications of the core histone tails. *Genes Develop*, 15, 2343–2360.

Zhang, KX, D'Souza S, Upton BA, Kernodle S, Vemaraju S, Nayak G, Gaitonde KD, Holt AL, Linne CD, Smith AN, Petts NT. (2020). Violet-light suppression of thermogenesis by opsin 5 hypothalamic neurons. *Nature*, *585*(7825), pp.420-425.

Zhao S, Fernald RD. (2005). Comprehensive algorithm for quantitative real-time polymerase chain reaction. *J Comp Biol*, *12*(8), pp.1047-1064.

Zimmer C, Boogert NJ, Spencer KA. (2013). Developmental programming: cumulative effects of increased pre-hatching corticosterone levels and post-hatching unpredictable food availability on physiology and behaviour in adulthood. *Horm Behav*, *64*(3), pp.494-500.

Zimmer C, Larriva M, Boogert NJ, Spencer KA. (2017). Transgenerational transmission of a stress-coping phenotype programmed by early-life stress in the Japanese quail. *Sci Rep*, 7(1), pp.1-19.